The Synthesis and Development of Fluorescent Analogues of L-Phenylalanine and L-Tyrosine.

Olivia Marshall, MSci

A thesis submitted in part fulfilment of the requirements for the degree of Doctor of Philosophy

School of Chemistry

College of Science and Engineering

University of Glasgow

May 2026

Abstract

Fluorescence spectroscopy plays a pivotal role chemical biology, enabling real-time monitoring and identification of protein structure and function. Fluorescent amino acids have emerged as a prominent alternative to extrinsic fluorescent labelling as their small size results in minimal perturbation of the protein of interest. The focus of this PhD was the development of short and efficient synthetic routes to small, but strongly fluorescent amino acids to be utilised as non-invasive peptidic probes. The first project describes the synthesis of dibenzofuran amino acids as rigid, fluorescent analogues of tyrosine, for which an improved synthesis involving a Negishi cross-coupling reaction was developed.

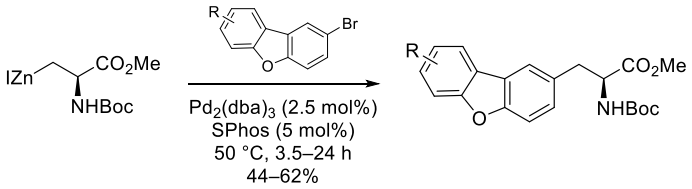

The second aim of this PhD was the development of one-pot methodologies in which a commercially available tyrosine derivative was activated by the installation of a nonaflate leaving group, followed by palladium catalysed cross-coupling reactions. This approach gave rapid access to novel libraries of biaryl and arylalkynyl analogues of phenylalanine. Photophysical analysis identified a strongly fluorescent and environmentally sensitive dimethylaminobiphenyl-substituted amino acid that was found to be an effective FRET donor and was incorporated into a peptide containing a 2,4-dinitrophenyl-lysine quencher, enabling evaluation of kinetic parameters of serine proteolysis.

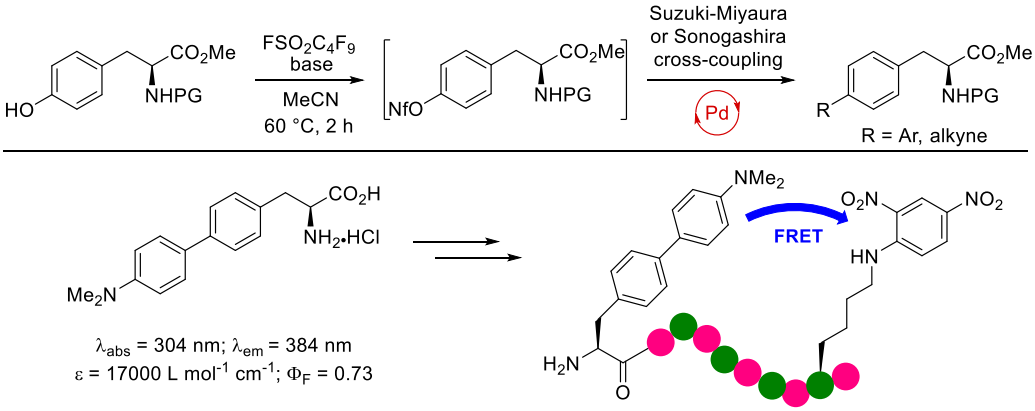

The one-pot tyrosine activation followed by Sonogashira cross-coupling strategy was subsequently used to access a phenylacetylene α-amino acid, a key synthetic intermediate for the introduction of more complex aryl substituents. This intermediate enabled the expansion of the arylalkyne amino acid library, generating red-shifted amino acids with high brightness. A lead BODIPY analogue displayed sensitivity to lipid-rich environments, showing potential in membrane imaging applications. Furthermore, the utility of the phenylacetylene α-amino acid intermediate for chemical biology applications was demonstrated by late-stage functionalisation of peptides and click chemistry with several azides.

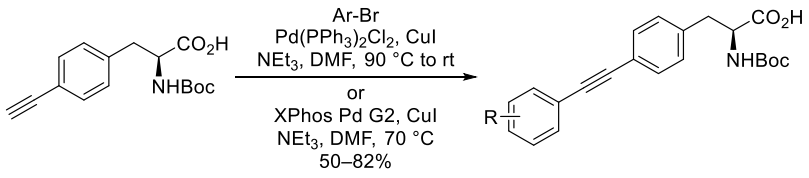

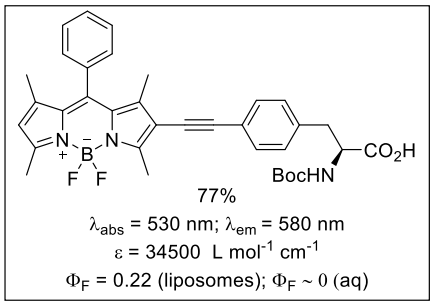

Finally, owing to the success of the alkyne-extended analogues of phenylalanine, a synthetic route was developed to access arylalkynyl analogues of tyrosine. This involved the preparation of an iodotyrosine intermediate that underwent successful Sonogashira cross-coupling reactions with TMS-acetylene.

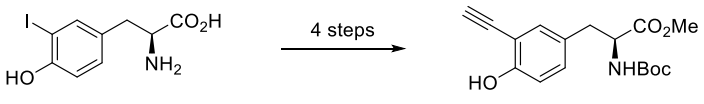

Table of Contents

Acknowledgements

Firstly, I would like to thank my supervisor Professor Andy Sutherland for allowing me to undertake this PhD research in his group. I am extremely grateful for all his support. Andy's feedback, guidance and high expectations have been invaluable in my development as a researcher. I would also like to thank my second supervisor, Dr Joelle Prunet, and section head, Professor Andrew Jamieson, for their feedback at annual progression meetings, as well as Dr Drew Thompson and his research group for their assistance with peptide synthesis.

I'd like to express my gratitude to all the members of the technical staff including Alec Mungall, Giovanni Rossi, Andrew Monaghan, Karen McLachlan, Finlay Smith, Stuart Mackay, Arlene Sloan and in particular, the Loudon lab technician Gillian Laidlaw.

Thank you to the Sutherland group members past and present, Leanne Amy, Rochelle, Nina, Lachlan, Valeria, Pankaj, Juwon, Eoghan and Hannah. I would like to give special thank you to Holly McErlain, who has always had time to help answer my questions. A shout out as well to the members of the Hartley group who make the Loudon lab a joy to work in as well as Hollie Miller in the Prunet group and Katie Hillan in the Peveler group for their constant support and friendship.

There are many friends and family I would like to thank outside of the lab, who's support and encouragement has allowed me to pursue my ambitions, for which I will be forever grateful. In particular, Eirinn-Rose, Ellie, Helen, Zoe, Molly, Sofia, Harmony, Sarah, Kit, Melody, Hayley, Freddy, Owen, my parents Grant and Julia, my brother Alex and my partner James.

Author's Declaration

I declare that, except where explicit reference is made to the contribution of others, this thesis represents the original work of Olivia Marshall and has not been submitted for any other degree at the University of Glasgow or any other institution. The research was carried out at the University of Glasgow in the Loudon Laboratory under the supervision of Professor Andrew Sutherland between October 2022 and March 2026. Aspects of the work described herein have been published elsewhere as listed below.

O. Marshall and A. Sutherland, Expanding the fluorescence toolkit: molecular design, synthesis and biological application of unnatural amino acids, *Chem. Sci.,* 2025, **16**, 16414–16432.

O. Marshall and A. Sutherland, One-pot synthesis of alkynyl-conjugated phenylalanine analogues for peptide-based fluorescent Imaging, *Org. Lett.*, 2025, **27**, 8023–8027.

Liyao Z., **O. Marshall**, R. McGrory, R. Clarke, R. J. Brown, M. Kadodwala, A. R. Thomson, and A. Sutherland, Synthesis of fluorescent dibenzofuran α-amino acids: conformationally rigid analogues of tyrosine, *Org. Lett.*, 2025, **27**, 2475–2479.

O. Marshall, R. McGrory, S. Songsri , A. R. Thomson and A. Sutherland, Expedient discovery of fluorogenic amino acid-based probes via one-pot palladium-catalysed arylation of tyrosine, *Chem. Sci.*, 2025, **16**, 3490-3497.

L. M. Riley, **O. Marshall**, A. H. Harkiss, H. M. Senn and A. Sutherland, Synthesis of β-pyridyl α-amino acids: conformationally sensitive charge transfer-based fluorophores, *Org. Lett.,* 2024, **26**, 5391–5395.

R. McGrory, R. Clarke, **O. Marshall** and A. Sutherland, Fluorescent α-amino acids via Heck–Matsuda reactions of phenylalanine-derived arenediazonium salts, *Org. Biomol. Chem.,* 2023, **21**, 6932–6939.

Signature

Printed Name Olivia Marshall

List of Abbreviations

Aad	7-Aminoacridon-2-ylalanine
Abs	Absorbance
ACC	7-Amino-4-carbamoylmethylcoumarin
Acd	Acridon-2-ylalanine
Anap	3-(6-Acetylnaphthalen-2-ylamino)-2-aminopropanoic acid
APCI	Atmospheric pressure chemical ionization
Boc	*tert*-Butyloxycarbonyl
BODIPY	Boron-dipyrromethene
br	Broad
BRT	Brightness
Cbz	Carboxybenzyl
CD	Circular dichroism
CDI	Carbonyldiimidazole
COSY	Correlated spectroscopy
d	Doublet
Dad	7-(Dimethylamino)acridon-2-ylalanine
DAPA	Diaminopimelic acid
DEPT	Distortionless enhancement polarisation transfer
DHFR	Dihydrofolate reductase
DIC	*N,N*'-Diisopropylcarbodiimide
DIPEA	*N,N*'-Diisopropylethylamine
DMEDA	*N,N*′-Dimethylethylenediamine
DMF	Dimethylformamide
DMNA	*N,N*-dimethylamino-1,8-naphthalimide
DMSO	Dimethyl sulfoxide
DNA	Deoxyribonucleic acid
DNP	2,4-Dinitrophenyl
ee	Enantiomeric excess
ESI	Electrospray ionisation
ESIPT	Excited state intramolecular proton transfer
FLIM	Fluorescence lifetime imaging microscopy
Fmoc	Fluorenylmethyloxycarbonyl
FRET	Förster resonance energy transfer
g	Grams
GFP	Green fluorescent protein
GMO	Genetically modified

h	Hour
HBTU	*O*-(Benzotriazol-1-yl)-*N,N,N′,N′*-tetramethyluronium hexafluorophosphate
HOBt	Hydroxybenzotriazole
HOMO	Highest occupied molecular orbital
Hpg	Homopropargylglycine
HPLC	High-performance liquid chromatography
HSQC	Heteronuclear single quantum correlation spectroscopy
Hz	Hertz
ICT	Intramolecular charge transfer
IQF	Internally quenched fluorescence
IR	Infrared
J	NMR spectra coupling constant
LE	Locally Excited
m	Multiplet
M	Molar
m/z	Mass to charge
mg	Milligrams
MHz	Milligrams
μM	Micromolar
mmol	Millimolar
mol	Mole
MOM	Methoxymethyl
MOPS	3-(*N*-morpholino)propanesulfonic acid
MW	Microwave
NBD	7-Chloro-4-nitrobenzo-2-oxa-1,3-diazole
NBS	*N*-Bromosuccinimide
Nf	Nonaflate
nm	Nanometers
NMR	Nuclear magnetic resonance
OLEDs	Organic light-emitting diodes
PBS	Phosphate-buffered saline
PC	Phosphatidylcholine
PET	Photo-induced electron transfer
Phe	Phenylalanine
PyBOP	Benzotriazol-1-yloxytripyrrolidinophosphonium hexafluorophosphate
q	Quartet
QTOF	Quadrupole time-of-flight

rt	Room temperature
s	Singlet
S.S.	Stokes shift
S_0	Ground state
S_1	First excited state
S_2	Second excited state
SPPS	Solid phase peptide synthesis
t	Triplet
T_1	First triplet excited state
TBAF	Tetra-*n*-butylammonium fluoride
TFA	Trifluoroacetic acid
THF	Tetrahydrofuran
TICT	Twisted intramolecular charge transfer
TIPS	Triisopropyl silane
TLC	Thin layer chromatography
Tm	*Thermotoga maritima*
TMP	Trimethoprim
TMS	Trimethylsilyl
tRNA	Transfer ribonucleic acid
Trp	Tryptophan
Tyr	Tyrosine
UV	Ultraviolet
Vis	Visible light
ε	Molar attenuation coefficient
λabs	Absorbance maximum
λem	Emission maximum
Φ	Fluorescence quantum yield
°C	Degrees centigrade
Δ	Reflux

1.0 Introduction

Fluorescence spectroscopy plays a critical role in the study of biological processes in providing non-invasive tools with temporal and spatial resolution.[1-6] In addition to tuneable physicochemical properties such as target affinity, reactivity and subcellular location, modification of the fluorescent properties can generate probes that respond to stimuli and provide quantitative measurements corresponding to changes in emission intensity. For example, small molecule fluorescent probes are widely used in live cell imaging to detect cellular microenvironments such as pH, viscosity and voltage, as well as to investigate dynamic changes in protein structure and function, including ligand binding events and protein-protein interactions.[5-8]

Traditional fluorescent labelling techniques, such as protein expression with green fluorescent protein (GFP) or formation of fusion proteins including HaloTag and SNAP tag have been widely employed.[9] However, a major limitation of these approaches is that the attachment of large fluorescent proteins (e.g. SNAP tag = 20 kDa)[9] can disrupt the function of the target protein. Furthermore, the synthesis of peptides containing bulky fluorescent labels, such as fluorescein, often requires further optimisation, including adjustment of linker length between the fluorophore and protein of interest and modification of the physicochemical properties.[10] Consequently, considerable effort has been directed towards the development of fluorescent amino acids.[11-15] Fluorescent amino acids offer several advantages, including straightforward incorporation into proteins *via* solid phase peptide synthesis (SPPS) or unnatural acid mutagenesis, while causing minimal perturbation to protein structure and function due to their small size.[11-14]

1.0 Fluorescence Fundamentals

The Perrin-Jablonski diagram shown in Figure 1 illustrates the photophysical pathways that may occur following the irradiation of a fluorophore.[16,17] The absorption of a photon promotes an electron from the electronic ground state (S_0) to an excited state (S_n). Each electronic state contains multiple vibrational levels, with most molecules occupying the lowest vibrational energy level at room temperature. The Franck-Condon principle states that electronic excitation occurs much faster than nuclear and vibrational motion, resulting in effectively vertical electronic transitions on a nuclear coordinate diagram.[17-19] Consequently, the probability of a transition is determined by the overlap integral of the vibrational wavefunctions, which corresponds to the intensity distribution within the absorption spectrum.

Following photon absorption, several competing relaxation pathways may occur. Typically, rapid relaxation to the lowest vibrational level of the first excited state (S_1) occurs through internal conversion ($S_n \rightarrow S_1$) and vibrational relaxation, including energy transfer to the surrounding solvent. Kasha's rule states that fluorescence emission will occur from the lowest excited state to the ground state ($S_1 \rightarrow S_0$).[20,21] Relaxation to higher vibrational levels of the ground state also follows the Franck-Condon principle, giving rise to vibrational fine-structure in the emission spectrum. Together, the Franck-Condon principle and Kasha's rule explain the approximate mirror-image relationship commonly observed between absorption and emission spectra (Figure 2).[17]

Several non-radiative processes compete with fluorescence, including thermal decomposition and intersystem crossing.[17] Intersystem crossing from the singlet excited state to the triplet excited state ($S_1 \rightarrow T_1$) is formally forbidden, but may occur through spin-orbit coupling. Due to the forbidden nature of the transition to S_0, triplet-states are longer-lived, or 'dark-states'. The release of a photon as a molecule relaxes from the triplet state to the ground state is termed phosphorescence. Processes' that dissipate excited-state energy prior to radiative decay are described as quenching. Quenching can occur through several mechanisms such as excited-state reactions, energy transfer and molecular collision.

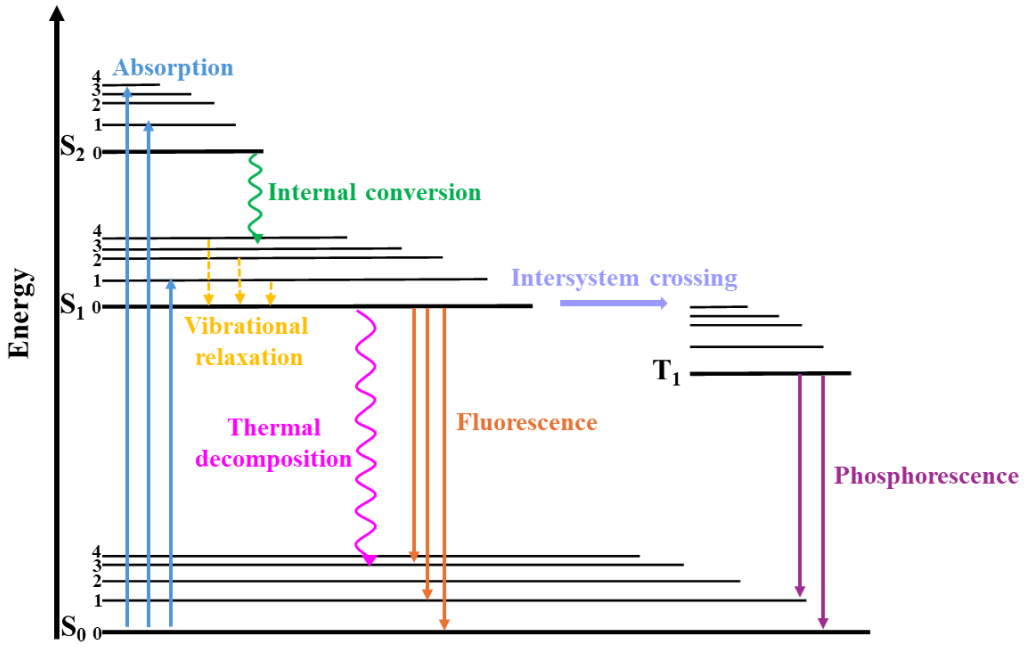

Figure 1: Perrin-Jablonski diagram.

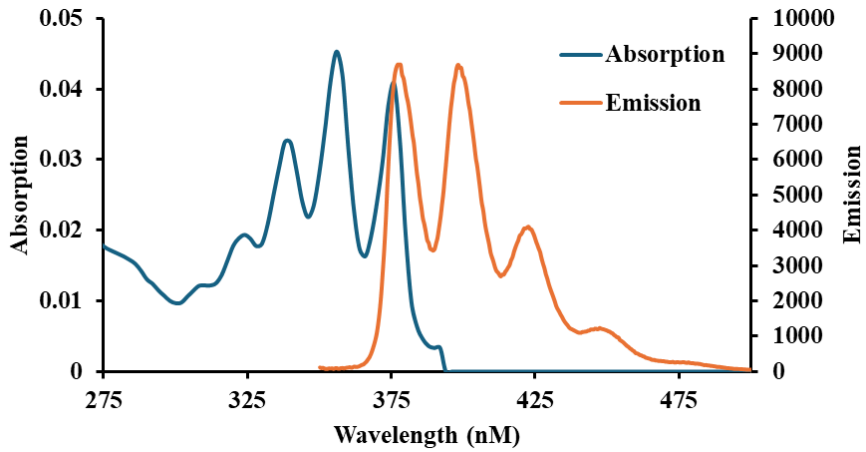

Figure 2: Absorption and emission spectra of anthracene (0.4 µM, EtOH).

Fluorescence occurs in organic molecules with conjugated π-systems in which the electrons are delocalised.[17] These conjugated π-systems can absorb UV or visible light at the wavelength specific to the π-π* or HOMO-LUMO energy gap. Rapid vibrational relaxation within the excited state results in emission at a lower energy, and therefore lower frequency, than the incident radiation, resulting in red-shifted emission relative to the absorption spectrum.

When discussing fluorescent molecules for bioimaging there are several metrics used: the Stokes shift, quantum yield (ϕ), extinction coefficient (ε) and brightness.[16]

The Stokes shift refers to the difference between the absorption and emission maxima. It is often desirable to have a large Stokes shift such that the emitted wavelength is not re-absorbed ("self-quenching"). The quantum yield is a dimensionless ratio of (photons absorbed) / (photons emitted) and is a measurement of the fluorophore's efficiency, with 1.0 indicating 100% efficiency. Factors such as quenching, pH and solvent polarity influence the quantum yield.[22-24] The extinction coefficient regards the efficiency with which light is absorbed as described by the Beer-Lambert Law where absorbance is equal to the molar extinction coefficient multiplied by the concentration and path length (Equation 1).[16] Finally, brightness is the extinction coefficient multiplied by the quantum yield.

$$A = \varepsilon c l$$

Equation 1: Beer-Lambert Law. Where $\boldsymbol{A}$ is the absorbance, $\boldsymbol{\varepsilon}$ is the absorption coefficient (M^{-1} cm^{-1}) $\boldsymbol{c}$ is the concentration (mol L^{-1}) and $\boldsymbol{l}$ is the path length (cm).

Various strategies have been employed to improve the fluorescent properties of small molecules, such as extending the π-conjugation and rigidification.[1,25] Increasing conjugation decreases the HOMO-LUMO energy gap resulting in absorption at longer wavelengths. Similarly, conformationally rigid, planar molecules allow for better π-orbital overlap and reduce deactivation through internal conversion.[26-28] For applications such as live-cell imaging, red-shifted absorption and emission are desirable because ultraviolet light can increase background autofluorescence and induce photodamage. Red and near-infrared fluorophores have been developed through strategies including enhancement of intramolecular charge transfer (ICT) or heteroatom engineering.[29] ICT is widely utilised in the design of fluorescent probes.[6] In these systems, an electron-donating and an electron-accepting group are positioned at opposing ends of the fluorophore, generating a strong dipole moment. Environmentally sensitive probes frequently employ ICT as the highly polarised excited state is better stabilised by more polar solvents, resulting in red-shifted emission.[17] Red-shifted emission has also been achieved by incorporation of heteroatoms including halogens, sulphur and selenium. As well as modifying the electronic structure of the fluorophore, heavy atoms can facilitate intersystem crossing and thus enhance phosphorescence.[17,29]

Alternatively, imaging techniques such as two-photon excitation spectroscopy can be used to excite a fluorophore at longer wavelengths. Two-photon excitation is the simultaneous absorption of two-photons with approximately twice the wavelength required for one-photon microscopy; for example, a fluorophore excited at 350 nm under one-photon excitation may be excited at 700 nm in a two-photon excitation process.[17,30] Consequently, the excitation wavelength may be longer than the emission wavelength, however it does also require a specialist, high-powered pulsed lasers with femtosecond pulse widths.[30] Each of these approaches, often in combination, have also been applied to the development of fluorescent amino acids.

1.1 Fluorescent Amino Acids

Fluorescent amino acids have received significant attention as minimally invasive peptidic probes.[11-15] As well as straightforward incorporation into a protein of interest *via* SPPS or genetic encoding, their small size has enabled fluorescent amino acids to be internally substituted within a peptide without perturbing the secondary structure and has facilitated investigation of challenging dynamic cellular processes previously inaccessible to chemical labelling.[31-33]

Proteinogenic amino acids phenylalanine, tyrosine and tryptophan are intrinsically fluorescent due to their aromatic side chains (Scheme **1**).[34] Despite relatively poor optical properties, the naturally fluorescent amino acids have been utilised in fluorescence measurements of peptides.[15] The fluorescence of tyrosine is pH dependent as deprotonation of the phenol side chain results in a bathochromic shift of its emission maxima from 310 to 340 nm, accompanied by a decrease in fluorescence intensity.[15,35] The indole moiety in tryptophan exhibits more favourable photophysical properties leading to its wider application as a fluorescent reporter.[15] Its higher brightness often results in it dominating the emission spectrum in peptides and its environmental sensitivity has been exploited in probing protein structure and dynamics.

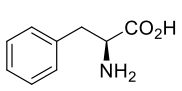

Phe, 1
λ_{ex} = 258 nm, λ_{em} = 282 nm
ε = 200 L mol^{-1} cm^{-1}
Φ_F = 0.024
BRT = 5 L mol^{-1} cm

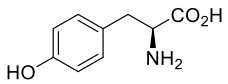

Tyr, 2
λ_{ex} = 275 nm, λ_{em} = 310 nm
ε = 1410 L mol^{-1} cm^{-1}
Φ_F = 0.14
BRT = 197 L mol^{-1} cm

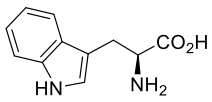

Trp, 3
λ_{ex} = 279 nm, λ_{em} = 365nm
ε = 5580 L mol^{-1} cm^{-1}
Φ_F = 0.20
BRT = 1116 L mol^{-1} cm

Scheme 1: Photophysical properties of proteinogenic amino acids phenylalanine, tyrosine and tryptophan.[34]

1.2 Design and Application of Novel Fluorescent Amino Acids

1.3.1 *De Novo* Fluorescent Amino Acids

In order to overcome the challenges associated with the naturally fluorescent amino acids, including the non-specific labelling of proteins and relatively poor optical properties, significant work has gone into the development of unnatural fluorescent amino acids. The approaches to achieve this can be broadly divided into the modification of the naturally fluorescent amino acids to improve their photophysical properties, or the *de novo* design of unnatural amino acids.

A common strategy in the *de novo* design of fluorescent amino acids is the incorporation of established fluorophores into the amino acid side chain. Coumarin-derived amino acids are a key example of this strategy and have been applied widely due to their relatively compact nature, yet strong fluorescence. Variation of the electron donating group that is conjugated to the acrylate has resulted in different, environmentally sensitive amino acid analogues which have been used in cell imaging,[36] protein-ligand binding[37,38] and analysis of nucleotide-induced conformational changes during DNA replication.[39] Coumarin amino acid analogues were further employed as FRET donors for modulating the fluorescence of cyan fluorescent protein.[40]

A scalable synthesis of coumarin-derived amino acid **6** was reported by Martin and co-workers starting from a protected glutamic acid analogue **4** (Scheme **2**).[36] Following activation of the side-chain carboxylic acid, reaction with freshly prepared ethyl magnesium malonate gave β-keto ester **5** in 90% yield. Condensation with resorcinol under strongly acidic conditions affords the desired coumarin moiety *via* a von Pechmann cyclisation in 64% yield. 7-Hydroxycoumarin ethylglycine **6** exhibits excellent photophysical properties, including a large stokes shift of 90 nm and a high quantum yield of 0.63 in its phenolate form.[41] Leveraging enantiopure amino acids in a chiral pool approach is favourable in the synthesis of unnatural amino acids, as it avoids the complexity and time-consuming optimisation of asymmetric catalysis and often utilises inexpensive, commercially available starting materials that can be readily diversified.[42]

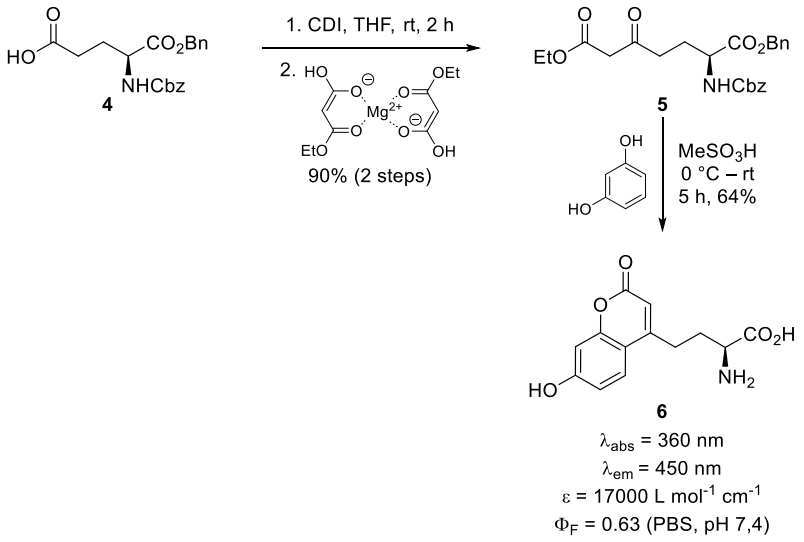

4 5 6

Scheme 2: Synthesis of hydroxy coumarin analogue 6.[36]

Several asymmetric syntheses have been reported that utilise the Williams' chiral auxiliary or a Ni(II) Schiff base as chiral glycine equivalents (Scheme **3**).[43,44] Following alkylation, decomposition of the chiral auxiliary is achieved using acid-mediated hydrolysis or hydrogenation to give dimethyl amino analogue **10** or methoxy analogue **13** in high enantiomeric excess and yield. The chiral glycine synthons have been widely utilised in the synthesis of unnatural amino acids.[45-48] More recently, the Ni(II) Schiff base first reported by Belokon, has gained particular attention owing to the broad range of reaction types including alkylation, aldol condensation and Michael addition performed with enantioselectivity. Furthermore, recovery of the chiral ligand after hydrolysis allows it to be recycled.[45,49,50] Second generation Ni(II) Schiff bases which aim to improve the diastereoselectivity have been reported, the most successful of which involve halogenation of the *N*-benzyl proline moiety.[51-54]

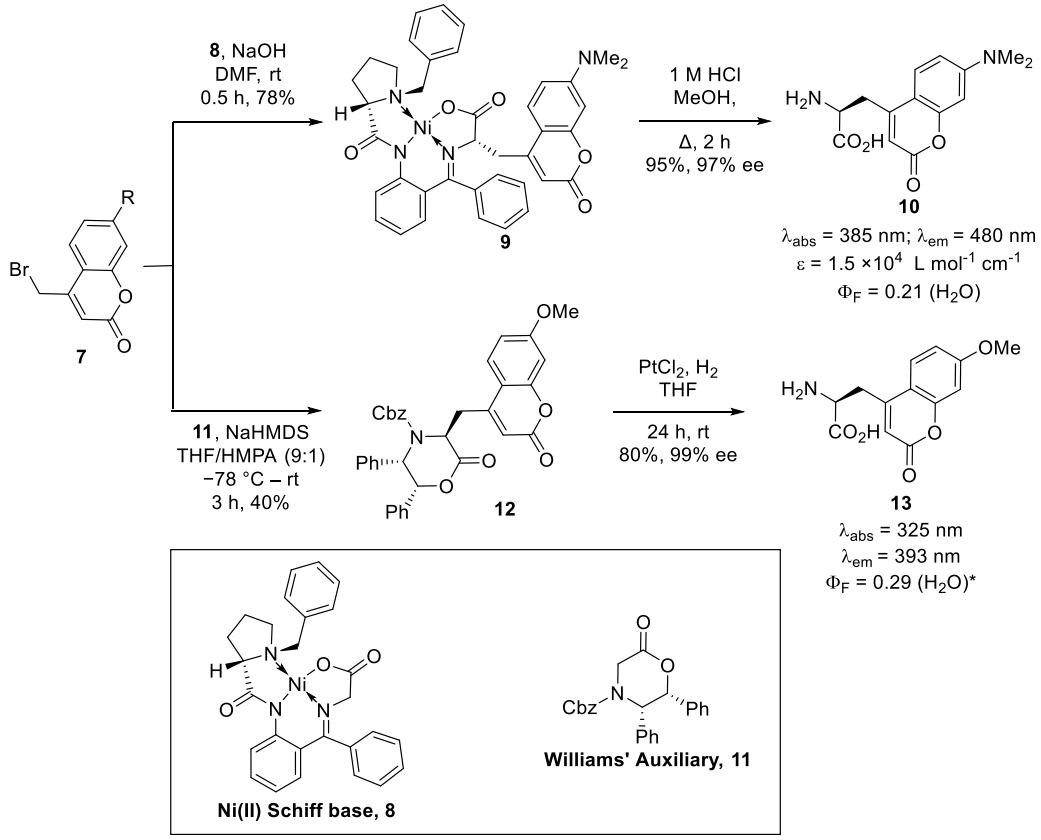

Scheme 3: Synthesis of coumarin-derived analogues 10 and 13 using chiral glycine equivalents.[43,44] Photophysical data of **10** is reported following incorporation into a di-alanine tripeptide. *reported quantum yield for 7-methxycoumarin.

The Mély group have reported several environmentally sensitive flavone-derived amino acid analogues, which have been utilised to probe peptide–nucleic acid interactions and in the determination of peptide orientation in lipid bilayers.[55-57] The synthesis started with Friedel-Crafts acylation of tyrosine (Scheme **4**). Following *N*-Boc-protection, acylated intermediate **15** was subjected to an aldol condensation with several aromatic aldehydes to give α,β-unsaturated ketones **16**–**18**. Subsequent Algar-Flynn-Oyamada reaction gave the cyclised flavonol core in 33–63% yields. Finally, Boc-deprotection gave the desired fluorescent amino acids.

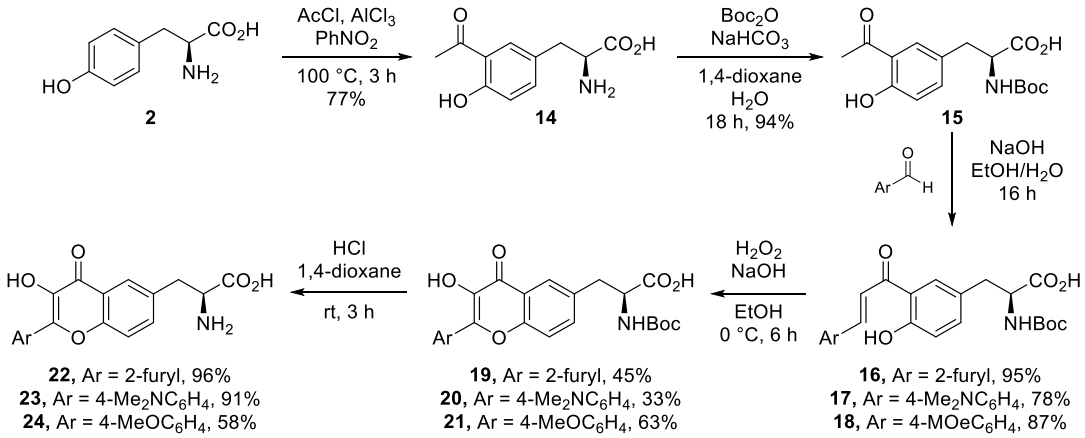

Scheme 4: Synthesis of flavone-derived amino acids.[55-57]

The environmental sensitivity arises from the formation of a push-pull chromophore, in which electron density is transferred from an electron-rich aromatic ring towards the ketone group (Scheme **5**). This donor-π-acceptor architecture promotes intramolecular charge transfer (ICT) and is often designed to induce a bathochromic shift in both the absorption and emission spectrum.[58] Emission from the charge-transfer excited state is further stabilised in polar solvents, resulting in environmental sensitivity in these systems.[17] Additionally, flavone-derived amino acids **22**, **23** and **24** exhibit excited-state intramolecular proton transfer (ESIPT). ESIPT is a process in which photoexcited molecules relax to a lower energy exited state *via* tautomerisation. In the case of flavone amino acid **24**, dual emission is observed, with longer-wavelength emission (520 nm) arising from the enol form (Scheme **5**). The relative intensities of emission from either the normal form N* and tautomer form T* are dependent on the local environment, particularly, charge distribution, polarity and exposure to aqueous solvent.[17] For flavone amino acid **24**, the ratio of the emission bands (N*/T*) significantly increased from 0.04 to 4.80 with increasing solvent polarity and hydrogen bond donating ability, as hydrogen bonding of the N* form suppresses ESIPT.[56] Furthermore, a two-fold increase in quantum yield was observed in changing solvent from aqueous buffer to 1,4-dioxane. The pronounced sensitivity to hydration was exploited by incorporating the amino acid into a HIV-1 nucleocapsid peptide enabling investigation of interactions with nucleic acid and lipid vesicles using fluorescence lifetime measurements, as longer fluorescence lifetimes were associated with ESIPT.

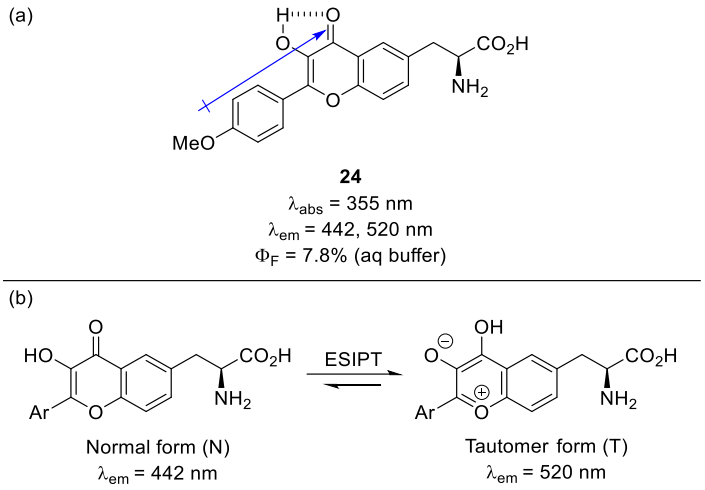

Scheme 5: (a) Photophysical properties of flavone-derived amino acid 24, highlighting the charge-transfer dipole on the structure.[56] (b) Tautomerisation of amino acid 24 *via* excited state intramolecular charge transfer (ESIPT).

Fluorescent amino acid acridon-2-ylalanine (Acd) **28** has found widespread applications due to its exceptionally high quantum yield in water (Φ = 0.95), long fluorescence lifetime ($\tau \sim$ 15 ns) and high photostability (<5% degradation after 3 h irradiation).[59] A recently reported improved synthesis involved formation of a triflate intermediate **26**, followed by Buchwald-Hartwig amination with methyl anthranilate to give **27** in 90% yield (Scheme **6**).[60] Cyclisation was achieved by subjecting **27** to an acid-catalysed Freidel-Crafts acylation using 13.5 M sulfuric acid, which simultaneously deprotected the amino acid backbone affording the desired amino acid **28** in 81% yield.

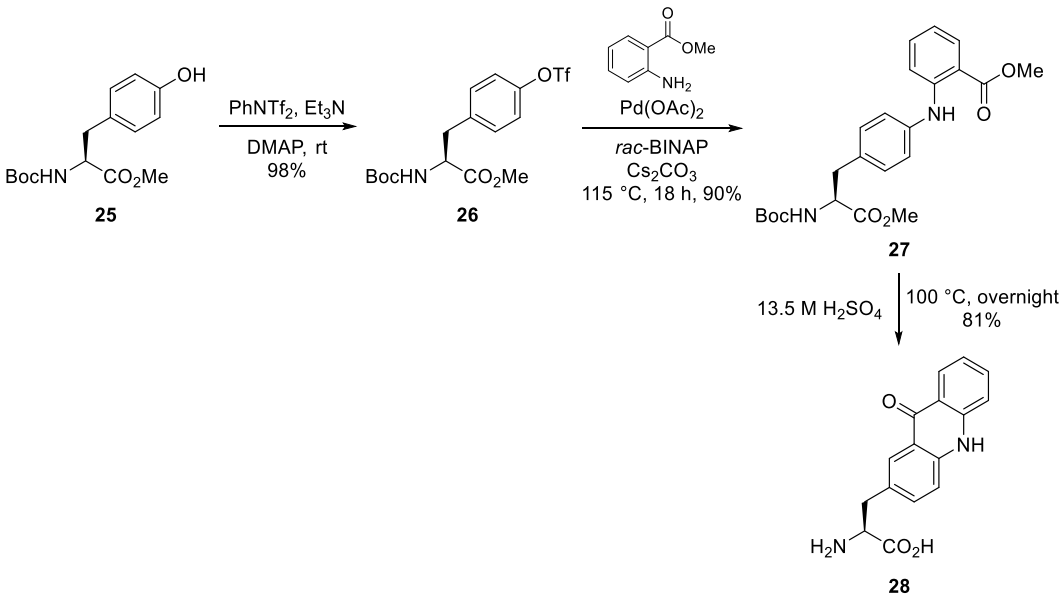

Scheme 6: Synthesis of Acd.[60]

The unnatural Acd amino acid has been incorporated into peptides *via* SPPS or gene encoding and utilised as a fluorescent probe in FRET measurements, partnered with either the natural amino acid tyrosine, an unnatural methoxycoumarin fluorescent amino acid, transition-metals, or thioamide residues (*via* a PET quenching mechanism).[59,61-65] Furthermore, the long fluorescence lifetime is particularly useful in photophysical studies such as fluorescence lifetime imaging microscopy (FILM), where the unnatural amino acid outperforms endogenous fluorophores such as GFP.[66] High quantum yield, environmental sensitivity and long fluorescence lifetime have also been exploited in fluorescence polarisability studies in the analysis of protein-protein binding.[67] Furthermore, to improve understanding of protein tolerance to unnatural amino acids incorporation, machine learning models were trained to predict mutant protein yield and solubility following Acd incorporation at different sites.[68] The model incorporated predicted parameters such as hydrophobic interactions, desolvation and amino acid angle preferences. Although the model was limited to Acd incorporation into the LexA and RecA proteins, it provides promising evidence for the development of predictive AI models that could broaden the use of fluorescent amino acids as chemical probes.

Following the success of Acd, several derivatives, Aad and Dad, have been developed (Scheme **7**).[69,70] Attachment of an amine donating group resulted in red-shifted absorption and emission, reducing the risk of photodamage when applied in peptide imaging. The low quantum yield of 7-aminoacridon-2-ylalanine **29** was subsequently overcome by alkylation. Alkylation of amino groups has been shown to disfavour twisted-intramolecular charge transfer, and enhance quantum efficiency.[71] More recently, a sulfur analogue **31** was reported by Wang and co-workers, in which heavy atom substitution was designed to extend triplet state lifetime. Sulfur analogue **31** possessed absorption and emission at similar wavelengths to those of Acd, however, the spectra were generally less defined (photophysical spectra were reported, but maxima values were not stated). A significant decrease in quantum yield of **31** relative to Acd correlated to an approximate 10-fold enhancement of phosphorescence. The phosphorescent properties were subsequently utilised to detect Eu(III) binding in lanthanide binding proteins.[72]

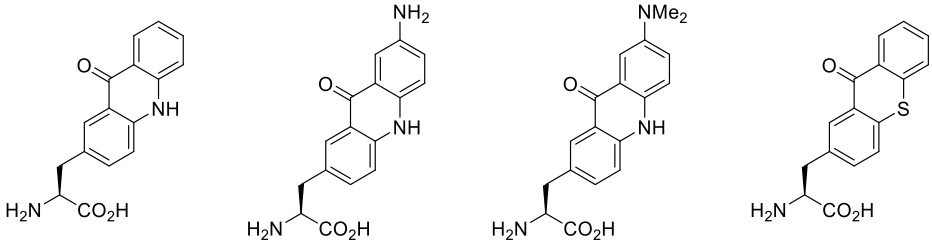

28 (Acd)
λ_{abs} = 262 nm
λ_{em} = 446 nm
Φ_F = 0.95 (H_2O)

29 (Aad)
λ_{abs} = 422 nm
λ_{em} = 530 nn
Φ_F = 0.10 (MeCN/PBS)

30 (Dad)
λ_{abs} = 430 nm
λ_{em} = 572 nm
Φ_F = 0.25 (MeCN/PBS)

31 (SAcd)

Scheme 7: Derivatives of Acd.

Xiang and Wang reported an improved, enantiospecific synthesis of 3-(6-acetylnaphthalen-2-ylamino)-2-aminopropanoic acid (L-Anap) (Scheme **8**).[73] 6-Hydroxy-2-acetylnaphthyl was subjected to a one-pot alkylation-Smiles rearrangement-hydrolysis sequence under conditions reported by Mizuno and Mitsuhano for the conversion of phenol substrates.[74] Due to challenging purification, **34** was hydrolysed under acidic conditions in order to isolate amino naphthalene intermediate **35** in a 73% yield over three steps. After protection with an *o*-nitrobenzenesulfonyl group, the key step in the synthesis involved a Fukuyama-Mitsunobu reaction, to couple the fluorophore with amino acid derivative **37**. A three-step deprotection gave desired amino acid **39**. The enantiopurity was assessed by the Mosher method in which the final product was reacted with a chiral derivatising agent, (*S*)-(+)-α-methoxy-α-trifluoromethylphenylacetyl chloride and concluded less than 3% racemisation occurred by ^{1}H NMR spectroscopy.[75]

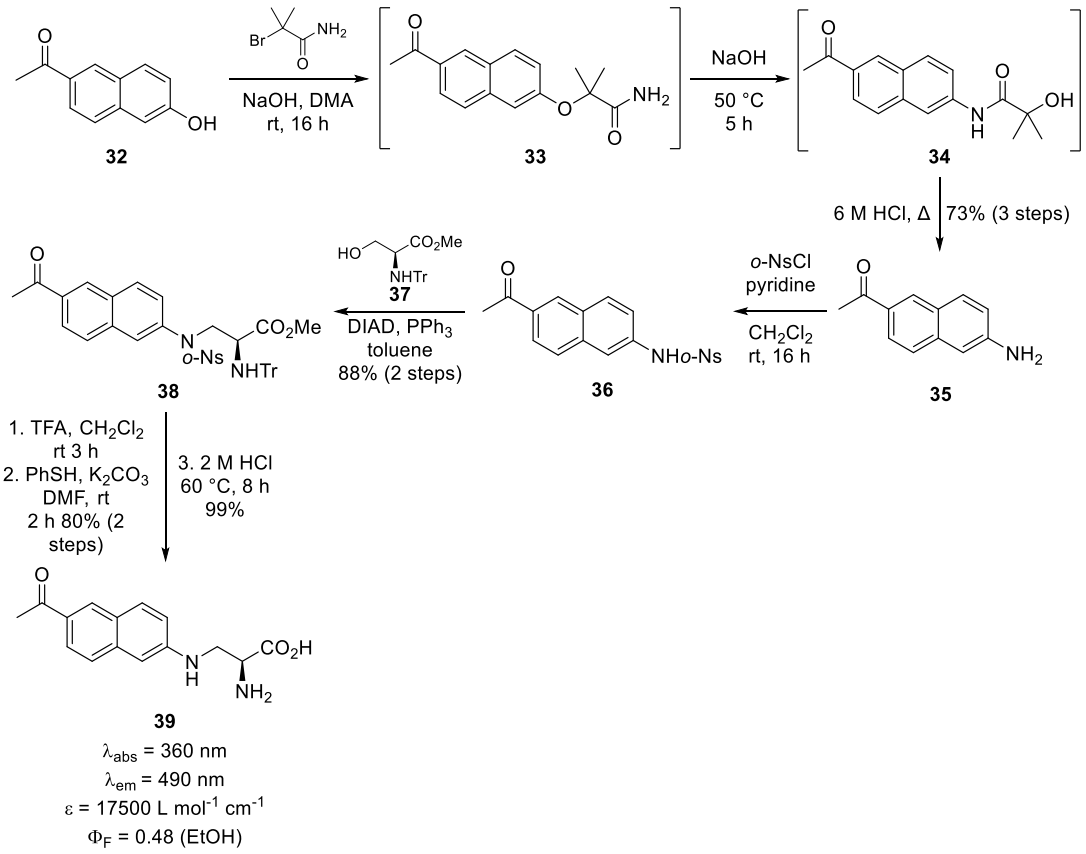

Scheme 8: Synthesis of Anap.[73]

Anap **39** exhibits a high degree of environmental sensitivity, demonstrated by a 70 nm shift in emission maxima from 420 nm in ethyl acetate to 490 nm in water. This property was exploited for the investigation of protein dynamics, including the opening of voltage-gated potassium ion channels at a cytosolic site previously inaccessible to chemical labelling,[33] as well as ligand binding analysis.[76] Additional applications include visualisation of proteins in cells, conformational changes *via* two-photon excitation and use as a FRET donor.[77-79]

In the development of a series of dimethylaminophthalimidoalanine amino acids, 4-*N,N*-dimethylamino-1,8-naphthalimide (4-DMNA) emerged as a lead owing to greater chemical stability, longer excitation wavelength and improved synthetic accessibility, whilst retaining the solvatochromic sensitivity which is exploited in its applications.[80] 4-DMNA was synthesised in three steps from commercially available 4-bromo-1,8-naphthalene anhydride **40** which was first transformed into dimethylamino compound **42** using 3-(dimethylamino)propionitrile **41** (Scheme **9**).[81] Condensation with 3-aminoalanine **44** gave desired amino acid 4-DMNA **44** in 55%

yield. 4-DMNA was incorporated internally into a KR peptide motif and the photophysical data recorded.

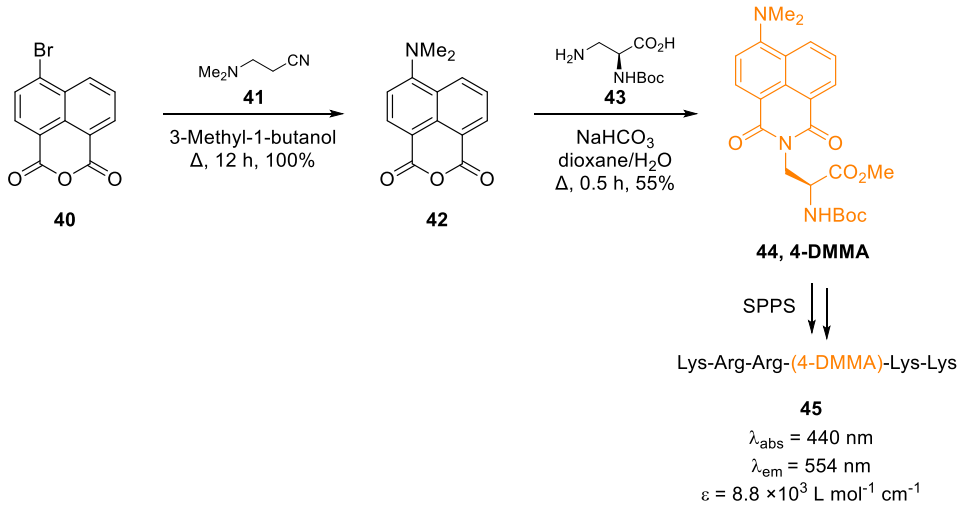

Scheme 9: Synthesis of 4-DMNA.[80]

In the synthesis of fluorescent amino acids, there is often a balance between enhancing the photophysical properties through extending the conjugation and maintaining a chromophore size small enough to avoid perturbing protein structure or function. In this regard, Liu and co-workers reported the rational design of a benzene scaffold substituted with multiple donor and acceptor groups that exhibited near-IR emission (Scheme **10**).[29] Computational screening was first employed to optimise the substitution pattern of electron donating and electron withdrawing groups. Frontier molecular orbital analysis identified positions that would stabilise the LUMO and destabilise the HOMO, thereby reducing the HOMO-LUMO energy gap, and indicated in an optimal 1,2,4,5-substitution pattern. Increasing the electron donating or electron withdrawing strength of the substituent resulted in further bathochromic shifting of the emission, due to enhanced charge-transfer. In addition to donor/acceptor strength, the authors demonstrated that steric hinderance from bulky substituents also had to be considered. For example, bulky dimethylamino **47** or azetidine groups **48** were shown to result in twisted or bent conformations due to steric repulsion with the aldehyde group, resulting in a hypsochromic shift in the calculated absorption and emission spectra relative to the methylamino donor **46** (Scheme **10**). Experimental data for the photophysical properties of the designed fluorophores generally agreed with the predicted data.

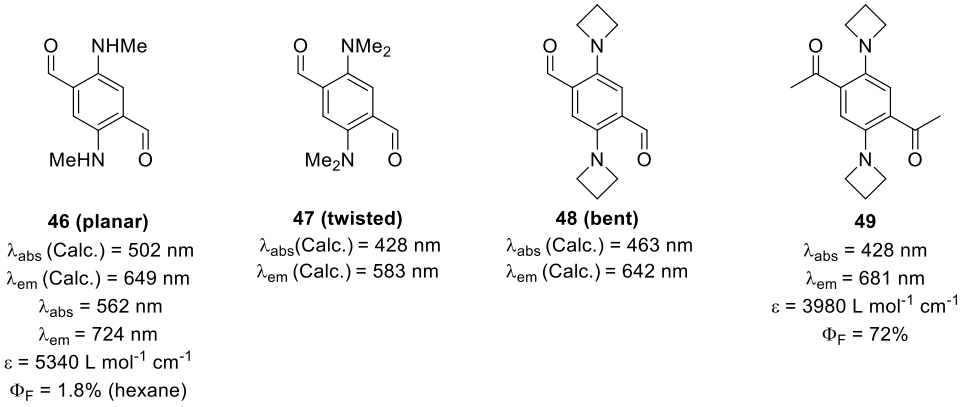

Scheme 10: Small, near-IR, benzene-derived fluorophores.[29]

Following rational fluorophore design, a fluorescent amino acid based on **49** was synthesised (Scheme **11**). Due to challenges described in the synthesis, an unusual one-pot microwave assisted palladium catalysed cross-coupling of dibrominated precursor with the Boc-protected D-amino acid and azetidine was used to give **53** in 14% yield. Deprotection afforded a novel, small, benzene-based, red fluorophore **53**, which replaced methionine in *E. faecium* bacterial cells and enabled wash-free imaging of peptidoglycan glycan in the bacterial cell wall.

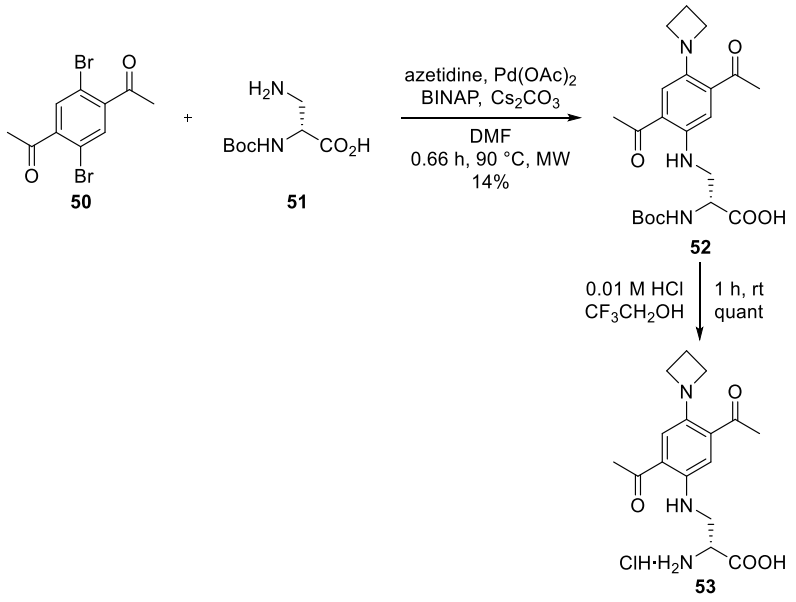

Scheme 11: Synthesis of compact, near-IR fluorescent amino acid.[29]

Nitrobenzodiazole (NBD) amino acids have also gained attention due to their small size and near-IR emission. Reported syntheses of NBD-derived amino acids include nucleophilic aromatic substitution of 4-chloro7-nitrobenzofurazan with 3-amino-

alanine,[82,83] copper-catalysed click-chemistry[84] and late-stage peptide labelling *via* manganese catalysis.[85] Similar approaches have been used to synthesise sulfur and selenium NBD analogues,[86,87] including a late-stage palladium arylation of cysteine residues which enabled real-time monitoring of peptide uptake and cellular trafficking.[88]

The Vendrell group systematically evaluated NBD-derived amino acids by variation of the atoms in positions 4 and 7, which directly contribute to the push-pull dipole of the fluorophore (Table **1**).[89] As well as evaluation of the optical properties, Vendrell and co-workers reported the chemical stability in conditions typically used in SPPS, which identified the cysteine analogues as generally less chemically stable than the DAPA derivatives. Analogue **54**, which contained a C-bridging group, had the longest emission wavelength but poor quantum yield resulted in weak emission and, instability in TFA or piperidine made it an unsuitable peptidic probe. Larger, heavier atoms such as sulfur and selenium are known to increase spin-orbit coupling (heavy atom effect), increasing the rate of intersystem crossing and decrease the quantum yield. However, except for oxygen bridged analogue **59** (Φ = 0.49), the NBD analogues exhibit relatively similar quantum yield values between 0.16 and 0.27. Longer emission wavelengths were observed for selenium bridged analogues **55** and **56** at ~600 nm, which also exhibited higher photostability than the more widely utilised oxygen analogue. The longer emission wavelengths of the selenium analogue were attributed to the involvement of d-orbital electrons in excitation and fluorescence processes.[90] To demonstrate an application of the near-IR fluorescent amino acid **55**, and exploit its weak emission observed in aqueous media, a lipid carboxamide analogue was synthesised and used for wash-free imaging of liposomes.

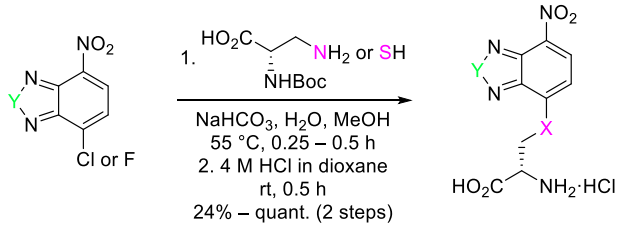

AA	X	Y	λabs (nm)	λ_{em} (nm)	QY	ε ($\times 10^3$ cm^{-1} M^{-1})
54	NH	CH_2	540	652	0.06	1.2
55	NH	Se	488	601	0.19	4.48
56	S	Se	485	600	0.16	6.89
57	NH	S	460	546	0.20	9.74
58	S	S	456	546	0.27	7.94
59	NH	O	472	545	0.49	9.72
60	S	O	468	550	0.25	11.4

Table 1: Synthesis and photophysical properties of NBD-derived amino acids.[89]

1.3.2 Fluorescent Analogues of L-Tryptophan

Another approach for the synthesis of fluorescent amino acids is the modification of naturally fluorescent proteinogenic amino acids to improve their photophysical properties. In this endeavour, there is often a balance between minimising structural modifications, so that the unnatural analogue can be readily substituted for the corresponding proteinogenic amino acid, and more extensive modification that confers stronger fluorescent properties, thereby enabling applications such as cell-imaging. Significant work in this area has focused on the modification of tryptophan, from minimal structural changes such as substitution of the indole ring or heteroatom engineering to more extensive modifications aimed at increasing π-conjugation.

4-Cyanotryptophan gained attention due to its increased quantum yield ($\Phi = 0.88$ compared to $\Phi_{Trp} = 0.12$) and emission in the blue visible region ($\lambda_{em} = 405$ nm). Its effectiveness as a minimally perturbing fluorescent probe has been utilised to report on the local environment of a peptide,[91,92] in FRET measurements of membrane and ligand binding events,[93,94] and in two-photon microscopy for visualising peptides.[95] Following an initial low yielding palladium catalysed cyanation of tryptophan,[96] there has been several attempts to improve the synthesis of 4-cyanotryptophan. Jo and co-workers reported the functionalisation of 4-cyanoindole **61**, however, the route involved a late-stage enzymatic kinetic resolution of a racemic mixture of the amino acid, reducing overall yield.[93] An asymmetric approach was reported by Smith and co-workers (Scheme **12**).[91] Facile access to 4-cyanoindole intermediate **62** was achieved in 4 steps in 64% yield. The indole was then subjected to phase-transfer asymmetric alkylation with glycine derived imine **63** and (−)-(*N*-(9-anthracenylmethyl)cinchonindinium **64** as the catalyst. This gave imine **65** in excellent enantioselectivity (>98%) and high yield (77%). Imine hydrolysis and subsequent deprotection under acidic conditions gave 4-cyanotryptophan **66** in 91% yield.

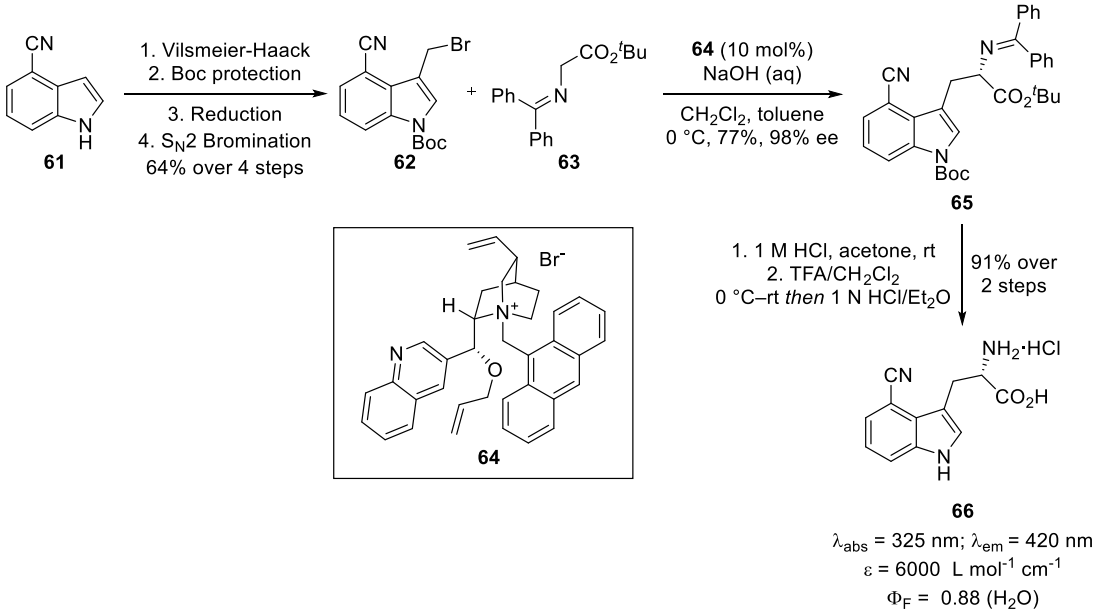

Scheme 12: Asymmetric synthesis of 4-cyanotryptophan.[91]

The structural similarities to the natural analogue has enabled several biosynthetic syntheses.[97,98] Biosynthesis often has the advantage of reduced synthetic steps and high enantioselectivity.[99] Arnold and co-workers utilised an engineered tryptophan synthetase from *Thermotoga maritima* (Tm9D8) to catalyse a nucleophilic substitution at the β-position of serine (Scheme **13**).[98] Despite a relatively long reaction time of 72 h and a moderate 49% yield, the avoidance of protecting group chemistry and a single step process make this an attractive approach.

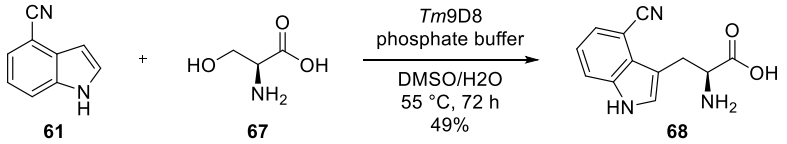

Scheme 13: Enzymatic synthesis of 4-cyanotryptophan.[98]

Tryptophan regioisosteres **69** and **70** reported by Harran and co-workers exhibited red-shifted absorption and emission from 279/365 nm to 352/434 and 342/447 nm, respectively (Scheme **14**).[100] Furthermore, under acidic environments (20% v/v TFA/DMSO) a distinct colour change from clear to purple/pink was observed with emission around 560 nm. Aza-tryptophans have also been explored as minimally modified fluorescent analogues of tryptophan, however, for 4- (**72**), 5- (**73**) and 6- (**74**) azatryptophan, the reported photophysical properties are based on the corresponding indole as opposed to the fluorescent amino acid itself.[101-105] The first

reported 7-azatryptophan **75** has been most extensively applied as a fluorescent probe.[106-111] However, increased quantum yield exhibited by the 6-azaindole as well as red-shifted absorption and emission of the 6-azatryptophan amino acid indicates future potential for this analogue. Similar to 4-cyanotryptophan, biosynthesis of aza-tryptophan analogues utilising an engineered tryptophan synthetase has been reported.[103]

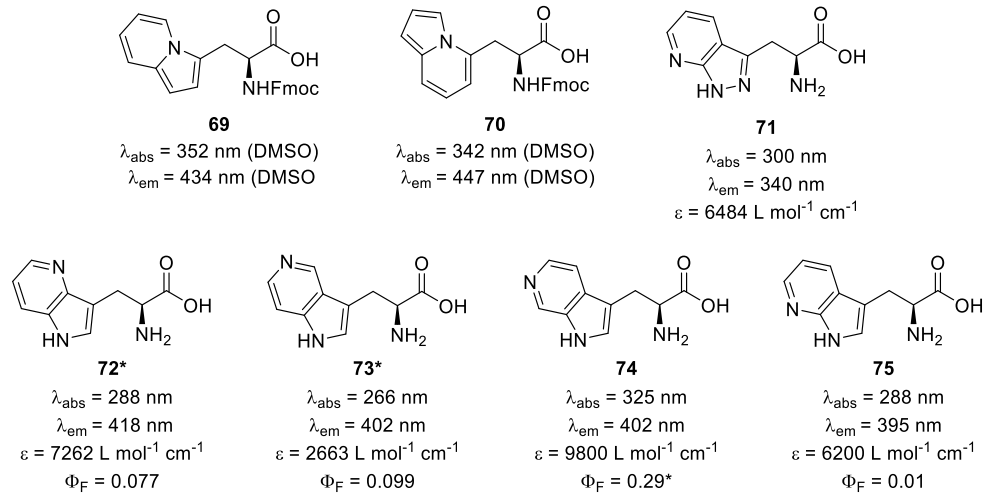

Scheme 14: Photophysical properties of minimally modified tryptophan analogues. *optical properties of the corresponding indole, not amino acid.

As well as point modifications such as carbon-nitrogen substitution and functionalisation of the indole ring, larger modifications to extend the conjugation of tryptophan has been widely explored. The Sutherland group reported carbazole-derived amino acids as rigid fluorescent analogues of tryptophan.[31] A Negishi cross-coupling reaction of β-iodoalanine **78** with various carbazoles, under conditions previously reported by Jackson and co-workers, provided access to a moderate library of carbazole tryptophan analogues in 42–68% yields (Scheme **15**).[31,112,113]

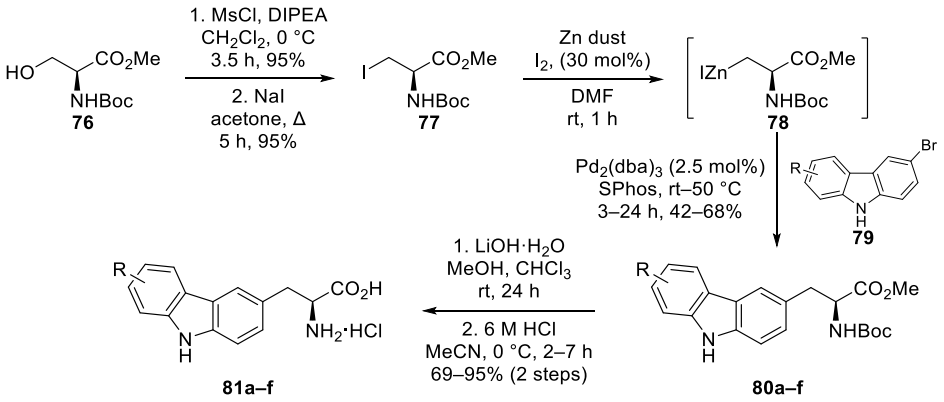

Scheme 15: Synthesis of carbazole analogues of tryptophan.[31]

The trifluoromethyl substituted carbazole analogue was subsequently substituted for an internal tryptophan of a beta hairpin peptide TrpZip1.[31] Circular dichroism (CD) characterisation revealed that the unnatural amino acid did not perturb the secondary structure of the peptide, demonstrating the carbazole to be a structural mimic of tryptophan. Additionally, cyano-substituted analogue **81a**, which exhibited the most red-shifted emission, was incorporated into a peptide ligand of a proline rich WW domain protein (Figure **3a**). The fluorescent amino acid enabled measurement of the peptide binding interaction that was consistent with literature (Figure **3b** and **3c**).

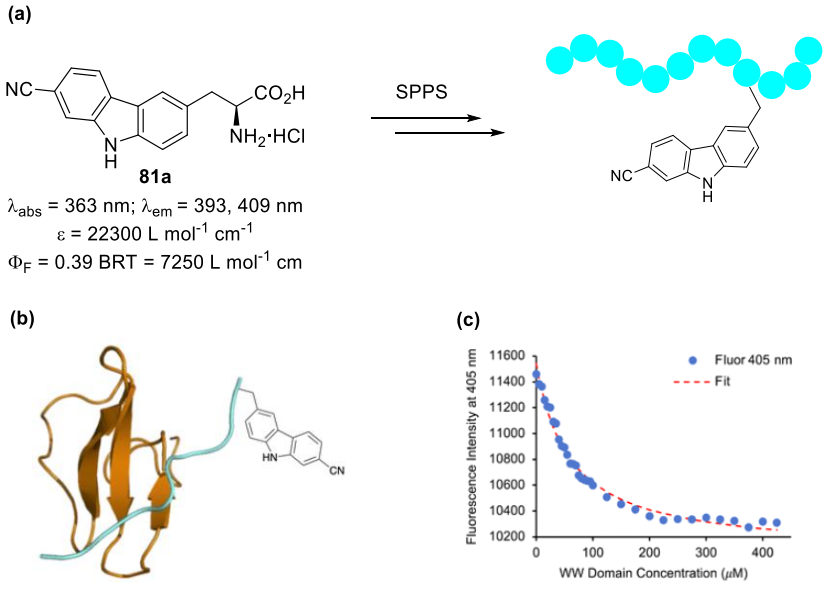

Figure 3: (a) Scheme showing incorporation of carbazole analogue 81a into dodeca-peptide ligand. (b) Schematic of peptide ligand interacting with WW domain peptide. (c) Fluorescence titration data of binding of modified peptide ligand 16 with WW domain.

The Sutherland group also reported a series of aryl-extended benzotriazole analogues.[114] L-3-Aminoalanine derivative **83** was accessed *via* Hofmann rearrangement of asparagine **82** and subsequent esterification (Scheme **16**). Nucleophilic aromatic substitution of **84** with 4-bromo-1-fluoro-2-nitrobenzene (**84**), followed by reduction of the nitro-group with tin dichloride gave the desired amine in good yields. Diazonium salt formation and subsequent cyclisation was achieved using a polymer-supported nitrite reagent and *p*-tosic acid in 66% yield. Bromide **87** was then subjected to Suzuki-Miyaura cross-coupling reactions with various aryl boronic acids to give the desired aryl-extended benzotriazole amino acids. Of this fluorescent amino acid library, methoxy analogue **89** exhibited strong fluorescence in the visible region. A bathochromic shift of the emission maxima with increasing solvent polarity from 372 nm (THF) to 417 nm (MeOH) and then further to 449 nm (PBS) was indicative of emission from a charge-transfer excited state.

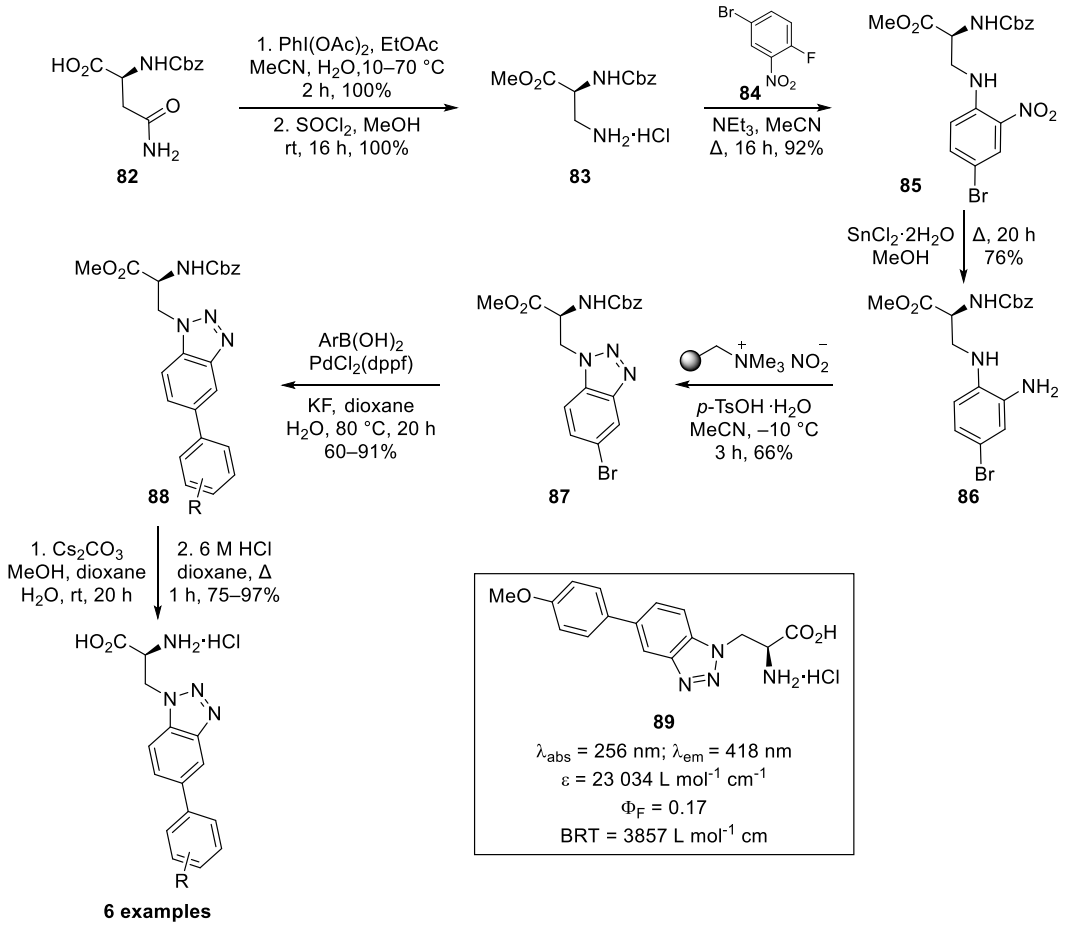

Scheme 16: Synthesis of biaryl benzotriazole analogues of tryptophan.[114]

Following on from this work, a series of alkyne-extended benzotriazole analogues were reported utilising the same general synthesis route but instead subjecting the

halogenated benzotriazole to a Sonogashira cross-coupling.[115] As well as analysis of the photophysical properties of the alkyne extended analogues, a chemo- and stereo-selective hydrogenation of the protected alkyne amino acid analogues utilising a palladium catalyst also enabled analysis of the corresponding alkene extended benzotriazoles (Scheme **17**). Both extended alkyne and alkene conjugation had the desired effect of red-shifting the absorption maxima to no-longer overlap with the proteinogenic amino acids, from 256 nm in the biaryl series to ~320 nm. Furthermore, rigid methoxy analogue **92** exhibited increased quantum yield and brightness.

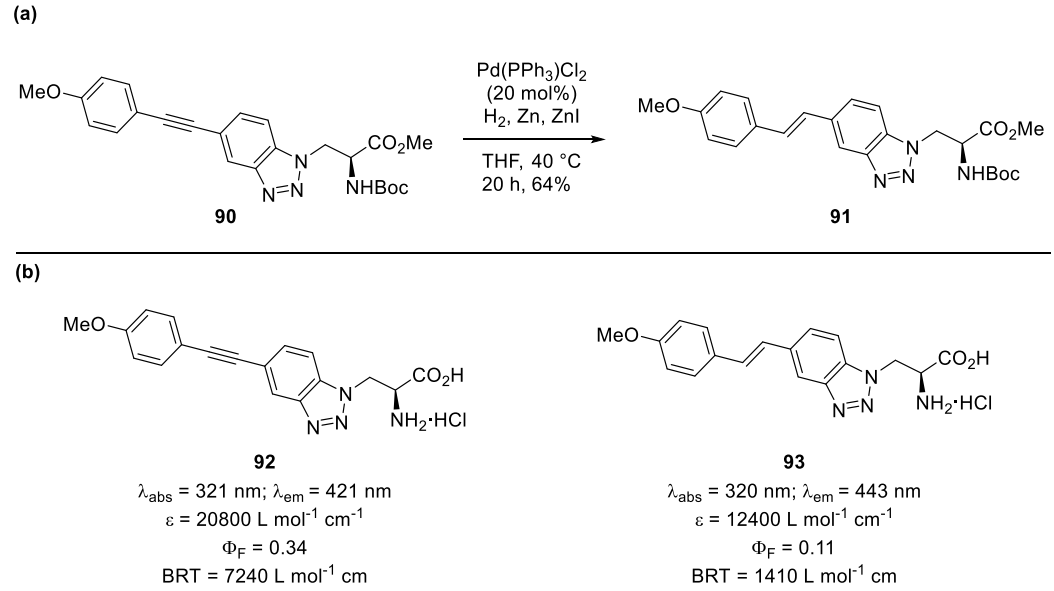

Scheme 17: (a) Selective hydrogenation of 90. (b) Photophysical properties of alkyne 92 and alkene 93 extended benzotriazole analogues.[115]

Further red-shifted absorption and emission was achieved by more extensive modification of the indole core (Scheme **18**).[116] Iron-catalysed C2-thioarylation of tryptophan analogue **94** was achieved by *in situ* formation of an iron-triflimide super Lewis acid catalyst (10 mol%) in conjunction with catalytic diphenyl selenide (10 mol%) to give **95** in 88% yield. An Ullmann-type reaction enabled cyclisation to form the [3,2-*a*]thioazoloindole ring at 110 °C in 81% yield. Bromination with *N*-bromo succinimide and catalytic HBr followed by Suzuki-Miyaura cross-coupling reactions utilising Buchwald XPhos Pd G2 catalyst, gave the extended analogues bearing electron withdrawing substituents **98** and **99**. The amino acids were deprotected prior to photophysical analysis, which, alongside red-shifted absorption, revealed a mega-stokes shift of 8112 cm^{-1} for acetyl analogue **100**. Additionally,

trifluoro analogue **101** exhibited strong brightness of 12000 cm^{-1} M^{-1}. Further photophysical analysis revealed these analogues to be amenable to two-photon absorption, enabling near-IR excitation.

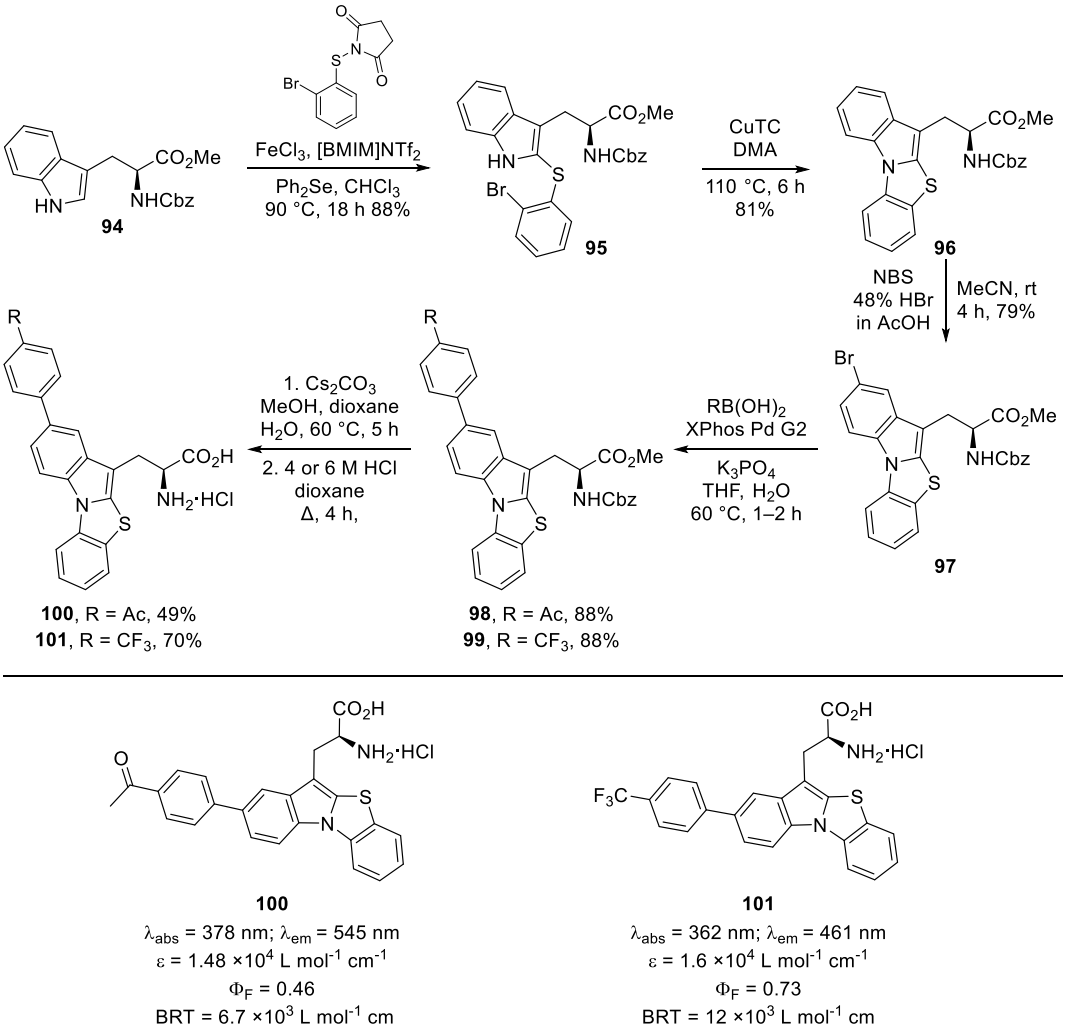

100
λ_{abs} = 378 nm; λ_{em} = 545 nm
ε = 1.48 ×10^4 L mol^{-1} cm^{-1}
Φ_F = 0.46
BRT = 6.7 ×10^3 L mol^{-1} cm

101
λ_{abs} = 362 nm; λ_{em} = 461 nm
ε = 1.6 ×10^4 L mol^{-1} cm^{-1}
Φ_F = 0.73
BRT = 12 ×10^3 L mol^{-1} cm

Scheme 18: Synthesis of thiazoloindole amino acid analogues of tryptophan.[116]

1.3.3 Fluorescent Analogues of L-Phenylalanine

Phenylalanine exhibits the weakest photophysical properties of the proteinogenic amino acids. This has resulted in fewer reports of phenylalanine modification for the synthesis of fluorescent amino acids. Despite this, there are key examples in which researchers have developed phenylalanine analogues with improved brightness and red-shifted absorption and emission.

The fluorescent properties of three cyano analogues of phenylalanine were described by Tucker and co-workers (Scheme **19**).[117] Each show an approximate four-fold increase in quantum yield and molar absorption compared to the native phenylalanine resulting in brightness closer to that of tyrosine and tryptophan. Moderate environmental sensitivity was observed as emission intensity increased in response to improved hydrogen bond donation ability of the solvent or increasing acidity.

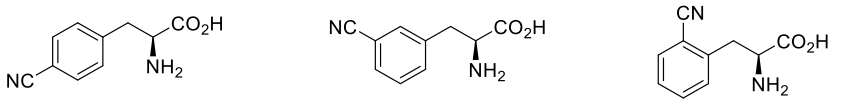

Scheme 19: Cyanophenylalanine analogues.

4-Cyanophenylalanine **102** has been most widely utilised as a chemical probe in which its sensitivity to its microenvironment (e.g. hydrogen bond donors) has enabled the study of small molecule binding to peptides,[118] peptide-membrane interactions,[119] including ion channels,[120] amyloid formation,[121,122] protein folding and hydration.[123] Furthermore, when situated near the N-terminus of a peptide, **102** displayed pH sensitivity resulting from quenching by the deprotonated N-terminus.[124] This feature was subsequently used to monitor the rate of membrane penetration into an acidic vesicle of a cell penetrating peptide.[125] The influence of local amino acids side chains to **102** has also been exploited in FRET measurements for studying protein folding, particularly through the use of naturally fluorescent amino acid tryptophan as a short-range fluorescence quencher (Förster distance 16 Å).[126-128]

The synthesis of 4-cyano-α-methyl-L-phenylalanine **108** was described by Stella and co-workers who used phase-transfer catalysis for the alkylation of **105**. Hydrolysis of the benzylidene **106** afforded **107** as a racemic mixture. Enzymatic resolution of the racemic amino acid was achieved using genetically modified *Ochrobactrum anrthopi* bacterium to give the D-amide as well as desired L-amino acid **108** in 34% yield, >98% ee.[119] 4-Cyano-α-methyl-L-phenylalanine **108** was subsequently utilised in analysis of peptide-membrane interactions. More recently, Kanjapur and co-workers reported the synthesis of 4-cyanophenylalanine *via* a three-step, one-pot, biocatalytic cascade from 4-cyanobenzaldehyde using a threonine transaldase (s-ObiH) followed by genetically modified phenylalanine dehydratase (*Rp*PSDH) and finally aminotransferase (TyrB) enzymes to give 4-cyanophenylalanine in >99% yield by HPLC and >99% ee.[129]

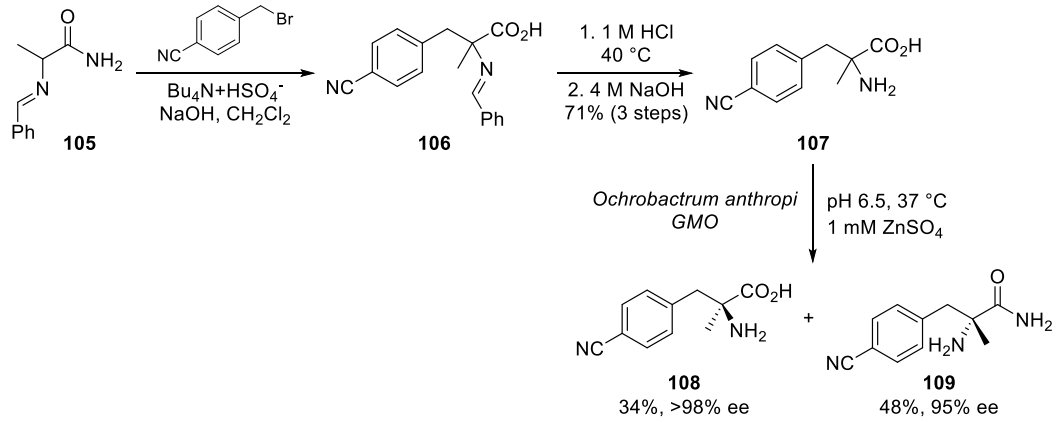

Scheme 20: Synthesis of 4-cyano-α-methyl-L-phenylalanine.[119]

Rigid, polyaromatic analogues of phenylalanine were synthesised by Frost and co-workers using rhodium catalysis (Scheme **21**).[130] *N,N*-Diprotected dehydroalanine starting materials were reacted with aryl boronic acids using $[Rh(COD)_2]BF_4$ and caesium fluoride to give naphthyl, phenanthrene, and pyrene substituted amino acids in good yields; however, they were isolated as racemic mixtures. The emission spectra exhibited fine vibrational structure commonly observed for rigid chromophores such as anthracene, with minimal variation observed between cyclohexane, acetonitrile and ethanol solvent systems. Pyrene analogue **112** exhibited the most promising fluorescent properties, with absorption between 236 and 343 nm, emission between 376 to 422 nm, a high molar absorptivity 3.52 ($\times 10^4$ M^{-1} cm^{-1}) and quantum a yield of 0.64.

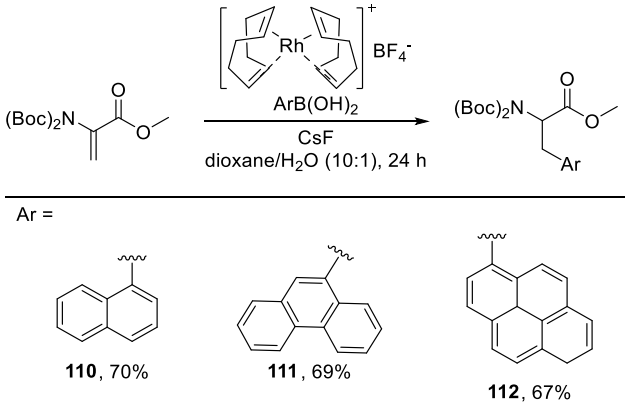

Scheme 21: Rhodium catalysed synthesis of rigid, polyaromatic phenylalanine analogues.[130]

Enantioselective synthesis of the pyrenyl amino acid was achieved by Hecht and co-workers (Scheme **22**).[131] The key step involved alkylation of the Belokon Ni(II) Schiff base complex **8** with 1-chloromethylpyrene **115** under basic conditions to give **116** in 78% yield. Hydrolysis of the alkylated complex gave pyrenyl amino acid **117** in a crude yield of 93%; however, the enantiomeric excess of **117** was not reported. Amino acid **117** was subsequently transposed onto a suppressor tRNA transcript and site specifically incorporated into two positions of a dihydrofolate reductase (DHFR) enzyme. Excimer formation (defined as an excited dimer in which the excited-state molecule associates with a ground-state molecule of the same type by intramolecular π–π stacking)[132, 133] between the two unnatural amino acids allowed for analysis of conformational changes upon enzyme-product binding. Similar polyaromatic structures have been used in the generation of fluorescent amino acids, however, the use of longer linkers precludes them from being classified as phenylalanine analogues.[134-136]

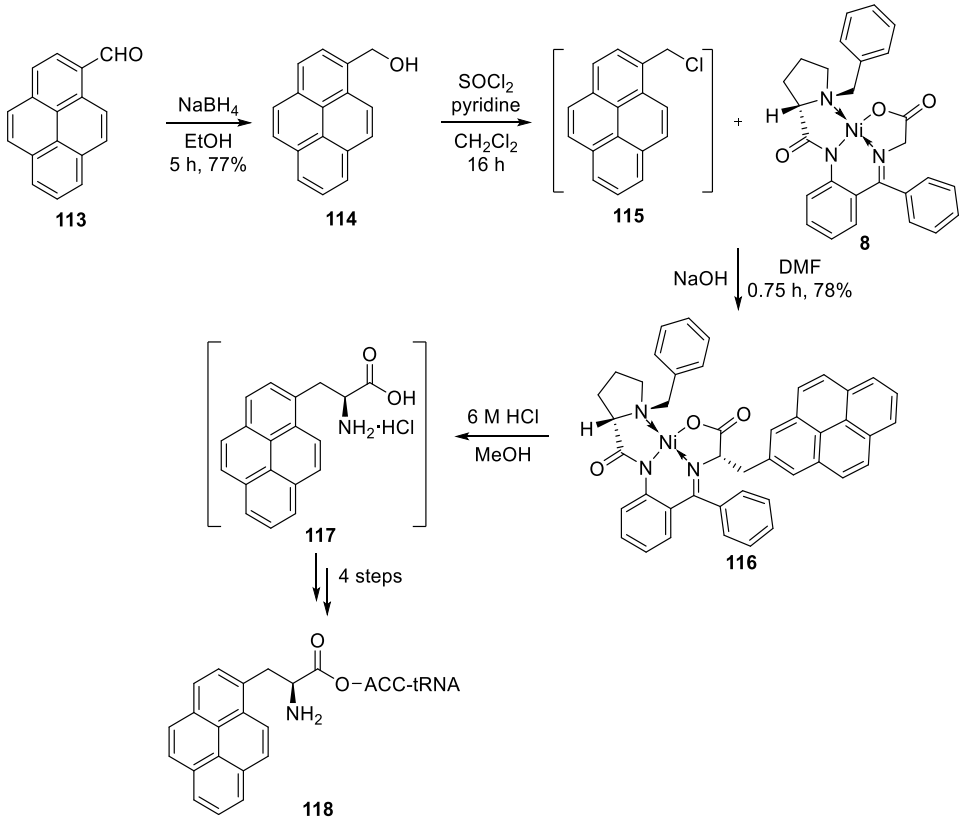

Scheme 22: Asymmetric synthesis of pyrenyl amino acid 118.[131]

Palladium catalysis has also been used to generate aryl and stilbene analogues of phenylalanine.[32,137-139] The Sutherland group previously reported the Heck-Matsuda cross-coupling of arenediazonium salts derived from phenylalanine gave various styrene analogues in 50–80% yield (Scheme **23**).[138] Whilst these analogues exhibited red-shifted absorption and emission relative to phenylalanine, they generally displayed weak emission resulting from the conformational flexibility of the alkene.

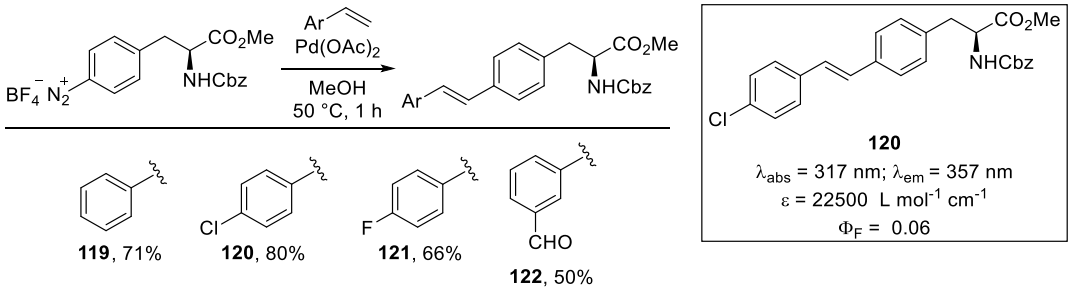

Scheme 23: Synthesis of styrene analogues of phenylalanine *via* palladium catalysed Heck-Matsuda cross-coupling reaction.[138]

Suzuki-Miyaura cross-coupling of a protected iodophenylalanine analogue and 9-phenanthracenylboronic acid provided access to polyaromatic phenylalanine

analogue **123**. The absorption and emission of phenylphenanthrene analogue **123** was dominated by the phenanthrene chromophore (Figure **4b**), exhibiting similar spectroscopic properties to analogues **111**, where the phenanthrene was directly attached to the amino acid backbone.[130,139] To demonstrate cell imaging applications Guo and co-workers subsequently incubated **123** with human HeLa cells at a concentration of 10 µM (Figure **4c**). Confocal microscopy revealed weak red fluorescent signals upon excitation at 405 nm; however, the absence of an absorption peak for phenanthrene amino acid **123** at this wavelength, together with its emission maximum at 400 nm, which would be expected to produce blue fluorescence, prompts reconsideration if the fluorescence observed in the human HeLa cells is originating from source other than amino acid **123**. Cell imaging has been more clearly demonstrated with fluorescent amino acids exhibiting absorption and emission wavelengths in the visible and near-IR region, highlighting the requirement for red-shifted fluorescent amino acids.[29]

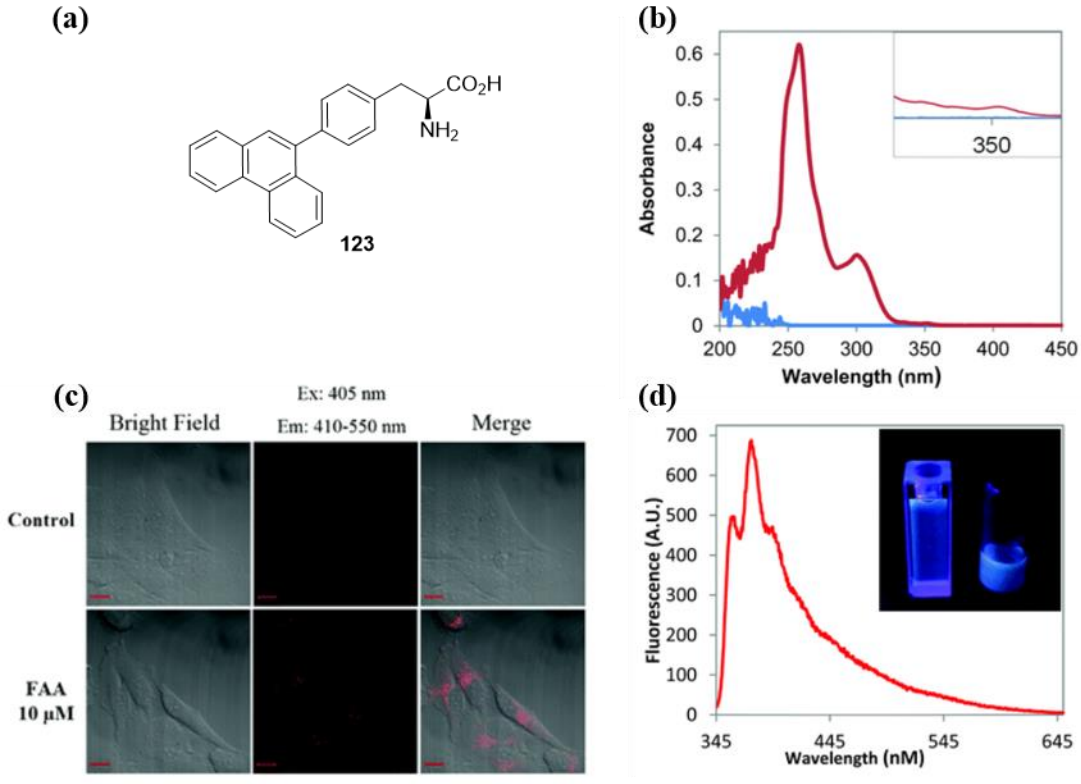

Figure 4: (a) Structure of phenanthrene analogue x. (b) Absorption spectra of 123 (10 µM, 1:1 DMSO: water). (c) Confocal microscopy images of human HeLa cells incubated with 10 µM 123. Scale bar 20 µm. (d) Emission spectra of 123 (20 µM, 1:1 MeCN: water). Reproduced from Ref. 139 with permission from the Royal Society of Chemistry.

Several terphenyl analogues were synthesised from an iodophenylalanine analogue in three steps (Scheme **24**).[32] Most promising photophysical properties were exhibited by linear analogue **124** (λ_{abs} = 283 nm; ε = 38250 L mol^{-1} cm^{-1}; λ_{em} = 344 nm; Φ = 0.73). Conformational flexibility around the biaryl bond allowed this analogue to be incorporated into folded regions of into dihydrofolate reductase (DHFR) from *E. coli*, without perturbing its catalytic function. Terphenyl analogue **124** was subsequently utilised as a FRET donor, paired with a L-(7-hydroxycoumarin-4-yl)ethylglycine acceptor, and utilised for monitoring conformation changes in DHFR upon inhibitor trimethoprim (TMP) binding.[140]

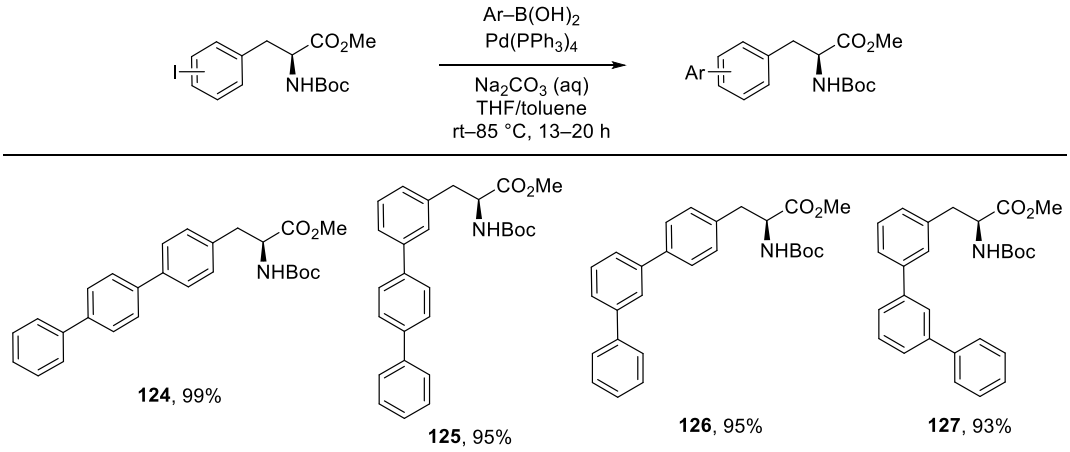

Scheme 24: Synthesis of terphenyl amino acids *via* Suzuki-Miyaura cross-coupling reaction.[32,140]

Instead of tuning the photophysical properties of phenylalanine, conjugation with a known chromophore can confer unique optical properties. Ackermann and co-workers described a palladium-catalysed C(sp^3)–H activation strategy for BODIPY fluorophore labelling of alanine residues, generating a series of BODIPY-derived phenylalanine analogues.[141] Although the methodology required both a triazole directing group and a phthalimide protecting group, resulting in a lengthy five-step deprotection, Ackerman reported high yields for the C(sp^3)–H activation across a variety of functionalised BODIPY chromophore substrates (Scheme **25**). The methodology was subsequently applied to a terminal peptide substrate for late-stage peptide labelling.

The BODIPY phenylalanine analogues exhibited red-shifted emission, with the *para*-methoxy analogue **130** showing the near-IR emission at 625 nm. BODIPY

analogue **130** also exhibited lipophilic sensitivity, as its fluorescence was quenched in aqueous solvents.[142] Following Ackerman's work, the Vendrell group demonstrated through computational studies that the BODIPY-derived phenylalanine derivatives could transition from an emissive planar conformation to a "butterfly-type" conformation in the excited state.[142] This butterfly-type conformation provided greater access to non-radiative decay pathways such as internal conversion. Consequently, the environmental sensitivity of these analogues was attributed to a relatively low energy barrier between the planar and butterfly conformations, with solvent interaction facilitating the crossing of this barrier.

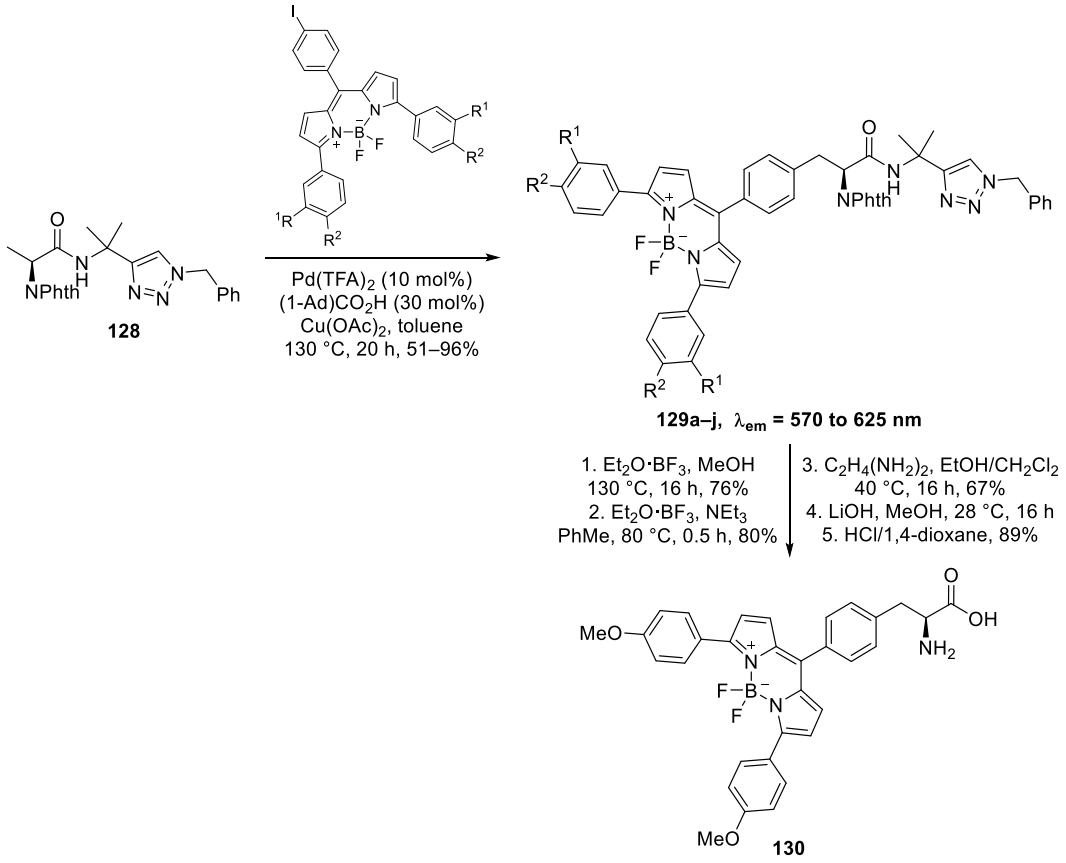

Scheme 25: Synthesis of BODIPY analogues of phenylalanine *via* C-H activation.[142]

1.3.4 Fluorescent Analogues of L-Tyrosine

Similar to phenylalanine, fluorescent analogues of tyrosine have remained relatively underexplored. Tyrosine possess an inherent environmental sensitivity arising from hydrogen bonding or deprotonation of the phenolic hydroxyl group.[15] The sensitivity has been modulated by incorporation of electron withdrawing groups; for example, the reduced pka values of 3-fluoro- or 3-nitrotyrosine resulted in longer wavelength absorption and emission and altered pH-sensitivity.[143,144] Poor emission from 3-nitrotyrosine has resulted in its application as a fluorescence quencher in the analysis of protein structure and protein-protein interactions.[145,146]

Verma and Singh reported 2-(2′-hydroxyphenyl)benzothiazole (HBT) analogues of tyrosine **132** and **133**.[147] Following synthesis of 3-formyltyrosine **131** by a Reimer-Tiemann reaction as described by Bane and co-workers,[148] Verma and Singh formed the fluorescent appendage by condensation of **131** with 2-aminophenothiol in 82% yield. Interestingly, the Fmoc-protected analogue **133**, showed the most useful fluorescent properties. By increasing the proportions of water in chloroform to induce aggregation of **133**, they demonstrated the formation of J-aggregates (or head-to-tail aggregates), which displayed increased fluorescence. In chloroform, emission is observed from the enol tautomer at 390 nm. Comparably, in 1:99 chloroform: water, the formation of J-aggregates, combined with excited state intramolecular proton transfer (ESIPT)- induced phototautomerisation to the keto-form, resulted in a pronounced red-shift and enhanced emission intensity at 525 nm. It was suggested that this was observed for **133**, but not **132**, due to π-stacking of the Fmoc protecting group, which further stabilised the aggregated state. In order to further demonstrate the strong fluorescent properties, Fmoc-analogue **133** was subsequently utilised in visualising latent fingerprints. **133** was shown to adhere to fingerprint residue on various surfaces and facilitated the high level characterisation that is required for forensic identification.

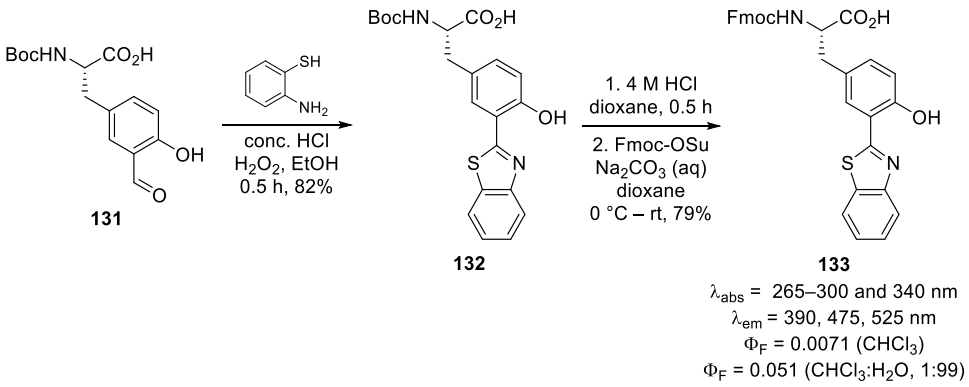

Scheme 26: Synthesis of benzothiazole functionalised tyrosine.[147]

A more systematic approach was taken by Wang and co-workers, who reported a library of *mono*- and *bis*-styryl tyrosine analogues *via* a palladium catalysed Heck cross-coupling reaction of 3-iodotyrosine (Scheme **27**).[149] Generally, the *mono*-styryl analogues emitted at shorter wavelengths (400–440 nm) than the *bis*-styryl analogues, for which the more extensive conjugation resulted in broad emission which covered the visible to near-IR region (400–800 nm). *Bis*-styryl analogues bearing an electron- donating methoxy substituent (**134**) exhibited strong emission at 420 nm with high quantum yield (0.94). Subsequently, **134** was incorporated into a Bax-inhibiting peptide and employed in cell imaging by laser scanning confocal microscopy.

Generation of a push-pull system resulted in near-IR emission at 630 nm for pyridine analogue **135**.[149] As anticipated, the tyrosine analogues displayed environmental sensitivity associated with deprotonation of the hydroxyl group. In particular, pyridine analogue **135** exhibited distinct blue-green-red colour changes resulting from deprotonation of the oxygen under basic conditions and protonation of the nitrogen under acidic conditions, both of which resulted in charge-transfer across the fluorophore.

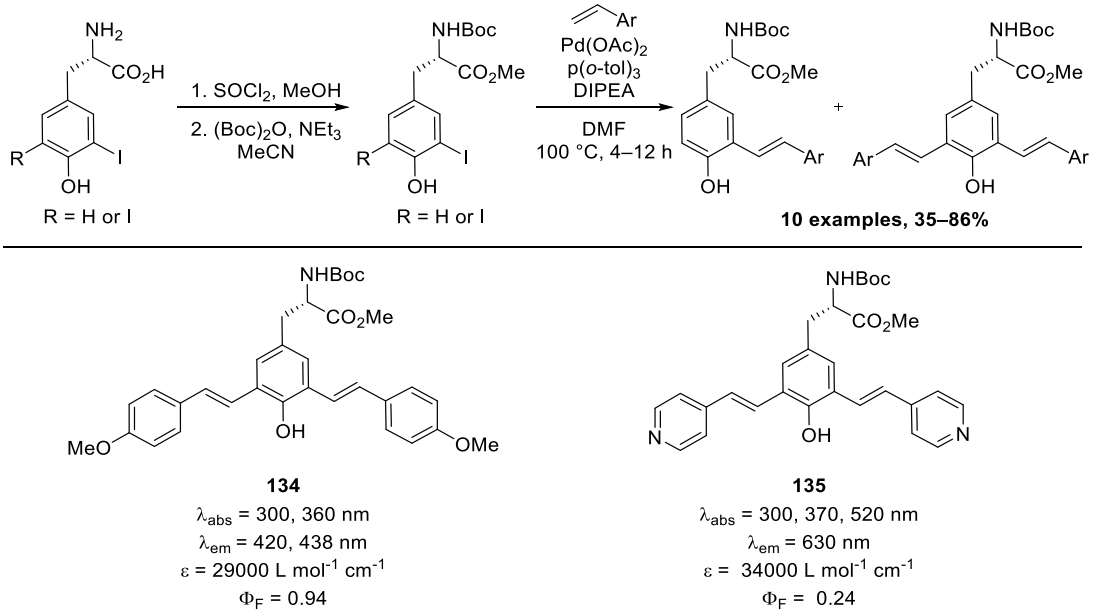

Scheme 27: Heck cross-coupling reaction of tyrosine.[149]

An alternative approach to C–C bond forming strategies for functionalisation of the aryl ring of tyrosine is substitution of the phenolic group. Ferriera and co-workers reported several fluorescent *O*-aryltyrosines analogues (Scheme **28**).[150] C–O bond formation was achieved *via* a copper-catalysed Ullmann-Goldberg type reaction using a bidentate *N*,*N*′-dimethylethylenediamine (DMEDA) ligand and caesium carbonate as the base in toluene to give **136** and **137** in 34 and 35% yields, respectively.

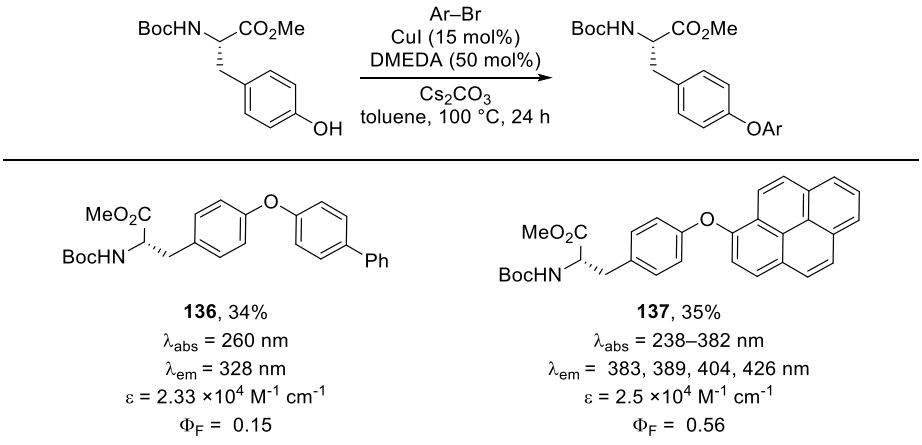

Scheme 28: Ullman-type reaction for tyrosine functionalisation.[150]

Tetrazine-functionalised tyrosine analogue **141** was synthesis by an S_NAr reaction of tyrosine with 3-bromo-6-methyl-1,2,4,5-tetrazine in 84% yield by Riera and co-

workers (Scheme **29**).[151] As well as being significantly red-shifted for a small molecule fluorophore (λ_{abs} = 531 nm; λ_{em} = 587 nm), the tetrazine moiety was demonstrated to serve as a handle for bioconjugation *via* inverse electron-demand Diels-Alder cycloaddition.

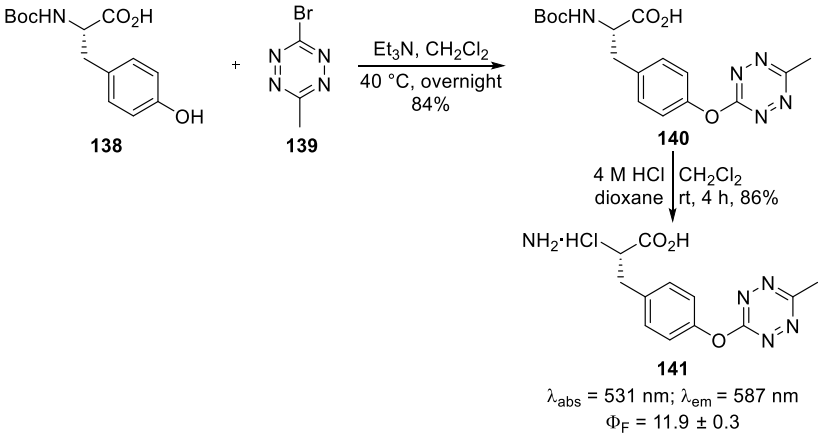

Scheme 29: Synthesis of tetrazine analogue of tyrosine 141.[151]

1.3 Summary and Thesis Outline

Fluorescence spectroscopy provides a powerful tool for elucidating complex biological processes. Compared to labelling with large, extrinsic fluorophores such as GFP, fluorescent amino acids are low-molecular-weight fluorophores that allow straightforward, selective incorporation into peptides.[11-14] Their photophysical properties can be tailored to red-shift the absorption or emission wavelengths, enhance quantum yield and brightness, or impart environmental sensitivity. In the development of fluorescent amino acids, researchers have employed strategies such as the attachment of known chromophores to the amino acid side chain, or structural modification of the proteinogenic amino acids tryptophan, tyrosine and phenylalanine. Fluorescent amino acids have consequently found broad application as peptidic probes for real-time cellular imaging and for investigating dynamic process like conformational changes and protein binding, through the application of techniques such as FRET.

Despite several classes of fluorescent amino acids being reported, there remains a desire to expand the available library. Since the tolerance for incorporating an amino acid into a protein at a given site depends on the resulting physicochemical properties,[68] access to a diverse set of fluorescent amino acids with varied photophysical and physicochemical characteristics is essential. Furthermore, there is a continued drive to discover amino acids that combine compact size with strong red fluorescence, using synthetically scalable and cost-effective methodologies.

The focus of this PhD is the development of novel fluorescent analogues of tyrosine and phenylalanine, an area which has been relatively underexplored. The first aim of this PhD is the synthesis of rigid dibenzofuran analogues of tyrosine, which complement the previous carbazole amino acid series reported by the Sutherland group (Section 2.1).[31] Following this, a key aim of this PhD was to develop one-pot methodologies for the rapid synthesis of biaryl and arylalkynyl analogues of phenylalanine (Section 2.2 and 2.3). As well as one-pot methodologies, alternative approaches that enable late-stage incorporation of fluorescent amino acids were explored (Section 2.3). Finally, the synthesis of arylalkyl analogues of tyrosine were investigated (Section 2.4).

2.0 Results and Discussion

2.1 Synthesis of Dibenzofuran Analogues of Tyrosine

2.1.1 Previous Work in the Sutherland Group

Previously in the Sutherland group, a series of biaryl tyrosine analogues were synthesised in five steps starting from a commercially available protected tyrosine starting material (Scheme **30**).[152] The key step involved a mild Suzuki-Miyaura cross-coupling reaction utilising the Buchwald pre-catalyst XPhos Pd G3 to access seven fluorescent amino acid analogues.

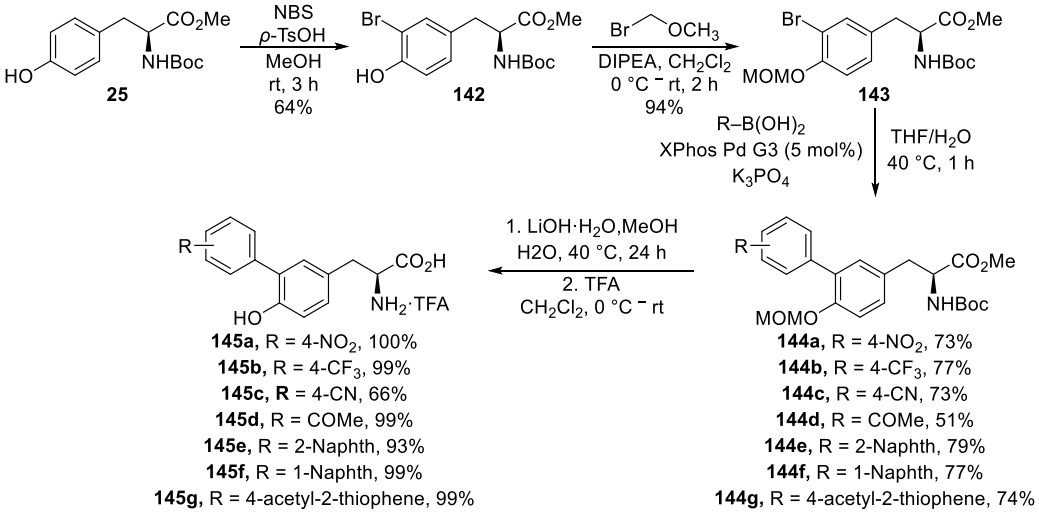

Scheme 30: Synthesis of biaryl analogues of tyrosine.

Photophysical analysis of the deprotected biaryl analogues revealed moderate red-shifting of the absorption and emission. For example, the 4-acetyl-2-thiophene analogue (**145g**) had an absorption and emission maximum of 350 nm and 448 nm respectively. However, low quantum yields gave brightness values below 1500 cm^{-1} M^{-1} across the series. Considering that conformationally rigid structures are known to show improved fluorescent properties as a result of more efficient π-overlap and reduced deactivation of the excited state by internal conversion,[26-28,31,153] cyclisation to give the dibenzofuran analogues was investigated. Cyclisation was achieved using

a palladium(II)-catalysed intramolecular C–H bond activation and C–O bond formation (Scheme **31**).[154]

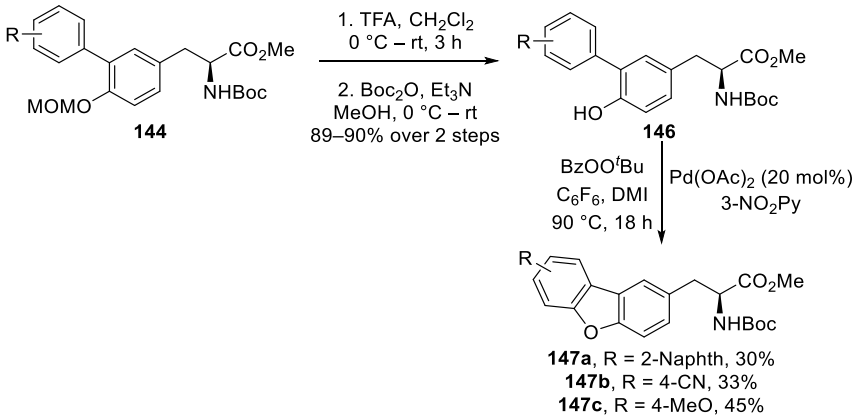

Scheme 31: Synthesis of dibenzofuran α-amino acids *via* the cyclisation of biaryl tyrosine analogues.

The dibenzofuran *α*-amino acids demonstrated promising fluorescent properties (Table **2**). Compared to the 2-naphthalene biaryl analogue, cyclisation afforded a ten-fold increase in brightness as well as red-shifted absorption and emission.

Amino Acid	λ_{Abs} (nm)	λ_{Em} (nm)	ε (cm^{-1} M^{-1})	Stokes Shift (nm)	Φ_F	Brightness (cm^{-1} M^{-1})
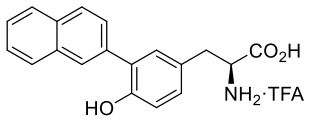 **145e**	286	358	10600	72	0.15	1120
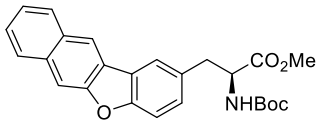 **147a**	320	**353**, 370	78000	33, 50	0.16	12100
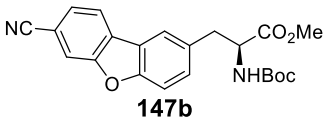 **147b**	295	353	21600	58	0.49	10600
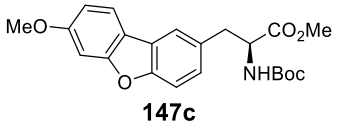 **147c**	306	323	23100	17	0.62	14300

Table 2: Photophysical properties of biaryl tyrosine analogue 145e and dibenzofuran amino acids 147a–c.

Due to the lengthy synthesis route involving multiple protection and deprotection steps, and the low yielding cyclisation step, a new synthesis plan was proposed in order to access other targets. Retrosynthetic analysis of the dibenzofuran amino acid analogue proposed Negishi cross-coupling of a brominated dibenzofuran and an organozinc reagent (Scheme **32**). This approach was inspired by Jackson and co-workers who have previously described the synthesis of phenylalanine analogues utilising an organozinc reagent derived from serine as the alanine β-anion synthetic equivalent.[112,113,155] Negishi cross-coupling of the β-alanine anion reagent was also previously successful in the synthesis of carbazole-derived α-amino acids by the Sutherland group. The carbazole α-amino acids were subsequently shown to be strongly fluorescent tryptophan mimics and used to measure protein binding interactions between a protein ligand and WW domain protein.[31]

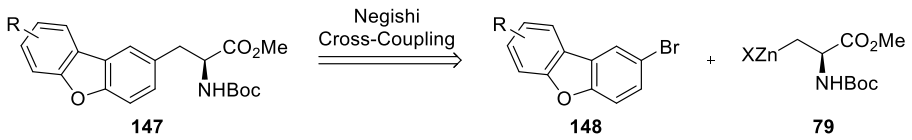

147 148 79

Scheme 32: Retrosynthesis of dibenzofuran amino acids.

2.1.2 Results and discussion

In order to synthesise the organozinc reagent **78** required for Negishi cross-coupling, a protected serine derivative was first mesylated followed by iodination under standard conditions to give **77** in a 67% yield over two steps (Scheme **33**). This was followed by a one-pot procedure involving in-situ generation of the organozinc reagent with iodine-activated zinc dust, followed by Negishi cross-coupling using tris(dibenzylideneacetone)dipalladium(0) and an SPhos ligand (2:1 ligand:palladium molar ratio) to give the dibenzofuran α-amino acids **147a**, **147e** and **147d** in 44–66% yields. Negishi cross-coupling afforded the 2-naphthalene analogue **147a** in 44% yield, a significant improvement over the 30% yield afforded from the cyclisation method previously described. The reaction conditions developed by Jackson and co-workers demonstrated that use of sterically bulky, electron rich ligands such as SPhos improved the yield of the Negishi cross-coupling reaction significantly.[10] Notably the use of SPhos, compared to their previous method employing P(o-tol)$_3$ as the

phosphine ligand,[112,113] greatly improved both the robustness of the reaction and the yield for *ortho*-substituted aryl halide coupling partners. The greater reactivity when utilising SPhos was attributed to the formation of the more reactive monoligated palladium species, as reported by Buchwald and co-workers.[156,157] Considering the relative instability of the serine-derived organozinc reagent, which is prone to decomposition by protonation and elimination,[158] a highly reactive palladium species is necessary. This is particularly important when the organozinc reagent is not present in excess, as is required in the one-pot, two-step synthesis of the dibenzofuran *α*-amino acids. Overall, this route demonstrates a simpler and more successful synthesis of the dibenzofuran amino acid analogues.

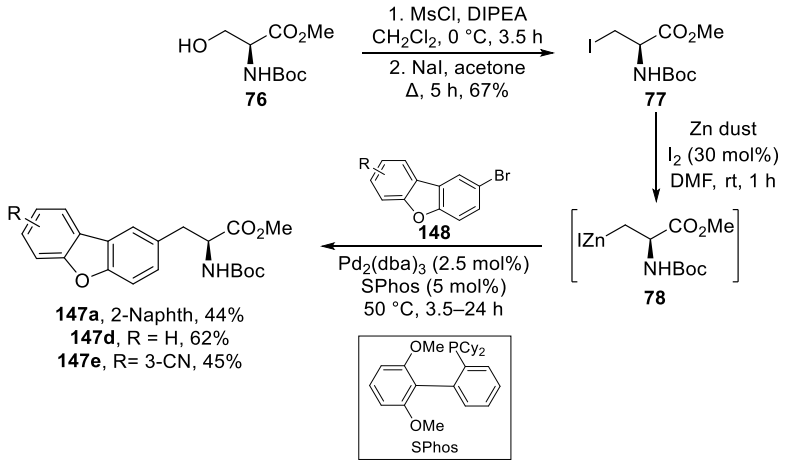

Scheme 33: Synthesis of dibenzofuran α-amino acids *via* Negishi cross-coupling.

The photophysical properties of the new analogues **147d** and **147e** were subsequently analysed (Figure **5**, Table **3**). As was previously seen, the dibenzofuran analogues both showed improved photophysical properties compared to the natural tyrosine and the biaryl tyrosine analogues previously synthesised. The unsubstituted analogue **147d** had a high quantum yield (0.60) and brightness (9840 cm^{-1} M^{-1}) for a relatively simple fluorescent amino acid. However, compared to the dibenzofuran *α*-amino acids previously synthesised (Table **2**), **147d** and **147e** possess lower brightness values.

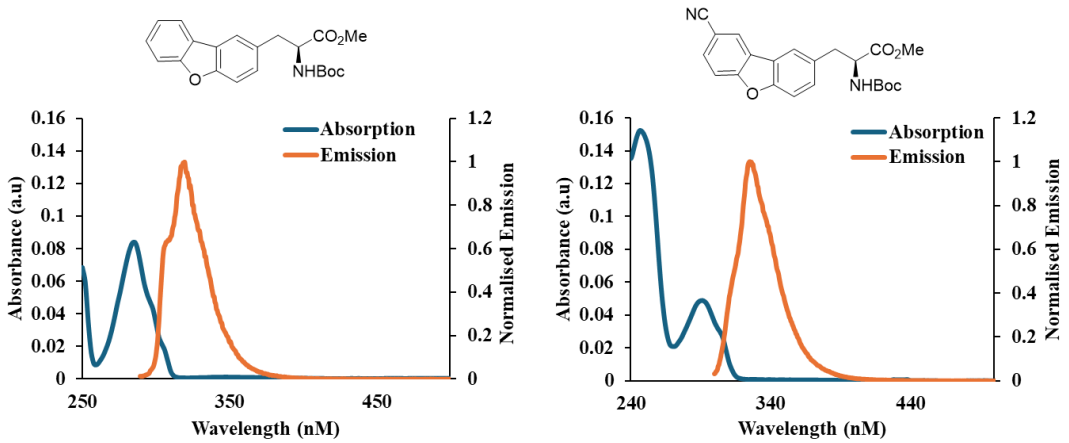

Figure 5: Absorption and normalised emission of dibenzofuran analogues 147d and 147e (5 µM in MeOH).

Amino Acid	λ_{Abs} (nm)	ε (cm^{-1} M^{-1})	λ_{Em} (nm)	S.S. (nm)	Φ_F	BRT (cm^{-1} M^{-1})
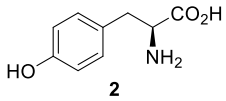 **2**	275	310	1410	35	0.14	197
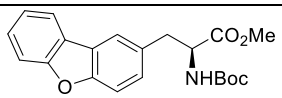 **147d**	286	319	15800	33	0.60	9480
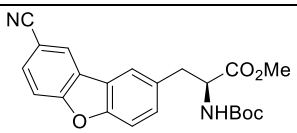 **147e**	290	325	10200	35	0.40	4110

Table 3: Photophysical properties of tyrosine and dibenzofuran α-amino acids 147d and 147e. Comparison of absorption (λ_{Abs}) and emission (λ_{Em}) maximum, molar absorption coefficient (ε), stokes shift (S.S.), quantum yield Φ_F and brightness (BRT) in methanol.

Methoxy analogue **147c** was subsequently selected as a lead owing to its high brightness (14300 cm^{-1} M^{-1}). Inspired by work published by Poreba and co-workers who developed a highly sensitive novel FRET (Förster resonance energy transfer) pair for studying protease kinetics, it was considered that **147c** could be utilised as a FRET donor.[159] Poreba and co-workers synthesised several short peptides (8–9 amino acid residues) which were *N*-terminally labelled with a 7-amino-4-carbamoylmethylcoumarin (ACC) fluorophore and contained fluorescence quencher 2,4-dinitrophenyl-lysine (Lys(DNP)) at either P2' or P3'. The peptide substrates

were then utilised in kinetic measurements for five commonly used protease enzymes. Internally quenched fluorescent (IQF) peptides, a specific FRET pair in which the acceptor molecule acts as a fluorescence quencher, are highly useful for analysis of post-translational modifications, informing on both catalytic activity and site specificity.[160] Whilst there are several utilised fluorophore/quencher IQF/FRET pairs, fluorescent amino acids offer simpler incorporation and do not require incorporation of a linker. Furthermore, they can offer a better balance of hydrophobicity and solubility owing to their small size. Several fluorescent amino acid FRET pairs have been reported for studying conformational changes in proteins including tryptophan/4-cyanotryptophan,[94] and 4-biphenyl-L-phenylalanine/L-(7-hydroxycoumarin-4-yl)ethylglycine.[32] Shin and co-workers used a FRET system consisting of a Bax protein containing fluorescent amino acid ANAP (6-acetyl(naphthalen-2-ylamino)-2-aminopropanoic acid) and a fluorescent fusion protein Hsp70-YFP to investigate disruption of the protein-protein interactions in response to several organelle-targeting substances in a time-dependent cellular assay.[79] In an analogous application, the well-studied fluorescent amino acid ACD (acridon-2-ylalanine) was quenched by a thioamide amino acid residue *via* PET (photoinduced electron transfer) in a distance dependent manner also enabling the evaluation of conformational changes in proteins.[65] It was considered that methoxy analogue **147c** could be applied as a FRET donor as it had considerable overlap with the Lys(DNP) quencher (Figure **6**). From the spectral overlap, $J(\lambda)$, the Förster distance (R_0) was calculated to be 34.2 Å, which is comparable to other commonly used FRET pairs.[159] R_0 describes the distance at which the efficiency of the energy transfer is 50%, thus informing on the spatial proximity between the donor and the acceptor.[17]

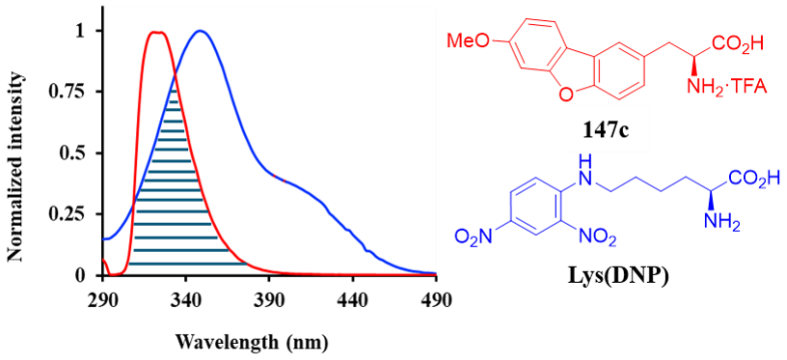

Figure 6: Spectroscopic overlap of *α*-amino acid 147c emission (red) and Lys(DNP) absorption (blue).

Following identification of α-amino acid **147c** as a promising FRET donor, **147c** was incorporated into a peptide containing the 2,4-dinitrophenyllysine quencher by Dr Liyao Zeng. This was achieved by first synthesising the nonapeptide **149** using standard SPPS methodology, followed by manual coupling of the unnatural amino acid using PyBOP (Scheme **34**). Decapeptide **150** was subsequently deprotected and cleaved from the resin using morpholine, followed by treatment with a TFA cocktail, and purified by reverse-phase HPLC.

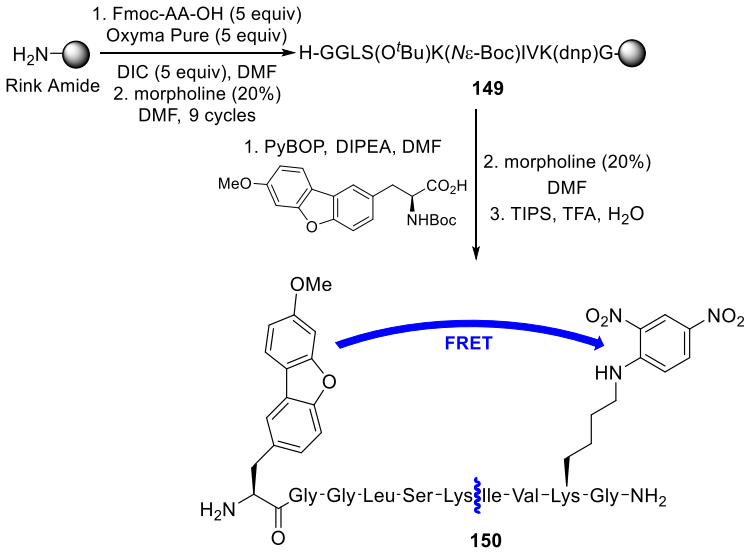

Scheme 34: Synthesis of peptide for proteolysis containing amino acid 147c and Lys(DNP). Synthesis performed by Dr Liyao Zeng.

Emission from α-amino acid **147c** was almost completely suppressed when incorporated into the peptide, exhibiting only 3% of the emission intensity of the free α-amino acid. The peptide was subsequently cleaved using trypsin, a commonly used serine protease,[161] and the emission was monitored over time (Figure **7**). The increase in emission intensity over time demonstrates the utility of α-amino acid **147c** as a novel FRET donor for monitoring trypsin-mediated hydrolytic cleavage.

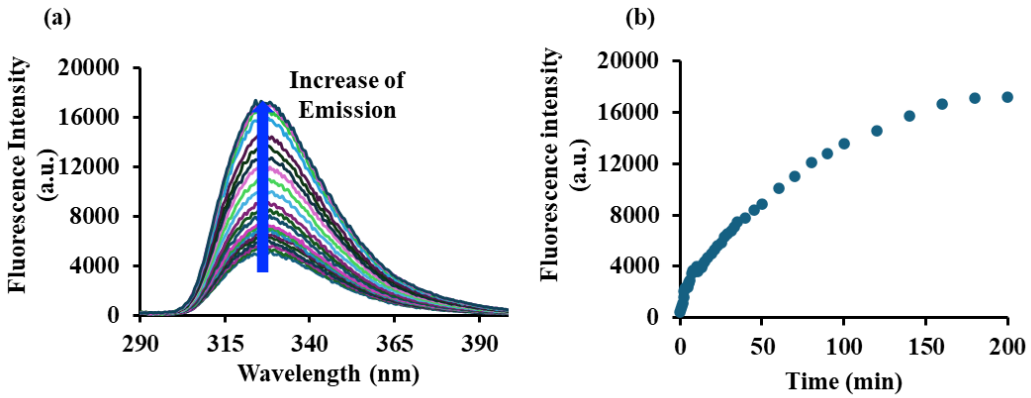

Figure 7: Enzyme hydrolysis of peptide 150 (10 µM) using trypsin (0.02 µM) in 3-morpholinopropanesulfonic acid (MOPS) buffer (20 mM) at pH 7.0. (a) Increase in emission over time during trypsin digestion of peptide 150. (b) Emission versus time during trypsin digestion of peptide 150. Experiment performed by Dr Liyao Zeng.

2.1.3 Conclusions and Future Work

In conclusion, the synthesis of dibenzofuran-derived tyrosine analogues was optimised to a four-step route incorporating a Negishi cross-coupling reaction. Two additional analogues were prepared: an unsubstituted derivative and an 8-cyano-substituted analogue. These compounds exhibited enhanced photophysical properties relative to both native tyrosine and the previously reported library of biaryl tyrosine analogues, although their brightness remained lower than that of the 7-methoxydibenzofuran analogue. Notably, the 7-methoxydibenzofuran analogue was subsequently demonstrated to function as an effective FRET donor in an assay for monitoring serine protease kinetic activity.

Having developed carbazole- and dibenzofuran-derived amino acid libraries, an analogous dibenzothiophene series is proposed. Whilst dibenzothiophene has a lower reported quantum yield than dibenzofuran (0.03 and 0.29, respectively),[162] substitution with heavier chalcogens has been shown to red-shift the absorption and emission spectra in rhodamine and [1,3]-dioxolo[4,5-*f*]benzodioxole (DBD) dyes.[163-165] It is envisaged that the reduced quantum yield could be mitigated by appropriate substitution of the dibenzothiophene core, yielding a novel series of fluorescent amino acids with improved photophysical properties. Retrosynthetic analysis of the

dibenzothiophene α-amino acids is presented in Scheme **35**, utilising a similar Negishi cross-coupling approach to that used previously in the synthesis of carbazole- and dibenzofuran-derived α-amino acids. The key cyclisation step will be achieved using a mild, nucleophilic intramolecular cyclisation of methylated diazonium salts reported by Lee and co-workers (Scheme **36**).[166] Overall, this project will aim to make a small library of dibenzothiophene α-amino acids from commercially available bromoanilines and investigate their photophysical properties.

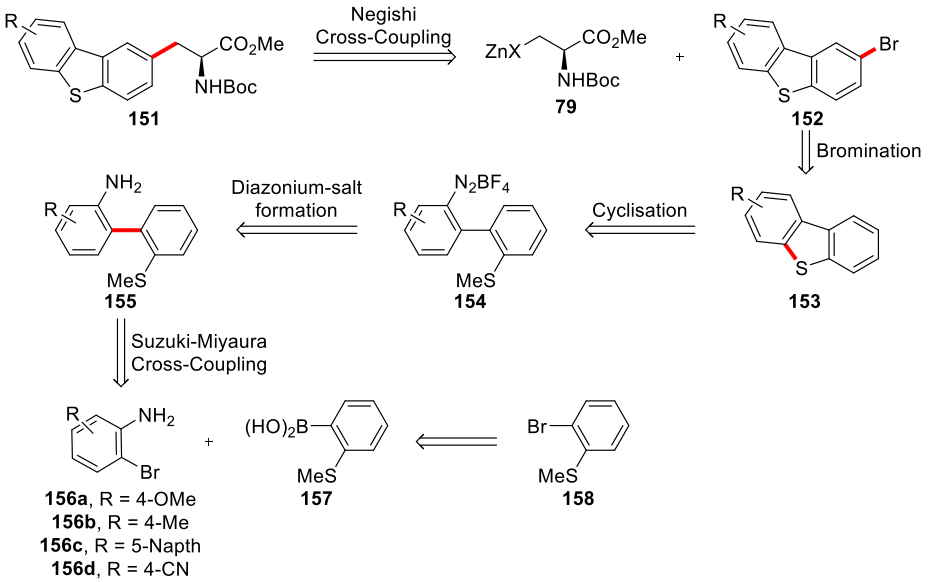

Scheme 35: Retrosynthesis of dibenzothiophene amino acids.

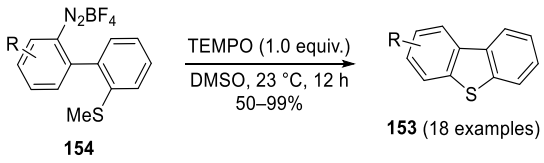

Scheme 36: Mild, catalyst free synthesis of substituted dibenzothiophenes.[166]

2.2 One-pot Synthesis of Biaryl Analogues of Phenylalanine

2.2.1 Previous work in the Sutherland Group

A recent focus in the Sutherland group has been the development of one-pot methods for the synthesis of fluorescent amino acids.[138,152,167] In addition to enabling rapid access to diverse fluorescent amino acid libraries, the operational simplicity and efficiency of one-pot protocols further increase their appeal. In this work, biaryl analogues of phenylalanine were synthesised *via* a one-pot method in which a commercially available tyrosine derivative was first activated by installation of a nonaflate leaving group, followed by a palladium-catalysed cross-coupling reaction. Akai and co-workers have previously reported palladium-catalysed cross-coupling of nonaflates from simple phenols, highlighting the benefits of aryl nonaflates which show higher reactivity and are more amenable to synthesis than the corresponding aryl triflates.[168] Optimisation of the one-pot cross-coupling of tyrosine to give **159a** found that addition of water as a cosolvent significantly improved the yield from 46% to 66%. Water is known to react with the base generating hydroxide ions, which facilitate transmetallation and reductive elimination.[169] Furthermore, batch addition of the Buchwald pre-catalyst XPhos Pd G2 (3 × 1 mol%) further increased the yield to 91%. Following optimisation, an initial library of biaryl amino acids were synthesised by Dr Rochelle McGrory and Dr Sineenard Songsri (Scheme **37**).

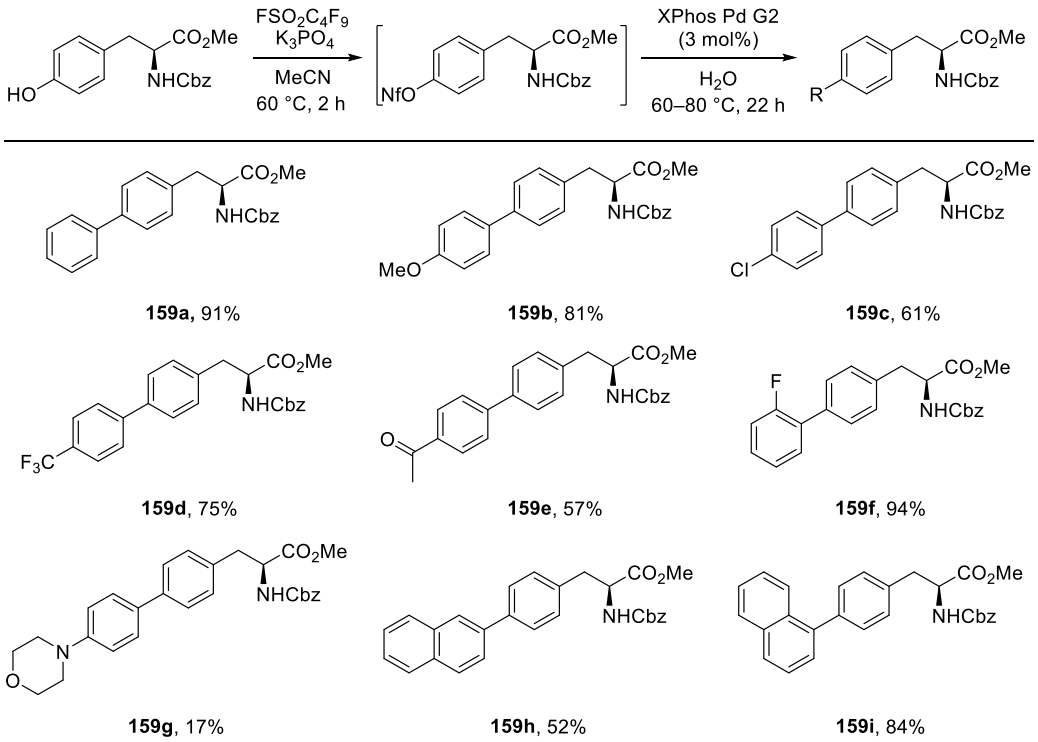

Scheme 37: Biaryl phenylalanine analogues previously synthesised in the Sutherland Group.

The biaryl amino acids were subsequently deprotected *via* methyl ester hydrolysis with caesium carbonate followed by removal of the Cbz group with 6 M hydrochloric acid (Scheme **38**). After deprotection, the photoluminescent properties were analysed. The biaryl analogues all showed increased brightness from the native phenylalanine (5 cm^{-1} M^{-1}). In particular, promising fluorescent properties were observed for the electron-donating 4-methoxybiphenyl α-amino acid **160b**, with relatively high quantum yield (0.24) and brightness (3430 cm^{-1} M^{-1}). The highly conjugated naphthyl derivatives **160g** and **160h** also showed improved properties including red shifted absorption (292 nm), high quantum yield (0.27) and brightness 2800 (cm^{-1} M^{-1}). Owing to these results, it was desirable to expand the substrate scope in order to further investigate the photoluminescent properties of the biaryl phenylalanine analogues.

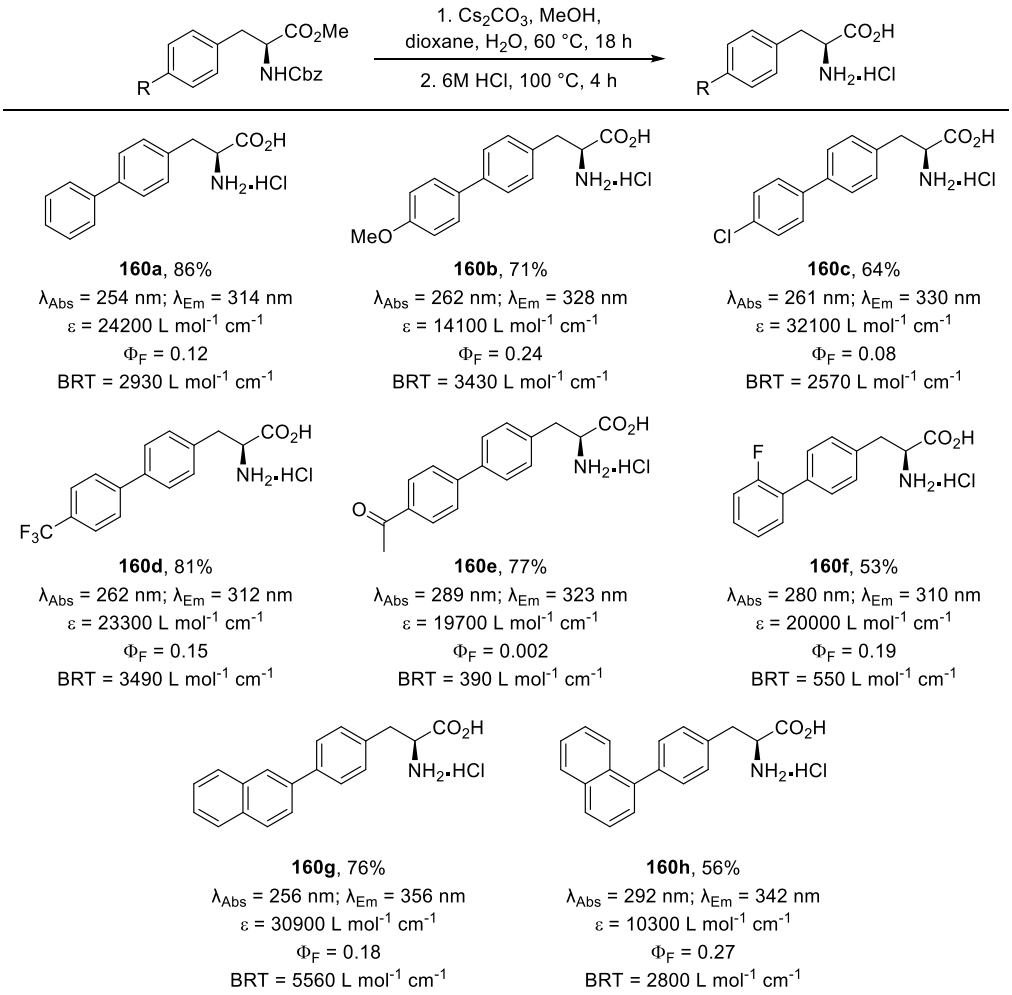

Scheme 38: Deprotection and photophysical properties of biaryl phenylalanine analogues previously synthesised in the Sutherland Group.

2.2.2 Results and discussion

The substrate scope for the one-pot nonaflate-formation and Suzuki-Miyaura cross-coupling of tyrosine was first expanded to include terphenyl analogue **159j**. Amino acid **159j** was previously synthesised by Hecht and co-workers from 4-iodophenylalanine *via* a Suzuki-Miyaura reaction and subsequently incorporated into a bacterial protein in order to study conformational changes *via* FRET measurements.[32,140] To further explore how electronics affect the photophysical properties of biaryl *α*-amino acids, the library was expanded to include 4-fluoro analogue **159k**, electron-withdrawing 4-cyano analogue **159l**, electron-donating 4-dimethylamino analogue **159o** and 2-methoxy analogue **159m** and thiophene analogue **159p** (Scheme **39**). Analogues **159h**, and **159e** were resynthesised to

improve yield and **159c** was resynthesised to improve purity. Dimethoxy analogue **159q** was proposed as restricted rotation was recently demonstrated within the group to result in dual emission *via* locally excited (LE) and twisted intramolecular charge transfer (TICT) states.[167] Unfortunately, poor conversion from the nonaflate intermediate due to steric hinderance of the 2,6-dimethoxyphenyl boronic acid prevented isolation. Similarly, steric hinderance resulted in poor conversion for the anthracene analogue **159r**. Lastly, the highly electron deficient 2-fluoropyridine substrate showed no conversion from the nonaflate intermediate. This was not surprisingly considering the notorious difficulty for the Suzuki-Miyaura cross-coupling of pyridines.[170,171]

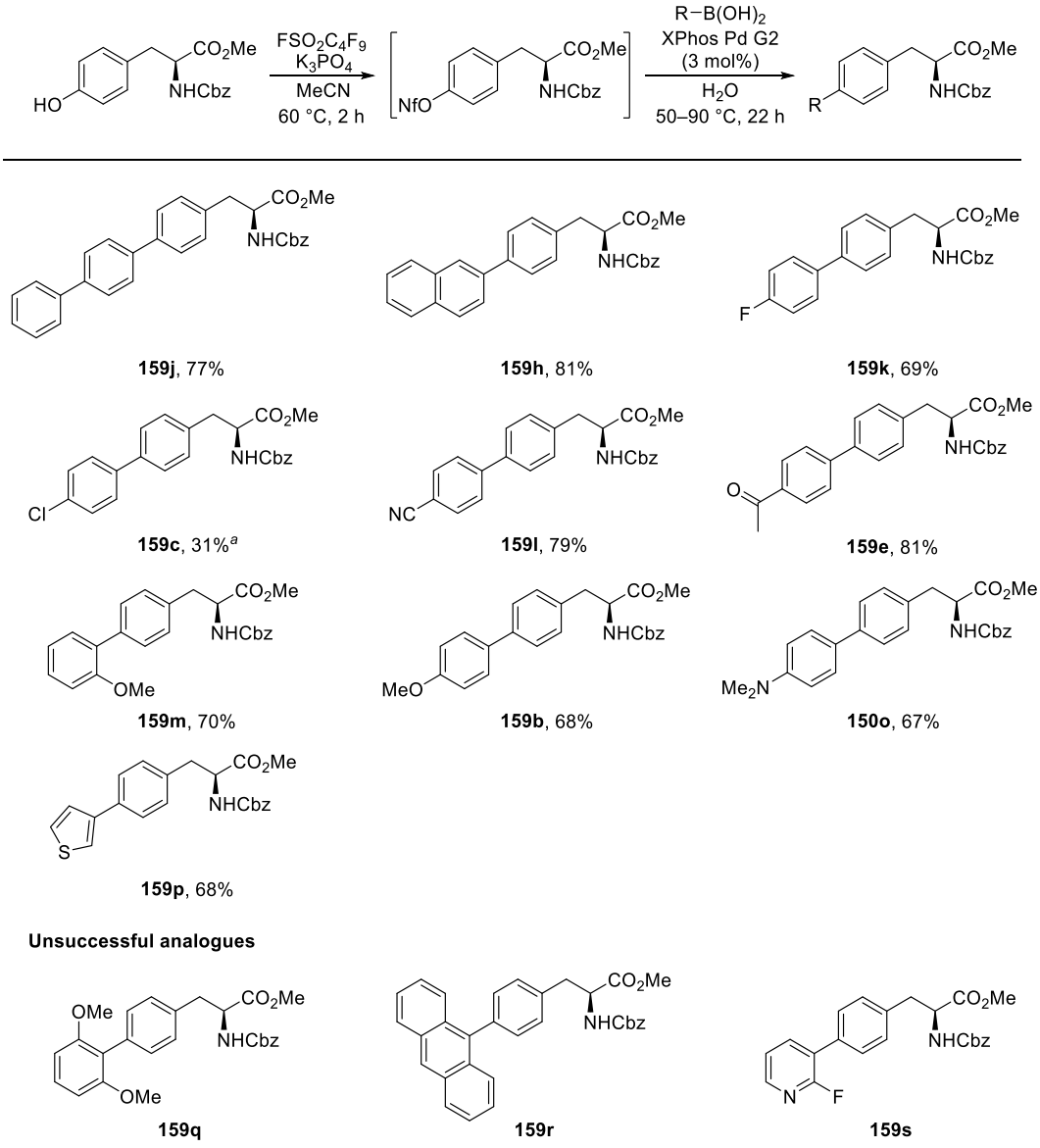

Scheme 39: One-pot synthesis of biaryl phenylalanine analogues. [a] 6 mol% XPhos Pd G2.

The biaryl α-amino acids were subsequently deprotected to give the deprotected amino acids as hydrochloric salts (Scheme **40**). The 4-cyanobiphenyl α-amino acid **159l**, could not be fully deprotected due to hydrolysis of the cyano group when attempting amine deprotection under acidic conditions.

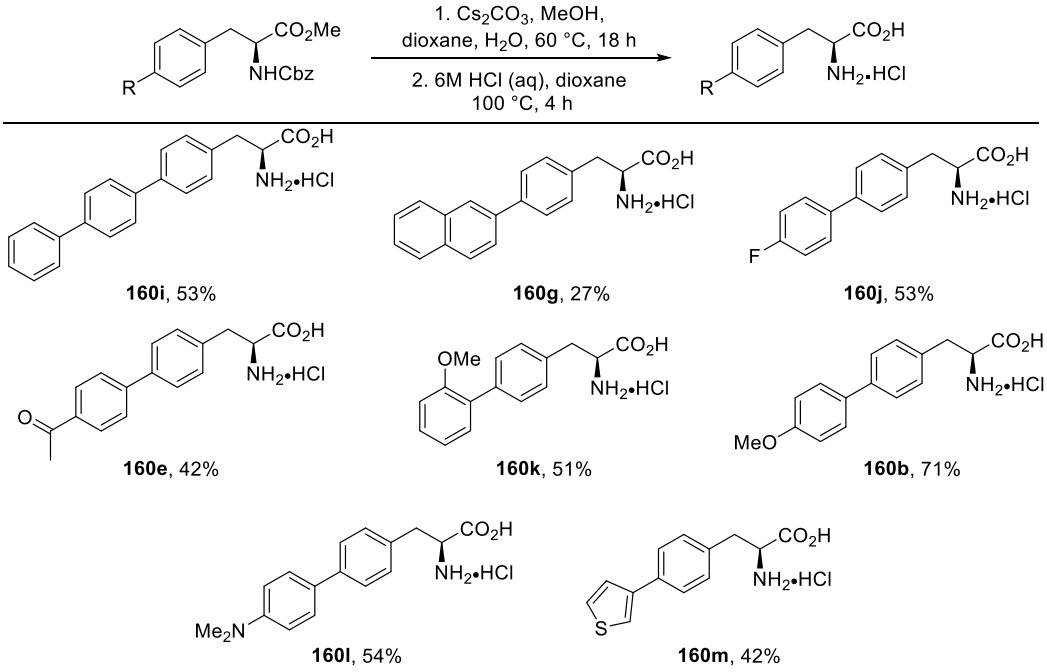

Scheme 40: Deprotection of biaryl amino acids.

The photoluminescent properties of the biaryl analogues of phenylalanine were subsequently investigated. Absorbance and emission spectra were recorded in methanol (Figure **8**). Due to the difficulties described for the deprotection of the 4-cyanobiphenyl α-amino acid, absorption and emission were recorded for the protected derivative **159l**. The photophysical data were then recorded (Table **4**). Except for the 4-fluorophenyl analogue **160j** (λ_{max} = 252 nm), the amino acids showed red shifted absorption bands (λ_{max} = 265–300 nm) compared to phenylalanine (λ_{max} = 258 nm)[15] as well as significantly improved photophysical properties. The protected 4-cyanobiphenyl α-amino acid **159l**, showed the strongest brightness (29100 cm^{-1} M^{-1}). Electron-rich 2-methoxyphenyl and 4-dimethylaminophenyl analogues resulted in a bathochromic shift in the absorption (λ_{max} = 288 and 300 nm, respectively).

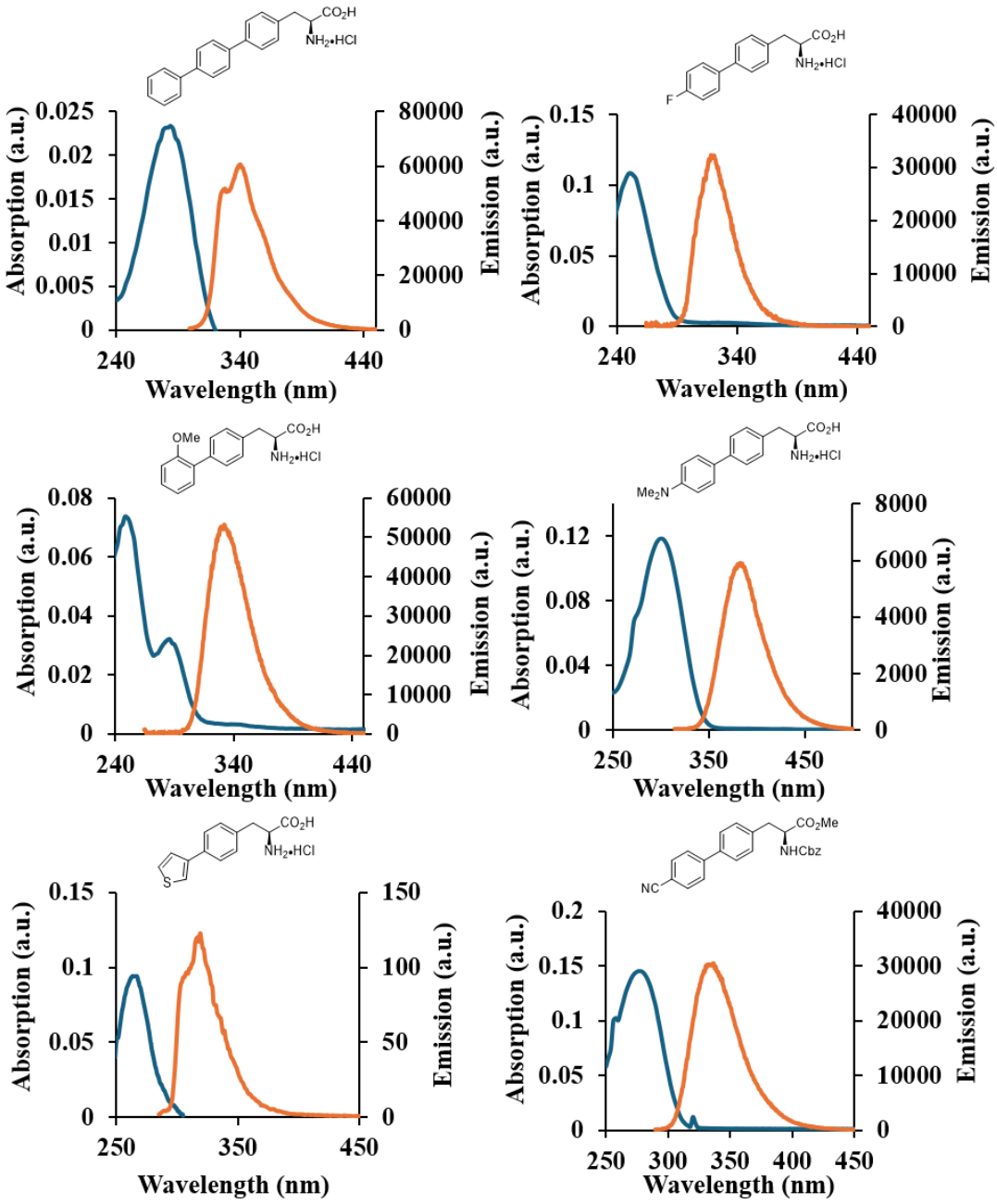

Figure 8: Absorption (blue) and emission (orange) of biaryl phenylalanine analogues 160i–160m and 159l (5 µM in MeOH).

Amino Acid	λ_{Abs} (nm)	ε (cm^{-1} M^{-1})	λ_{Em} (nm)	S.S. (nm)	Φ_F	BRT (cm^{-1} M^{-1})
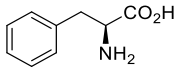 **1**	258	200	282	24	0.024	5
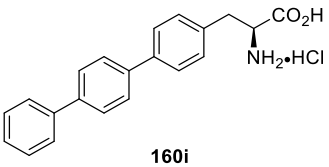 **160i**	284	14100	332, **341**	48, 57	0.83	11740
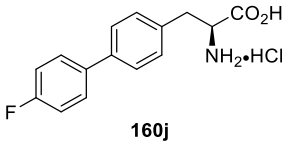 **160j**	252	20000	321	69	0.11	2200
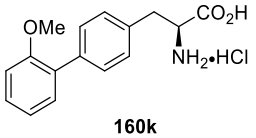 **160k**	**248**, 288	13800	333	85, 45	0.38	5140
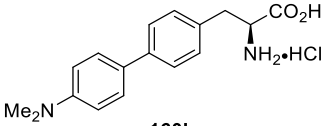 **160l**	300	17000	384	84	0.73	12460
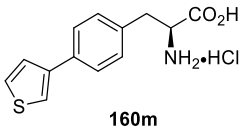 **160m**	265	18100	320	55	0.11	1900
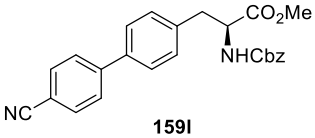 **159l**	278	29100	334	56	1.0	29100

Table 4: Photophysical properties of biaryl phenylalanine analogues 160i–160m and 159l. Comparison of absorption (λ_{Abs}) and emission (λ_{Em}) maximum, molar absorption coefficient (ε), stokes shift (S.S), quantum yield Φ_F and brightness (BRT) in methanol.

It was also desirable to synthesise coumarin analogue **159t**. Coumarins (or 1,2-benzopyranones) are found in numerous natural and pharmaceutical products and have been incorporated into various amino acid analogues owing to their strong fluorescent properties.[12,13,172] For example, L-(7-hydroxycoumarin-4-yl)ethylglycine has a red shifted emission of 450 nm in its anionic form and displays both pH and solvent sensitivity.[41] However, the synthesis of the coumarin boronic acid from the corresponding amine, as described by Blanchet and co-workers,[173] proved

challenging, affording a 25% yield (Scheme **41**). The Suzuki-Miyaura cross-coupling proceeded in a similarly low yield (25%).

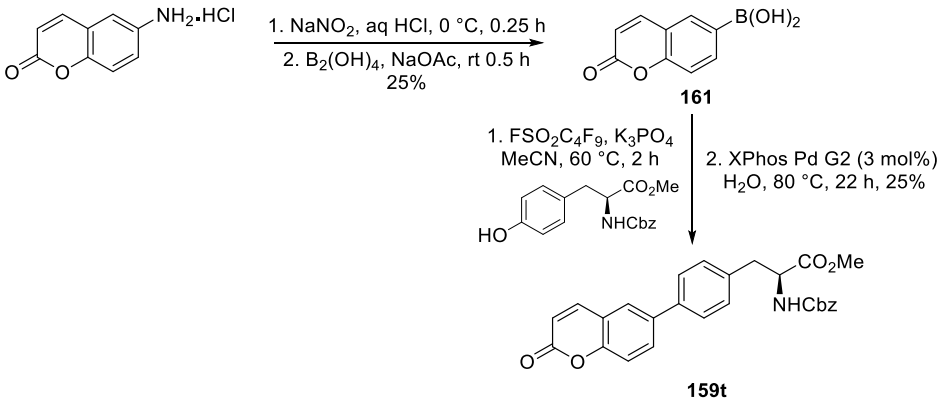

Scheme 41: Synthesis of coumarin-derived phenylalanine analogue 159t.

The photophysical properties of the protected coumarin analogue **159t** were subsequently investigated (Figure **9**, Table **5**). Whilst **159t** had a more red-shifted emission (439 nm) compared to the other biaryl amino acids (Table **4**), the low quantum yield (0.02) and brightness (750 cm^{-1} M^{-1}) resulted in analogue **159t** not being considered for further chemical biology applications.

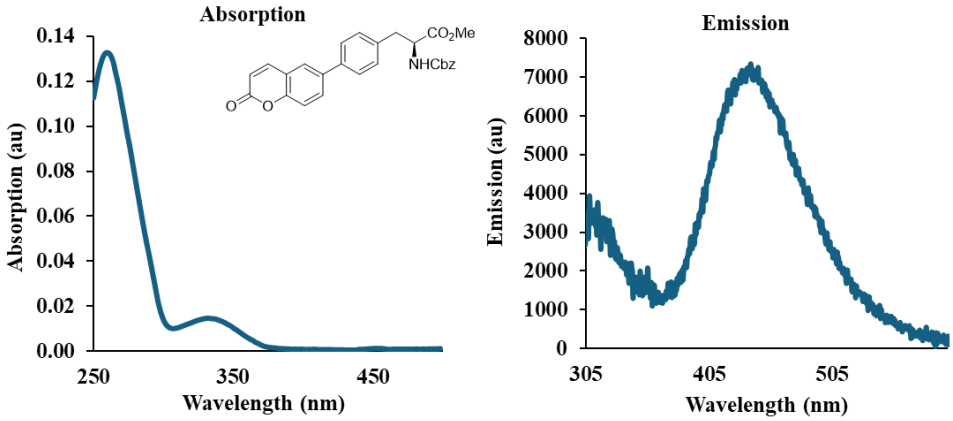

Figure 9: Absorption and emission of coumarin-derived phenylalanine analogue 159t (4 µM in MeOH).

Amino Acid	λ_{Abs} (nm)	ε (cm^{-1} M^{-1})	λ_{Em} (nm)	S.S. (nm)	Φ_F	Amino Acid
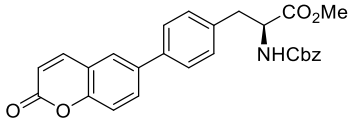 159t	262	33700	439	177	0.02	750

Table 5: Photophysical properties of coumarin analogue 159t. Comparison of absorption (λ_{Abs}) and emission (λ_{Em}) maximum, molar absorption coefficient (ε), stokes shift (S.S), quantum yield Φ_F and brightness (BRT) in methanol.

Consequently, 4-dimethylaminophenyl analogue **160l** was identified as the lead biaryl amino acid. As well as the most red-shifted absorbance, *α*-amino acid **160l** possessed a high extinction coefficient (17000 cm^{-1} M^{-1}), quantum yield (0.73) and brightness (12460 cm^{-1} M^{-1}). Furthermore, analogue **160l** possesses a stronger brightness than terphenyl analogue **160i** which has previously been used as an intrinsic peptidic probe,[32,140] and a higher quantum yield than other, rigid, polyaromatic phenylalanines reported by Ferreira and co-workers.[130]

2.2.3 Photophysical properties of lead dimethylaminobiphenyl analogue 160l.

The photoluminescent properties of lead *α*-amino acid **160l** were further investigated to gain insight into the environmental sensitivity and potential applications. The spectroscopic properties of *α*-amino acid **160l** were found to be pH-dependent, with acidification from pH 6 to pH 5 using 6 M hydrochloric acid resulting in a hypsochromic shift in the absorption maxima from 300 nm to 256 nm (Figure **10**). The emission spectra exhibited a corresponding hypsochromic shift from 385 nm to 315 nm, accompanied by an eightfold decrease in emission intensity in acidic environments. No significant change in the absorption and emission spectra was observed following the addition of triethylamine to adjust to pH 7 and pH 9. The pH sensitivity was attributed to protonation of the dimethylamino group (pK_aH of dimethylaminobenzene = 5.06),[174] leading to suppression of the stronger, charge transfer fluorescence at 385 nm and instead emission from a locally excited state at 315 nm. The emission at 315 nm is comparable to the emission of unsubstituted analogue **160a**, supporting that this corresponds to a locally excited state following attenuation of the electronic effects of the dimethylamino substituent. pH sensitivity

can be highly useful when designing fluorescent probes as microenvironments within the cell possess different pH values, such as the cytosol (pH 7.2), lysosomes (pH 4.5–5.5) and mitochondria (pH 8.0).[175] Fluorescent pH probes have been used to indicate cargo delivery to the desired cellular locations, as well as real time reporting of pH changes and tumour imaging.[176,177] pH sensitivity has been demonstrated in di-substituted pyridyl analogues of tyrosine,[149] however, there are not examples of fluorescent amino acids being utilised as pH sensitive probes.

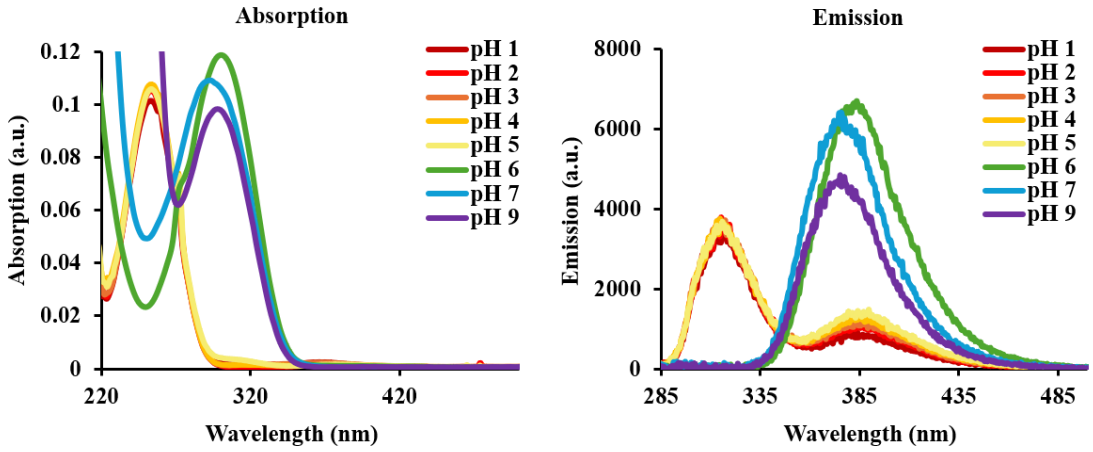

Figure 10: Absorption and emission spectra of *α*-amino acid 160l between pH 1 and pH 9 (5 µM in MeOH).

The solvatochromic properties of *α*-amino acid **160l** were next investigated (Figure **11**). Whilst no clear trend was observed in the absorption maxima in various solvents, a bathochromic shift in the emission maxima was observed with increasing solvent polarity. Specifically, the emission maxima shifted from 371 nm in non-polar solvents such as ethyl acetate and tetrahydrofuran to 404 nm in polar solvents including water and phosphate-buffered saline (PBS).

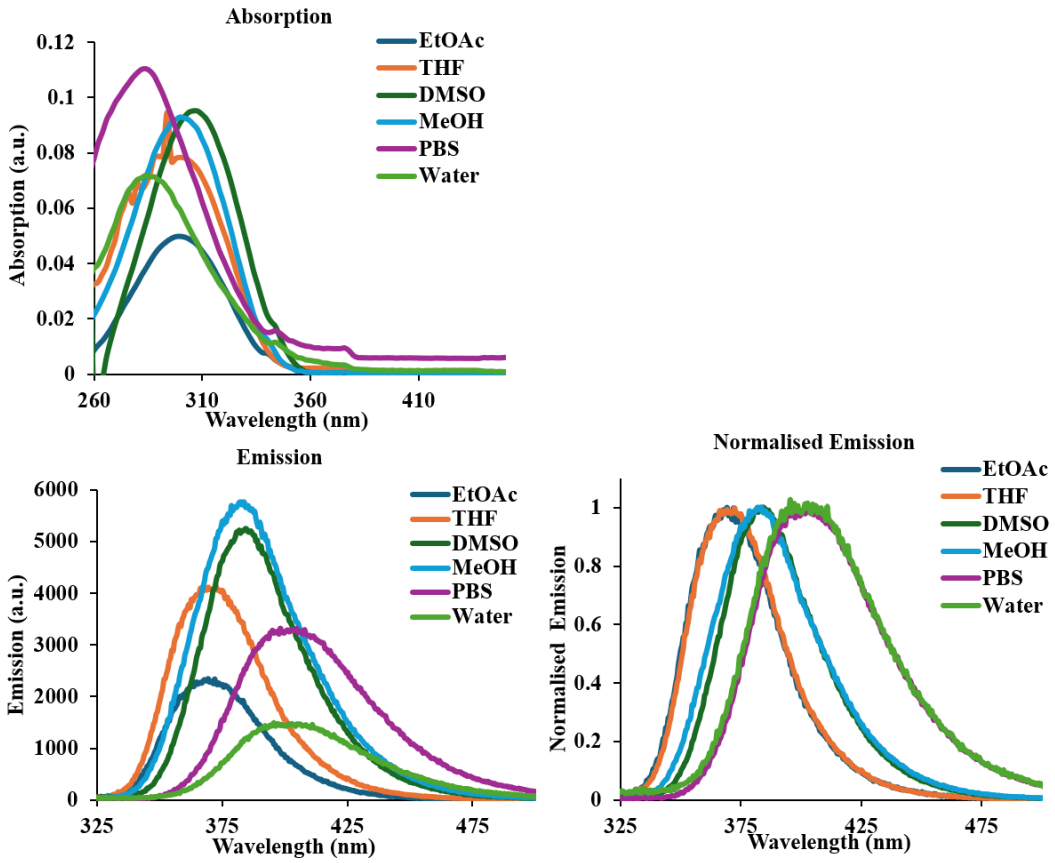

Figure 11: Solvatochromic properties of *α*-amino acid 160l.

A bathochromic shift in the emission maxima in polar solvents is indicative of emission from a charge-transfer excited state. The solvent molecules reorientate around the dipole in the excited state, lowering the excited state energy and increasing the emission wavelength (Figure **12**).[17]

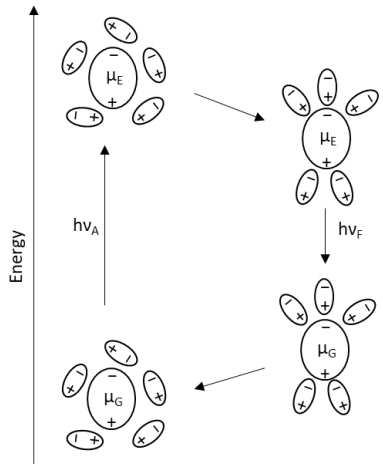

Figure 12: Stabilisation of the excited state by polar solvents.

The observed solvatochromism was further validated by a Lippert-Mataga plot (Figure **13**). The Lippert-Mataga plot is generated in accordance with Equation **2**, which equates the Stokes shift to the solvent orientation polarizability.[178] The Lippert-Mataga plot for α-amino acid **160l** shows a positive correlation between the solvent orientation polarisability and the Stokes shift (Figure **13**).

$$\lambda_{Abs} - \lambda_{Em} = \frac{2\Delta f}{hca^3}(\mu_E - \mu_G)^2 + c$$

$$\text{Where, } \Delta f = \frac{\varepsilon - 1}{2\varepsilon + 1} - \frac{\eta^2 - 1}{2\eta^2 + 1}$$

Equation 2: Lippert-Mataga Equation. Where $\boldsymbol{\lambda_{Abs}}$ and $\boldsymbol{\lambda_{Em}}$ are the absorption and emission maxima (cm^{-1}), h is Planck's constant (6.6256×10^{-34} m^2 kg s^{-1}), c is the speed of light (2.997×10^8 m s^{-1}), a is the fluorophore cavity radius, $\boldsymbol{\mu_E}$ and $\boldsymbol{\mu_G}$ are the excited- and ground- state dipole moments respectively and c is a constant. $\boldsymbol{\Delta f}$ is the orientation polarisability of the solvent which is dependent on the dielectric constant ($\boldsymbol{\varepsilon}$) and solvent refractive index ($\boldsymbol{\eta}$).

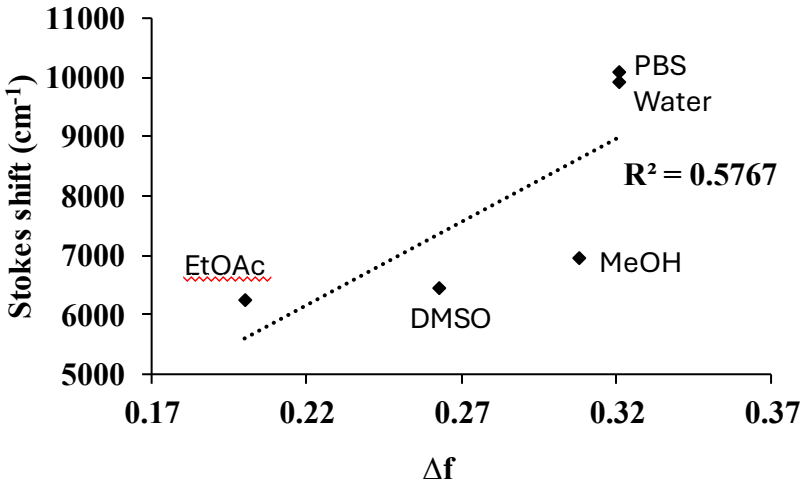

Figure 13: Lippert-Mataga plot for α-amino acid 160l.

In order to confirm the charge-transfer properties of α-amino acid **160l**, DFT calculations were performed. An energy minimised model (Figure **14b**) was optimised using B3LYP/6-31G basis sets,[179] which showed the expected twisted conformation of the biaryl side chain. Following this, frontier molecular orbital analysis was performed to visualise the highest occupied molecular orbital (HOMO) (Figure **14c**) and the lowest unoccupied molecular orbital (LUMO) (Figure 14d). Comparison of the electron density distribution between the HOMO and LUMO

indicates a redistribution from the electron-rich dimethylamino substituent to the aryl ring system upon excitation. Therefore, the DFT calculations supports the observed charge-transfer properties in the solvatochromic and pH studies.

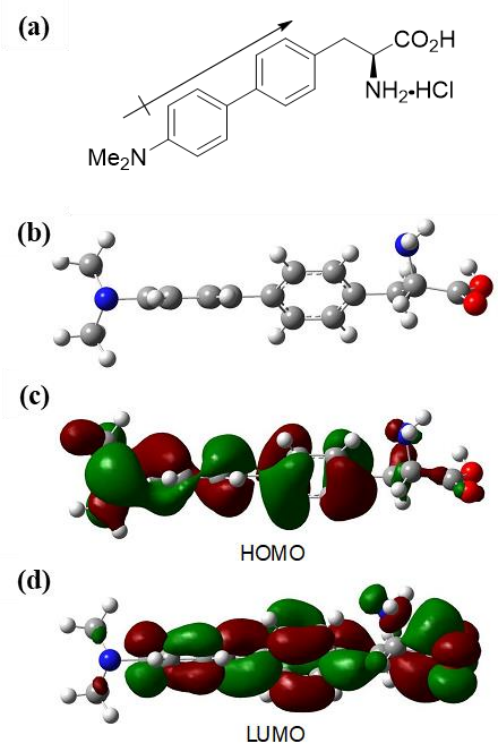

Figure 14: DFT calculations for *α*-amino acid 160l. (a) Structure of amino acid 160l indicating charge-transfer dipole; (b) Energy minimised DFT structure using B3LYP/6-31G basis sets; (c) HOMO calculated isosurface plot; (d) LUMO calculated isosurface plot.

The last solvatochromic property that was investigated was the absorption and emission of *α*-amino acid **160l** in lipophilic environments. Serial dilution of a 7 mg/mL liposome solution prepared from cholesterol: phosphatidylcholine (7:1) gave 0.23, 0.94 and 3.75 mg/mL liposome solutions to which *α*-amino acid **160l** was added (Figure **15**). The phospholipid bilayer in the liposomes is designed to mimic the environment at cellular membranes. Moderate sensitivity to lipophilic environments was observed with a 46% decrease in emission intensity upon increasing the concentration of liposomes from 0.23 to 3.75 mg/mL. Reduced emission intensity in highly lipophilic environments could result from aggregation. However, the change in emission intensity was not considered significant enough to be utilised in applications related to cell-based studies, so further exploration of the emission in lipophilic environments was not undertaken.

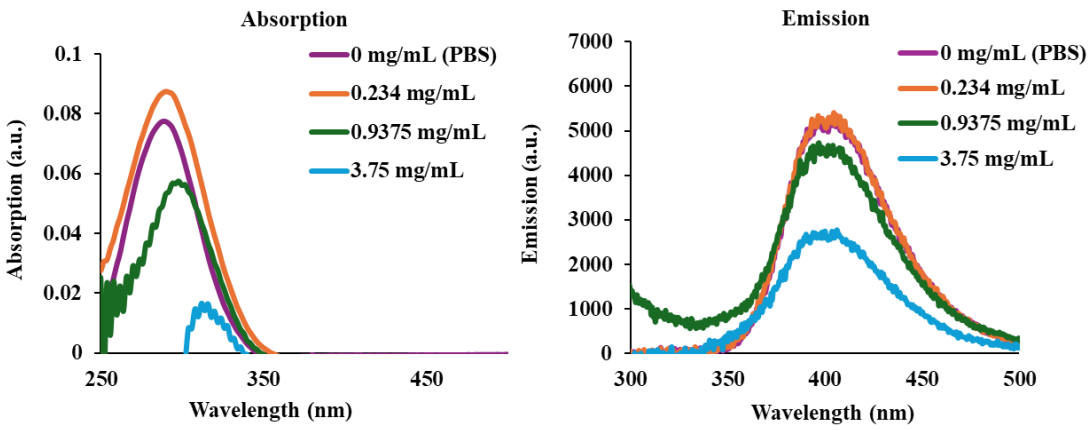

Figure 15: Effect of increasing liposome concentration in phosphate buffer on the absorption and emission spectra of *α*-amino acid 160l (5 µM).

Having demonstrated the pH and solvent sensitivity of *α*-amino acid **160l**, viscosity studies were next performed. Solutions of *α*-amino acid **160l** were prepared in methanol (viscosity $\eta = 0.59$ mPa s),[180] with increasing quantities of ethylene glycol ($\eta = 13.5$ mPa s)[180] and the absorption and emission spectra recorded. No significant change in the absorption or emission spectra was observed with increased viscosity (Figure **16**). These results indicate that the charge-transfer excited-state is not associated with twisted intramolecular charge transfer (TICT) which was previously been shown to occur in conformationally flexible aryl systems.[183]

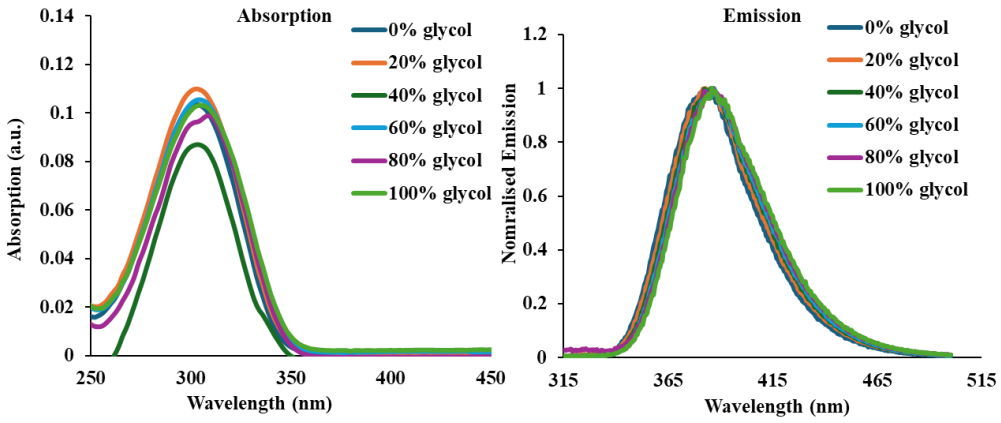

Figure 16: Effect of solvent viscosity on the absorption and emission spectra of *α*-amino acid 160l (5 µM).

Finally, an aggregation study was performed. The absorption and emission spectra of α-amino acid **160l** were recorded in methanol over a concentration range of 5–500 µM (Figure **17**). The absorption intensity increased with concentration. The emission intensity increased up to 50 µM, after which aggregation-induced quenching was observed.

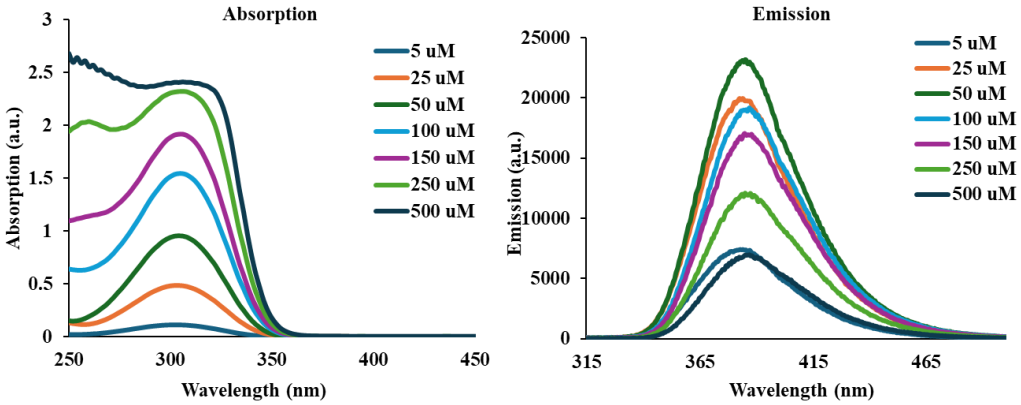

Figure 17: Effect of concentration on the absorption and emission spectra of α-amino acid 160l (MeOH).

2.2.4 Enantiopurity of α-amino acid 160l.

In order to assess the enantiomeric excess (ee) of this synthetic approach, the (*R*)-enantiomer of α-amino acid **160l** was synthesised (Scheme **42**). Starting from D-tyrosine methyl ester hydrochloride, Cbz-protection was achieved using benzyl chloroformate and sodium hydrogencarbonate in an 85% yield. The Cbz-protected starting material was then subjected to the one-pot nonaflate-formation and Suzuki-Miyaura coupling reaction. A lower yield of **163** was obtained (22%), compared to synthesis of the L-amino acid (67%). Whilst the reason for the low yield was not clear, there were sufficient quantities of **163** to progress forward. Intermediate **163** was subjected to the two-step deprotection involving base-mediated methyl ester hydrolysis followed by acid-mediated Cbz-group removal to give the required D-enantiomer **164**.

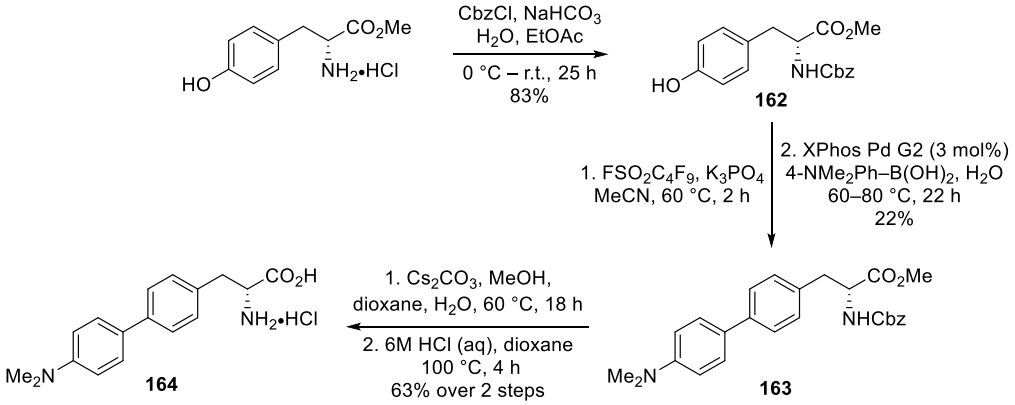

Scheme 42: Synthesis of *R*-enantiomer of *α*-amino acid 160l.

Separately, the D- and L- amino acids were reacted with Marfey's reagent **165** to give diastereomers **166** and **167** (Scheme **14**).[181] Comparison of the (*R,S*) diastereomer **166** with the (*S,S*) diastereomer **167** by ^{1}H NMR spectroscopy showed that the aromatic proton highlighted in Scheme **43** appeared as a distinct singlet at a different chemical shift for each diastereomer. Integration of this highlighted proton provided the ratio of diastereomers.

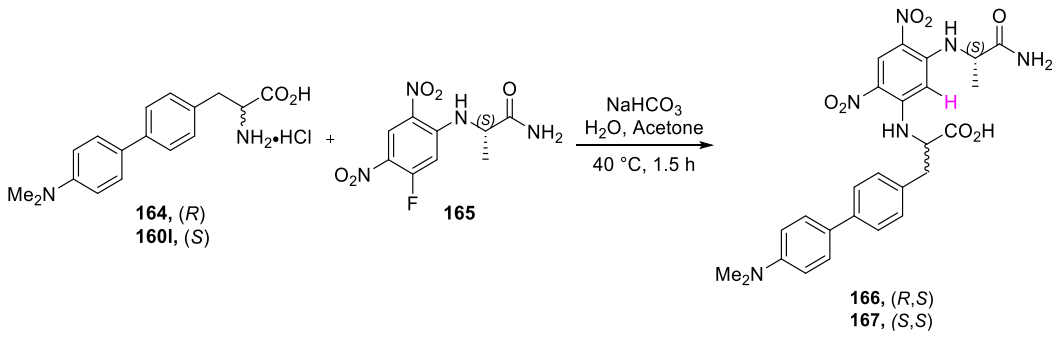

Scheme 43: Reaction of *R* and *S* biaryl amino acids with Marfey's reagent

^{1}H NMR spectroscopy of the (*S,S*) diastereomer **167** is shown in Figure **18**, from which a diastereomer ratio of 1:25 was measured, giving an ee of 93%. This indicates minimal erosion of the enantiomeric purity from the starting material *via* the various synthetic reactions employed to access the biaryl amino acids.

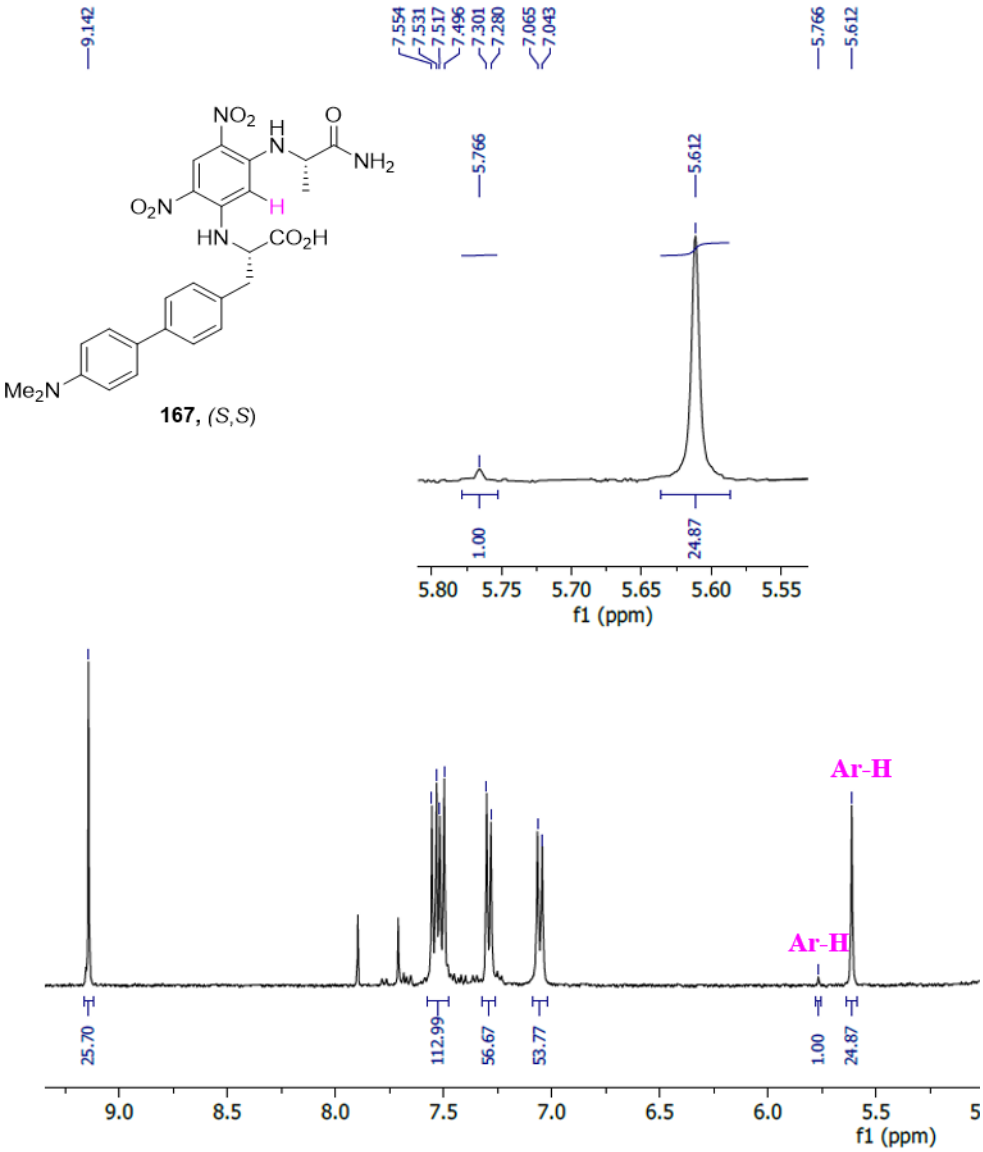

Figure 18: ^{1}H NMR spectrum of (*S,S*) diastereomer 167. Expansion highlights peaks at 5.61 and 5.78 ppm used to calculate ratio of diastereomers. Assignment of diastereomer peaks aided by comparison to ^{1}H NMR spectrum of (*R,S*) diastereomer **166**.

2.2.5 Application of lead 4-dimethylaminobiphenyl analogue as FRET donor for evaluating serine protease kinetics.

It was envisaged that *α*-amino acid **160l** could also be utilized as a FRET donor, as was demonstrated for 7-methoxydibenzofuran *α*-amino acid **147c** in section 2.2.1. Biaryl *α*-amino acid **160l** was found to have greater spectroscopic overlap with 2,4-dinitrophenyl lysine compared to 7-methoxydibenzofuran *α*-amino acid **147c** ($J(\lambda)$ = 1.71×10^{14} and 1.37×10^{14} M^{-1} cm^{-1} nm^{4} respectively). This gave a Förster distance

(R_0) value for biaryl α-amino acid **160l** and Lys(DNP) of 36.7 Å, which is comparable to other commonly used FRET pairs (Figure **19**).[159]

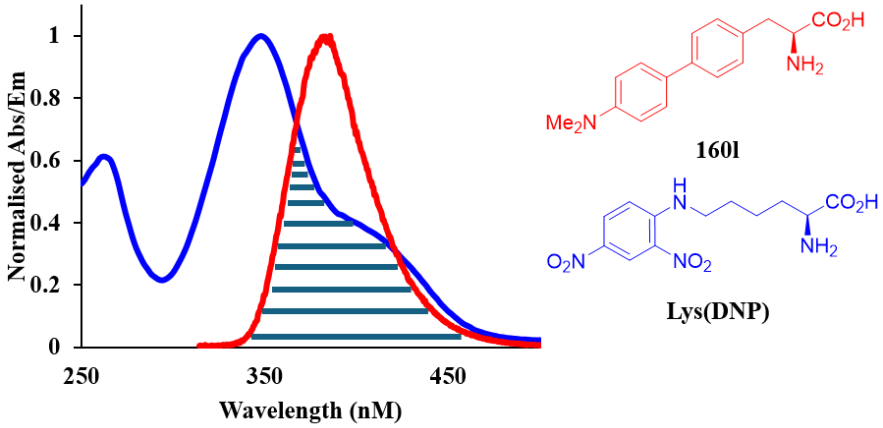

Figure 19: Spectroscopic overlap of α-amino acid 160l emission (red) and Lys(DNP) absorption (blue).

Prior to demonstrating the application of **160l** as an intrinsic peptide probe, Fmoc-protection of **160l** was undertaken. Fmoc is frequently used as an orthogonal amine-protecting group in solid phase peptide synthesis. Fmoc-protection of **160l** was achieved using Fmoc-succinimide and sodium hydrogencarbonate under standard conditions to give **168** in a 48% yield (Scheme **44**).

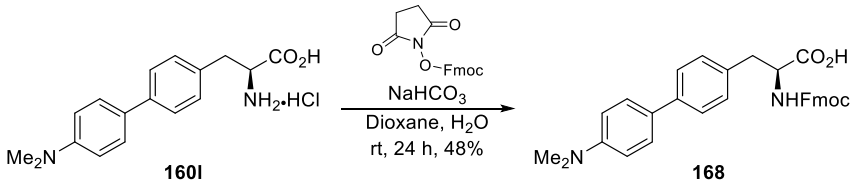

Scheme 44: Fmoc-protection of 160l.

To highlight the imaging potential of α-amino acid **160l** a similar decapeptide to the one described in section 2.2.1 was synthesised (Scheme **45**). Nonapeptide **149** was synthesised using standard solid-phase peptide synthesis, employing *N,N*'-diisopropylcarbodiimide (DIC) in combination with Oxyma pure as coupling reagents. Fmoc-deprotection was achieved using morpholine generating **149** in nine cycles. Amino acid **168** was subsequently manually coupled with **149** using PyBOP to give the desired decapeptide. Following morpholine-mediated Fmoc-deprotection, global deprotection and resin cleavage was achieved using a TIPS/TFA cocktail.

Decapeptide **169** was purified by reverse-phase HPLC (>99% purity) and characterised by high resolution electrospray ionisation mass spectrometry to confirm its identity.

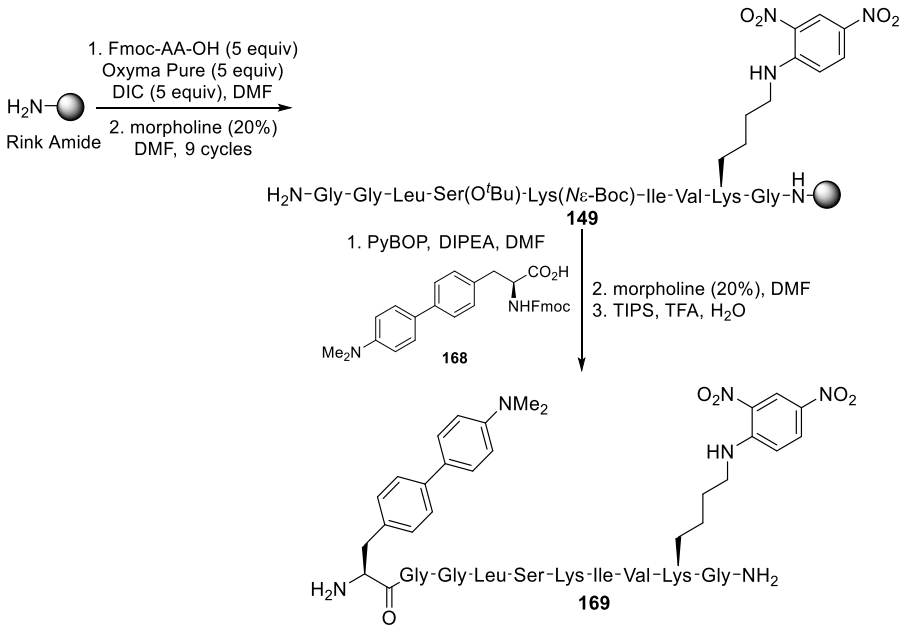

Scheme 45: Synthesis of decapeptide 169.

Decapeptide **169** was subsequently digested by the serine protease trypsin in MOPS buffer (Scheme **46**). Prior to digestion, the emission from amino acid **160l** in decapeptide **169** was nearly completely suppressed to 10% that of the free amino acid (Figure **20**). Upon digestion, the emission was restored, enabling real-time monitoring of the reaction.

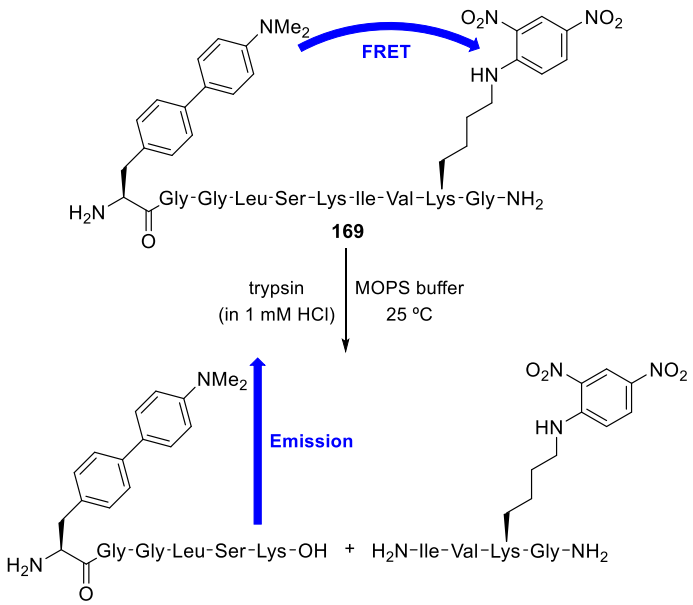

Scheme 46: Trypsin-mediated hydrolysis of peptide 169. The enzyme hydrolysis of peptide **169** used trypsin (0.01 µM), a range of peptide concentrations (0.50–2.50 µM) in 3-morpholinopropoanesulfonic acid (MOPS) buffer (20 mM) at pH 7.0 (n = 3).

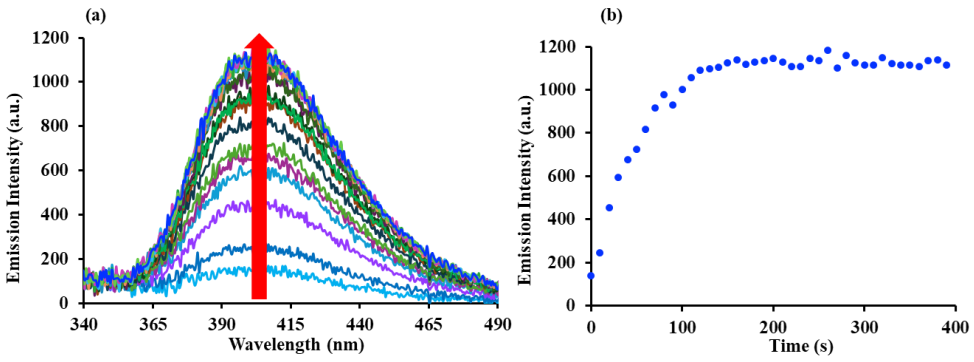

Figure 20: (a) Emission spectra showing increasing fluorescence over time during trypsin cleavage of decapeptide 169 (0.5 µM). (b) Plot of emission intensity *versus* time during trypsin hydrolysis of decapeptide 169 (0.5 µM).

In order to calculate enzymatic parameters K_M and k_{cat} for trypsin digestion of substrate **169** using Michaelis-Menten kinetics, the peptide concentration was varied (Figure **21**). The initial velocity over the first fifty seconds, where pseudo-first order kinetics is observed, was calculated using Origin software.[182] The reciprocal of initial velocity [V] *vs* substrate concentration [S] was plotted (Lineweaver-Burk plot, Figure 18), and used to calculate a K_M value of 0.33 ± 0.073 µM and a k_{cat} value of 0.73 ± 0.057 s^{-1} (n = 3). This gives a k_{cat}/K_M ratio of 2.2^{-1} µM s^{-1}. K_M, the Michaelis constant, is the substate concentration at which the reaction rate reaches half of Vmax

(the maximum reaction velocity). K_M thereby informs on the affinity of the enzyme for the substrate, with a lower K_M indicating a higher affinity. The catalytic constant, $k_{cat,}$ is calculated by dividing the maximum reaction rate Vmax by the total enzyme concentration to give the catalytic turnover for the reaction. The values of K_M and k_{cat} for peptide **169** are lower than those reported by Poreba and co-workers for an analogous peptide substrate which incorporated 7-amino-4-carbamoylmethylcoumarin (ACC) as the fluorescence donor ($K_M = 2.8$ μM, $k_{cat} = 4.2$ s^{-1}, $k_{cat}/K_M = 1.5$ s^{-1} μM^{-1}). This suggests that whilst trypsin had a strong affinity for the peptide substrate **169** the catalytic turnover was relatively low. However, in order to directly compare the decapeptide substrate affinity, a more rigorous evaluation with the same enzyme batch is required. Nonetheless, the proof-of-concept experiment demonstrates biaryl amino acid **160l** can function effectively as a FRET donor capable of reporting on proteolytic cleavage by a measurable increase in fluorescence intensity. Further validation of **160l** as a fluorescence reporter could involve incorporation of **160l**/Lys(DNP) into other peptide substrates for protease enzymes, which would further establish **160l**/Lys(DNP) as a fluorescence tool for investigating post-translational modifications.

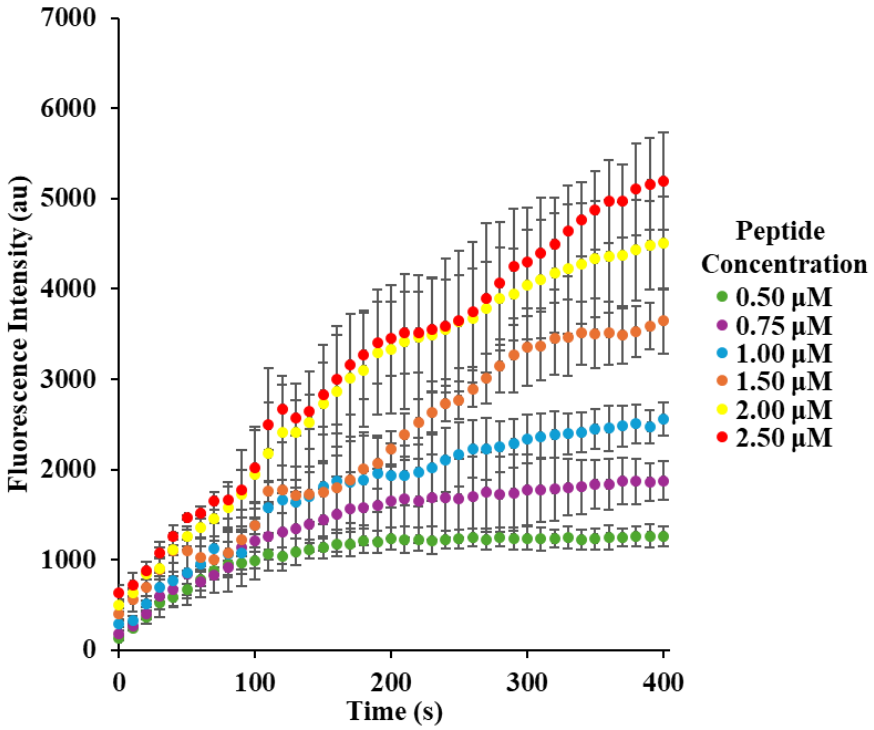

Figure 21: Fluorescence intensity *vs* time for trypsin-mediated hydrolysis of 169 at various concentrations.

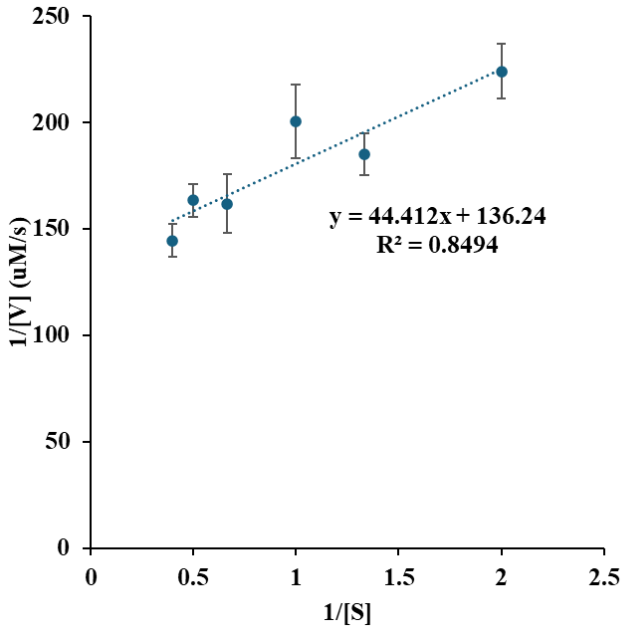

Figure 22: Lineweaver-Burk Plot.

Overall, biaryl α-amino acid **160l** has been shown to be both compatible with solid-phase peptide synthesis and applicable as a chemical probe for protease kinetics through the establishment of a novel FRET pair.

2.2.6 Conclusions

To conclude, a one-pot nonaflate-formation and Suzuki-Miyaura cross-coupling reaction has been developed for the rapid synthesis of novel biaryl α-amino acids. Compared to the natural amino acid phenylalanine, these analogues showed improved photophysical properties, particularly those bearing highly conjugated and electron-donating substituents. This led to the identification of the 4-dimethylaminobiphenyl analogue **160l**, which displayed red-shifted absorption (300 nm) and emission (384 nm) along with a high quantum yield (0.73) and brightness (12460 cm^{-1} M^{-1}). Furthermore, **160l**, was shown to exhibit both solvatochromic and pH sensitivity associated with emission from a charge-transfer excited state. Consequently, **160l** was successfully incorporated into a decapeptide as a novel FRET donor, paired with a 2,4-dinitrophenyllysine quencher. Compared to the dibenzofuran α-amino acid **147c**, **160l** exhibited greater spectroscopic overlap with

the quencher, resulting in an increased Förster distance (R_0) of 36.7 Å. The decapeptide was shown to be a suitable substrate for serine protease trypsin, and the increase in the emission of **160l** during hydrolysis of the peptide was used to calculate kinetic parameters K_M and k_{cat}. Overall, this approach enabled the synthesis and evaluation of a diverse range of biaryl fluorescent amino acids and has demonstrated an application of the lead analogue as an intrinsic peptide probe for monitoring enzymatic activity.

2.3 Synthesis of Arylalkynyl Analogues of Phenylalanine.

2.3.1 One-pot synthesis of arylalkynyl analogues of phenylalanine

Following the successful synthesis of biaryl analogues of phenylalanine from an aryl nonaflate intermediate *via* Suzuki-Miyaura cross-coupling reactions, it was proposed that a similar one-pot methodology utilising Sonogashira cross-coupling reactions would allow access to arylalkynyl analogues. It is well established that extending conjugation results in a bathochromic shift of a chromophore's absorption.[26-28] Furthermore, non-symmetric acetylene derivatives display strong fluorescence, particularly when a 'push-pull' donor acceptor system is bridged by an acetylene unit.[184,185] Interest in such donor-π-acceptor moieties is often driven by potential applications including organic light-emitting diodes (OLEDs), solar cells or molecular wires.[186, 187] Despite this, there are limited examples of alkyne conjugated fluorescent amino acids. Wiczk and co-workers reported a benzoxazole-derived amino acid, in which an alkyne bridged an arylated benzoxazole (acceptor) and a 4-methoxyphenyl (donor) moiety.[188] This amino acid exhibited favourable fluorescent properties, including absorption at 340 nm and emission at 428 nm. The amino acid also displayed a very high molar extinction coefficient (57330 M^{-1} cm^{-1}) and quantitative quantum yield. Previously, within the Sutherland group, installation of an alkyne moiety resulted in a red-shifted absorption and increased quantum yields relative to the biaryl analogue in a series of benzotriazole-derived α-amino acids (Scheme **47**).[114,115]

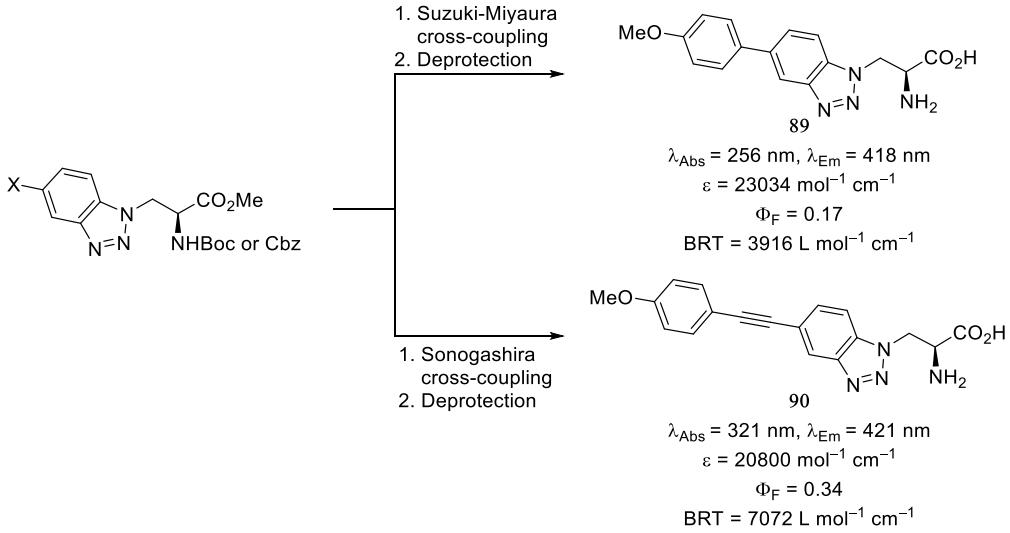

Scheme 47: Benzotriazole analogues of tryptophan previously synthesised in the Sutherland group *via* Suzuki-Miyaura and Sonogashira cross-coupling.

The first aim of this project was to optimise the one-pot nonaflate-formation and Sonogashira cross-coupling reaction of a protected tyrosine-derivative (Table **6**). The Sonogashira cross-coupling reaction of the isolated nonaflate intermediate was first attempted under conditions previously developed within the Sutherland group utilising $Pd(PPh_3)Cl_2$ and a copper iodide co-catalyst,[115] however, only the phenylacetylene homo-coupled product was observed (entry 1). Surprisingly, conditions reported by Akai and co-workers for the one-pot Sonogashira cross-coupling of simple phenols using a $PdCl_2(MeCN)_2$ catalyst and an XPhos ligand showed no conversion from the nonaflate (entry 2).[168] The Buchwald pre-catalyst XPhos Pd G2, which had been successful in the one-pot nonaflate formation and Suzuki-Miyaura cross-coupling reaction, gave an improved yield of 37% (entry 3). It was decided to optimise the copper-free Sonogashira reaction (or Heck-Cassar reaction) conditions in order to prevent the formation of the homo-coupled byproduct, which is mediated by the copper(I) salt in a Glaser reaction.[189] In order to prevent a plug of caesium carbonate forming in the reaction vial, which prevented sufficient mixing, the addition of water as a co-solvent or switching solvent system to *N,N*-dimethylformamide was investigated, however, both were unsuccessful due to poor conversion from, or failure to form the nonaflate intermediate respectively (entries 4 and 5). Increasing the catalyst loading to 10 mol% resulted in an improved yield of 78% (entry 6). Lastly, it was found that a lower catalyst loading of 5 mol% could be tolerated by increasing the temperature to 70 °C, which gave full conversion from the nonaflate (entry 7).

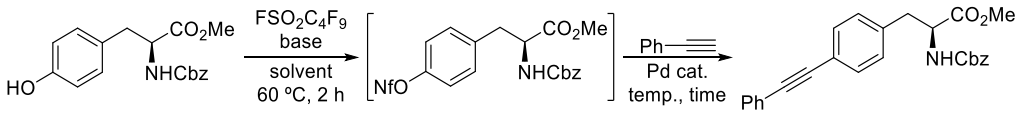

Entry	Catalyst System	Catalyst Loading (mol%)	Solvent	Base	Temp. (°C)	Time (h)	NMR Conversion (%)
1[a]	$Pd(PPh_3)Cl_2$ / CuI	10 / 20	DMF	Et_3N	100 – rt	3.5	0
2	$Pd_2(MeCN)_2$ / Xphos	1 / 2	MeCN	Cs_2CO_3	60	4.0	0
3	XPhos Pd G2	1	MeCN	Cs_2CO_3	60	4.0	37
4	XPhos Pd G2	1	MeCN, H_2O	Cs_2CO_3	60	4.0	0
5[b]	-	-	DMF	Cs_2CO_3	60	-	0
6	XPhos Pd G2	10	MeCN	Cs_2CO_3	60	4.0	78
7	**XPhos Pd G2**	**5**	**MeCN**	**Cs_2CO_3**	**70**	**3.5**	**100**

Table 6: One-pot synthesis nonaflate-formation and Sonogashira cross-coupling optimisation. [a] Nonaflate isolated prior to Sonogashira cross coupling reaction. [b] Nonaflate formation not observed.

The mechanism for the Sonogashira reaction is generally accepted to proceed *via* two independent catalytic cycles, in which the copper co-catalyst forms a copper acetylide intermediate required for transmetallation with the palladium species (Scheme **48a**). The highly reactive copper acetylide intermediate enables Sonogashira reactions to be performed at room temperature, however, the presence of the copper(I) catalyst can also result in the formation of the homo-coupled byproduct.[190] The Heck-Cassar reaction overcomes copper-mediated homocoupling by removing the co-catalyst, however, the mechanism for this reaction is still debated.[190-192] In 2018, Košmrlj and co-workers proposed a tandem palladium/palladium cycle, similar to the palladium/copper cycle of the Sonogashira

reaction, in response to reportedly high energy barriers calculated for the formation of the η^2-alkyne–palladium intermediate.[192] They proposed a transmetallation step between the oxidative addition complex and a *trans*-[$Pd^{II}(C{\equiv}CPh)_2(PPh_3)_2$] complex. This was supported by DFT calculations, kinetic studies and ^{31}P NMR analysis of intermediate complexes. More recently, analysis of the tandem palladium cycle by Cabri and co-workers suggested that transmetallation was less efficient than direct reaction between the oxidative addition complex and the alkyne substrate.[190] Cabri went on to propose that the mechanism proceeds *via* either a cationic or neutral mechanism depending on the counterion. For a pseudohalide counterion ($^-$OTf), the pseudohalide dissociates from the metal following oxidative addition, allowing the secondary amine to enter the coordination sphere, forming a cationic complex (Scheme **48b**). Subsequent deprotonation of the alkyne results in the η^1-alkyne–palladium intermediate, and final reductive elimination affords the cross-coupled product.

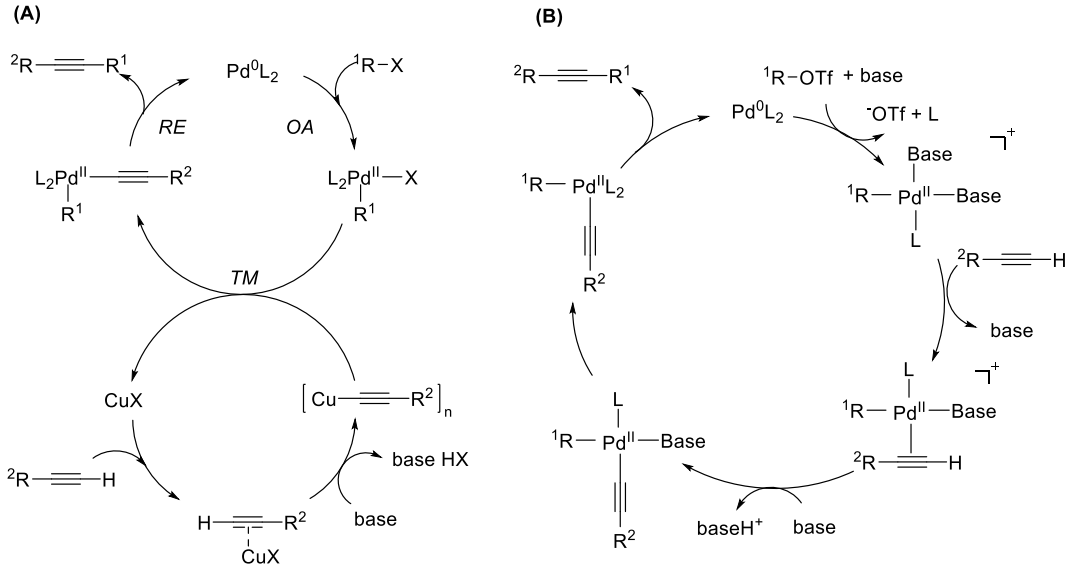

Scheme 48: Mechanism for the Sonogashira reaction (A) and Heck-Cassar or copper-free Sonogashira reaction (B). OA stands for oxidative addition, TM stands for transmetallation and RE stands for reductive elimination.

Following optimisation, the one-pot Sonogashira cross-coupling reaction with phenylacetylene and 4-methoxyphenylacetylene substrates was achieved to give the desired α-amino acids in 80% and 65% yields, respectively (Scheme **49**).

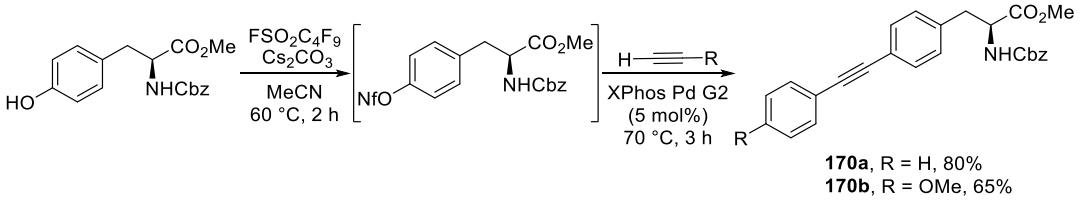

Scheme 49: Synthesis of Cbz-protected arylalkynyl phenylalanine analogues 170a and 170b.

Prior to the synthesis of further arylalkynyl α-amino acid analogues, the deprotection of these analogues was explored. Methyl ester hydrolysis of the phenyl analogue **170a** using caesium carbonate gave deprotected carboxylic acid **171** in 91% yield (Scheme **50**). However, removal of the Cbz-group under strongly acidic conditions was unsuccessful. ^{1}H NMR spectroscopy indicated a mixture of products and starting material. Since the polarity of deprotected amino acids make their purification more challenging, it was decided to switch to a Boc-protecting group, which can be cleaved under mild acidic conditions. Another advantage of the one-pot synthesis route is that switching to the Boc-protected tyrosine starting material was relatively straightforward.

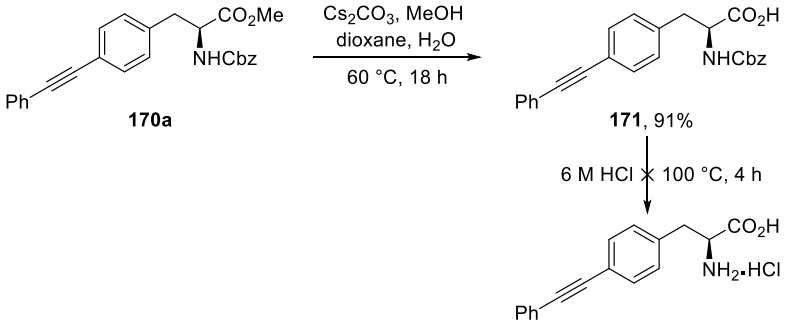

Scheme 50: Attempted deprotection of arylalkynyl analogue 170a.

The optimised reaction conditions were not affected by the change in protecting group and so, the substrate scope for the one-pot nonaflate formation and Sonogashira cross-coupling of Boc-protected tyrosine was explored (Scheme **51**). The one-pot methodology enabled the rapid synthesis of a diverse range of alkyne-conjugated phenylalanine analogues (**172a**–**172i**) in moderate to excellent yields (51–95%). A lower yield of 30% was obtained for heteroaryl analogue **172h**, despite an elevated temperature of 85 °C. Only 50% conversion from the nonaflate was

observed for the 4-nitrophenyl acetylene substrate, resulting in this product not being isolated due to difficult purification.

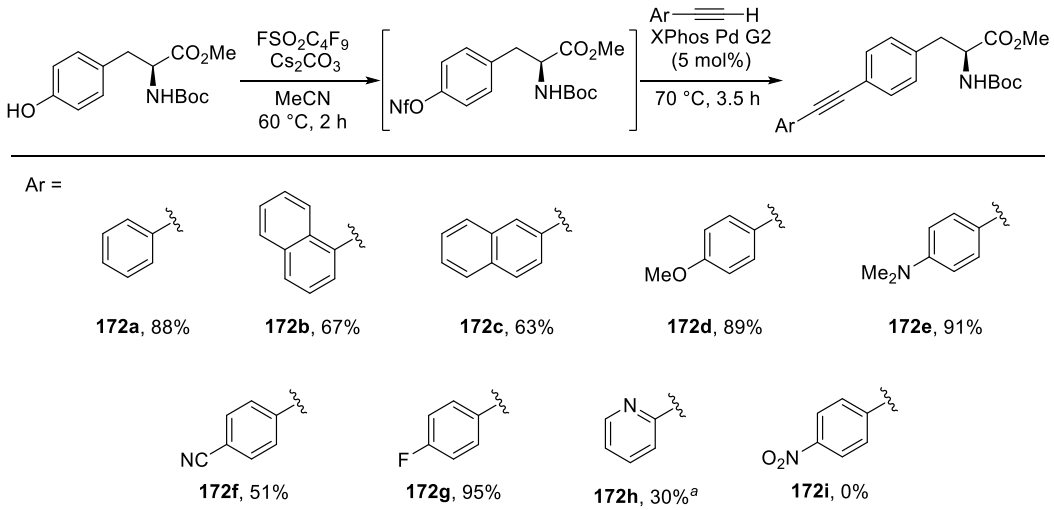

Scheme 51: Substrate scope for one-pot nonaflate formation and Sonogashira cross-coupling reaction of Boc-protected tyrosine. [a] Reaction performed at 85 °C.

Deprotection of the arylalkynyl α-amino acid analogues was subsequently investigated. Caesium carbonate mediated methyl ester hydrolysis was successful at generating carboxylic acid products for the electron rich and halogenated analogues (Scheme **52**). Removal of the Boc-group was achieved for unsubstituted phenylacetylene analogue **172a** using 4 M hydrochloric acid in dioxane at room temperature in 42% yield. However, for analogues **172d, 172e** and **172g**, the Boc-group could not be cleanly removed using hydrochloric acid.

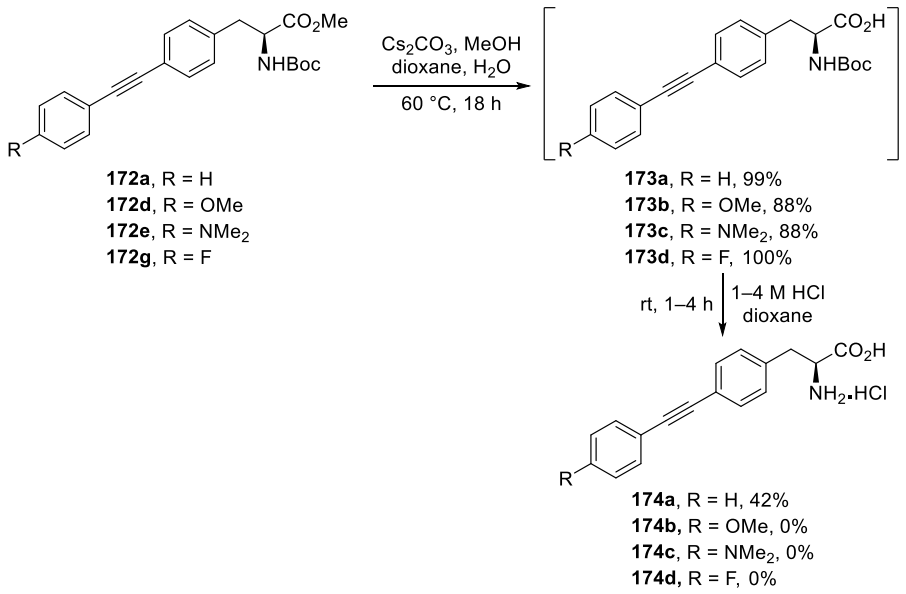

Scheme 52: Attempted deprotection of Boc-protected arylalkynyl *α*-amino acid analogues.

Methods for Boc-deprotection were explored for the electron rich 4-methoxy analogue, which was expected to be the most challenging. It was considered that trifluoroacetic acid, which is often used as a mild Boc-deprotecting reagent,[193] would be less likely to form adducts with the alkyne moiety. However, on reaction with trifluoroacetic acid at room temperature, significant starting material degradation was observed by ^{1}H NMR spectroscopy (Scheme **53**).

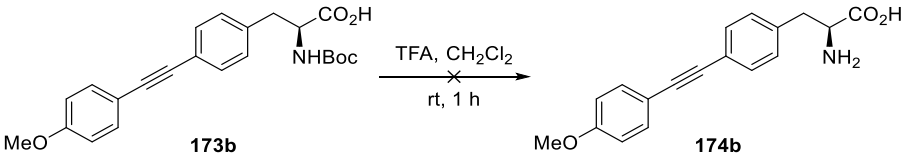

Scheme 53: Attempted TFA deprotection of 173b.

As traditional Boc-deprotection methods proved unsuccessful, alternative methods were investigated. A mild, Lewis acid-mediated Boc-deprotection using iron(III) chloride, reported by Mandal and co-workers,[193] was successful in Boc-removal from the fully protected analogue **172d** to give amine **175** in 41% yield (Scheme **54**). However, the subsequent methyl ester hydrolysis with caesium carbonate was not successful as **174b** could not be extracted from the aqueous layer. Iron(III) chloride mediated Boc-deprotection of the carboxylic acid product **173b** was also unsuccessful due to product solubility and purification challenges. Although

isolation of free amino acid **174b** was not achieved, this method may still be applicable to Boc-deprotection on resin, for which purification is simplified, as demonstrated by Mandal and co-workers.[65]

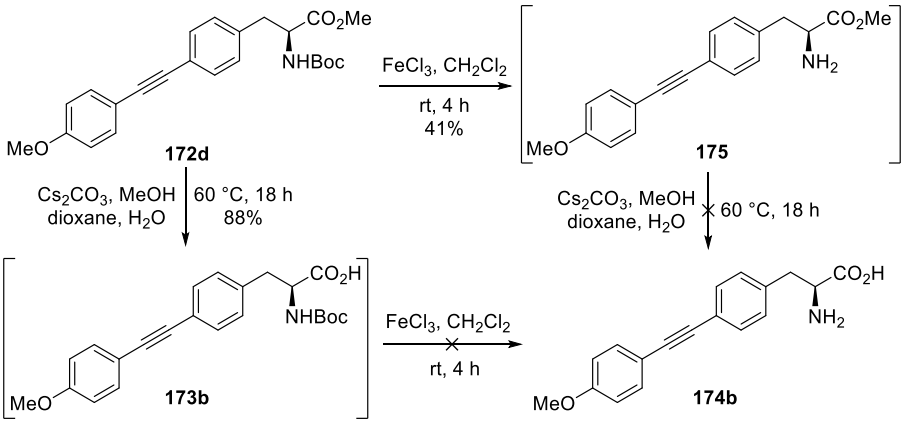

Scheme 54: Deprotection studies using iron(III) chloride.

Oxalyl chloride was reported by Awuah and co-workers as a Boc-deprotection method suitable for acid-sensitive substrates.[194] However, after treatment with oxalyl chloride for 4 h, the reaction mixture showed degradation of the starting material and incomplete Boc-removal by ^{1}H NMR spectroscopy (Scheme **55**). The final Boc-deprotection attempted was reported by Cravatt and co-workers, who used iodotrimethylsilane and *N*-methylmorpholine on an alkyne containing substrate.[195] It was considered that this methodology could be used to fully deprotect amino acid **172d**, as the silyl ester intermediate could form at both the carbamate and ester positions. Treatment of **172d** with iodotrimethylsilane and *N*-methylmorpholine resulted in a mixture of silyl ester and deprotected products. Nonetheless, after attempted recrystallisation, the deprotected product was not isolated. The reaction was also performed without *N*-methylmorpholine, however, ^{1}H NMR spectroscopy indicated reduction of the alkyne moiety after 1 h.

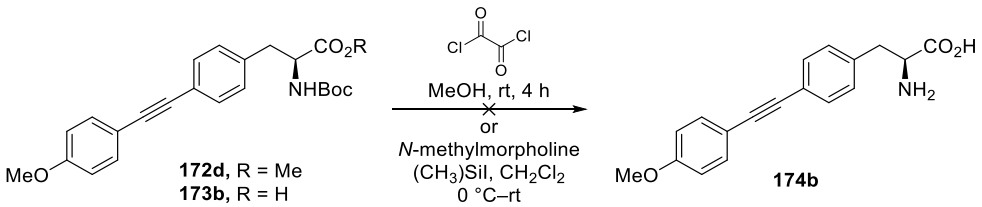

Scheme 55: Attempted deprotection of 172d and 173b with oxalyl chloride and iodotrimethylsilane.

2.3.2 Photophysical properties of arylalkynyl analogues of phenylalanine

Due to the challenging deprotection of the electron-rich phenylacetylene *α*-amino acid analogues, it was decided to proceed with photophysical analysis of the protected *α*-amino acids. Whilst deprotection is necessary for incorporation of unnatural amino acids into peptides, it could be argued that the photophysical properties of the protected analogues better represents the properties of the amino acid after it is embedded within a peptide.

After initial analysis revealed that 4-methoxyphenylacetylene *α*-amino acid **172d** displayed poor emission in methanol, a brief solvatochromic study was undertaken (Figure **23**). However, no increase in the emission intensity was observed in non-polar or aprotic solvents. Subsequently, the absorption and emission for the other arylalkynyl *α*-amino acid analogues **172a**–**172h** were recorded in methanol (Figure **24**).

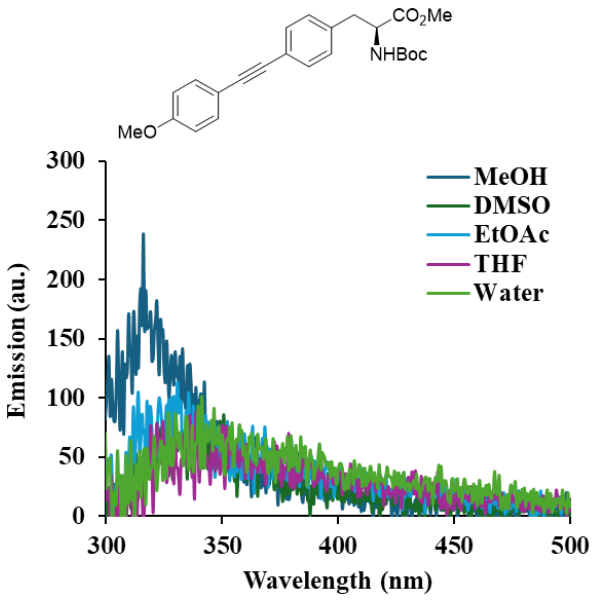

Figure 23: Solvatochromic study for *α*-amino acid x.

Compared to the biaryl analogues described in section 2.2, as well as the parent amino acid phenylalanine, the arylalkynyl analogues all displayed red-shifted absorption as a result of the extended conjugation (Table **7**). Furthermore, high molar extinction coefficients were recorded across the series. Unsubstituted analogue **172a**, as well as 4-methoxy (**172d**), 4-dimethylamino (**172e**), and 4-fluoro (**172g**) were

poorly emitting, resulting in quantum yield data not being measured. It was considered that the low emission was a result of non-radiative relaxation pathways such as photoinduced electron transfer (PET) or intramolecular intersystem crossing.[196] Improved fluorescent properties were observed for naphthyl analogues **172b** and **172c**, as well as analogues bearing electron-withdrawing substituents (**172f**). In particular, 1-naphthyl analogue **172b** demonstrated strong fluorescence, exhibiting mirrored vibrational bands in both absorption and emission spectra, as well as high quantum yield (0.65) and brightness (15550 cm^{-1} M^{-1}).

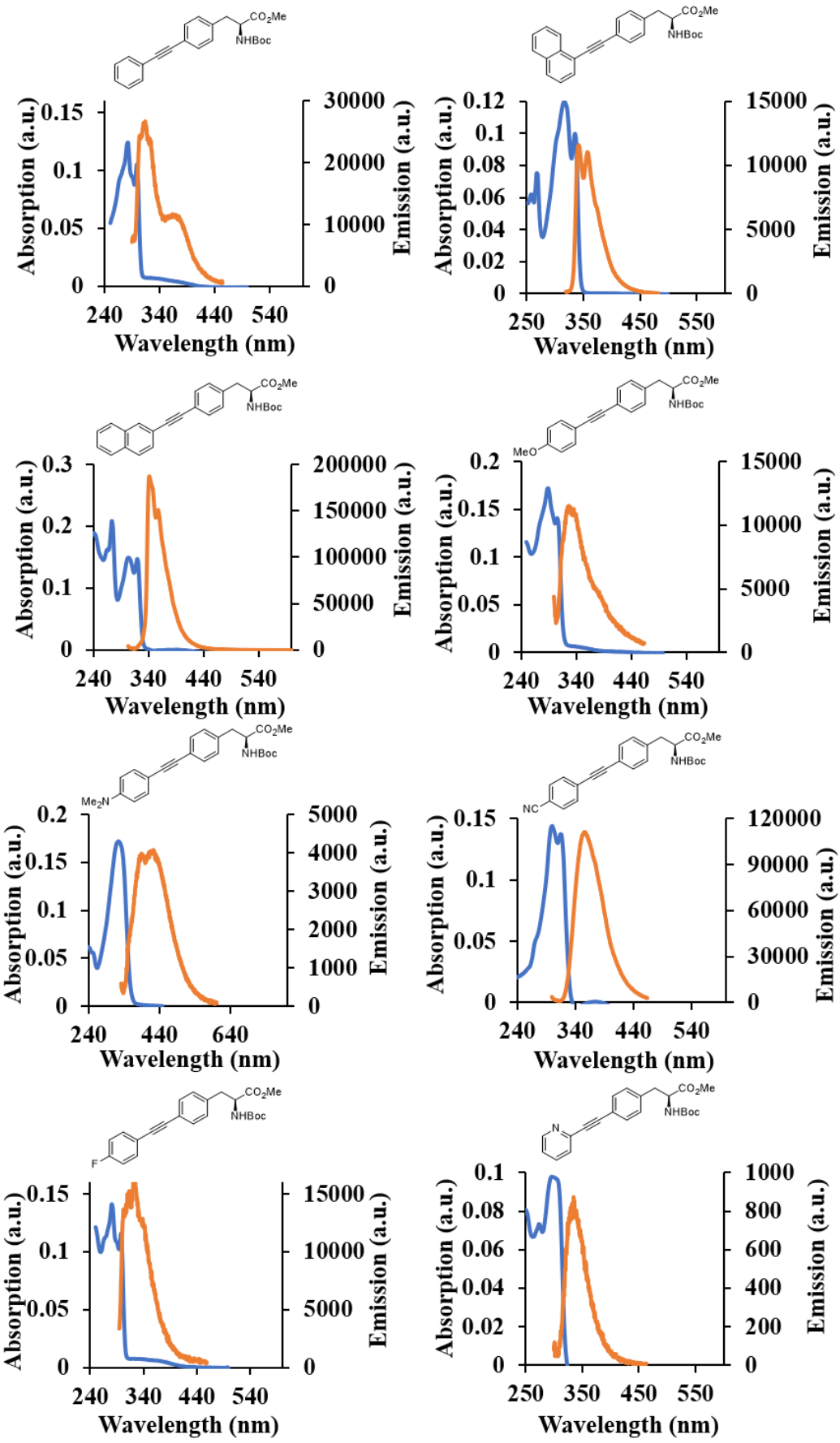

Figure 24: Absorbance (blue) and emission (orange) spectra for arylalkynyl phenylalanine analogues 172a–172h (5 µM in MeOH).

Amino Acid	λ_{Abs} (nm)	ε (cm^{-1} M^{-1})	λ_{Em} (nm)	S.S. (nm)	Φ_F	BRT (cm^{-1} M^{-1})
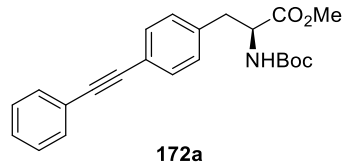 **172a**	284	24900	312	30	-	-
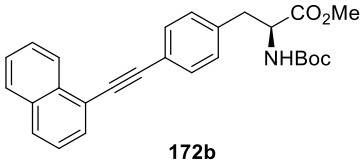 **172b**	316 336	24100	**343** 359	27 7	0.69	15550
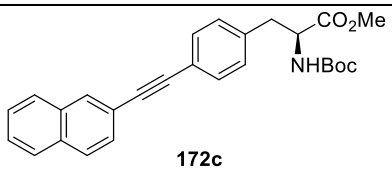 **172c**	274	39200	341	67	0.23	8950
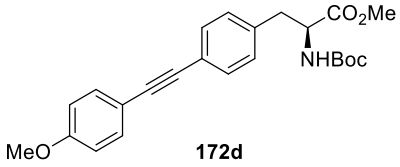 **172d**	292	30200	326	34	-	-
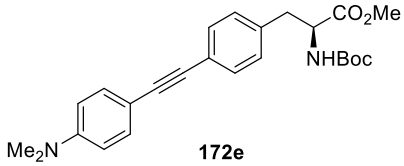 **172e**	326	35400	423	97	0.03	1050
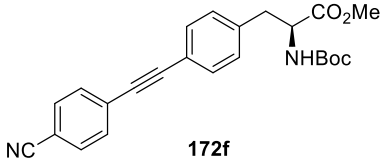 **172f**	302	34400	356	54	0.21	7340
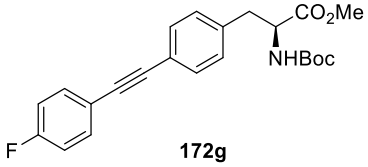 **172g**	282	29400	324	42	-	-
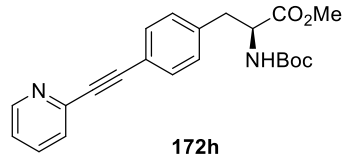 **172h**	296	20400	334	38	0.06	1270

Table 7: Photophysical properties of arylalkynyl phenylalanine analogues 172a–172h. Comparison of absorption (λ_{Abs}) and emission (λ_{Em}) maximum, molar absorption coefficient (ε), stokes shift (S.S), quantum yield Φ_F and brightness (BRT) in methanol.

2.3.3 Photophysical properties of lead 1-naphthyl analogue 172b.

Following identification of 1-naphthyl analogue **172b** as the lead arylalkynyl *α*-amino acid owing to its high brightness (15550 cm^{-1} M^{-1}), additional photophysical analysis was performed. No significant spectroscopic change was observed in response to increasing solvent viscosity, which was achieved by increasing the proportion of ethylene glycol in solution (Figure **25**). This suggests emission is not affected by conformational rearrangement between twisted and planar geometries.

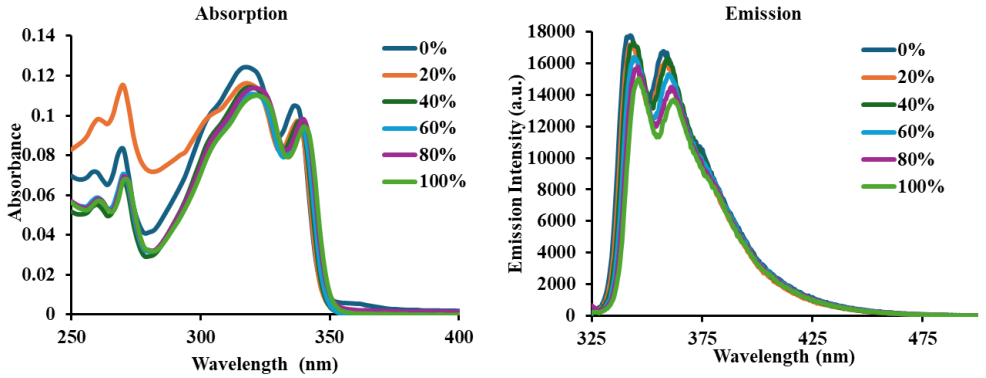

Figure 25: Effect of solvent viscosity on the absorption and emission spectra of *α*-amino acid 172b. Absorption and emission recorded in increasing quantities of ethylene glycol (η = 13.5 mPa s)[180] in methanol (viscosity η = 0.59 mPa s)[180] (5 μM).

An aggregation study showed an increase in fluorescence intensity from 5 μM to 80 μM, after which aggregation induced quenching was observed (Figure **26**).

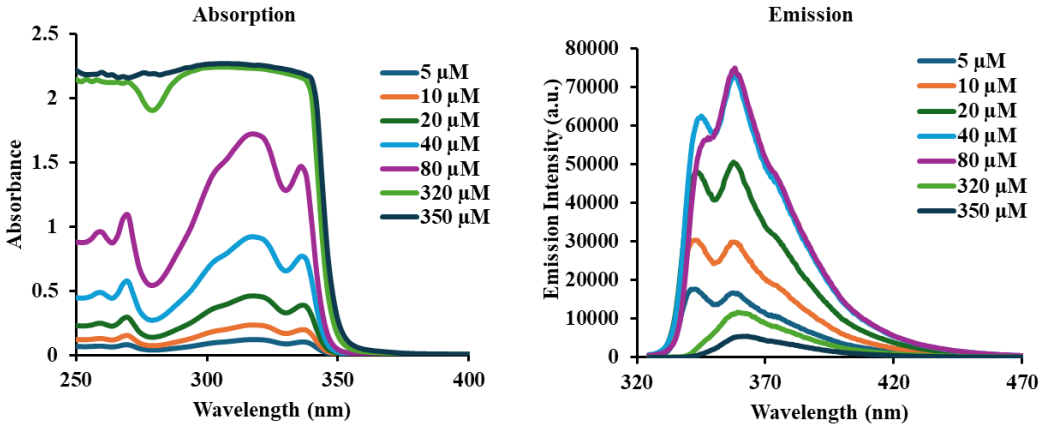

Figure 26: Effect of concentration on the absorption and emission spectra of *α*-amino acid 172b (MeOH).

The most notable spectroscopic properties were observed in response to changing solvent (Figure **27**). Whilst minimal differences in the absorption and emission were observed in various organic solvents, a significant reduction in emission intensity and a bathochromic shift from 322 nm to 390 nm was seen in water.

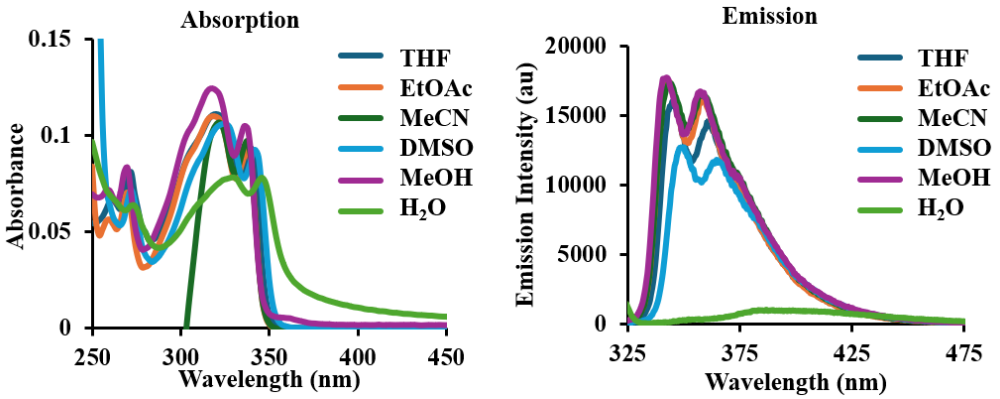

Figure 27: Solvatochromic properties of *α*-amino acid 172b.

Given the marked change in emission intensity in water, the absorption and emission properties were compared between phosphate-buffered saline (PBS) and liposomes prepared from phosphatidylcholine (PC) and cholesterol (7:1) (Figure **28**). In PBS, weak emission of **172b** was observed, potentially resulting from aggregation of the lipophilic *α*-amino acid. However, in a lipophilic environment, an 8.5-fold increase in emission intensity is observed. This was attributed to insertion of **172b** into the bilayer, where it adopts a highly emissive conformation. Sensitivity to lipophilic environments can be exploited in fluorescence probes designed to target cellular membranes. This targeting strategy has been utilised by Vendrell and co-workers, who developed a series of lipid-sensitive BODIPY amino acid analogues of the three naturally fluorescent amino acids.[142,197-200] In particular, Vendrell and co-workers have highlighted how the sensitivity to lipophilic environments and low/negligible emission in buffer can be exploited for "wash-free" cellular imaging techniques.

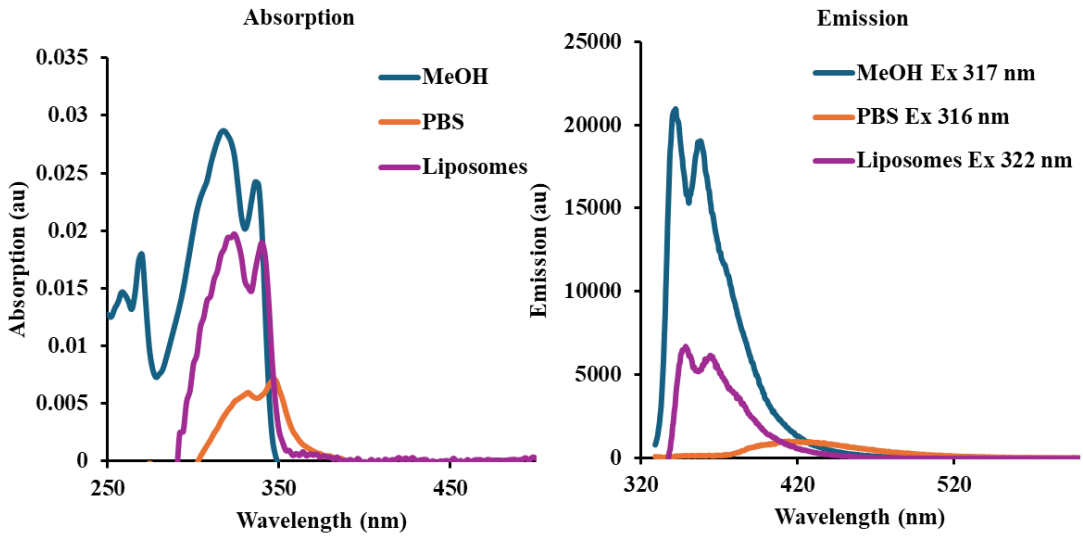

Figure 28: Absorption and emission spectra of 172b in polar solvents MeOH and PBS *vs* liposomes (PC: cholesterol, 7:1) (5 µM).

Lead 1-naphthyl analogue **172b** was successfully deprotected over two steps in 64% yield *via* base mediated hydrolysis of the ester followed by removal of the Boc-protecting-group with 2 M hydrochloric acid (Scheme **56**). Photophysical analysis of **176** showed that **176** retained the desirable photophysical properties upon deprotection. Direct comparison of the alkyne-conjugated α-amino acid **176** to the corresponding 1-naphthyl biaryl analogue **160h** revealed the intended benefit of installing the alkyne moiety; **176** exhibits red-shifted absorption from 282 nm to 346 nm and a five-fold increase in brightness.

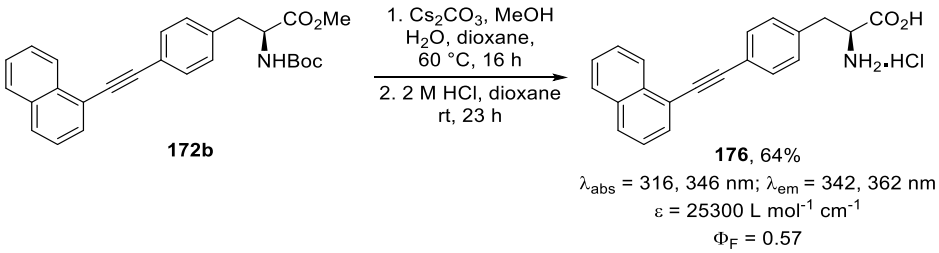

Scheme 56: Deprotection of 172b.

Red-shifted unnatural amino acids are designed to avoid spectroscopic overlap with the naturally fluorescent amino acids in order to prevent quenching and reduce background fluorescence when inserted into a peptide. To demonstrate **176** retains its strong fluorescence even when adjacent to the naturally fluorescent amino acids, dipeptides **178** and **179** were synthesised. The ester of **172b** was first hydrolysed

using caesium carbonate followed by amide coupling with the methyl esters of L-phenylalanine and L-tryptophan employing HOBt and PyBOP as coupling reagents (Scheme **57**). This gave dipeptides **178** and **179** in 79% and 76% yield, respectively.

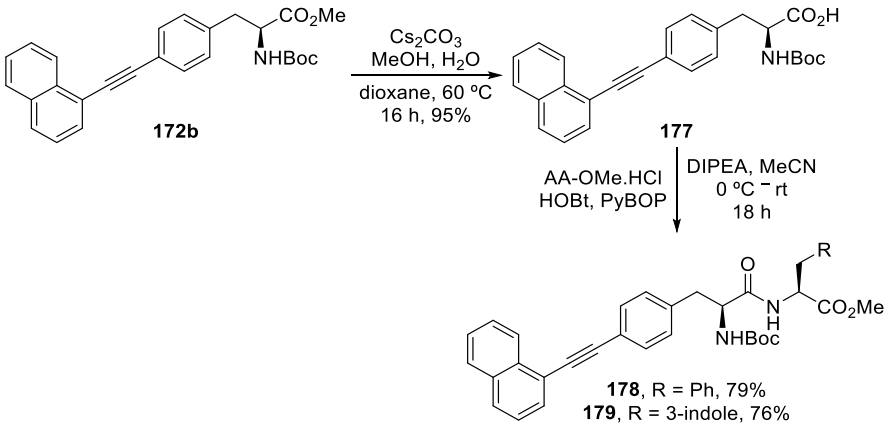

Scheme 57: Dipeptide synthesis 178 and 179.

The absorption and emission of dipeptides **178** and **179** were recorded (Figure **29**). Upon excitation at either the absorption maximum of the unnatural α-amino acid **172b** (316 nm), or the naturally fluorescent amino acids (L-phenylalanine: 260 nm; L-tryptophan: 275 nm), the emission spectra were dominated by the unnatural analogue. This indicates that the unnatural fluorescent α-amino acid **172b** can be incorporated into a peptide where its emission will not be affected by intrinsic fluorescence from the natural amino acids.

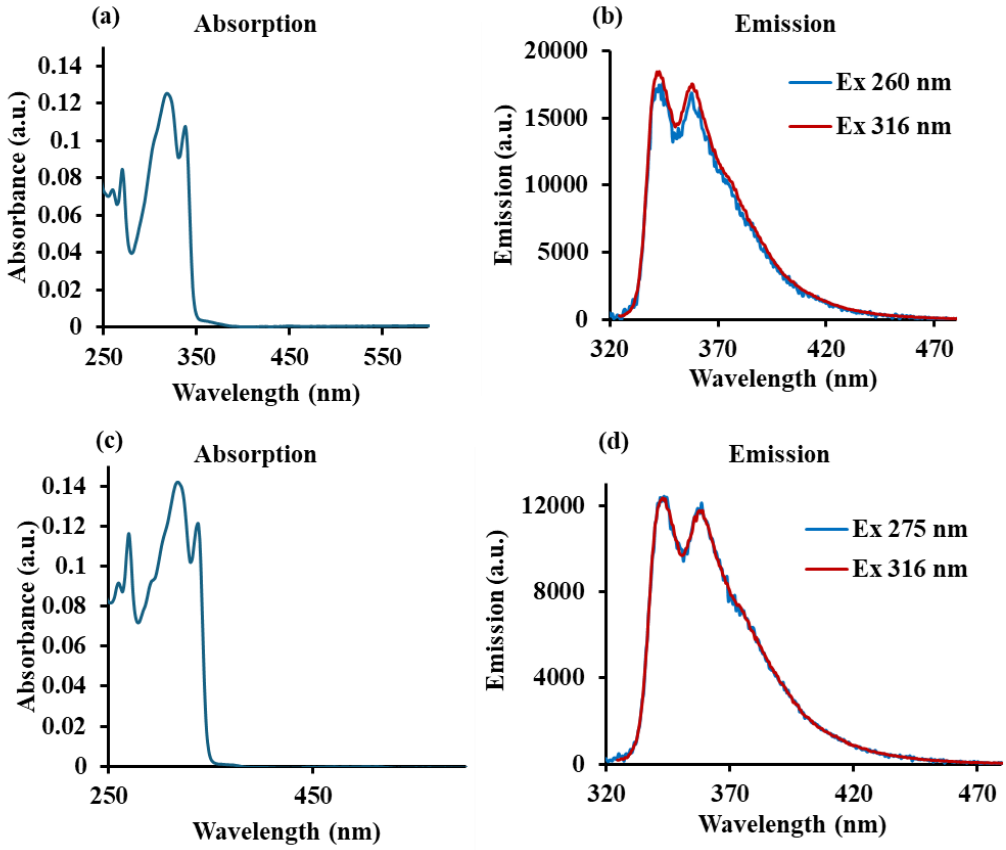

Figure 29: (a) Absorption and (b) emission of dipeptide 178 (5 µM, MeOH). (c) Absorption and (d) emission of dipeptide 179 (5 µM, MeOH).

2.3.4 Conclusions

In summary, following the successful one-pot nonaflate-formation and Suzuki-Miyaura cross-coupling reaction of tyrosine to access biaryl α-amino acids, a similar method incorporating copper-free Sonogashira cross-coupling reactions was developed to access alkyne-conjugated phenylalanine analogues. Installation of the alkyne moiety resulted in a red-shift of the absorption maximum relative to the biaryl series. In particular, analogues bearing electron-withdrawing substituents or highly conjugated naphthalene moieties exhibited promising fluorescent properties. The highest brightness was observed for 1-naphthyl analogue **172b** with a value of 15550 cm^{-1} M^{-1}, representing a five-fold increase relative to the corresponding biaryl compound. Naphthyl analogue **172b** also demonstrated high sensitivity to lipophilic environments, with an eight-fold enhancement in emission intensity in liposomes compared to phosphate buffer. Lastly, the unnatural α-amino acid **172b** was

incorporated into dipeptides containing the naturally fluorescent amino acids L-phenylalanine and L-tryptophan. Clearly defined emission from the 1-napthyl analogue was observed upon excitation of the dipeptides, without interference from the intrinsic fluorescence of the proteinogenic amino acids.

2.3.5 Expansion of the arylalkynyl *α*-amino acid library

The one-pot synthesis of alkyne extended phenylalanine analogues from tyrosine by hydroxyl group activation followed by copper-free Sonogashira cross-coupling was limited by the availability of aryl alkyne substrates. To address this limitation, and expand the arylalkynyl *α*-amino acid library, an alternative synthetic approach was explored. The new approach involved the preparation of an alkyne-derived phenylalanine which could undergo Sonogashira cross-coupling with more readily available aryl bromides. To access the key phenylacetylene intermediate, a one-pot coupling of a protected tyrosine analogue with TMS-acetylene was developed (Table **8**). Under the one-pot nonaflate-formation and copper-free Sonogashira cross-coupling reaction conditions described previously (section 2.3.1), carbonate-mediated TMS-deprotection was observed, giving **181** in 22% yield (entry 1). TMS-deprotection was mitigated by substituting to triethylamine as the base, giving **180** in 46% yield (entry 2). After an unsuccessful attempt to improve the yield by increasing the temperature (entry 3), it was found that batch addition of the catalyst (2 × 3 mol%) over a 23 h reaction period resulted in full conversion from the nonaflate and isolation of **180** in an excellent yield of 96% (entry 4).

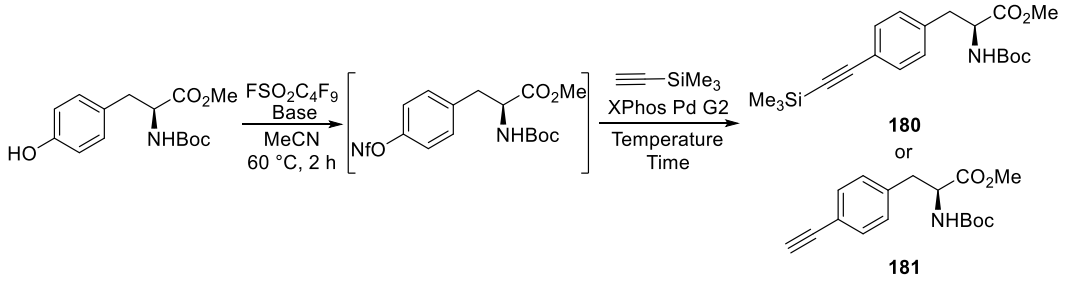

Entry	Base	Catalyst Loading (mol%)	Temperature (°C)	Time (h)	Yield
1	Cs_2CO_3	5	70	5	22% (**181**)
2	Et_3N	5	70	5	46% (**180**)
3	Et_3N	5	85	5	39% (**180**)
4	Et_3N	2 × 3	70	23	96% (**180**)

Table 8: One-pot synthesis of TMS-protected phenylacetylene analogue 180.

TMS-deprotection using tetrabutylammonium fluoride (TBAF) was subsequently explored. Conditions reported by Xia and co-workers[201] utilising 1.1 equivalents of (TBAF) at room temperature proved sluggish, resulting in an additional 0.6 equivalents being added after 1.5 h, then a further 1.1 equivalents being added after 3.5 h, to give **181** in a low yield of 15% (Table **9**, entry 1). To increase the reaction rate 3 equivalents of TBAF were added dropwise over 5 minutes then the reaction stirred for a further 15 minutes (entry 2). The reaction was also cooled to 0 °C to mitigate degradation. This gave key phenylacetylene intermediate **181** in 90% yield.

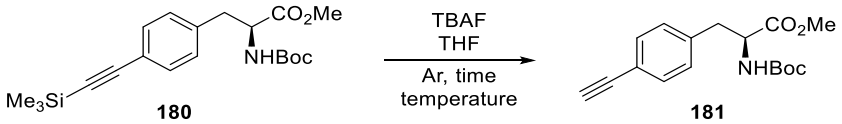

Entry	TBAF Equivalents	Time (h)	Temperature (°C)	Yield
1	1.1 then 1.7	9.5	Room temperature	15%
2	3	0.3	0	90%

Table 9: Deprotection of 180.

Phenylacetylene intermediate **181** was then subjected to Sonogashira cross-coupling reactions with various commercially available aryl bromides. For this, reaction conditions previously developed within the group, utilising $Pd(PPh_3)_2Cl_2$ and a

copper cocatalyst, were employed.[115] The reaction mixture was initially heated to 90 °C in order to facilitate formation of the active palladium(0) catalyst, after which it was allowed to return to room temperature. A brief optimisation was undertaken for the Sonogashira cross-coupling of **181** with 4-iodobenzonitrile (Table **10**). Increasing the initial heating period from 0.1 to 0.5 hours increased the yield from 65% to 82% (entry 2). Batch addition of the catalyst after 3 hours further increased the yield to 93% (entry 3). This was a significant improvement compared to the one-pot cross-coupling from tyrosine, which gave **172f** in 51% yield (section 2.3.2), indicating this approach is better suited for the synthesis of arylalkynyl *α*-amino acids bearing electron withdrawing groups.

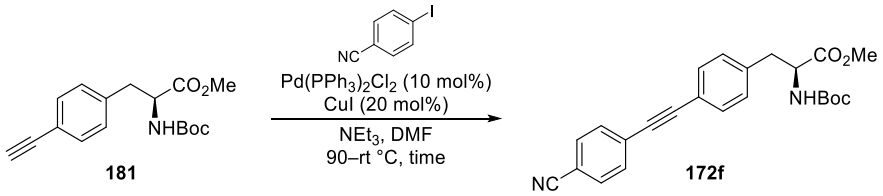

Entry	Time held at 90 °C (h)	Total time (h)	Catalyst Addition	Yield (%)
1	0.1	21 h	Single	65
2	0.5	21 h	Single	82
3	0.5	21 h	Batch	93

Table 10: Optimisation of Sonogashira cross-coupling reaction of 181.

Considering the poor photophysical properties observed for analogues bearing electron donating groups in the initial library of arylalkynyl analogues (section 2.3.3), the substrate scope was focussed on highly conjugated and electron withdrawing substrates (Scheme **58**). The method tolerated both *ortho*- and *para*-substituted aryl bromides which gave **172j**, **172k** and **172l** in 52%, 84% and 61% yields, respectively. Cross-coupling with 1-bromonaphthalene gave **172b** in 33% yield, a significantly lower yield than that achieved *via* the direct one-pot cross-coupling of tyrosine (67%). Substituted naphthyl bromide substrates were also successful and gave **172m** and **172n** in 65% and 61% yields, respectively. Several quinoline analogues **172o**–**172r** were synthesised in 50–87% yields. In addition to functioning as an electron-deficient heteroatom motif, the position of the nitrogen atom and the substitution pattern on the quinoline ring, can significantly impact the electronic configuration and conformation of the system, thereby modulating the photophysical properties.[202,203] For example, in a series of fluorescent pyridine

compounds, *ortho*- or *para*-substitution promoted emission from a charge-transfer excited state, whereas *meta*-substitution favoured emission from a locally excited state.[204]

Analogues **172s**–**172w** were inspired by known chromophores that have previously been exploited in the synthesis of fluorescent α-amino acids (Scheme **58**). Nitrobenzodiazole analogue **172s** was synthesised in a moderate yield of 49%. Despite milder conditions at room temperature, purification of **172s** was challenging due to the formation of brightly coloured byproducts. Nitrobenzodiazole (NBD) derived amino acids are attractive for fluorescence imaging owing to their small size yet far red-shifted absorption ($\geq$ 450 nm) and emission ($\geq$ 540 nm).[83-85,88,89,205] This has led to the development of several amino acid probes by Liao, Van Nieuwenhze and Vendrell groups in which the NBD-derived amino acids has been used for monitoring proteolysis in high-density microarrays,[84] visualisation of peptidoglycan synthesis in bacterial cells,[205] late stage peptide labelling of cell penetrating peptides[88] and real-time monitoring of bacterial cultures.[85] Coumarin derived amino acids are also widely used due to their compact, yet strongly fluorescent nature.[36,41,206,207] Specifically, coumarin analogues bearing electron-donating groups have shown improved photophysical properties, resulting from conjugation to the enone. As such, coumarin analogue **172t** was synthesised in a low yield of 33%. The low yield was attributed to challenging separation from minor byproducts and notable formation of the homocoupling byproduct.

Two xanthone analogues **172u** and **172v** were synthesised in 48% and 78% yields, respectively (Scheme **58**). The xanthone moiety has been utilised as a component of several fluorescent dyes.[208,209] Compared to unsubstituted xanthone, which is poorly emissive due to ultrafast intersystem crossing (ISC),[210] substitution at the 2-position with electron donating groups has been shown to significantly improve the photophysical properties resulting in red-shifted fluorescent compounds (λ_{Em} = 493–532 nm).[209] The photophysical properties of xanthone have been exploited in cysteine-reactive fluorescent probes[211] and photo-reactive fluorescent amino acids designed to investigate protein folding.[212] Finally, analogue **172w** was inspired by the 2-acrydonylalanine fluorescent amino acid that has been utilised in various applications including protein-protein interactions,[67] fluorescent lifetime imaging microscopy[66] and several FRET studies of protein conformational changes[63] and

protease sensing.[60] To avoid synthesis of the acridinone core, a truncated analogue **172w** was synthesised utilising commercially available 7-bromoquinolin-4-ol in 30% yield. The relatively low yield of this analogue was due to difficult separation from the homo-coupled byproduct.

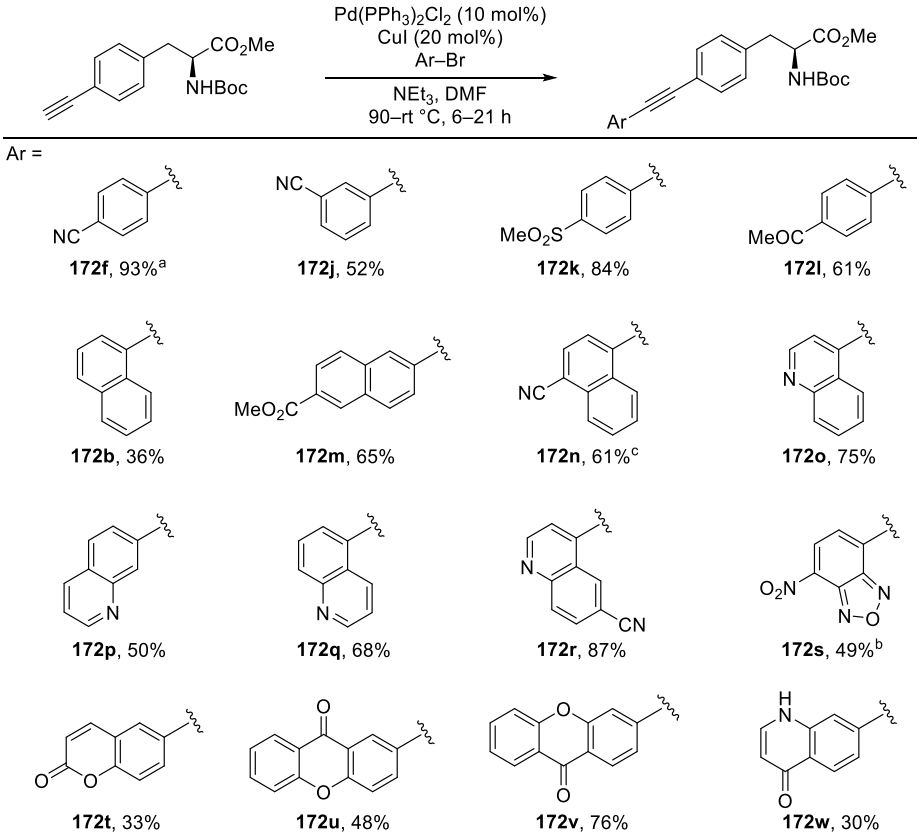

[a]Aryl-iodide substrate; [b]Aryl-chloride substrate; [c]XPhos Pd G2 catalyst

Scheme 58: Expansion of arylalkynyl phenylalanine analogue library.

Following the synthesis of the expanded arylalkynyl α-amino acid library, the photophysical properties were analysed. Consistent with the initial library discussed in section 2.3.2, the alkyne extended analogues exhibited red-shifted absorption and high molar extinction coefficients relative to both the biaryl series and L-phenylalanine. Absorption and emission spectra for analogues **172j**–**172q** in methanol is shown in Figure **30**, and the photophysical properties summarised in Table **11**. Methyl naphthoate **172m** analogue exhibited a quantum yield of 0.98, resulting in an exceptionally high brightness of 36740 cm^{-1} M^{-1}. This value is comparable to that of fluorescein isothiocyanate (39000 cm^{-1} M^{-1}), a commonly used fluorescent reagent.[213] Similarly, cyanonaphthalene analogue **172n** displayed strong fluorescence properties including red-shifted absorption (356 nm) and high

brightness (22800 cm^{-1} M^{-1}). Among the quinoline analogues, the 7-ethynyl analogue **172p** exhibited the highest brightness (14600 cm^{-1} M^{-1}) as well as relatively red-shifted emission (344 nm). In contrast, the 4-ethynyl quinoline analogue **172o** exhibited a significantly lower brightness of 2200 cm^{-1} M^{-1}, which could be attributed to non-radiative relaxation pathways arising from low lying $n \rightarrow \pi^*$ transitions involving the quinoline nitrogen lone pair.[202,214]

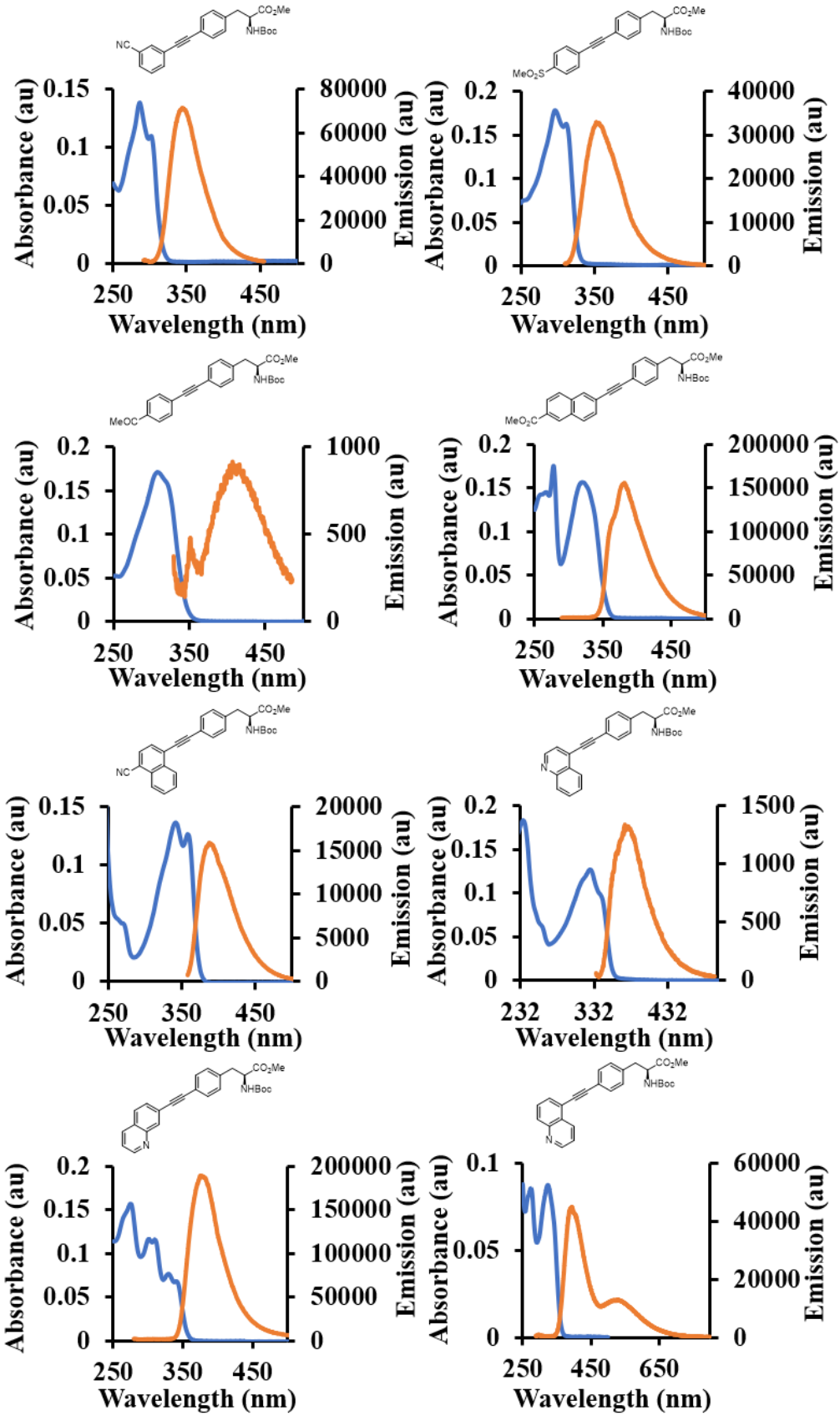

Figure 30: Absorption (blue) and emission (orange) of arylalkynyl phenylalanine analogues 172j–172q (5 µM in MeOH).

Amino Acid	λ_{Abs} (nm)	ε (cm^{-1} M^{-1})	λ_{Em} (nm)	S.S. (nm)	Φ_F	BRT (cm^{-1} M^{-1})
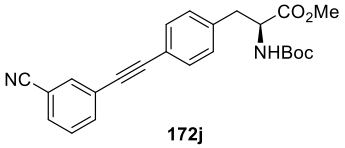 **172j**	**286** 302	27900	349	37	0.21	5850
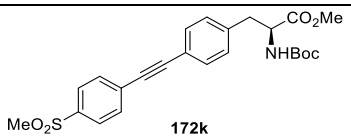 **172k**	296	34900	352	56	0.12	4020
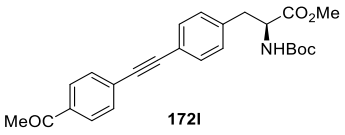 **172l**	308	34300	413	105	-	-
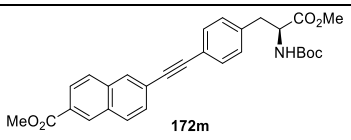 **172m**	**278** 320	37200	380	102	0.98	36740
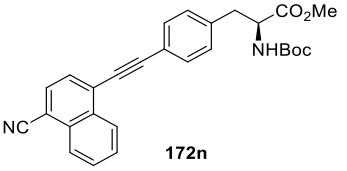 **172n**	**242** 343 356	26200	387	145	0.87	22800
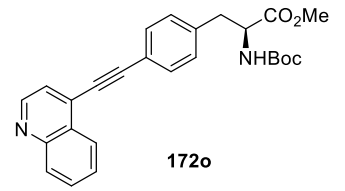 **172o**	326	24900	380	54	0.09	2200
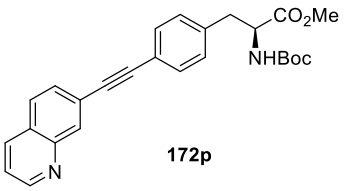 **172p**	**274** 312 344	34000	380	106	0.42	14600
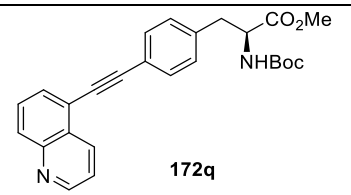 **172q**	274 **324**	17000	**396** 529	72	0.38	6450

Table 11: Photophysical properties of arylalkynyl phenylalanine analogues 172j–172q. Comparison of absorption (λ_{Abs}) and emission (λ_{Em}) maximum, molar absorption coefficient (ε), stokes shift (S.S), quantum yield Φ_F and brightness (BRT) in methanol.

Absorption and emission spectra for analogues **172r**–**172q** is shown in Figure **31**, and the photophysical properties summarised in Table **12**. It was postulated that a cyano quinoline analogue could combine the red-shifted emission of the quinoline analogue **172n** and the high brightness of **172p**, however, whilst **172r** displayed moderate red-shifted emission (419 nm), a low quantum yield of 0.07 resulted in a poor brightness of 1300 cm^{-1} M^{-1}. Analogues incorporating chromophores previously exploited in fluorescent amino acids (**172s**–**172w**), all exhibited weak fluorescence.

NBD analogue **172s** is reported in acetonitrile, following a brief solvatochromic study revealed this analogue to be essentially non-emissive in other polar solvents (MeOH, H_2O, DMSO) or non-polar solvents (EtOAc, THF). NBD analogue **172s** displayed red-shifted absorption (414 nm) and emission (561 nm) but poor quantum yield (0.03) and brightness (300 cm^{-1} M^{-1}) in acetonitrile. Lower quantum yields can be tolerated for amino acids near the IR region as reduced background fluorescence (e.g. autofluorescence from lysosomes) at near IR wavelengths results in higher signal-to-noise ratio of emission from fluorescent amino acids, even at relatively low brightness values. However, **172s** was still considered to have insufficient brightness to be utilised as a fluorescent probe. Nitro-groups are well known to act as fluorescence quenchers, primarily resulting from non-radiative ($n \rightarrow \pi^*$) transitions associated with the non-bonding electrons. Furthermore, the strong electron withdrawing capability results in an electron sink at the nitro-group, forming a charge-transfer state that suppresses the radiative decay channel.[215]

Of the α-amino acids containing known chromophores, xanthone analogue **172u** displayed the highest brightness (5172 cm^{-1} M^{-1}) as well as moderately red-shifted absorption (290 nm, 353 nm) and emission (453 nm). However, **172u** exhibits considerably weaker fluorescence compared to the naphthyl analogues **172m** and **172n** (Table **11**). This highlights the benefit of *de novo* design of fluorescent α-amino acids and how modification of the naturally fluorescent amino acids with known chromophores can result in weaker emission from the chromophore, despite extended conjugation.

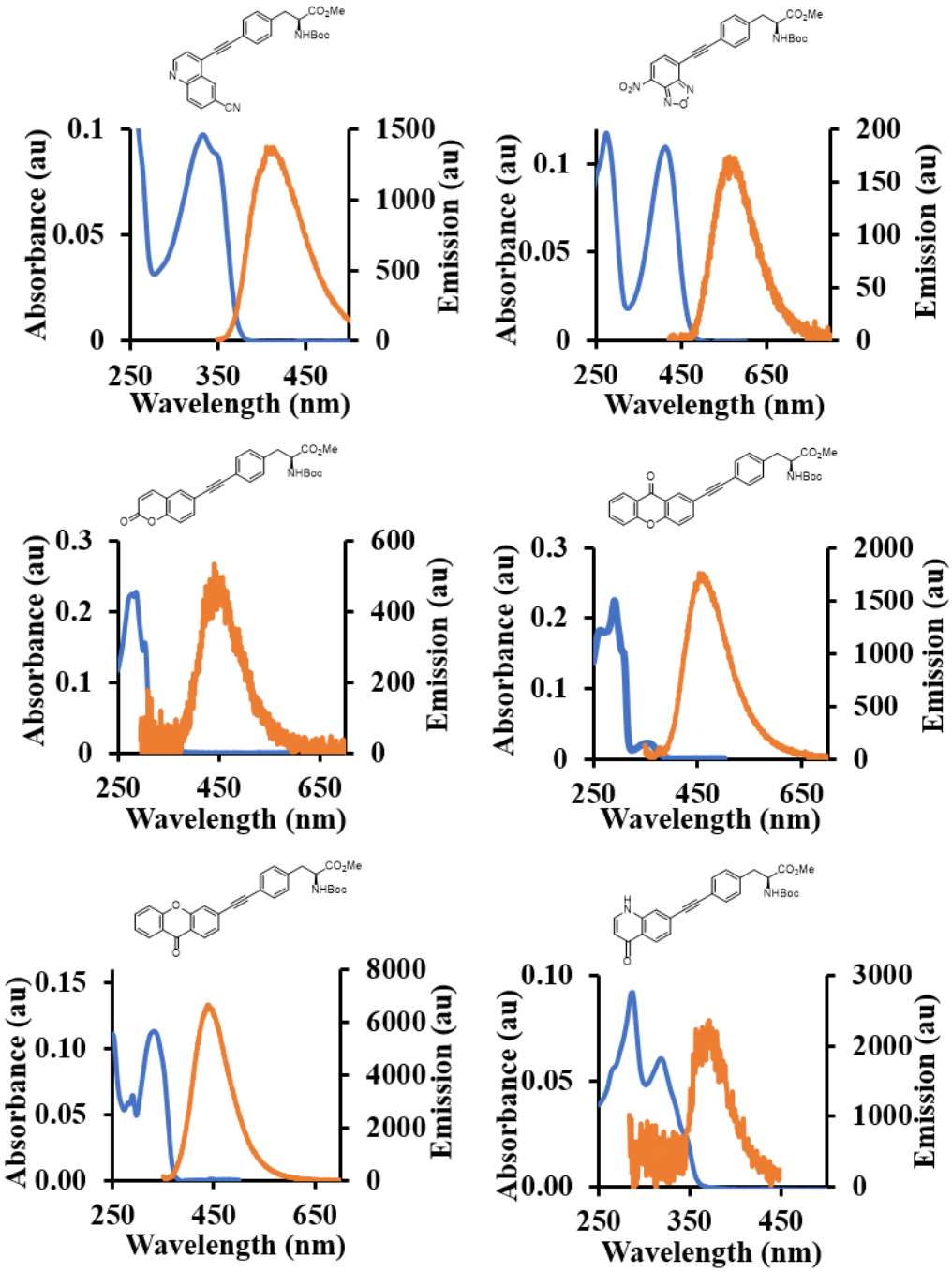

Figure 31: Absorption (blue) and emission (orange) of arylalkynyl phenylalanine analogues 172r–172w (5 μM in MeOH). NBD analogue was recorded in MeCN (5 μM).

Amino Acid	λ_{Abs} (nm)	ε (cm^{-1} M^{-1})	λ_{Em} (nm)	S.S. (nm)	Φ_F	BRT (cm^{-1} M^{-1})
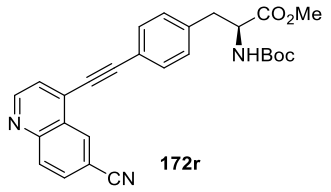 **172r**	332	19200	419	87	0.07	1300
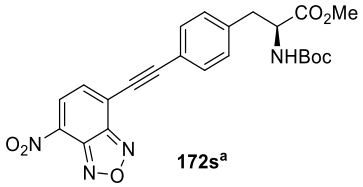 **172s**[a]	**274** 414	9800	561	287 147	0.03	300
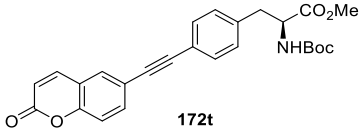 **172t**	385	39700	448	163	0.03	1000
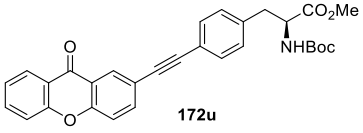 **172u**	**290** 353	43100	453	163	0.12	5172
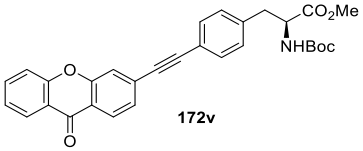 **172v**	332	32400	437	105	0.08	2630
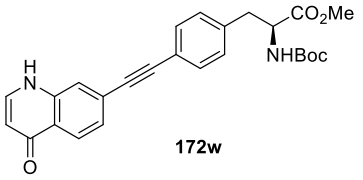 **172w**	**286** 322	39800	372	86	-	-

Table 12: Photophysical properties of arylalkynyl phenylalanine analogues 172r–172w (MeOH). [a]Recorded in MeCN. Comparison of absorption (λ_{Abs}) and emission (λ_{Em}) maximum, molar absorption coefficient (ε), stokes shift (S.S), quantum yield Φ_F and brightness (BRT).

In summary, the one-pot methodology for the cross-coupling with aryl alkyne substrates was most successful for substrates that were highly conjugated and bearing electron donating groups. An alternative approach to extend the scope of electron deficient substrates was developed. A key phenylacetylene intermediate was synthesised utilising a similar one-pot cross-coupling methodology from tyrosine with a TMS-acetylene substrate. Following deprotection, this intermediate enabled Sonogashira cross-coupling reactions with electron-deficient and commercially available aryl bromides. Notably, the polycyclic analogues bearing electron withdrawing groups exhibited very promising photophysical properties. Cyanonapthalene **172n**, methyl naphthoate **172m** and quinoline analogue **172p**

exhibited excellent brightness values for small fluorescent *α*-amino acids (36740, 22800 and 14600 cm^{-1} M^{-1}, respectively).

2.3.6 Additional photophysical and Raman spectroscopy studies

Considering the significant lipophilic sensitivity displayed by lead 1-naphthyl analogue **172b** (Section 2.3.3), several polycyclic analogues, which exhibited high brightness in methanol, were analysed in lipophilic environments (7:1 PC: cholesterol in PBS). Naphthyl analogues bearing electron withdrawing groups **172m** and **172n** exhibited high lipophilic sensitivity (Figure **32**). Methyl naphthoate analogue **172m** exhibited a bathochromic shift in PBS (λ_{Em} = 423 nm) compared to liposomes (λ_{Em} = 358 nm) which coincided with a 10.5-fold decrease in emission intensity (Figure **32b**). Similarly, the emission maxima of cyanonaphthalene analogue **172n** shifted from 378 nm in liposomes to 546 nm in PBS along with a 4-fold decrease in emission intensity (Figure **32d**).

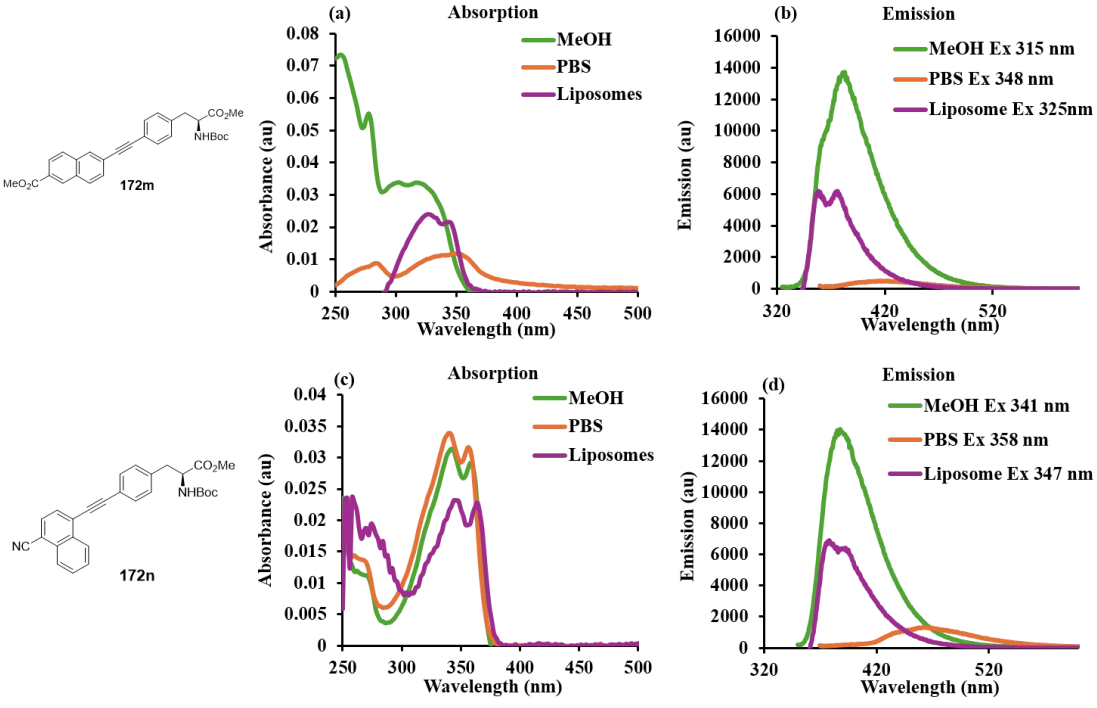

Figure 32: Absorption and emission of 172m and 172n in liposomes, PBS and MeOH (5 µM).

Quinoline analogues **172p** and **172o** were also examined in lipophilic environments (Figure **33**). For **172p**, the emission maximum shifted from 374 nm in liposomes to 494 nm in PBS, accompanied by a moderate 2.7-fold decrease in emission (Figure **33b**). Overall, **172p** displayed reduced fluorescence in PBS and liposomes compared to methanol. In contrast, **172q** was shown to be the most sensitive to lipophilic environments. In methanol, **172q** showed dual emission, arising from a locally excited state at 396 nm and a weaker charge-transfer excited state at 529 nm. In liposomes, emission from the locally excited state dominated, compared to emission from the charge-transfer excited state in PBS which was significantly weaker. The emission intensity decreases 16-fold between the lipophilic and aqueous environments.

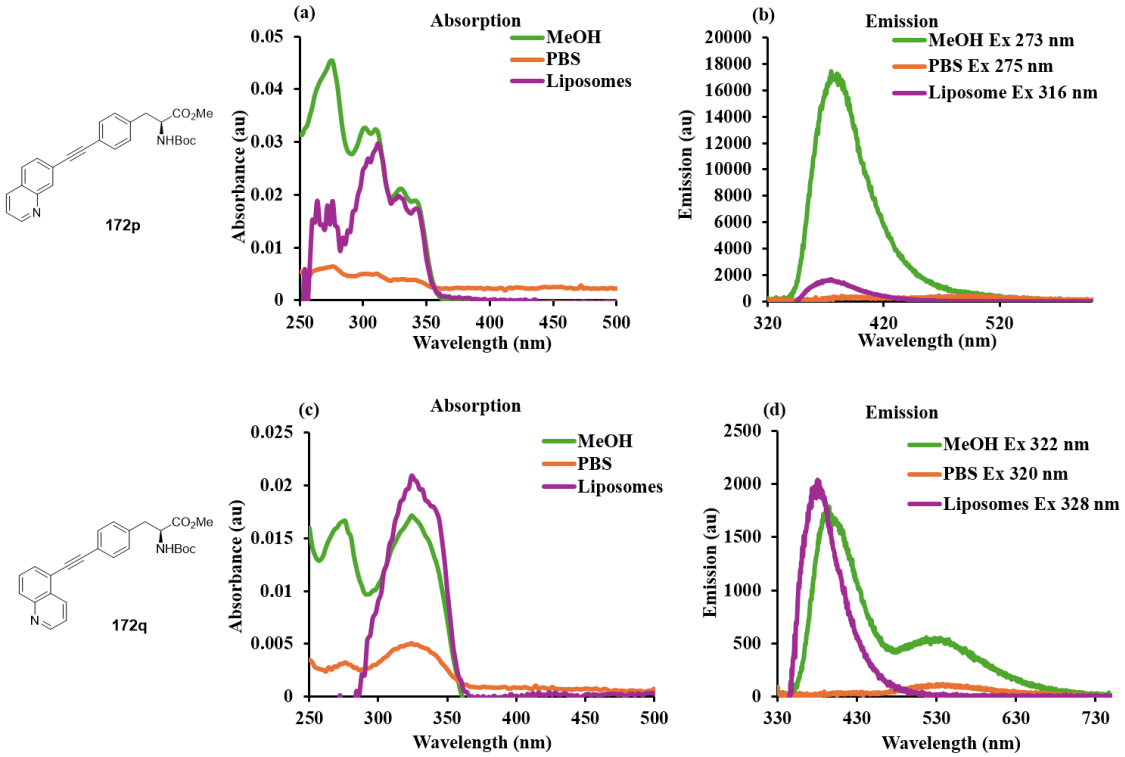

Figure 33: Absorption and emission of 172p and 172q in liposomes, PBS and MeOH. (5 µM).

Additional solvatochromic and pH studies were performed for quinoline analogues **172p** and **172q**. With the exception of water, the absorption was mostly unaffected by solvent (Figure **34a**). For **172p**, as well as weak emission in water, the solvatochromic study revealed weak emission in THF and DMSO (Figure **34b**). The absorption spectrum of **172p** was generally less defined in acidic environments compared to neutral or basic which also displayed moderate-red shifting in the

absorption maximum to 366 nm (Figure **34c**). In the emission spectra, a 117 nm shift from 385 nm to 502 nm was observed upon acidification to pH 6 (Figure **34d**). This observation was somewhat unexpected given that the pKa of isoquinoline is 5.14,[174] which would suggest a change in emission should occur closer to pH 5 than pH 6. The discrepancy could be attributed to inaccurate pH adjustment or the substitution of the quinoline could have increased the pKa. Nonetheless, the significant pH sensitivity demonstrates the potential of **172p** as a pH fluorescent probe. Quinoline-based fluorescent probes have been reported for lysosome detection and intracellular pH changes, in which a change in pH is associated with a detectable colour change in the emission.[216-218]

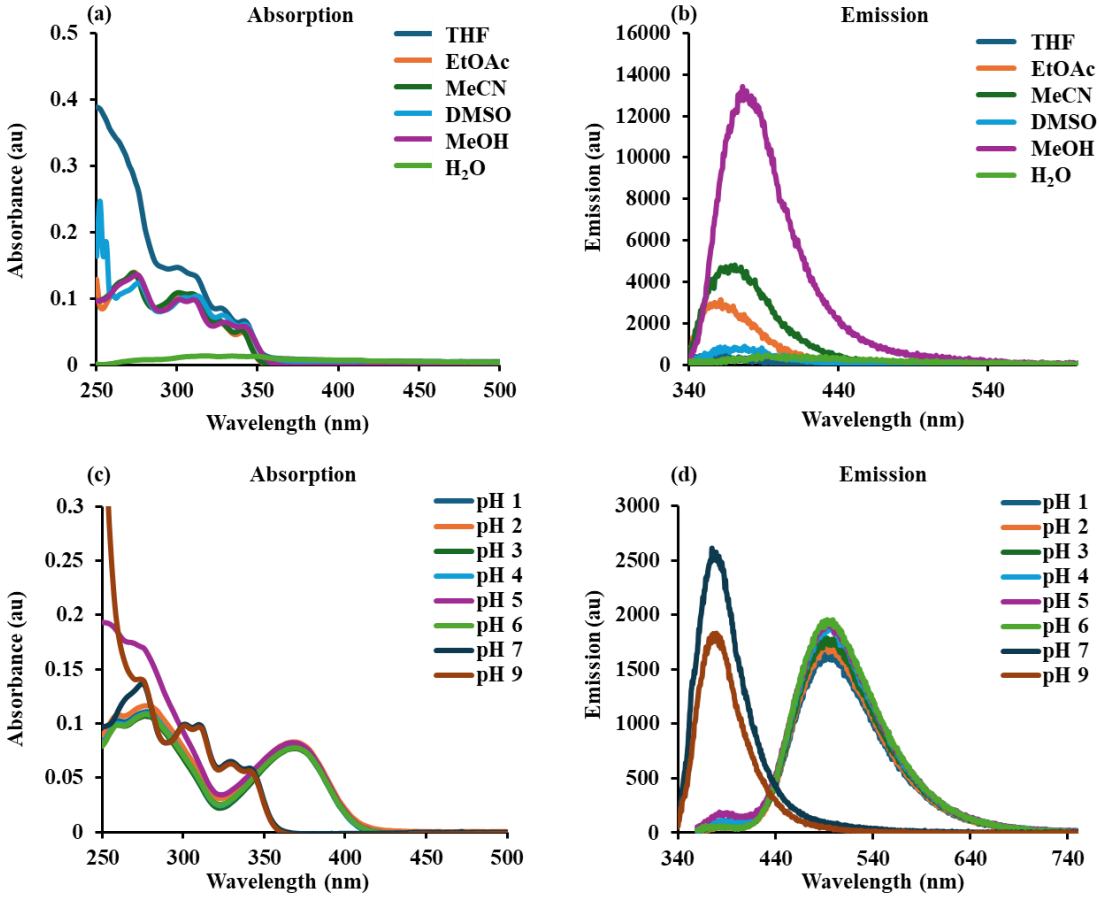

Figure 34: Solvatochromic and pH sensitivity of 7-ethynyl quinoline analogue 172p (5 µM in MeOH).

Similarly, quinoline analogue **172q** exhibited a significant change in absorption and emission in water compared to other solvents (Figure **35**). As previously observed for lipophilic/aqueous environments (Figure **33**), the emission maximum shifted from 397 nm (THF, EtOAc, MeCN, DMSO, MeOH) to 529 nm (H_2O) (Figure **35b)**.

Emission at 529 nm increased by 94% in acidic environments (Figure **35d**). This is consistent with emission at 529 nm resulting from charge-transfer, which becomes the dominant emission upon protonation of the quinoline nitrogen.

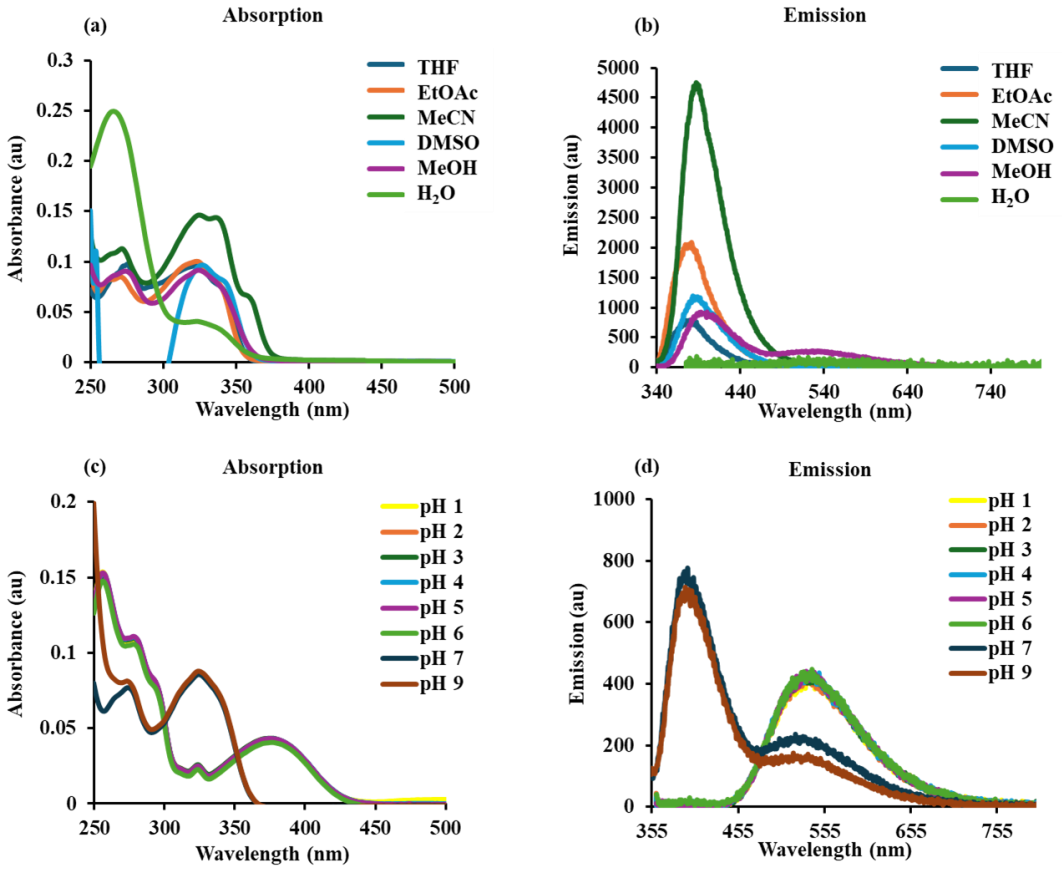

Figure 35: Solvatochromic and pH sensitivity of 5-ethynyl quinoline analogue 172q (5 µM in MeOH).

2.3.7 Raman Spectroscopy

Raman spectroscopy was also considered as a potential imaging modality for the arylalkyne *α*-amino acid analogues of phenylalanine. As with fluorescent spectroscopy, Raman spectroscopy is highly valuable as a non-invasive imaging technique. Raman tags such as nitrile, azide and alkynes exhibit distinct vibrational frequencies between 1800–2800 cm^{-1}, or the 'cell-silent' region. Named for the lack of background signal from biological molecules, Raman probes targeting the 'cell-silent' region have wide biomedical applications including analyte detection/monitoring, biomarker profiling and live cell imaging.[219,220] Unnatural amino acid Raman probes include 4-cyanophenylalanine,[221] *p*-ethynyl

phenylalanine,[222] and β-ethynyl alanine (also referred to as homopropargyl glycine (HPG)).[222-224] Whilst the reported unnatural amino acid Raman tags have gained attention due to their very small size, it is proposed, that alkyne extended phenylalanine analogues **172m**, **172n** and **172q** could function as dual fluorescence and Raman spectroscopy labels, enabling multimodal imaging with a single probe.

Raman spectra of analogues **172m**, **172n** and **172q** (Figure **36**), reveal a distinct peak in the 'cell silent' region for each of these α-amino acids, corresponding to the C≡C vibrational stretch. Due to significant baseline-distortion resulting from background fluorescence, the spectra shown in Figure **36** are preliminary. Repeated measurement of the Raman spectra of **172m**, **172n** and **172q** in which a background is measured and subtracted from the final spectra, along with smoothing using either Origin[182] software, is required. However, the preliminary data does indicate the potential for these α-amino acids to be used as biorthogonal Raman tags.

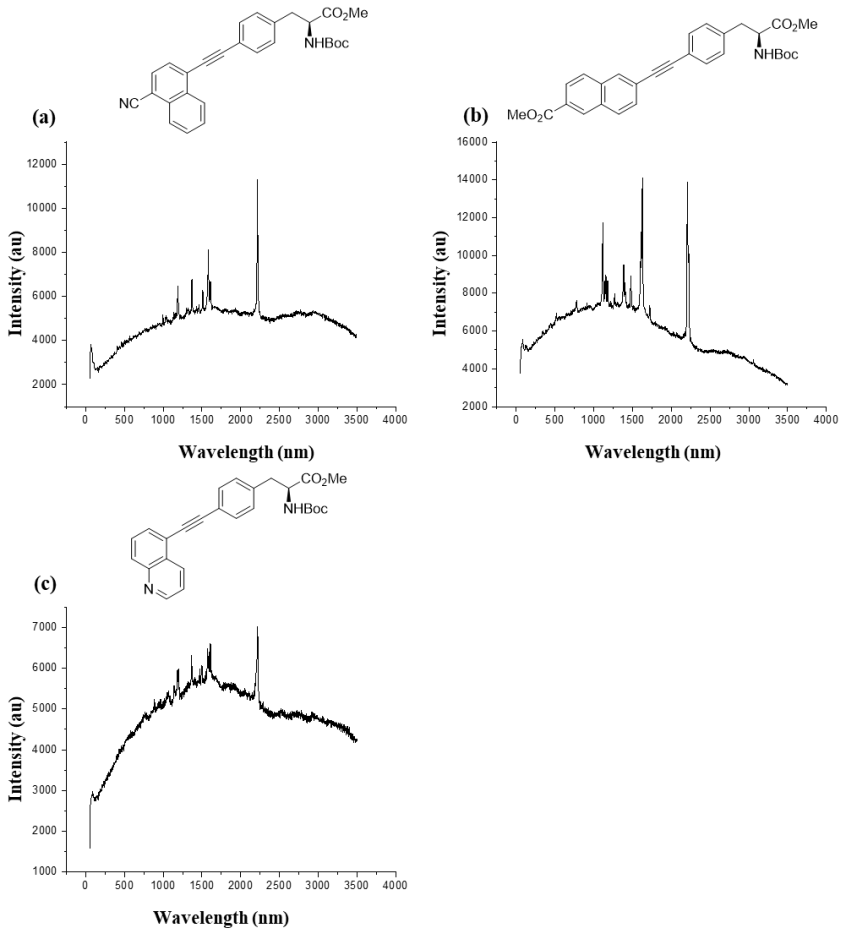

Figure 36: Preliminary Raman spectra of 172n, 172m and 172q.

2.3.8 Enantiopurity of arylalkynyl analogues of phenylalanine

In order to assess the enantiopurity of the synthetic route, dipeptide **178** was resynthesised. The previous synthesis of dipeptide **178** (Section 2.3.3) employed the one-pot preparation of the 1-naphthyl analogue **172b** from the protected tyrosine analogue. Caesium carbonate- mediated methyl ester hydrolysis followed by amide coupling utilising PyBOP and HOBt coupling reagents gave dipeptide **178**. In the alternative route, the protected tyrosine analogue was first converted to TMS-protected phenylacetylene analogue **180** (Scheme **59**). Subsequent deprotection with tetrabutylammonium fluoride afforded the phenylacetylene analogue **181**, which underwent a Sonogashira cross-coupling with 1-bromonaphthalene to give 1-napthyl analogue **172b**. Intermediate **172b** was subjected to the same methyl ester hydrolysis and amide coupling as before to give dipeptide **178**.

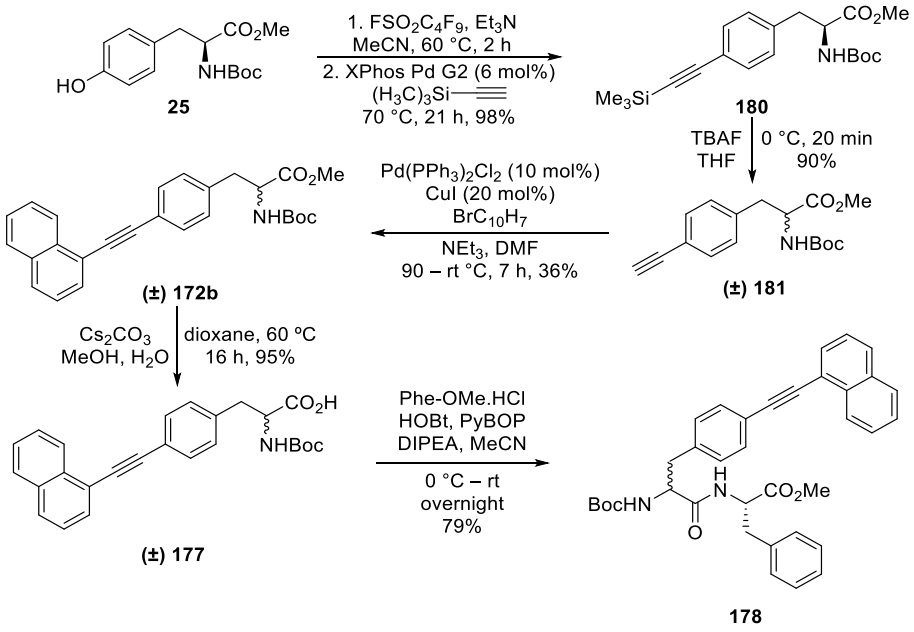

Scheme 59: Resynthesis of dipeptide 178.

It became apparent, however, that dipeptide **178**, as synthesised *via* the route outlined in Scheme **59**, comprised a mixture of diastereomers. Figure **37** shows the ^{1}H NMR spectrum of dipeptide **178** previously synthesised using 1-ethynylnaphthalene (Section 2.3.3), with the expanded region highlighting the N-H doublet and the doublet of doublets observed for the indicated aromatic protons. Whereas the earlier synthesis afforded the (*S*,*S*)-diastereomer (Figure **37a**), synthesis of **178** *via* the route

outlined in Scheme **59** yielded a mixture of diastereomers that were partially separable by column chromatography. The ^{1}H NMR spectra of the two sets of collected fractions are shown in Figure **37b** and **37c**. By comparison to the (*S*,*S*)-diastereomer in Figure **37a**, fraction set A was found to contain predominantly the (*R*,*S*)-diastereomer, whereas fraction set B predominantly contains the (*S*,*S*)-diastereomer. The diastereomeric ratio of dipeptide **178** was not determined, as a ^{1}H NMR spectrum of the crude material was not recorded prior to purification and the complete separation of the diastereomers by column chromatography was not achieved.

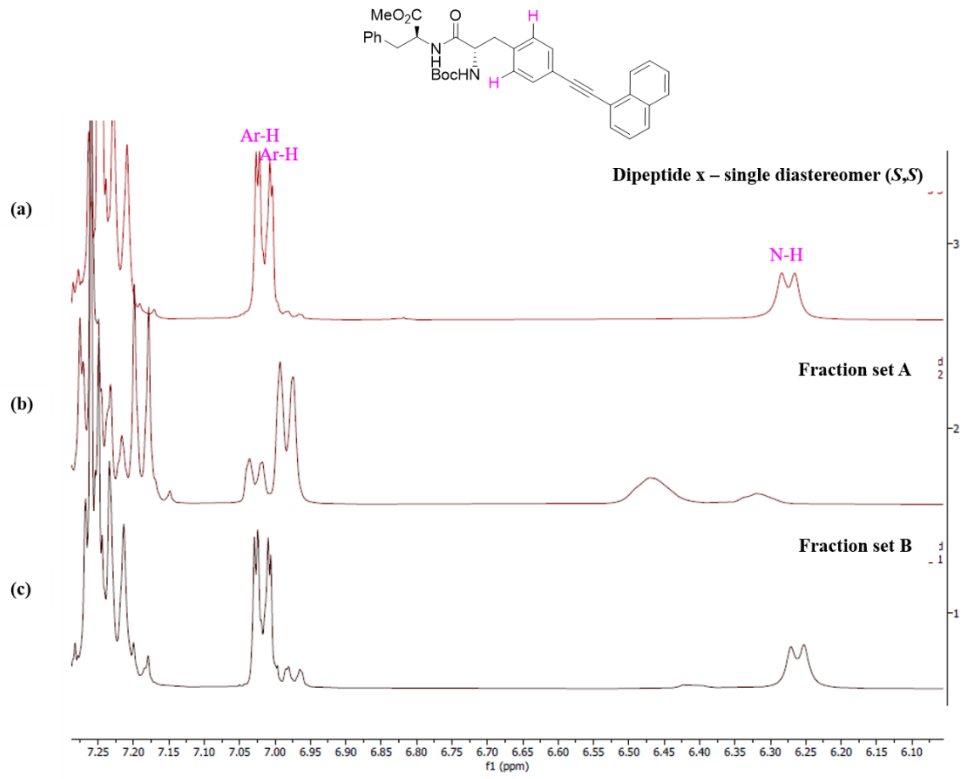

Figure 37: Comparison of ^{1}H NMR spectra of dipeptide 178 ($CDCl_3$). ^{1}H NMR spectrum of single diasteromer as synthesised in section 2.3.3 (top) compared to mixture of diasteromers obtained as outlined in Scheme 59 which were partially separated into fraction set A and B.

Having identified **178** as a mixture of diastereomers, chiral HPLC analysis was performed to determine the stage at which racemisation was occurring. In order to obtain a racemic mixture for chiral HPLC analysis, the synthetic route was repeated using protected D-tyrosine as the starting material. Chiral HPLC analysis of the TMS-phenylacetylene intermediate **180** was carried out using a Chiralpak® AD-H column with a 0.5% IPA in hexane solvent system (Figure **38**). A racemic mixture of **180** was

first analysed (Figure **38a**), followed by separate analysis of the *R* (Figure **38b**) and *S* (Figure **38c**) enantiomers to enable peak identification. Despite some peak broadening for the *R* enantiomer, good separation of the *R* and *S* enantiomers was achieved. Analysis of the *S* enantiomer reveals >99% enantiopurity, indicating that the one-pot nonaflate-formation and copper-free Sonogashira cross-coupling reaction did not induce racemisation of the starting material.

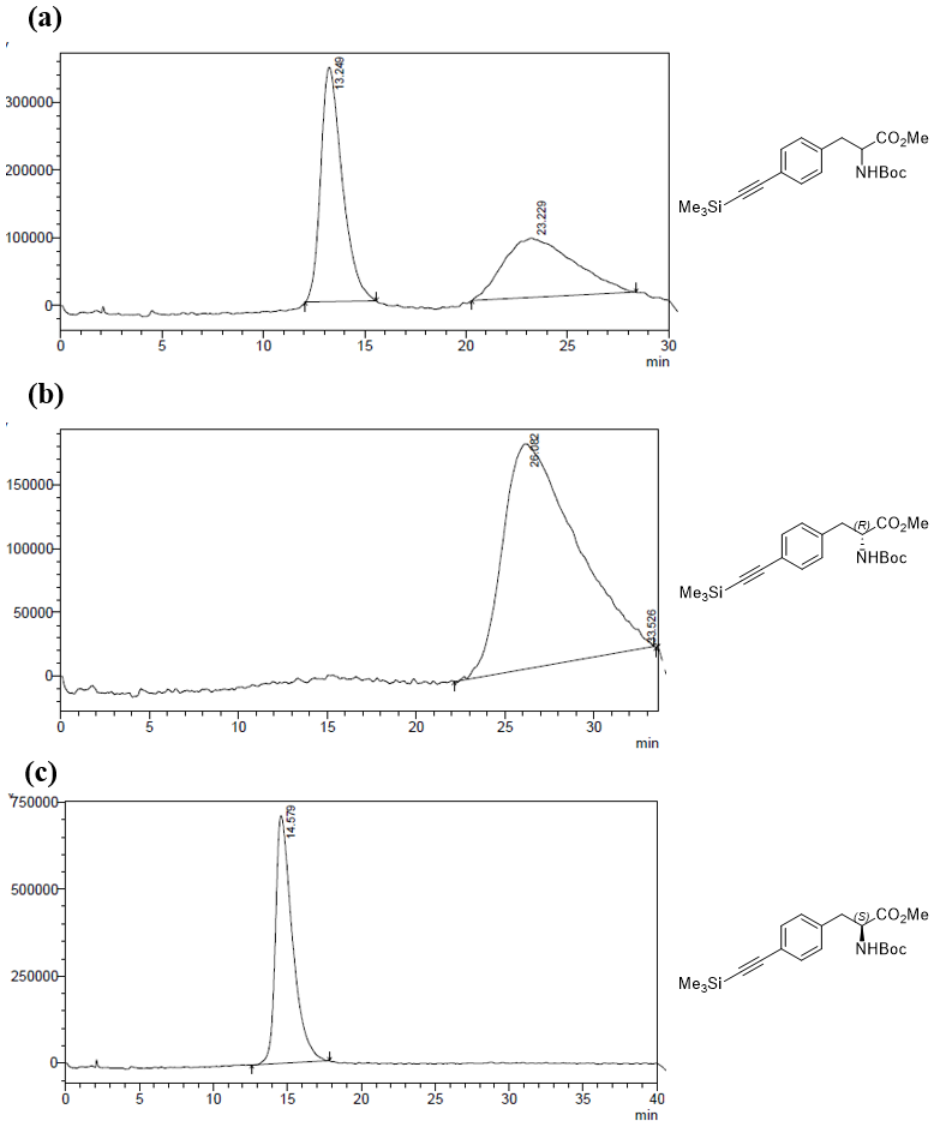

Figure 38: Chiral HPLC analysis of TMS-phenylacetylene intermediate 180.

Next, chiral HPLC analysis of product **181** following TMS removal with TBAF was performed. Unfortunately, separation of the *R* and *S* enantiomers was not achieved. Inconsistencies between chiral HPLC runs, despite several column cleaning methods and extended equilibration being employed indicated an issue with the chiral HPLC column. Although baseline separation was not achieved, two peaks were clearly

observed for the racemic mixture (Figure **39a**). Subsequent analysis of **181** indicated an approximately 1:1 mixture of enantiomers (Figure **39b**). While accurate determination of the ee was not possible due to poor separation, it was evident that TMS deprotection utilising three equivalents of tetrabutylammonium fluoride (TBAF) in THF induced racemisation. Under anhydrous conditions, the 'naked' fluoride ion acts as a base and abstracts the acidic α-hydrogen atom, resulting in racemisation.[225] Deprotection of the same *α*-amino acid analogue using TBAF has been reported in literature with fewer equivalents (1.1 or 2), however, the enantiopurity of the product was not discussed.[201,226] It was therefore necessary to identify an alternative method of deprotection.

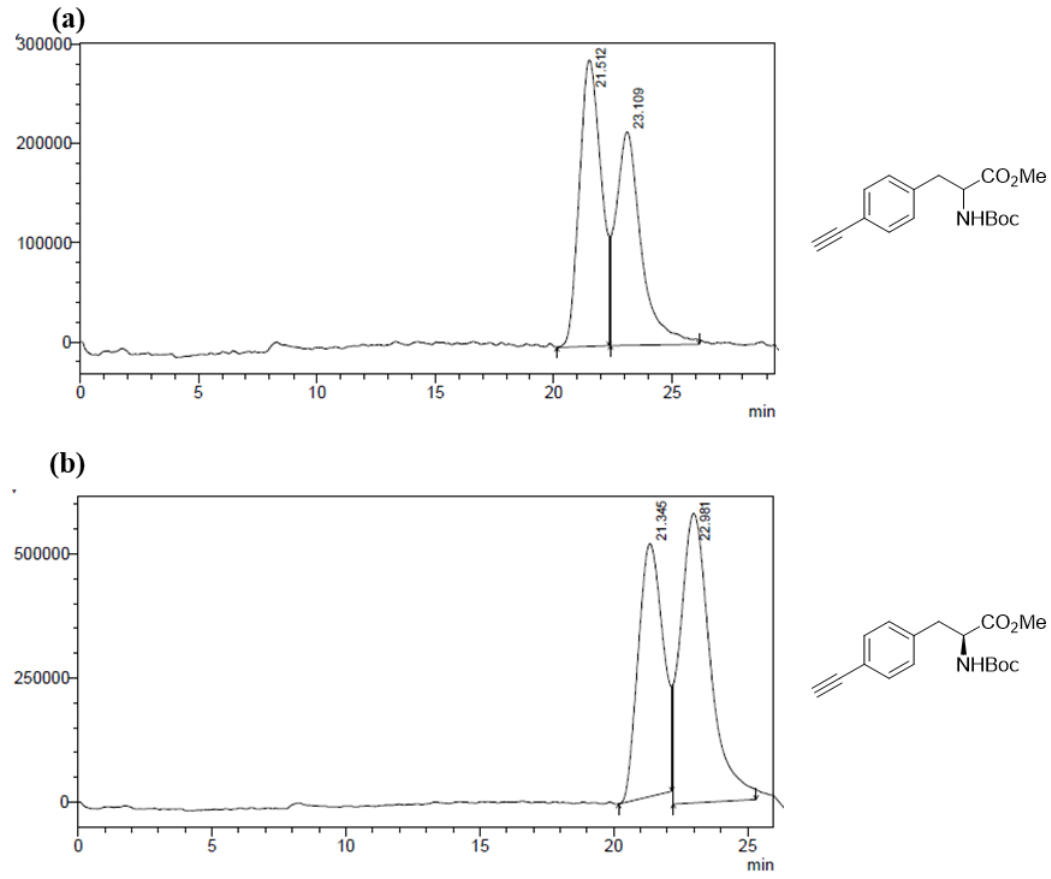

Figure 39: Chiral HPLC analysis of phenylacetylene intermediate 181.

Verlinden *et. al.* reported the use of sodium hydroxide (0.23 M, 1.6 equivalents) for the TMS-removal and methyl ester hydrolysis of **180** in 60% yield.[227] A modified procedure using sodium hydroxide (0.23 M, 6.2 equivalents) gave **182** in 91% yield (Scheme **60**). As well as removal of the TMS group, this approach gave carboxylic acid product **182**, which was considered beneficial for subsequent amide coupling.

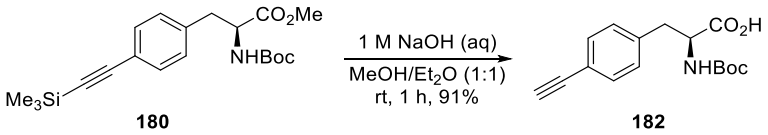

Scheme 60: Deprotection of 180 using 1 M sodium hydroxide.

As the Chiralpak® AD-H chiral column previously failed to give consistent results or fully separate **181**, an alanine dipeptide **183** was synthesised in order to assess the enantiopurity of **182** (Scheme **61**). Alanine dipeptide **183** was synthesised from the deprotected α-amino acid **182**, using HOBt and PyBOP coupling reagents in 78% yield. A racemic mixture was also synthesised using TBAF mediated desilylation followed by methyl ester hydrolysis with caesium carbonate to give **(±) 182**. The racemate was also subjected to amide coupling with alanine to give **183** as a mixture of diastereomers.

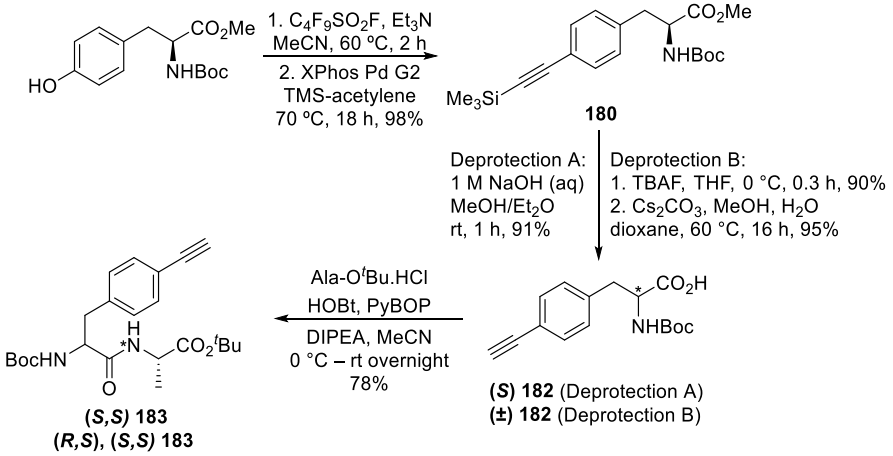

Scheme 61: Synthesis of alanine dipeptide 183.

The ^{1}H NMR spectra of dipeptides **183** and **183** are shown in Figure **40**. For diastereomeric mixture **183**, distinct signals corresponding to each diastereomer are observed for both methyl and N-H groups. By comparison, the ^{1}H NMR spectrum of **183** shows a single set of signals, consistent with the presence of one diastereomer. These results indicate that TMS-removal and methyl ester hydrolysis with sodium hydroxide does not result in racemisation.

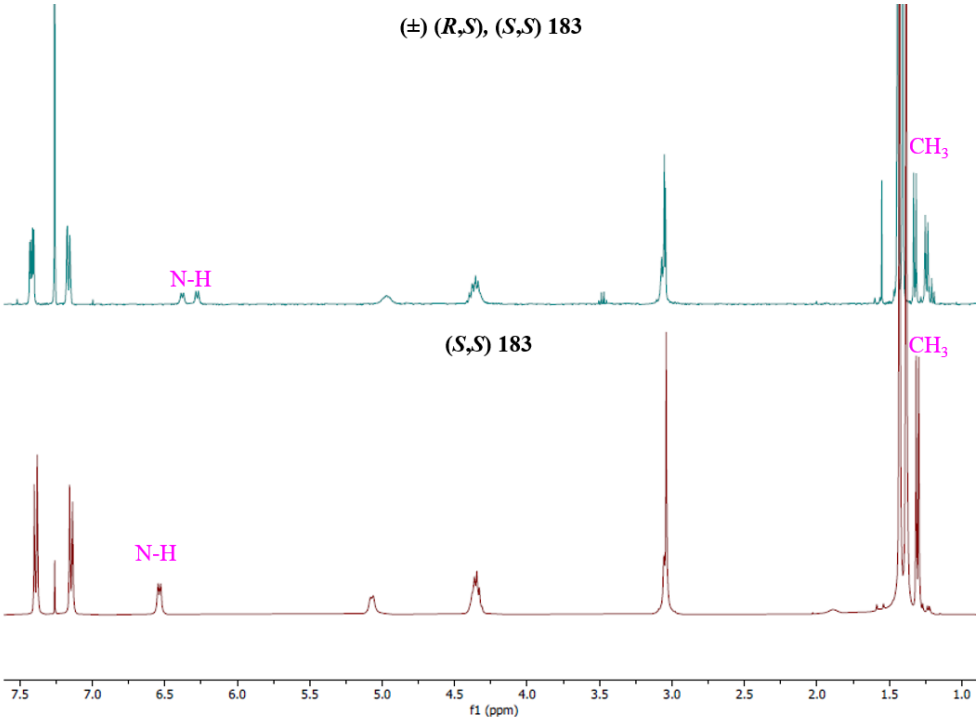

Figure 40: ^{1}H NMR spectra of 183 [(*R*,*S*), (*S*,*S*)] and 183 (*S*,*S*).

Having established a method for the synthesis of arylalkynyl α-amino acid analogues that does not result in racemisation, α-amino acids **184a**–**184f** were synthesised as the carboxylic acid analogues in moderate to good yields (49–82%) (Scheme **62**). For analogues **184c** and **184d**, an impurity which was challenging to separate by silica gel chromatography was observed when utilising the $Pd(PPh_3)_2Cl_2$ catalyst. The impurity was identified by undefined multiplets in the aromatic region of the ^{1}H NMR spectrum, as well as a singlet at 23 ppm in the ^{31}P NMR spectrum. Whilst the NMR spectra did not align with that of the triphenylphosphine ligand or triphenylphosphine oxide (a common byproduct), the signal in the ^{31}P NMR spectrum indicated it was resulting from the catalyst. Switching to XPhos Pd G2 resulted in more straightforward chromatography and isolation of **184c** and **184d** both in 73% yield.

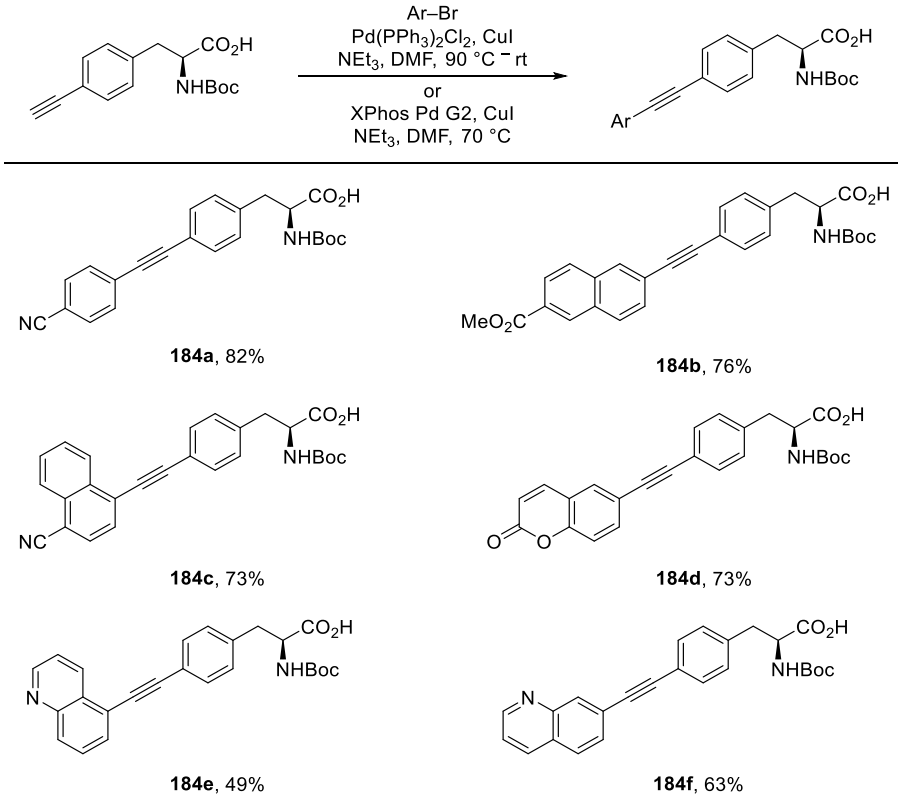

Scheme 62: Synthesis of *α*-amino acids 184a–184f.

The photophysical properties of **184a**–**184f** were recorded (Figure **41**, Table **13**). Generally, the fluorescence intensity of the partially deprotected *α*-amino acids was lower than exhibited by the protected analogues. Increased polarity of the partially deprotected *α*-amino acids and increased hydrogen-bond formation from the carboxylic acid could result in non-radiative relaxation pathways such as vibrational coupling either intermolecularly or *via* solvent interactions. As the *α*-amino acids are primarily intended to be applied as intrinsic peptidic probes, the photophysical properties observed for the fully protected analogues better indicate the fluorescence that would be expected once embedded within a peptide.

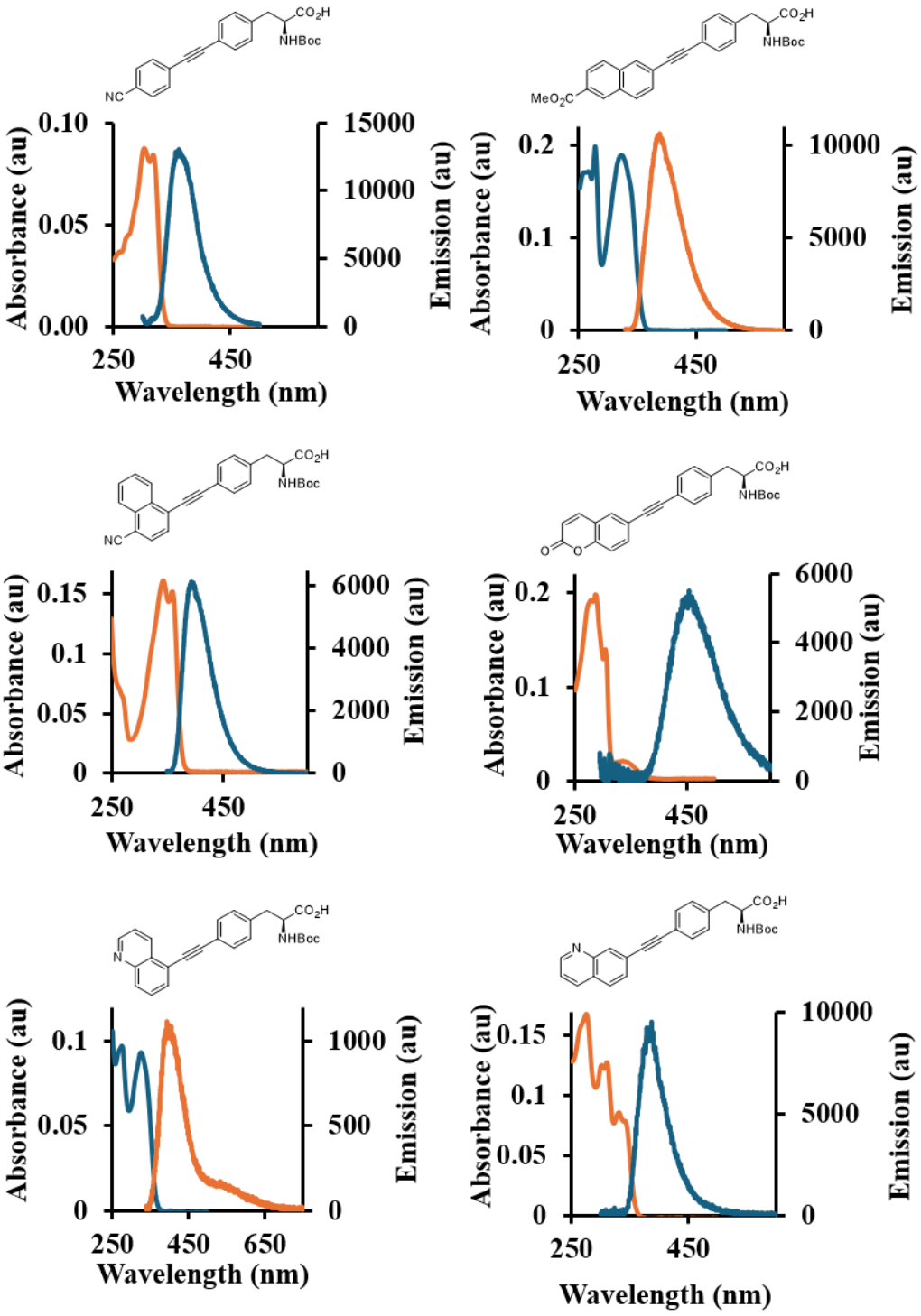

Figure 41: Absorption and emission spectra for *α*-amino acids 184a–184f (5 µM in MeOH).

Amino Acid	λ_{Abs} (nm)	ε (cm^{-1} M^{-1})	λ_{Em} (nm)	S.S. (nm)	Φ_F	BRT (cm^{-1} M^{-1})
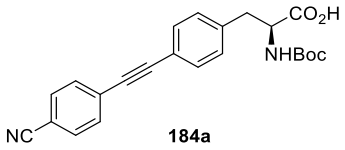 184a	**302** 318	28200	365	65	0.10	2950
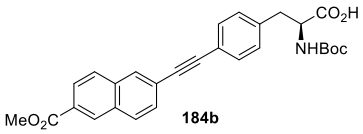 184b	**278** 322	39400	388	66	0.57	22290
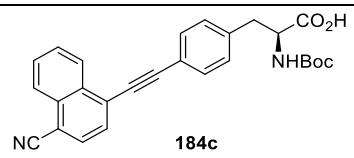 184c	**342** 360	33500	394	52	0.53	17680
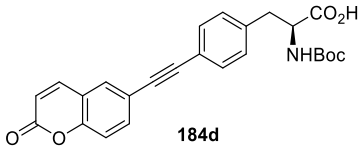 184d	286	47300	455	169	0.03	1380
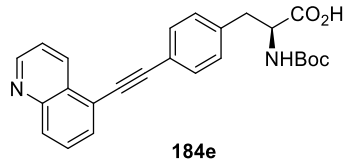 184e	**274** 324	17100	394	120	0.53	9150
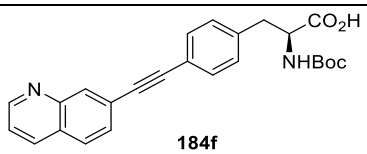 184f	**274** 312 334	30700	383	109	0.28	8600

Table 13: Photophysical properties of *α*-amino acids 184a–184f. Comparison of absorption (λ_{Abs}) and emission (λ_{Em}) maximum, molar absorption coefficient (ε), stokes shift (S.S), quantum yield Φ_F and brightness (BRT) in methanol.

The pH sensitivity of the quinoline analogues was demonstrated as before in which protonation of the nitrogen at pH 6 resulted in a bathochromic shift in the emission maxima consistent with emission from a charge-transfer excited state (Figure **42**).

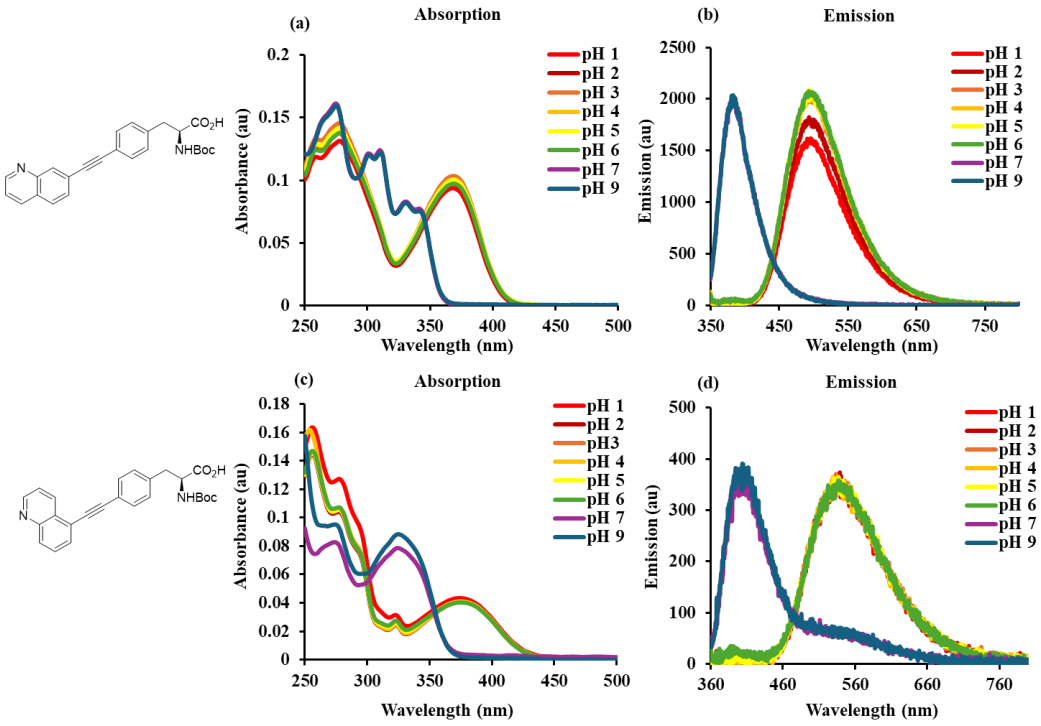

Figure 42: pH sensitivity of quinoline analogues 184e and 184f (5 µM in MeOH).

The expansion of the arylalkynyl *α*-amino acid library to include additional analogues bearing electron withdrawing groups successfully identified red-shifted, highly emissive analogues **184b** and **184c**, as well as pH sensitive quinoline analogues **184e** and **184f**. Notably, these analogues outperformed those conjugated to small, electron deficient chromophores such as coumarin or NBD. The strong photophysical properties of the arylalkynyl *α*-amino acids relative to the proteinogenic analogues highlight their potential as intrinsic peptidic probes in fluorescence-based techniques such as FRET, fluorescence anisotropy or two-photon excitation. However, it was also desirable to find an analogue for cell imaging applications. Cell imaging requires the absorption and emission maxima to be within the visible light region to ensure compatibility with optical light microscopes – which typically filter out UV light – and to prevent cell damage from UV light exposure.

2.3.9 Synthesis of an arylalkynyl BODIPY analogue

In order to improve the photophysical properties for cell imaging applications, a new analogue containing a BODIPY chromophore was desirable. Environmentally sensitive BODIPY chromophores have been designed by Nagano and co-workers.[228] Conjugation of the BODIPY core to electron-donating groups resulted in poor emission in polar solvents resulting from PET induced quenching and therefore, 'turn-on' fluorescence in non-polar solvents. Several environmentally sensitive amino acid analogues in which the BODIPY core is conjugated to naturally fluorescent amino acids have been reported by the Vendrell and Ackermann groups (Scheme **63**).

Tryptophan analogue **185** was first reported by Vendrell in 2016.[229] Conjugation of the BODIPY core to the electron-rich indole moiety was achieved *via* palladium-catalysed C–H activation in a 74% yield. BODIPY-tryptophan conjugate **185** exhibited very high extinction coefficient of 121000 M^{-1} cm^{-1} and high sensitivity to lipophilic environments [QY (PBS): 0.03; QY (membranes): 0.22]. Tryptophan analogue **185** was subsequently incorporated into a linear antimicrobial hexapeptide analogue of PAF26, which was utilised to report fungal infection in human samples. A cyclised analogue of the linear fluorescent peptide was also synthesised to improve stability, and binding affinity for fungal cells. Tryptophan analogue **185** was further incorporated into a cyclic peptide c-Lac-1, which is known to bind to phosphatidylserine that are presented on the outer membrane of apoptic bodies (vascular structures released in the early stages of apoptosis).[230] The cLac-BODIPY peptide was able to report on apoptic bodies in flow cytometry experiments.

Following the success of Trp-BODIPY amino acid **185**, it was shown that thiophene conjugation (**186**) red shifted absorption/emission from 503/517 nm to 570/590 nm, respectively.[200] A significant drawback of the BODIPY fluorescent amino acid analogues was the acid sensitivity of the BODPIY core. This led to challenges in solid phase peptide synthesis requiring careful removal of the protecting groups and resin cleavage (5 × 1 minute cycles of 1% TFA in dichloromethane).[231] Acid resistant analogue **187** was synthesised by nucleophilic substitution of the fluoride substituents with cyano groups.[232] Tryptophan-BODIPY **187** was stable in 95% TFA

for one hour. Dicyano substitution has been reported to strengthen the B–N bond and increase the aromaticity of phenyl-BODIPY analogues.[233] Furthermore, the strong-electron withdrawing effect of the cyano group reduces the charge on the boron atom and increases stability (mesomeric effect). Late-stage BODIPY functionalisation of tryptophan residues *via* manganese catalysed C-H activation using a *N*-pyridine directing group gave **188**. The conjugated alkenyl spacer resulted in **188** being highly sensitive to viscosity.[234] Further development of late-stage peptide functionalisation was reported for tyrosine and phenylalanine analogues **189** and **130** *via* an azo coupling of a diazonium BODIPY species and palladium catalysed C(sp^3)–H activation of alanine residues respectively.[141, 199]

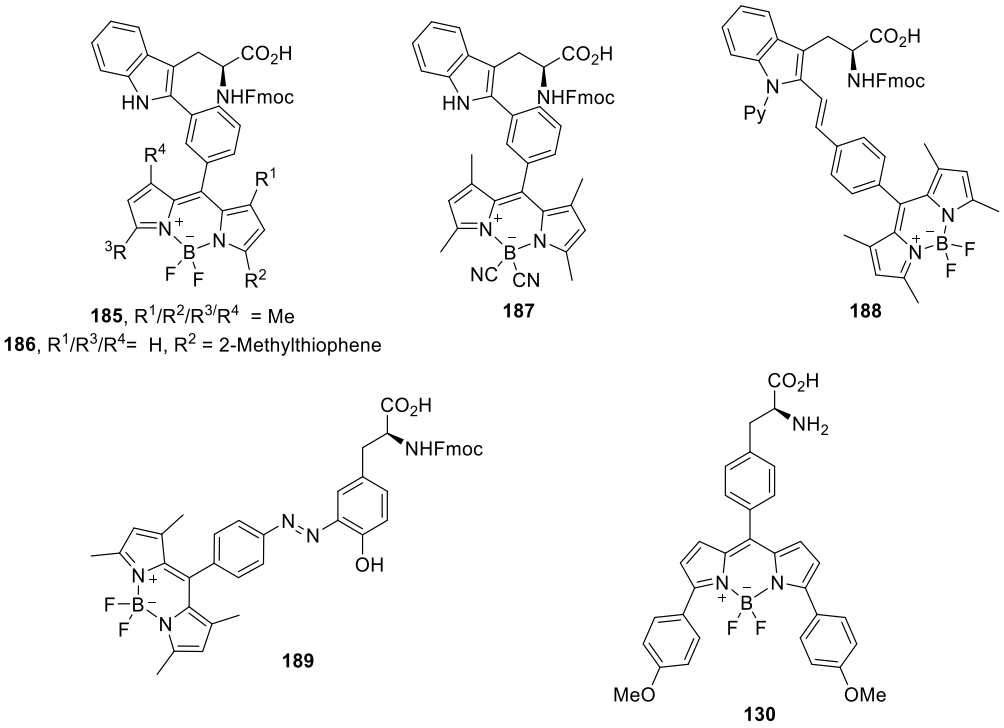

Scheme 63: BODIPY amino acids reported in literature.

Owing to the success described in literature for cell imaging utilising BODIPY derived amino acids, alkynyl BODIPY analogue **192** was proposed (Scheme **64**). Amino acid functionalisation directly attached to the BODIPY core was designed to obtain a more compact alkynyl structure. For the synthesis of **192**, the BODIPY core was first synthesised utilising modified conditions reported by Duan *et. al.*[235] The two-step, one-pot reaction, started with acid catalysed condensation of 2,4-dimethylpyrrole and benzaldehyde, followed by oxidative dehydrogenation with tetrachloro-*p*-benzoquinone (*p*-chloranil) and finally complexation with BF_3OEt_2.

Phe-BODIPY **190** was isolated in 20% yield, a significantly lower yield than reported by Duan *et. al*. (80%) who utilised a benzyl chloride starting material. The yield for **190** is generally in accord with other reported yields for BODIPY synthesis.[236] Low yields could be attributed to competing polymerisation of the pyrrole.[237] Alternatively, water from the base, which was not stored under strict anhydrous conditions, is known to strongly chelate the BF_3 Lewis acid, reducing its availability for chelation with the dipyrrin.[238] Despite the low yield, **190** was synthesised in sufficient quantities (>200 mg) for subsequent steps. Iodination of **190** was achieved utilising *N*-iodosuccinimide. Distinctly coloured pink, orange, and yellow spots were observed by TLC (30% dichloromethane in hexane) for the *di*- and *mono*-iodinated products and starting material, respectively, allowing straightforward isolation of **191** by column chromatography in 66% yield. Sonogashira cross-coupling of **182** and **191** was achieved the same conditions as described for amino acids **184a–184f** to give alkyne-extended BODIPY *α*-amino acid **192** in 77% yield.

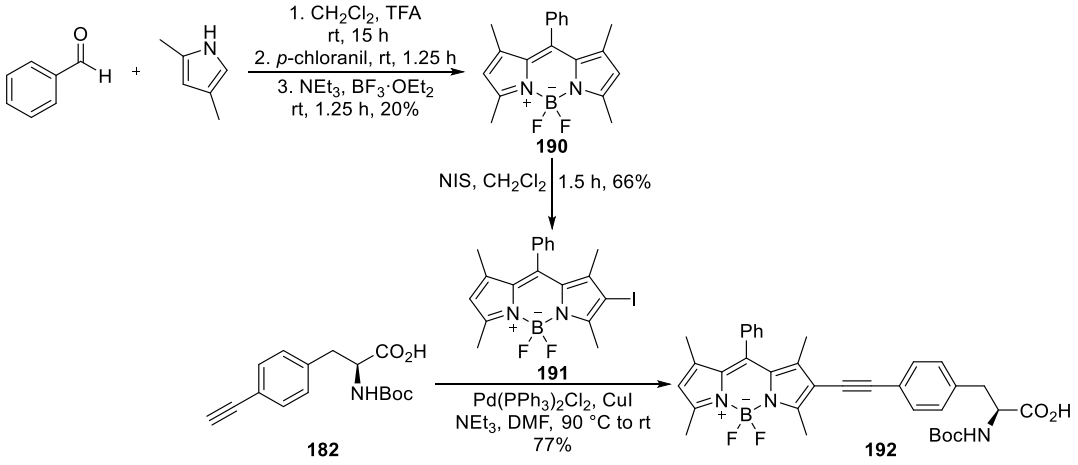

Scheme 64: Synthesis of BODIPY alkynyl *α*-amino acid 192.

Owing to the known solvatochromic properties of aryl-substituted BODIPY chromophores,[228] the photophysical properties were recorded in polar solvent methanol and non-polar solvent tetrahydrofuran (Figure **43** and Table **14**). As expected, the absorption (530 nm) and emission (580 nm) were sufficiently red-shifted for cell imaging applications. Alkyne extended amino acid **192** was also red-shifted relative to the Trp-BODIPY and Tyr-BODIPY analogues **185** and **189**.[199,229] A higher quantum yield (0.35) in non-polar solvent tetrahydrofuran resulted in enhanced brightness (14480 cm^{-1} M^{-1}) relative to the polar solvent methanol (9780 cm^{-1} M^{-1}) (Table 14). The solvatochromic properties of phenyl-BODIPY

chromophores has been attributed to charge-transfer or PET from the aryl ring to the BODIPY core. The charge-transfer and PET pathways, which result in fluorescence quenching, are better stabilised in high polarity solvents.[228,239]

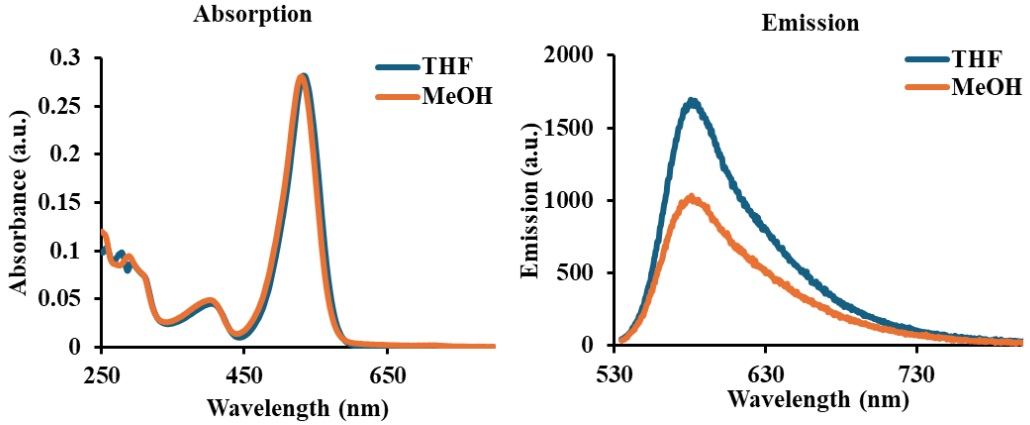

Figure 43: Absorption and emission of 192 in methanol and tetrahydrofuran (5 µM).

Amino Acid	λ_{Abs} (nm)	ε (cm^{-1} M^{-1})	λ_{Em} (nm)	S.S. (nm)	Φ_F	BRT (cm^{-1} M^{-1})
192	530	56300 (MeOH) 42200 (THF)	580	50	0.17 (MeOH) 0.35 (THF)	9780 (MeOH) 14480 (THF)

Table 14: Photophysical properties of *α*-amino acid 192. Comparison of absorption (λ_{Abs}) and emission (λ_{Em}) maximum, molar absorption coefficient (ε), stokes shift (S.S), quantum yield Φ_F and brightness (BRT) in methanol and tetrahydrofuran.

Following the strong emission observed in tetrahydrofuran, the photophysical properties of **192** in phosphate-buffered saline and in a lipophilic environment (7:1 PC:cholesterol) were examined (Figure **44**). A 6-fold increase in absorption intensity at 530 nm and an impressive 82-fold increase in emission intensity at 580 nm was observed in a lipophilic environment compared to phosphate buffer. The quantum yield in liposomes was measured to be 0.22 and the brightness was calculated to be 7540 cm^{-1} M^{-1}. Quantum yield data in phosphate-buffered saline was not measured due to insufficient emission. As a result of fluorescence quenching in aqueous environments, the emission is 'turned-on' in lipophilic environments. As previously discussed with 1-naphthalene analogue **172b**, this type of behaviour can be exploited

in 'wash-free' cell imaging targeting cellular membrane structures.[142,197-200] Despite having a lower brightness value than some of the other lead arylalkynyl α-amino acids in the series, the reduced autofluorescence from cellular components at further red-shifted wavelengths enables fluorescence imaging at lower brightness values.[142,197,198,229-231]

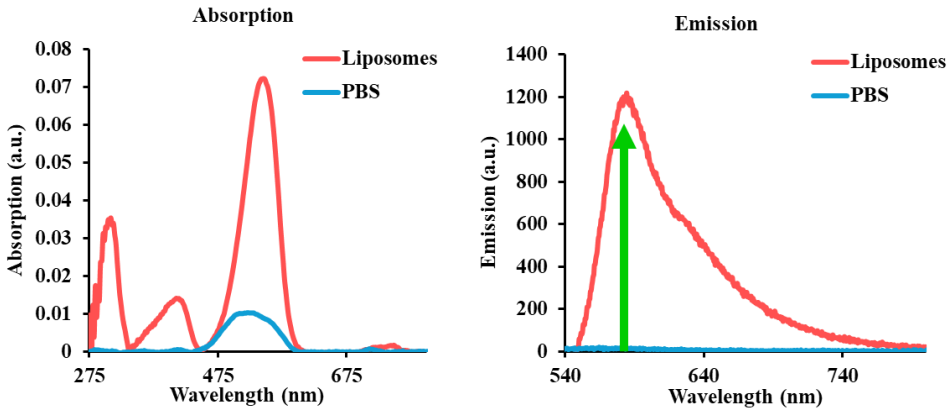

Figure 44: Absorption and emission of 192 in phosphate buffer and liposomes (5 µM).

Further to the lipophilic sensitivity, aggregation and viscosity studies were undertaken (Figure **45**). Aggregation induced quenching was observed in methanol above 25 µM. For the viscosity study, no significant change was observed in the absorption spectra at higher proportions of ethylene glycol in methanol. In the emission spectra, an initial 41% decrease in intensity was observed from 0% to 20% ethylene glycol and a further 23% decrease from 60% to 100% ethylene glycol in methanol. It had been anticipated that the increased viscosity would increase the emission intensity, as previously reported for tryptophan derived BODIPY analogues such as **188**.[234] However, the increase in hydrogen-bonding capability of ethylene glycol compared to methanol could stabilise non-radiative charge transfer or PET mechanisms.[17]

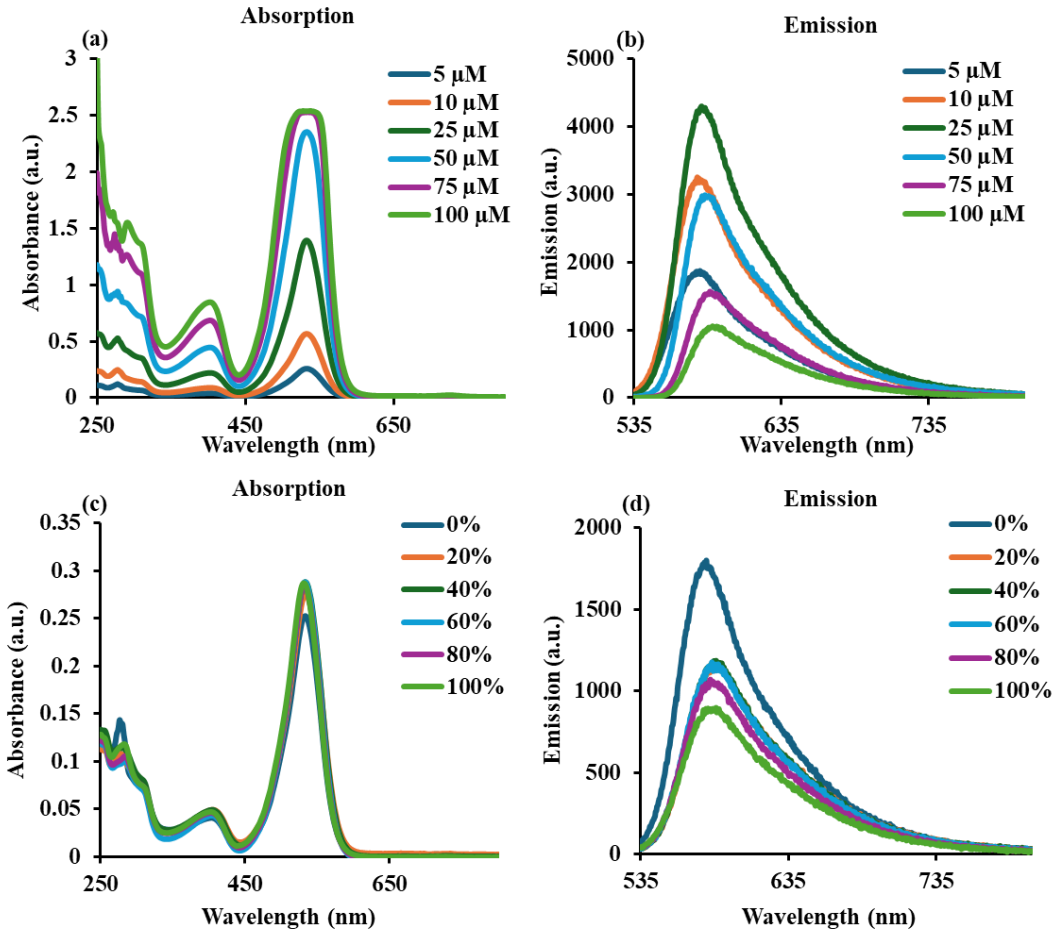

Figure 45: Aggregation study: absorption (a) and emission (b) at increasing concentration of 192 in methanol. Viscosity study: Absorption (c) and emission (d) of 192 in increasing quantities of ethylene glycol in methanol (5 µM).

In order to exploit the sensitivity of **192** to lipophilic environments, it was desirable to develop a fluorescent probe that would direct the α-amino acid to lipophilic environments within the cell. Therefore, attachment of a lipid chain was proposed to anchor the α-amino acid into membrane-structures and 'turn-on' the fluorescence. Probes such as lipid-conjugated dyes, have been utilised for visualisation, tracking and chemical sensing at the cell membrane.[240,241] A lipid-conjugated analogue of the tryptophan-derived BODIPY **188** (Scheme **63**), which displayed high sensitivity to membrane fluidity was used to anchor the amino acid into cholesterol cell membranes in a fluorescence-based screening platform.[234] As an initial proof-of-concept that **192** could be used for imaging of cellular membranes, lipid-conjugate analogue **194** was proposed (Scheme **65**). However, acid-mediated Boc-deprotection of **192** to give the amine required for amide coupling with palmitic acid was unsuccessful. An initial attempt at deprotection with 2 M hydrochloric acid showed incomplete Boc-removal after 1 hour. In order to leave the reaction for longer, the

reaction was repeated at a lower concentration of 1 M hydrochloric acid, however, after a further 2.5 hours, the reaction showed a complex mixture by ^{1}H NMR spectroscopy. An alternative deprotection using 2% trifluoroacetic acid in dichloromethane, as reported by Vendrell for the deprotection and cleavage of peptides containing BODIPY-derived amino acids, was attempted.[231] However, after 3 hours, minimal Boc-deprotection was observed by ^{1}H NMR spectroscopy.

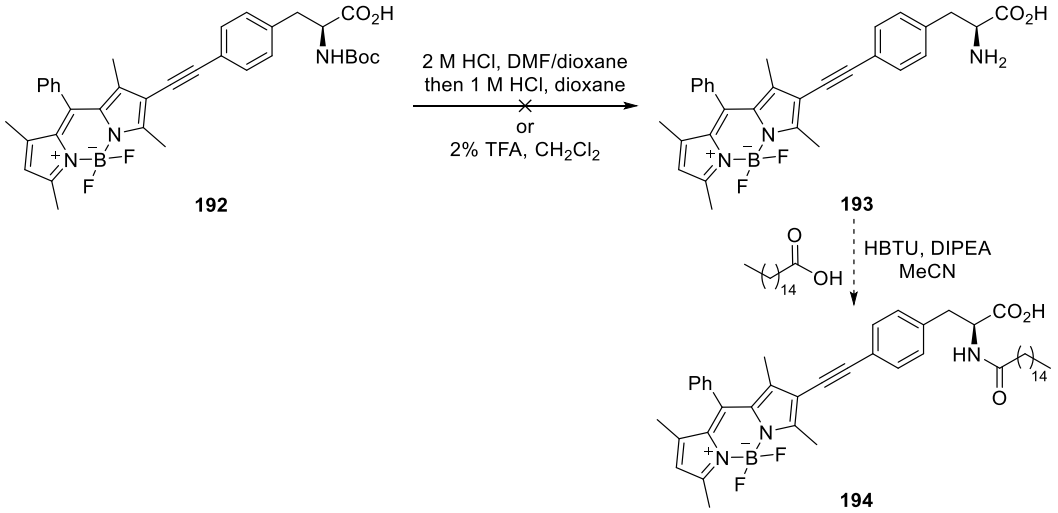

Scheme 65: Attempted initial synthesis of 194.

Due to the described difficulties of deprotecting acid-sensitive BODIPY analogue **192**, an alternative route in which the lipid moiety was installed earlier was employed (Scheme **66**). Starting with TMS-protected phenylacetylene *α*-amino acid **180**, Boc-deprotection was achieved using 2 M hydrochloric acid in dioxane in 90% yield. Amide coupling with palmitic acid using HBTU coupling reagent and *N,N*-diisopropylethylamine gave the lipid-conjugated product **196** in 87% yield. Removal of the TMS-protecting group and methyl ester hydrolysis was achieved using 1 M sodium hydroxide in 96% yield. Finally, a Sonogashira cross-coupling reaction with the iodinated-BODIPY substrate was achieved under the same conditions used for Boc-protected BODIPY **192**, which gave desired lipid-conjugated BODIPY analogue **194** in 63% yield.

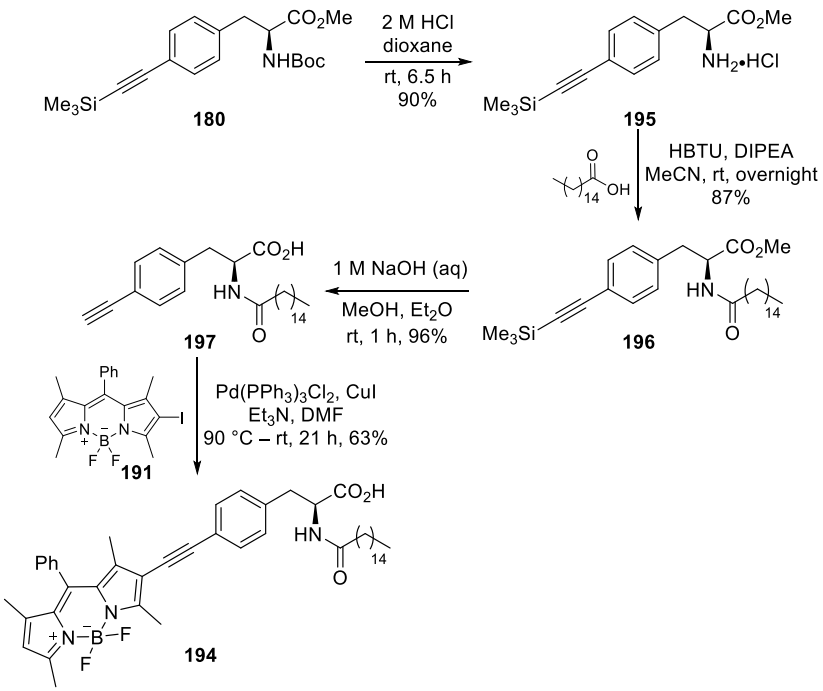

Scheme 66: Synthesis of lipid *α*-amino acid analogue 194.

The absorption and emission of lipid-conjugated analogue **194** was confirmed to be the same as exhibited by the Boc-protected analogue (Figure **46**).

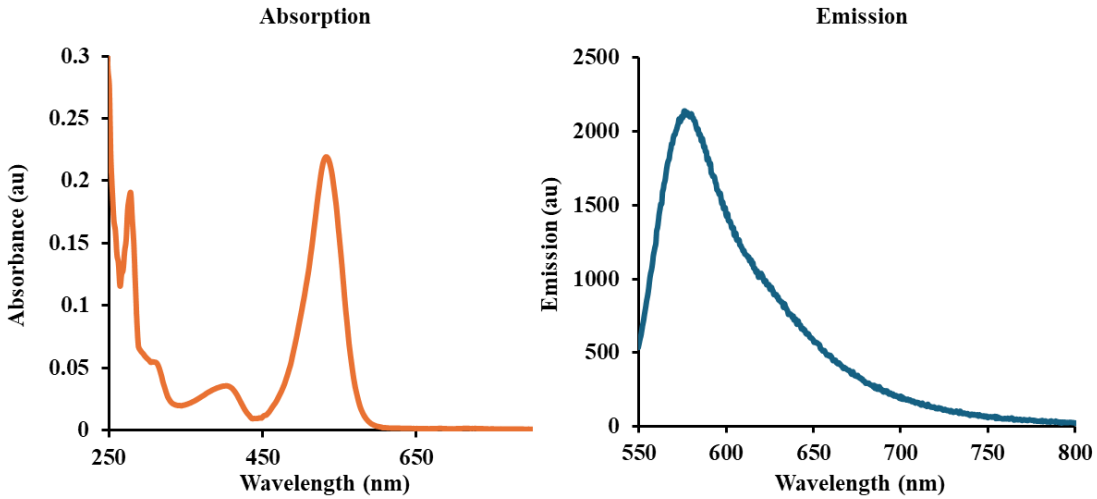

Figure 46: Absorption and emission of 194 (5 µM in THF).

2.3.10 Application of BODIPY analogue 194

A benefit of fluorescent amino acids is their broad applicability in fluorescence spectroscopy for *in vitro* assays and whole cell imaging across a wide range of biological systems. With the lipid-conjugated BODIPY analogue **194** in hand, it was desirable to utilise this analogue in cell imaging owing to its absorption and emission in the visible light region. As such, analogue **194** was given to our collaborator Professor Michael Barrett at the University of Glasgow, who's research focuses on African trypanosome (*T. brucei*) pharmacology. Despite significant research into trypanosome infection, there still requires better understanding of trypanosome-host interactions and the impact of co-infections.[242] Fluorescence microscopy provides an essential tool for characterisation and study of trypanosomes including localisation of trypanosome proteins and the detection of intracellular drugs.[243,244] Furthermore, trypanosomes can be utilised as model eukaryotic organisms for understanding cell division, molecular trafficking and organelle biosynthesis.[243] Membrane targeting is an attractive approach for visualisation of trypanosomes as they are known to undergo morphology changes throughout their lifecycle between 'slender' and 'stumpy' forms.[245] Research is ongoing in the Barrett group to utilise **194** for the visualisation of trypanosome cell membranes.

2.3.11 Phenylacetylene *α*-amino acid 182 as a key synthetic intermediate

The one-pot activation of tyrosine followed by Sonogashira cross-coupling with TMS-acetylene provided facile access to **180**, which was subsequently treated with 1 M sodium hydroxide to enable TMS-removal and methyl ester hydrolysis to give **182** without inducing racemisation (Scheme **67**). This two-step process, encompassing four functional group transformations, allowed for the multigram synthesis of **182** in an excellent overall yield of 89%.

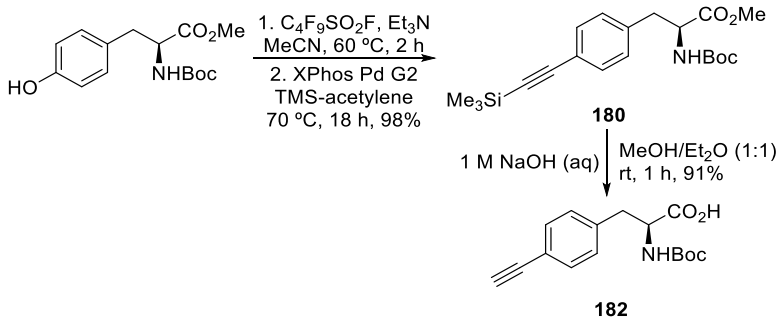

Scheme 67: Synthesis of key phenylacetylene *α*-amino acid intermediate 182.

Having already utilised phenylacetylene *α*-amino acid intermediate **182** to expand the library of arylalkynyl *α*-amino acids, it was desirable to further demonstrate **182** as a key synthetic intermediate. Alkynes are versatile intermediates capable of undergoing addition, cycloaddition and radical reaction as well as metal-catalysed cross-coupling reactions.[246-255] Specifically, phenylacetylene *α*-amino acid analogues have been used as substrates for the cycloaddition with nitrosoarenes to give indole derivatives and copper-catalysed "click chemistry" for incorporation of a fluorine-18 radiolabel for PET imaging (Scheme **68**).[256,257]

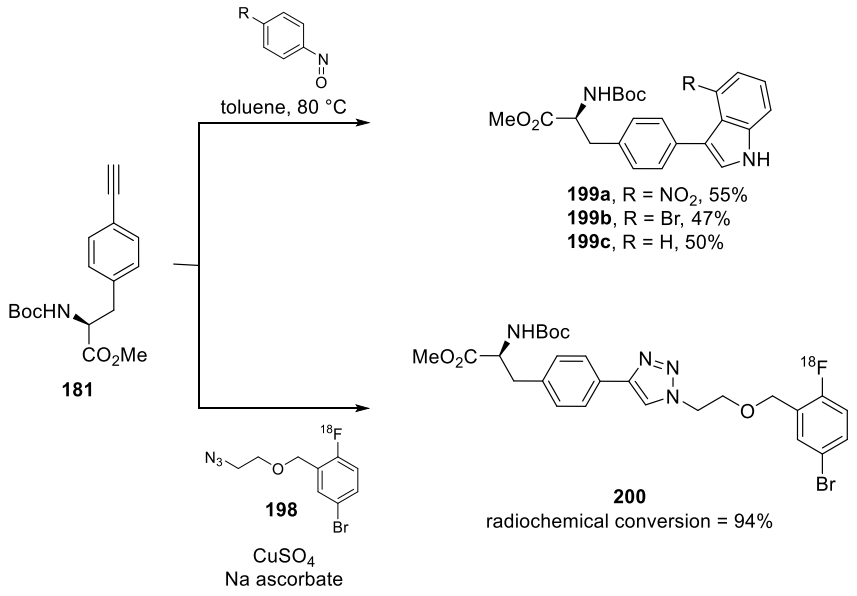

Scheme 68: Phenylacetylene *α*-amino acid substrate examples in literature.

It was envisaged that incorporation of **182** into a peptide would provide a handle for late-stage functionalisation, enabling fluorescence imaging, isolation or quantification. One such method explored was 'click chemistry,' which facilitates the formation of heteroatom-linked (C–X–C) conjugates. First coined by Kolb, Finn and

Sharpless, 'click chemistry' reactions are defined by fast reaction rates, wide scope, stereospecificity, high yields and the formation of easily removable byproducts.[258] The regioselective copper(I)-catalysed Huisgen [3 + 2] cycloaddition between an azide and an alkyne is among the most widely used click reactions. The reaction was further advanced through strain-promoted azide-alkyne cycloadditions, commonly employing cyclooctyne derivatives in which the distorted conformation of the alkyne increases its reactivity and enables copper-free reactions. The removal of copper enabled the application of *in vivo* 'click chemistry' for biorthogonal labelling of proteins. The reaction rate, stability, aqueous solubility and biocompatibility have further been improved by the incorporation of heteroatoms, electron withdrawing groups or aryl groups adjacent to the alkyne.[259-262]

Biosynthetic incorporation of unnatural amino acids bearing alkyne handles for 'click chemistry' has been demonstrated by Tirell and co-workers. Homopropargylglycine (Hpg) showed uptake in place of methionine in cells grown under methionine depleted conditions,[263] and ethynylphenylalanine was incorporated using engineered phenylalanine tRNA synthetase (PheRS*) in *E. coli*.[264] Newly synthesised proteins were subsequently visualised by a copper-catalysed reaction between the ethynylphenylalanine unnatural amino acid and an azide-bearing coumarin analogue.[265] The robustness of 'click chemistry' has also facilitated its application in the synthesis of fluorescent amino acids.[87,266-269] Whilst most approaches attach known chromophores, Bag *et. al.* described the conjugation of diverse polyaromatic structures to generate novel fluorescent amino acids.[269,270] The application of azide-alkyne cycloaddition reactions for bioconjugation is made more appealing by the 1,2,3-triazole ring products, which are resistant to hydrolysis, oxidation and reduction and have been exploited as metabolically stable bioisosteres of amide and ester bonds.[271,272] An additional advantage for the synthesis of fluorescent amino acids is that the triazole moiety can be used to extend the conjugation or act as a conjugated bridge.

Dipeptide **183**, containing phenylacetylene α-amino acid analogue **182**, was first subjected to copper(I)-catalysed 'click chemistry' with relatively simple azides (Scheme **69**). Copper(II) was reduced to copper(I) *in situ* by sodium ascorbate. The click reaction with methyl azido acetate under conditions reported by Li *et. al.* gave **201** in 83% yield. For the benzyl azide substrate, increasing the reaction

concentration from 0.025 M to 0.26 M increased the conversion from 7% to 100%, resulting in isolation of triazole **202** without the need for purification by silica gel chromatography.

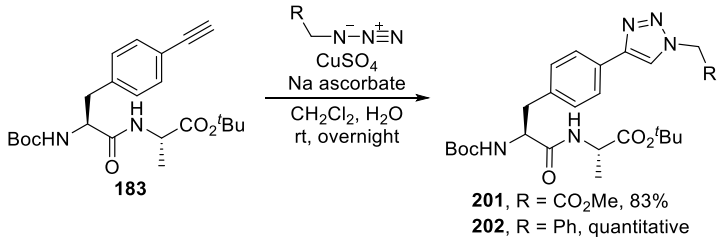

Scheme 69: 'Click chemistry' of dipeptide 183 with relatively simple azides.

In order to demonstrate the click chemistry of **183** with azides more relevant to chemical biology, fluorescein isocyanate was reacted with 3-azidopropylamine to give urea product **204** in 52% yield (Scheme **70**). However, due to poor solubility of the fluorescein azide, the click reaction was unsuccessful. Despite better solubility of the fluorescein azide observed in dimethyl sulfoxide, no reaction between the azide and the alkyne was observed by ^{1}H NMR spectroscopy after 16 h.

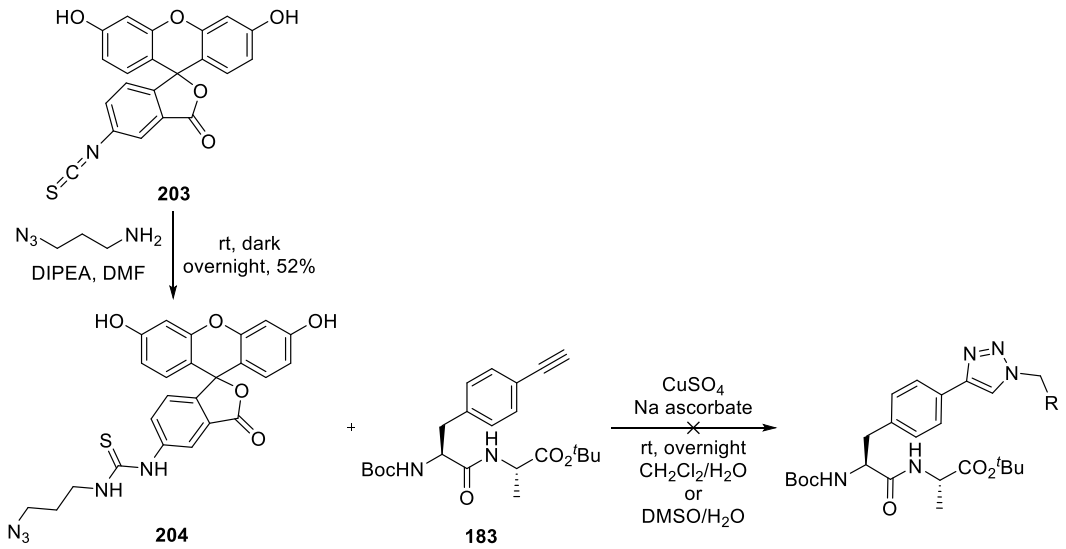

Scheme 70: Attempted click chemistry with fluorescein azide 204.

Consequently, a dansyl-azide was synthesised as an alternative fluorophore. Amide coupling of dansyl chloride with 3-azidopropylamine under basic conditions gave desired azide **206** in 98% yield (Scheme **71**). The dansyl-azide underwent copper(I)-catalysed click chemistry under standard conditions to afford triazole **207** in 85%

yield. The dansyl fluorophore dominated the absorption and emission spectra (Figure **47**). Triazole **207** displayed an absorption maximum at 254 nm and emission maximum at 536 nm, which is consistent with other dansyl-derived fluorescent probes.[273]

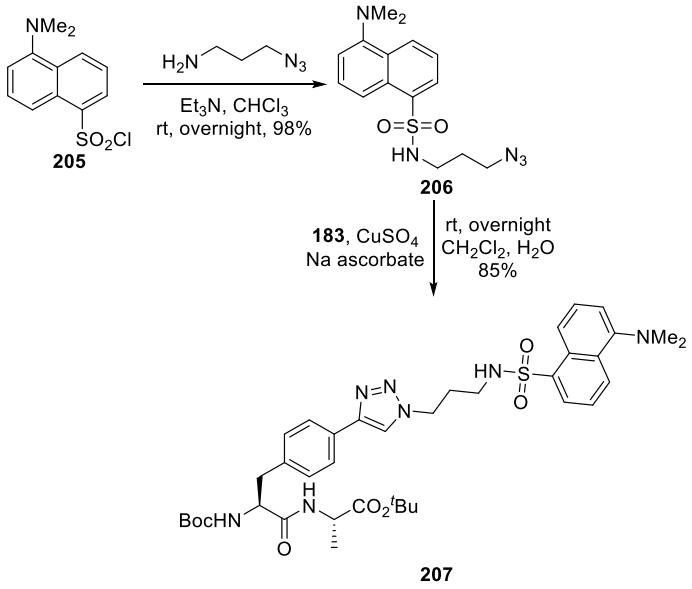

Scheme 71: Dansyl-azide click chemistry with 183.

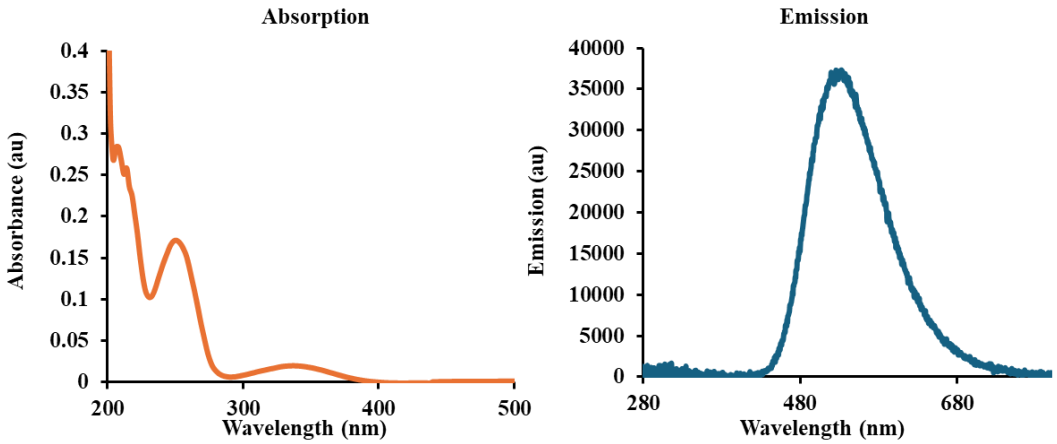

Figure 47: Absorption and emission of 207 (5 µM in MeOH).

Lastly, click chemistry with a biotin-azide was explored. Biotin is widely used as an affinity tag for protein isolation. Following biotinylation, avidin-coated beads are employed to isolate the tagged protein from complex mixtures (dissociation constant of biotin-avidin, $K_d = 10^{-14}$ mol L^{-1}).[274] Biotin-azide **209** was synthesised as described by Liu and co-workers.[275] The carboxylic acid was first activated with

carbonyldiimidazole (CDI) prior to amide coupling with 3-azidopropylamine to afford **209** in 45% yield (Scheme **72**). The azide was subjected to the copper(I)-catalysed click reaction as before with the addition of *tert*-butanol to help solubilise the starting materials. The click reaction afforded triazole **210** in 86% yield.

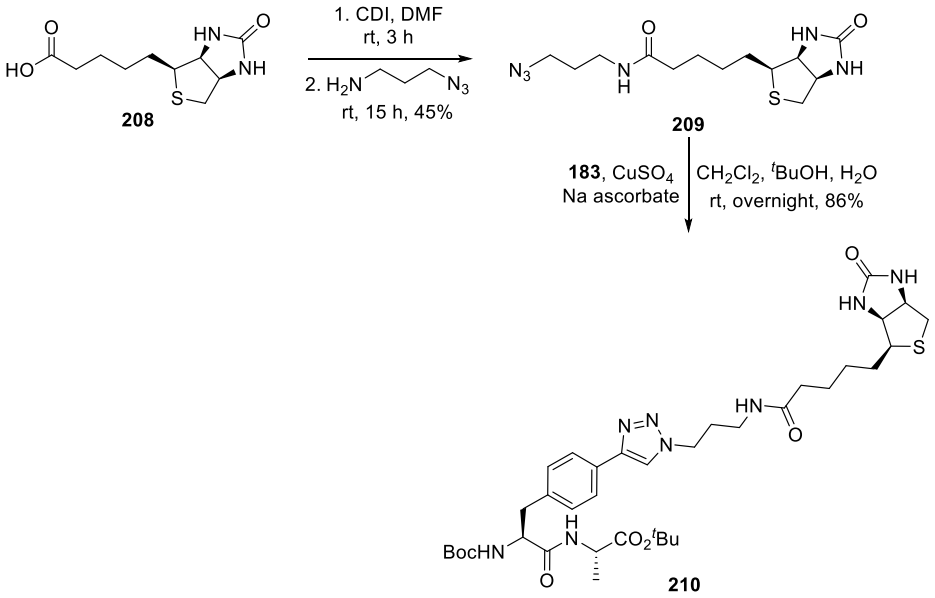

Scheme 72: Biotin-azide click chemistry with 183.

Having demonstrated phenylacetylene α-amino acid analogue **182** as a key synthetic intermediate for the late-stage functionalisation of peptides *via* copper(I)-catalysed click chemistry, we sought to further demonstrate that **182** could also undergo Sonogashira cross-coupling reactions for late-stage fluorescent labelling. The Sonogashira reaction has been widely applied to peptide functionalisation.[276-282] For example, Li and co-workers reported a biorthogonal copper-free Sonogashira cross-coupling using a water-soluble aminopyrimidine-palladium(II) complex to attach a fluorescein iodide to an Hpg-encoded ubiquitin in *E. coli*.[277] A fluorescein label was also employed by Hauke and co-workers who incorporated a mutant aryl iodide in a peptide sequence using an *E. coli.* enzyme prior to copper-free palladium-catalysed Sonogashira cross-coupling reactions.[278] Saha and co-workers describe the late stage modification of ribosomal proteins *via* selective enzymatic bromination of a tyrosine residue, followed by Sonogashira cross-coupling with various functional handles.[279] Additional examples include labelling with organometallic species and peptide stapling.[280-282] Whilst previous studies have focussed on installing large fluorescent tags *via* Sonogashira cross-coupling reactions, it was proposed that this work would

demonstrate the modification of phenylalanine residues to generate small, unnatural fluorescent α-amino acid residues.

For an initial proof of concept, a variety of dipeptides containing the phenylacetylene analogue **182** were synthesised (Scheme **73**). Amide coupling was achieved as before, using peptide coupling reagents PyBOP and HOBt, to give L-alanine, L-phenylalanine and L-aspartic acid dipeptides in 78–86% yields.

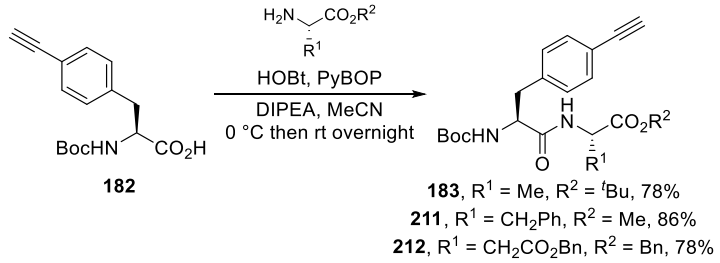

Scheme 73: Dipeptide synthesis 183, 211 and 212.

The dipeptides were then subjected to Sonogashira cross-coupling with 4-iodobenzonitrile, utilising $Pd(PPh_3)_2Cl_2$ and a copper cocatalyst, to give functionalised dipeptides **213**–**215** in good yields of 68–78% (Scheme **74**). This proof-of-concept study demonstrates that the alkynyl-phenylalanine analogue **182** could be used for *in situ* functionalisation of peptides.

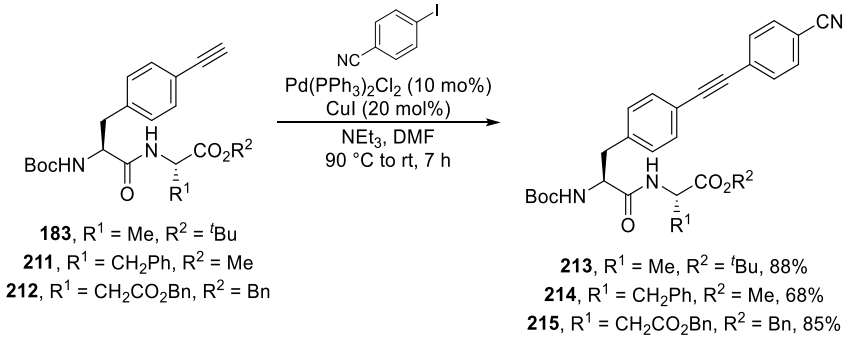

Scheme 74: Sonogashira cross-coupling of dipeptides 213–215.

2.3.12 Conclusions and future work.

In summary, following the successful synthesis of a library of biaryl fluorescent α-amino acid analogues of phenylalanine in section 2.2, a library of alkyne extended analogues were generated, which further red-shifted the absorption and led to improved photophysical properties. A one-pot methodology involving activation of a tyrosine analogue followed by copper-free Sonogashira cross-coupling provided rapid access to an initial library and identification of a highly fluorescent 1-naphthalene analogue **172b**. Compared to the biaryl analogue, the alkyne extended 1-naphthalene analogue exhibited a five-fold increase in brightness and its emission was not quenched when adjacent to naturally fluorescent amino acids in dipeptides.

The library of arylalkynyl α-amino acids was further expanded by the synthesis of a key phenylacetylene intermediate, which underwent Sonogashira cross-coupling with more readily available aryl bromides. Initial issues regarding racemisation during the TBAF-mediated removal of the TMS group were overcome using sodium hydroxide, which allowed generation of key alkynylphenylalanine intermediate **182**. Use of this intermediate led to the discovery of highly emissive and environmentally sensitive polycyclic analogues **184b** and **184c**, as well as quinoline analogues **184e** and **184d**. Furthermore, a novel, alkyne-extended BODIPY-derived α-amino acid analogue **192** was developed for cell-imaging applications. Motivated by the on/off fluorescence exhibited by **192** in lipophilic/aqueous media, a lipid-conjugated analogue **194** was prepared, with ongoing research in utilising this analogue for the visualisation of trypanosome cell membranes currently underway in the Barrett research group.

Lastly, the utility of phenylacetylene α-amino acid **182** as a synthetic handle for late-stage functionalisation of peptides was explored. 'Click-chemistry' enabled the installation of tags for both fluorescence and isolation. Furthermore, Sonogashira cross-coupling enabled *in situ* generation of fluorescent amino acids for a series of dipeptides. Future work will involve installation of phenylacetylene amino acid **182** into a peptide to demonstrate the late-stage functionalisation on a more complex substrate (Scheme **75**). This work will also expand the substrates to other aryl-bromides to enable *in situ* generation of the lead α-amino acids discovered in this

series. Raman spectroscopy of the alkyne functionalised peptides will also be undertaken to better evaluate the potential of the α-amino acids as dual fluorescence and Raman spectroscopy labels, enabling multimodal imaging.

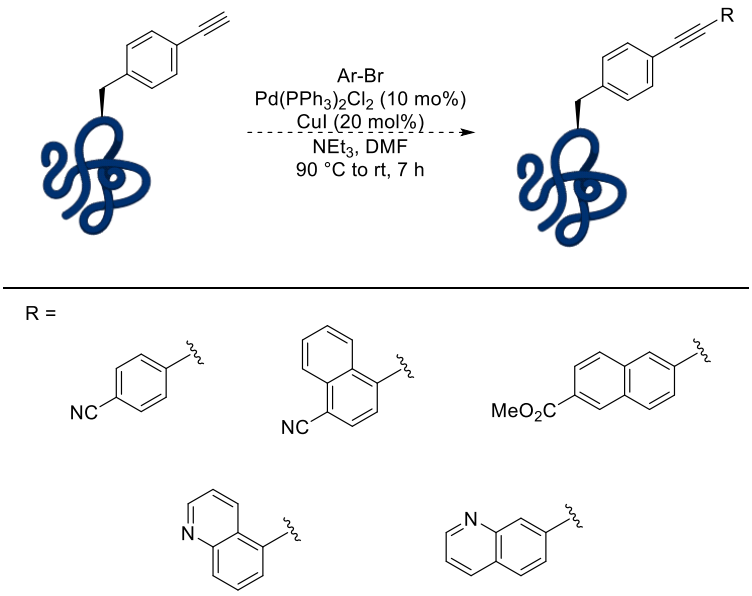

Scheme 75: Proposed late-stage peptide functionalisation.

2.4 Synthesis of Arylalkynyl Analogues of Tyrosine

2.4.1 Synthesis of a terminal alkyne analogue of tyrosine.

In the library of arylalkynyl analogues of phenylalanine discussed in section 2.3, analogues bearing electron-withdrawing groups exhibited more promising fluorescent properties. Based on this observation, it was considered that construction of a push-pull chromophore by increasing the electron density in the aryl ring closest to the α-amino acid backbone would result in increased intramolecular charge-transfer and improved fluorescence properties. Due to tyrosine naturally possessing a more electron rich aryl ring than phenylalanine, alkyne-extended analogues of tyrosine were therefore identified as attractive targets for the development of push-pull chromophores.

Sonogashira cross-coupling of 3-bromotyrosine was initially investigated (Scheme **76**). A protected tyrosine starting material was first brominated with *N*-bromosuccinimide in the presence of *p*-tosic acid to afford **142** in 79% yield. Sonogashira cross-coupling of bromotyrosine **142** utilising $Pd(PPh_3)_2Cl_2$ and a copper cocatalyst showed no conversion from the starting material by ^1H NMR spectroscopy. It was considered that the unprotected hydroxyl group could be hindering the reaction by binding to the palladium centre. However, installation of a MOM-protecting group was unsuccessful at improving the subsequent Sonogashira cross-coupling reaction. Sonogashira cross-coupling of **143** was attempted using both the $Pd(PPh_3)_2Cl_2$/CuI catalyst system as well as the copper-free Sonogashira reaction conditions utilising XPhos Pd G2, however, both showed no conversion from the starting material.

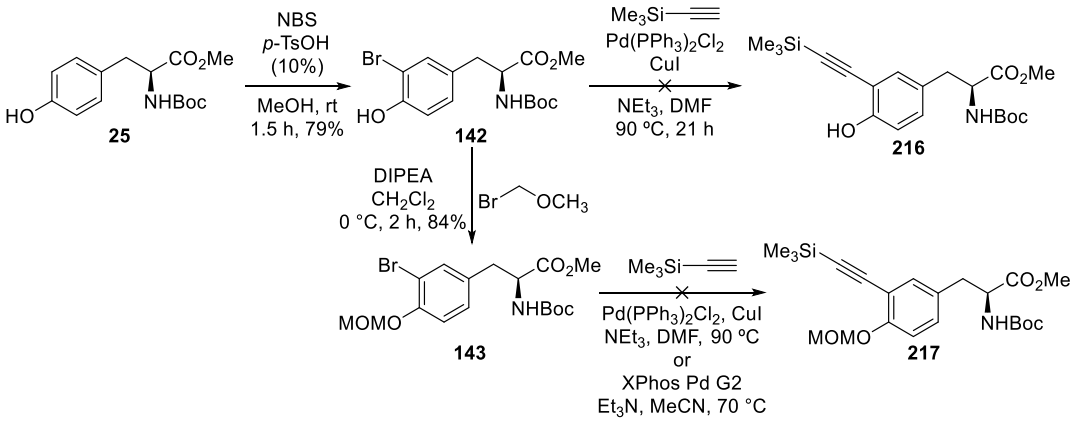

Scheme 76: Attempted initial synthesis of arylalkynyl tyrosine analogue.

In order to increase the reactivity of the starting material towards Sonogashira cross-coupling, a more reactive 3-iodotyrosine analogue was deemed necessary. Esterification of commercially available 3-iodotyrosine analogue **218** was achieved utilising thionyl chloride in 73% yield (Scheme **77**). Despite reports in literature that the esterified product did not require further purification,[283] the product was washed with a 4:1 chloroform:isopropyl alcohol in order to remove a dark brown impurity and give a crystalline white solid.

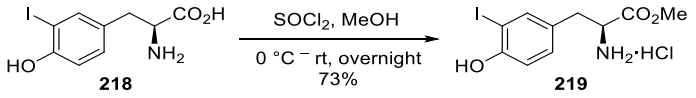

Scheme 77: Esterification of iodotyrosine 218.

Despite numerous reports of high yields of Boc-protection of **219** to give **220**,[283-285] significantly lower yields were obtained. Under conditions reported by Rokita and co-workers in which sodium hydroxide was used as a base, a complex mixture of products was observed by ^{1}H NMR spectroscopy (Table **15**, entry 1).[165] Triethylamine, as reported by Moody and co-workers, gave a cleaner reaction, however significant formation of a byproduct **221**, in which the phenol was also Boc-protected was observed by ^{1}H NMR spectroscopy (entry 2).[283] A brief solvent screen was undertaken to try and improve the solubility of the starting material and decrease byproduct formation (entries 3–5). Switching the solvent to water resulted in no reaction (entry 3) and a 4:1 mixture of dioxane:water resulted in increased byproduct formation (entry 4). Methanol proved to be the most effective solvent, although the crude mixture still contained 22% of **221** (entry 5). Purification by silica gel

chromatography afforded **220** in 56% yield, corresponding to a 41% yield over two-steps for the protection of 3-iodotyrosine. Whilst further optimisation of the protection step is required, these conditions provided sufficient material to enable progression to subsequent steps.

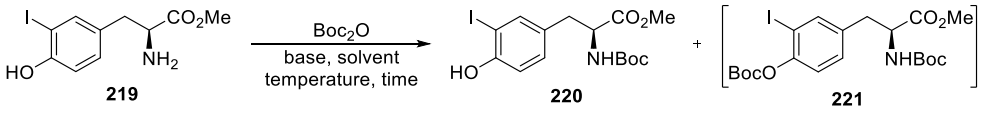

Entry	Base / additive	Solvent	Temp. (°C)	Time (h)	^{1}H NMR Product (220): byproduct (221)	Yield
1	NaOH	dioxane	rt	0.5	-	-
2	Et_3N	CH_2Cl_2	0–rt	5.8	2.3:1	39%
3	Et_3N	H_2O	rt	15	-	-
4	Et_3N	dioxane/ H_2O	rt	5.6	1.3:1	31%
5	Et_3N	MeOH	0–rt	22	3.7:1	56%

Table 15: Optimisation of Boc-protection of 219.

Sonogashira cross-coupling of iodotyrosine **220** with TMS-acetylene was achieved at 30 °C utilising $Pd(PPh_3)_2Cl_2$ and a copper cocatalyst to give alkynyltyrosine **216** in 89% yield (Scheme **78**). For the deprotection to the terminal alkyne, it was desirable to avoid sodium hydroxide as simultaneous methyl ester hydrolysis to the carboxylic acid results in more polar compounds that are challenging to purify by silica gel chromatography. Straightforward purification is advantageous for the synthesis of larger libraries of novel α-amino acids. Usuki and co-workers reported TBAF-mediated removal of a TMS-group using ethanol as a cosolvent without inducing racemisation.[286] Under these conditions, the TMS group was removed to give terminal alkynyltyrosine **222** in 70% yield. A similar value was obtained for the optical rotation of **222** (+53.6) as was obtained for the precursor (+39.9). Whilst the enantiomeric excess cannot be inferred from the optical rotation, this is indicative that complete racemisation has not occurred.

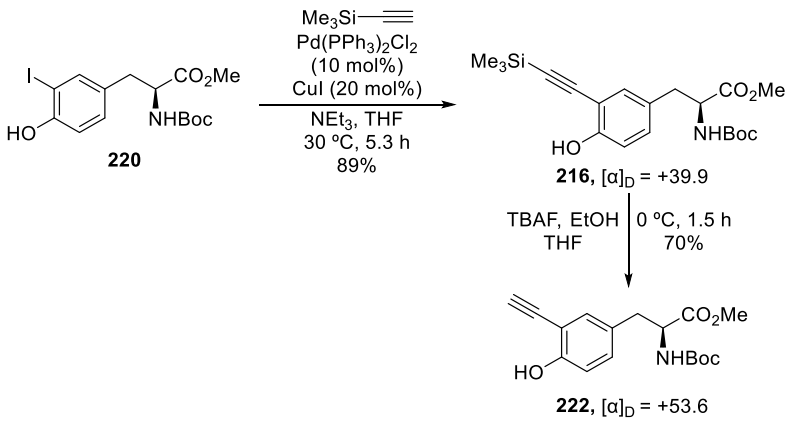

Scheme 78: Sonogashira cross-coupling of iodotyrosine 220 and subsequent deprotection.

In order to evaluate the enantiopurity, PhD student, Hannah Green who has continued this project went on to hydrolyse alkynyltyrosine **222** with lithium hydroxide and subject the product to amide coupling to give dipeptide **224** (Scheme **79**). The ^{1}H NMR spectrum of **224** showed a single diastereomer, demonstrating that the synthesis of **222** using TBAF in ethanol and tetrahydrofuran did not induce racemisation (Figure **48**).

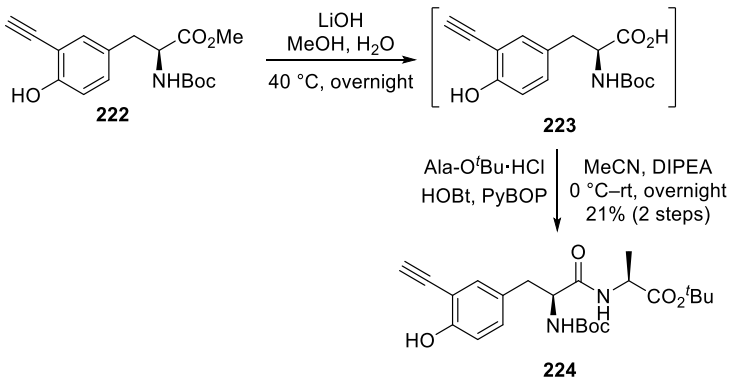

Scheme 79: Synthesis of dipeptide 224 by Hannah Green.

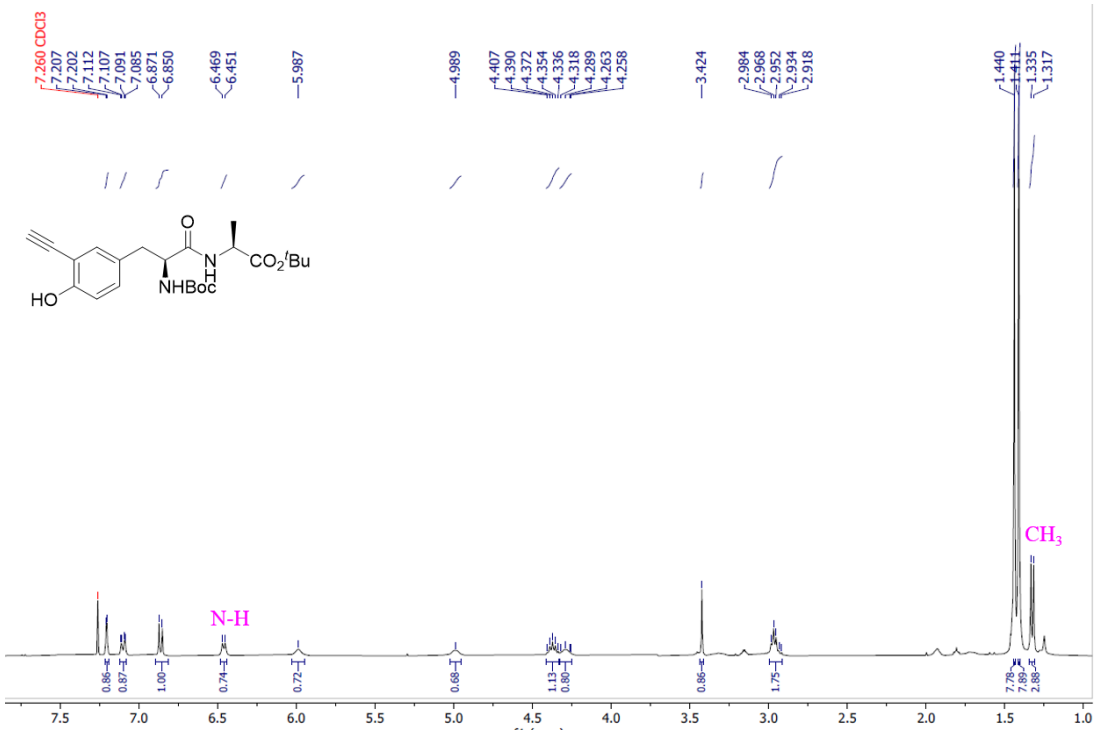

Figure 48: ^{1}H NMR spectrum of dipeptide 224 showing a single diastereomer. Highlighted methyl and N-H peaks, previously used to distinguish multiple diastereomers in alanine dipeptides containing unnatural phenylalanine analogues, indicate the presence of a single diastereomer of **224**.

2.4.2 Conclusions and Future work

Following the successful synthesis of alkyne extended phenylalanine analogues described in section 2.3, it was desirable to develop a series of alkyne extended tyrosine derived amino acids. Due to tyrosine possessing an electron donating hydroxyl group, it was considered that arylalkynyl analogues bearing electron withdrawing groups could result push-pull chromophores with improved fluorescent properties. Following protection of an iodinated tyrosine analogue, a Sonogashira cross-coupling reaction with TMS-acetylene was achieved in 89% yield. Removal of the TMS-group was achieved using TBAF using ethanol as a cosolvent to mitigate racemisation. This gave the desired terminal alkyne tyrosine analogue **222** in 70% yield.

Future work will involve optimisation of the Sonogashira cross-coupling reaction to give alkyne extended analogues of tyrosine (Scheme **80**). An initial library will focus

on highly conjugated adducts bearing electron withdrawing groups which were the most successful in the alkyne extended phenylalanine series. The photophysical properties of the α-amino acids will subsequently be evaluated. The aim for this series of α-amino acids containing push-pull chromophores is to identify a novel fluorescent α-amino acid that can be used for cell-imaging, without the need to attach larger chromophores such as BODIPY.

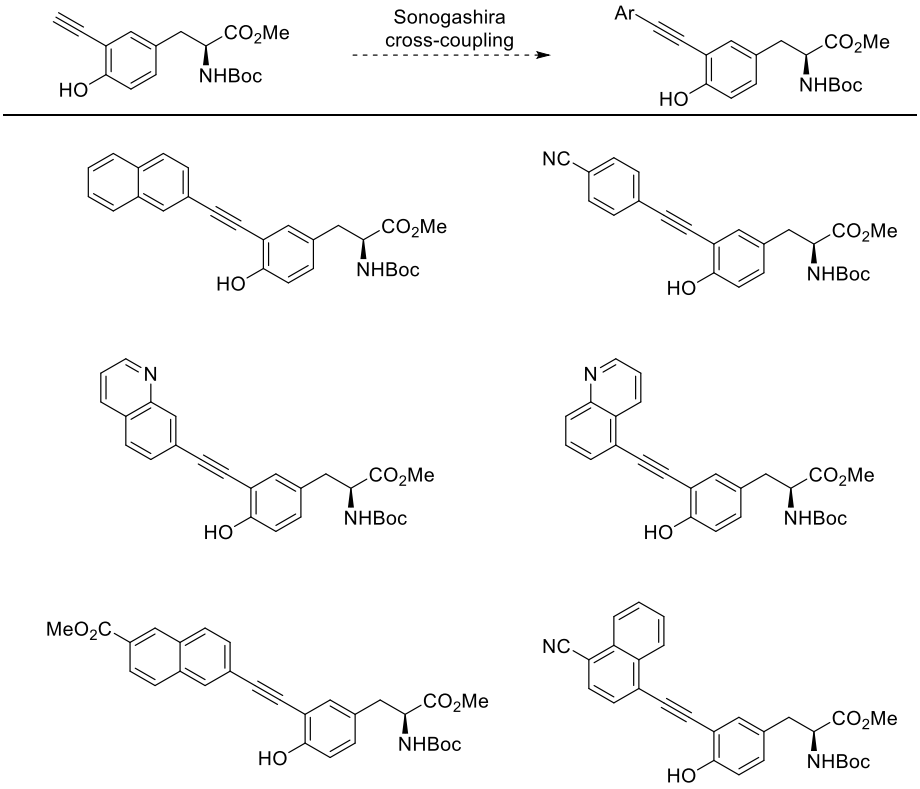

Scheme 80: Arylalkynyl tyrosine analogue targets.

3.0 Experimental

3.1 General Experimental

All reagents and starting materials were obtained from commercial sources and used as received. Dry *N,N*-dimethylformamide was purchased from ThermoFisher and anhydrous methanol was purchased from Alfa Aesar. All other dry solvents were purified using a PureSolv 500 MD solvent purification system. Dry glassware was oven-dried at 140 °C for a minimum of 16 h, cooled to room temperature and then purged with argon. Solvents were degassed by sonication under a flow of argon. Brine refers to a saturated solution of sodium chloride. Flash column chromatography was carried out using Fisher matrix silica 60. Macherey-Nagel aluminium-backed plates pre-coated with silica gel 60 (UV_{254}) were used for thin layer chromatography and visualised by staining with $KMnO_4$, vanillin or ninhydrin. ^1H NMR and ^{13}C NMR spectra were recorded on a Bruker DPX 400 or 500 spectrometer with chemical shift values in ppm relative to TMS (δ_H 0.00 and δ_C 0.0), or residual $CDCl_3$ (δ_H 7.26 and δ_C 77.2), DMSO-d_6 (δ_H 2.50 and δ_C 39.5) or CD_3OD (δ_H 3.31 and δ_C 49.0) as standard. ^1H and ^{13}C assignments are based on two-dimensional COSY, HSQC, HMBC and DEPT experiments. Mass spectra were obtained using an Agilent 1260 Infinity II HPLC coupled with an Agilent 6546 QTOF or Bruker Microtof-q for ESI. Infrared spectra were obtained neat using a Shimadzu IR Prestige-21 spectrometer. Melting points were determined on a Reichert platform melting point apparatus. Optical rotations were determined as solutions irradiating with the sodium D line (λ= 589 nm) using an Autopol V polarimeter. $[\alpha]_D$ values are given in units 10^{-1} deg cm^2 g^{-1}. Chiral HPLC spectra were recorded on Shimadzu LC-20AD prominence liquid chromatograph with a CBM-20A prominence communications bus module, DGU-20A5 prominence degasser, SPD-M20A prominence diode array detector (210 or 254 nm) and a Shimadzu CTO-20AC prominence column oven (25 °C). Analysis was performed using 20 μL sample injections and methods were calibrated with the corresponding racemic mixtures. Data acquisition and processing was performed using LabSolutions 1.21 SP1 chromatography software.

Absorption and emission data were recorded using the following instruments:

1. UV-Vis spectra were recorded on a Perkin Elmer Lamda 25 instrument. Fluorescence spectra were recorded on a Shimadzu RF-5301PC spectrofluorophotometer. Emission data were measured using excitation and emission bandpass filters of 3 nm.

2. Both UV-Vis spectra and fluorescence spectra were recorded on a Horiba Duetta Fluorescence and Absorbance spectrometer. Absorbance spectra were recorded with an integration time of 0.05 s, and a band pass of 5 nm. Fluorescence spectra were recorded with and excitation and emission band pass of 5 nm, an integration time of 0.1 s, 1 s or 2 s, and with detector accumulations set to 1.

Quantum yields were determined using a comparative method against L-tryptophan (Φ = 0.14 in methanol),[287] anthracene (Φ = 0.27 in ethanol)[288] or rhodamine 6G (Φ = 0.94 in ethanol)[288] as a standard reference. The integrated fluorescence intensity of each compound was determined from the emission spectra given. Measurements were performed at a minimum of five different concentrations. Concentrations were chosen to ensure the absorption value was below 0.1 to avoid re-absorption effects. Integrated fluorescence intensity was plotted as a function of the measured absorbance and a linear fit was calculated. The resultant gradient was then used to calculate the quantum yield, using the equation below:

$$\phi_x = \phi_{ST}\left(\frac{Grad_{ST}}{Grad_x}\right)\left(\frac{\eta_x^2}{\eta_{ST}^2}\right)$$

Subscript *ST* signifies the quantities associated with the quantum yield standard. Subscript X signifies the quantities associated with the novel compound. $Grad_X$ is the determined gradient associated with the novel compound. $Grad_{ST}$ is the determined gradient associated with quantum yield standard. η is the refractive index of the solvent used in the fluorescence measurements. η = 1.333 for water, 1.361 for ethanol 1.331 for methanol and 1.36 for liposomes.[289]

3.2 Dibenzofuran Analogues of Tyrosine Experimental

3.2.1 Synthesis of dibenzofuran amino acids

Methyl (2*R*)-2-[(*tert*-butoxycarbonyl)amino]-3-iodopropanoate (77)[290]

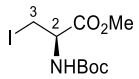

In an oven dry flask under argon, methyl (2*S*)-2-[(*tert*-butoxycarbonyl)amino]-3-hydroxypropanoate (624 mg, 2.85 mmol) was dissolved in dry dichloromethane (12 mL) and cooled to 0 °C. Diisopropylethylamine (0.550 mL, 3.13 mmol) was added followed by dropwise addition of methanesulfonyl chloride (0.240 mL, 3.13 mmol). The reaction mixture was stirred for 3.5 h at 0 °C. The reaction quenched with water (12 mL). The product was extracted with dichloromethane (2 × 100 mL) and washed with brine (100 mL). The solvent was removed under reduced pressure to give methyl (2*S*)-2-[(*tert*-butoxycarbonyl)amino]-3-(methylsulfonyloxy)propanoate as a colourless crude oil. The crude methyl (2*S*)-2-[(*tert*-butoxycarbonyl)amino]-3-(methylsulfonyloxy)propanoate product was subsequently dissolved in acetone (18 mL). Sodium iodide (855 mg, 5.70 mmol) was added. The reaction mixture was heated to 60 °C and stirred for 3 h. The reaction mixture was cooled and filtered and the filtrate concentrated *in vacuo*. Purification by flash column chromatography eluting in 20% ethyl acetate in hexane gave methyl (2*R*)-2-[(*tert*-butoxycarbonyl)amino]-3-iodopropanoate (**77**) (628 mg, 67%) as a yellow solid. Mp 43–45 °C; $[\alpha]_D^{24}$ +37.4 (c 1.0, $CHCl_3$) [lit.[290] +40.3 (*c* 1.0, $CHCl_3$)]; δ_H (400 MHz, $CDCl_3$) 5.35 (1H, br d, *J* 7.0 Hz, NH), 4.54–4.48 (1H, m, 2-H), 3.78 (3H, s, OMe), 3.58 (1H, dd, *J* 10.4, 3.8 Hz, 3-*H*H), 3.54 (1H, dd, *J* 10.4, 4.1 Hz, 3-H*H*), 1.44 (9H, s, 3 × CH_3); δ_C (101 MHz, $CDCl_3$) δ 170.2 (C), 155.0 (C), 80.5 (C), 53.8 (CH_3), 53.1 (CH), 28.4 (3 × CH_3), 7.9 (CH_2); MS (ESI) *m/z* 352 (MNa^+, 100).

Methyl (2*S*)-2-((*tert*-butoxycarbonyl)amino)-3-(naphtho[2′′,3′′-*b*]benzofuran-2′-yl)propanoate (147a)

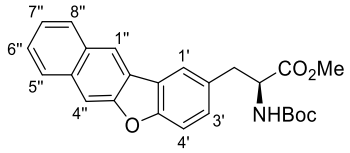

To an oven-dried Young flask under argon was added zinc dust (90.8 mg, 1.39 mmol) and iodine (17.9 mg, 0.0705 mmol). Methyl (2*R*)- 2-[(*tert*-butoxycarbonyl)amino]-3-iodopropanoate (**78**) (150 mg, 0.456 mmol) was added as a solution in dry *N*,*N*'-dimethylformamide (1.0 mL). A further portion of iodine (18.4 mg, 0.0725 mmol) was added and a colour change from yellow to colourless was observed, along with a noticeable exotherm. The reaction mixture was stirred at room temperature for 1 h. Tris(dibenzylideneacetone)dipalladium(0)-chloroform ($Pd_2(dba)_3$) adduct (12.4 mg, 0.0120 mmol) and 2-dicyclohexylphosphino-2′,6′-dimethoxybiphenyl (SPhos) (9.90 mg, 0.0241 mmol), 2-bromonaphtho[2,3-b]benzofuran (176 mg, 0.593 mmol) were added to the reaction mixture. A further 1.5 mL *N*,*N*'-dimethylformamide was added and the reaction stirred at 40 °C for 3.5 h. The reaction mixture was diluted with ethyl acetate (50 mL) and washed with an aqueous lithium chloride solution (5% w/w, 2 × 50 mL). The organic layer was dried ($MgSO_4$) and concentrated under reduced pressure. Purification by flash column chromatography eluting with 15% ethyl acetate in hexane gave methyl (2*S*)-2-((*tert*-butoxycarbonyl)amino)-3-(naphtho[2,3-*b*]benzofuran-2-yl)propanoate (**147a**) (84.4 mg, 44%) as a yellow solid. Mp 120–124 °C; $[\alpha]_D^{15}$ +67.2 (c 0.1, $CHCl_3$); ν_{max}/cm^{-1} (neat) 3357 (NH), 2921 (CH), 1700 (C=O), 1504, 1481, 1394, 1242, 1167, 747; δ_H (400 MHz, $CDCl_3$) 1.44 (9H, s, 3 × CH_3), 3.23 (1H, dd, *J* 13.8, 6.0 Hz, 3-*H*H), 3.31 (1H, dd, *J* 13.8, 5.6 Hz, 3-H*H*), 3.75 (3H, s, OCH_3), 4.64–4.74 (1H, m, 2-H), 5.11 (1H, d, *J* 8.4 Hz, 2-NH), 7.27 (1H, dd, *J* 8.4, 2.0 Hz, 3′-H), 7.43–7.54 (3H, m, 4′-H, 6′′-H and 7′′-H), 7.82 (1H, d, *J* 2.0 Hz, 1′-H), 7.89 (1H, s, 1′′-H), 7.95 (1H, d, *J* 8.4 Hz, 5′′-H), 8.02 (1H, d, *J* 7.6 Hz, 8′′-H), 8.34 (1H, s, 4′′-H); δ_C (101 MHz, $CDCl_3$) 28.4 (3 × CH_3), 38.4 (CH_2), 52.4 (CH_3), 55.0 (CH), 80.1 (C), 107.1 (CH), 111.6 (CH), 119.2 (CH), 122.0 (CH), 124.3 (C), 124.4 (CH), 125.3 (C), 126.0 (CH), 127.9 (CH), 128.5 (CH), 129.5 (CH), 130.2 (C), 130.8 (C), 133.2 (C), 155.18 (C), 155.25 (C), 156.9 (C), 172.5 (C); *m/z* (ESI) 442.1639 (MNa^+ . $C_{25}H_{25}NNaO_5$ requires 442.1625).

Methyl (2*S*)-2-((*tert*-butoxycarbonyl)amino)-3-(dibenzo[*b,d*]furan-2′-yl)propanoate (147d)

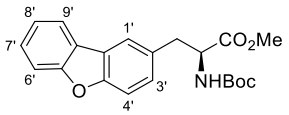

Methyl (2*S*)-2-((*tert*-butoxycarbonyl)amino)-3-(dibenzo[*b,d*]furan-2-yl)propanoate (**147d**) was synthesised as described for methyl (*S*)-2-((*tert*-butoxycarbonyl)amino)-3-(naphtho[2′′,3′′-*b*]benzofuran-2′-yl)propanoate (**147a**), using zinc dust (89.9 mg, 1.374 mmol), iodine (2 × 17.0 mg, 0.137 mmol), methyl (2*R*)- 2-[(*tert*-butoxycarbonyl)amino]-3-iodopropanoate (**78**) (150 mg, 0.456 mmol), $Pd_2(dba)_3$ (12.4 mg, 0.0120 mmol), SPhos (9.50 mg, 0.0231 mmol), and 2-bromodibenzo[b,d]furan (147 mg, 0.595 mmol) in *N*,*N*'-dimethylformamide (2.5 mL) at 40 °C for 4 h. Purification by flash column chromatography, eluting in 10–20% ethyl acetate in hexane, gave methyl (2*S*)-2-((*tert*-butoxycarbonyl)amino)-3-(dibenzo[*b,d*]furan-2-yl)propanoate (**147d**) as an off-white solid (104 mg, 62%). Mp 100–102 °C; $[\alpha]_D^{18}$ +51.4 (*c* 0.1, $CHCl_3$); ν_{max}/cm^{-1} (neat) 3350 (NH), 2984 (CH), 2958 (CH), 2934 (CH), 2014, 1734 (C=O), 1688 (C=O), 1515, 1281, 1192, 1157, 995; δ_H (400 MHz, $CDCl_3$) 1.42 (9H, s, 3 × CH_3), 3.21 (1H, dd, *J* 14.0, 6.0 Hz, 3-*H*H), 3.29 (1H, dd, *J* 14.0, 6.0 Hz, 3-H*H*), 3.72 (3H, s, OCH_3), 4.59–4.69 (1H, m, 2-H), 5.03 (1H, d, *J* 7.6 Hz, 2-NH) 7.21 (1H, dd, *J* 8.4, 1.6 Hz, 3′-H), 7.34 (1H, t, *J* 7.6 Hz, 7′-H), 7.42–7.52 (2H, m, 4′-H and 8′-H), 7.56 (1H, d, *J* 8.0 Hz, 9′-H), 7.72 (1H, d, *J* 1.6 Hz, 1′-H), 7.92 (1H, d, *J* 7.6 Hz, 6′-H); δ_C (101 MHz, $CDCl_3$); 28.4 (3 × CH_3), 38.5 (CH_2), 52.4 (CH_3), 55.0 (CH), 80.1 (C), 111.8 (CH), 111.9 (CH), 120.7 (CH), 121.4 (CH), 122.9 (CH), 124.1 (C), 124.6 (C), 127.4 (CH), 128.4 (CH), 130.7 (C), 155.2 (C), 155.5 (C), 156.6 (C), 172.5 (C); *m/z* (ESI) 270.1128 ($[(MH-CO_2{}^tBu)+H]^+$. $C_{16}H_{14}NO_3H$ requires 270.1125).

Methyl (2*S*)-2-((*tert*-butoxycarbonyl)amino)-3-(8′-cyanodibenzo[*b,d*]furan-2′-yl)propanoate (147e)

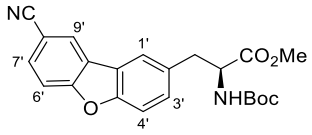

Methyl (2*S*)-2-((*tert*-butoxycarbonyl)amino)-3-(6-cyanodibenzo[*b,d*]furan-2-yl)propanoate (**147e**) was synthesised as described for methyl (*S*)-2-((*tert*-butoxycarbonyl)amino)-3-(naphtho[2′′,3′′-b]benzofuran-2′-yl)propanoate (**147a**), using zinc dust (58.6 mg, 0.896 mmol), iodine (2 × 11.5 mg, 0.0909 mmol), methyl (2*R*)- 2-[(*tert*-butoxycarbonyl)amino]-3-iodopropanoate (**78**) (99.7 mg, 0.303 mmol), $Pd_2(dba)_3$ (7.80 mg, 0.00760 mmol), SPhos (6.2 mg, 0.0152 mmol), and 8-bromodibenzo[b,d]furan-2-carbonitrile (108 mg, 0.397 mmol) in *N*,*N*'-dimethylformamide (1.0 mL) at 20 °C for 24 h. Purification by flash column chromatography eluting in 15 ethyl acetate in petroleum ether gave methyl (2*S*)-2-((*tert*-butoxycarbonyl)amino)-3-(6-cyanodibenzo[*b,d*]furan-2-yl)propanoate (**147e**) as a brown solid (54.8 mg, 45%). Mp 135–138 °C; $[\alpha]_D^{18}$ +49.1 (*c* 0.1, $CHCl_3$); ν_{max}/cm^{-1} (neat) 3339 (NH), 2919 (CH), 2223 (CN), 1735 (C=O), 1689 (C=O), 1553, 1483, 1455, 1250, 1157, 1052, 822; δ_H (400 MHz, $CDCl_3$) 1.41 (9H, s, 3 × CH_3), 3.20 (1H, dd, *J* 14.0, 6.0 Hz, 3-*H*H), 3.32 (1H, dd, *J* 14.0, 5.6 Hz, 3-H*H*) 3.74 (3H, s, OCH_3) 4.60–4.69 (1H, m, 2-H), 5.05 (1H, d, *J* 8.8 Hz) 7.32 (1H, dd, *J* 8.8, 2.0 Hz, 3′-H), 7.54 (1H, d, *J* 8.8 Hz, 4′-H), 7.64 (1H, d, *J* 8.4 Hz, 6′-H), 7.71–7.76 (2H, m, 1′-H and 7′-H), 8.23 (1H, d, *J* 2.0 Hz, 9′-H); δ_C (101 MHz, $CDCl_3$) 28.4 (3 × CH_3), 38.5 (CH_2), 52.5 (CH_3), 54.9 (CH), 80.3 (C), 106.8 (C), 112.2 (CH), 113.1 (CH), 119.3 (C), 121.8 (CH), 123.0 (C), 125.2 (C), 125.5 (CH), 130.1 (CH), 131.1 (CH), 132.1 (C), 155.2 (C), 156.1 (C), 158.4 (C), 172.3 (C); *m/z* (ESI) 295.1076 ($[(MH-CO_2{}^tBu)+H]^+$. $C_{17}H_{13}N_2O_3H$ requires 295.1077).

3.2.2 Determination of Förster distance (R_0) for amino acid 147c/lysine(DNP) pair

Forster distance, R_0, was determined using the following equation[17]:

$$R_0 = 0.211[\kappa^2 \eta^{-4} Q_D J(\lambda)]^{1/6}$$

where, κ" is a factor describing the relative orientation in space between two transition dipoles(typically assumed to be equal to 2/3); η is the refractive index of the medium and QD is the quantum yield of the donor in the absence of the acceptor. J(λ) is the overlap integral between the donor emission and acceptor absorption and can be calculated using the following equation:

$$J(\lambda) = \frac{\int_0^\infty F_D(\lambda)\varepsilon_A(\lambda)\lambda^4 d\lambda}{\int_0^\infty F_D(\lambda) d\lambda}$$

where λ is the wavelength and ε A is the extinction coefficient of the acceptor. J(λ) can also be expressed by the following equation for calculating the spectral overlap in excel[159]:

$$J(\lambda) = \frac{\sum_{\lambda=300,\lambda\in N}^{600} F_D(\lambda)\varepsilon_A\lambda^4}{\sum_{\lambda=300,\lambda\in N}^{600} F_D(\lambda)}$$

Emission and absorption spectra of amino acid **147c** and lysine(dnp) were recorded in methanol at a concentration of 5 μM. Forster distance calculation was performed in excel using template provided by Hink and Visser.[291] This gave a Forster distance between the FRET pair of 34.20 A.

3.3 Biaryl Analogues of Phenylalanine Experimental

3.3.1 Synthesis of biaryl amino acids

General Procedure 1: One-pot Nonaflate Formation and Suzuki-Miyaura Cross-Coupling Reaction. In an oven dry sealed tube, a solution of methyl (2*S*)-2-(benzyloxycarbonylamino)-3-(4-hydroxyphenyl)propanoate (1 equiv.) and potassium phosphate (3 equiv.) in acetonitrile (3 mL per mmol) was degassed under argon with sonication for 0.2 h. To this was added perfluoro-1-butanesulfonyl fluoride (1.5 equiv.). The reaction mixture was heated to 60 °C and stirred for 2 h. To this was added boronic acid (1.5 equiv.), XPhos Pd G2 (1 mol%) and water (2 mL per mmol). The reaction mixture was stirred at 60, 80 or 90 °C for 2 h. Additional XPhos Pd G2 (1 mol%) was added and the reaction mixture was stirred at 60, 80 or 90 °C for 2 h. A final portion of XPhos Pd G2 (1 mol%) was added and the reaction mixture was stirred at 60, 80 or 90 °C for 18 h. After cooling to room temperature, the reaction mixture was diluted in ethyl acetate (30 mL) and washed with water (3 × 30 mL). The organic layer was dried ($MgSO_4$), filtered and concentrated *in vacuo*. Purification by flash column chromatography gave the arylated products.

General Procedure 2: Ester Hydrolysis and Acid Mediated Removal of the Cbz-Protecting Group. To a stirred solution of the protected amino acid (1 equiv.) in methanol (3 mL), 1,4-dioxane (1.75 mL) and water (1.75 mL) was added caesium carbonate (1.3 equiv.). The reaction mixture was heated to 60 °C and stirred for 18 h. The reaction mixture was cooled to room temperature and concentrated *in vacuo*. The reaction mixture was diluted in water (5 mL), acidified to pH 1 using 1 M aqueous hydrochloric acid and extracted with ethyl acetate (3 × 20 mL). The organic layers were combined, dried ($MgSO_4$), filtered and concentrated *in vacuo* to give the desired carboxylic acid product. Without further purification, the carboxylic acid product was subsequently dissolved in 6 M hydrochloric acid (3 mL) and dioxane (3 mL) and heated under reflux for 4 h. The reaction mixture was cooled to room temperature and concentrated *in vacuo* to give the final amino acids. The amino acids were purified by recrystallisation from the specified solvent system.

Methyl (2*S*)-2-(benzyloxycarbonylamino)-3-(4”-phenylbiphen-4’-yl)propanoate (159j)

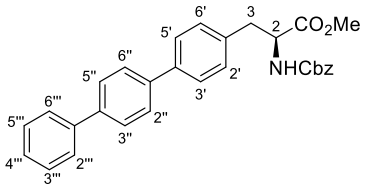

Methyl (2*S*)-2-(benzyloxycarbonylamino)-3-(4’’-phenylbiphen-4’-yl)propanoate (**159j**) was synthesised as described in general procedure 1 using methyl (2*S*)-2-(benzyloxycarbonylamino)-3-(4-hydroxyphenyl)propanoate (0.155 g, 0.471 mmol), perfluoro-1-butanesulfonyl fluoride (0.120 mL, 0.680 mmol), 4-biphenylboronic acid (0.136 g, 0.687 mmol), XPhos Pd G2 (0.0120 g, 0.0150 mmol, 3 mol%) and potassium phosphate (0.303 g, 1.43 mmol) in acetonitrile (1.5 mL) and water (1 mL) at 60 °C. After cooling to room temperature, the reaction mixture was diluted in chloroform (100 mL) and washed with water (3 × 50 mL). The organic layer was dried ($MgSO_4$), filtered and concentrated *in vacuo*. Purification by flash column chromatography, eluting with 80–100% dichloromethane in hexane gave methyl (2*S*)-2-(benzyloxycarbonylamino)-3-(4’’-phenylbiphen-4’-yl)propanoate (**159j**) (0.169 g, 77%) as a white solid. Mp 184–185 °C; ν_{max}/cm^{-1} (neat) 3709 (NH), 3357, 2980 (CH), 2866, 1724 (C=O), 1052; $[\alpha]_D^{23}$ +47.8 (*c* 0.1, $CHCl_3$); δ_H (400 MHz, $CDCl_3$) 3.14 (1H, dd, *J* 14.0, 6.0 Hz, 3-*H*H), 3.20 (1H, dd, *J* 14.0, 5.6 Hz, 3-H*H*), 3.76 (3H, s, OCH_3), 4.66–4.76 (1H, m, 2-H), 5.10 (1H, d, *J* 8.0 Hz, C*H*HPh), 5.13 (1H, d, *J* 8.0 Hz, CH*H*Ph), 5.27 (1H, d, *J* 8.0 Hz, 2-NH), 7.19 (2H, d, *J* 8.2 Hz, 2’-H and 6’-H), 7.28–7.41 (6H, m, 6 × ArH), 7.43–7.51 (2H, m, 2 × ArH), 7.56 (2H, d, *J* 8.2 Hz, 3’-H and 5’-H), 7.61–7.75 (6H, m, 6 × ArH); δ_C (101 MHz, $CDCl_3$) 38.0 (CH_2), 52.5 (CH_3), 54.9 (CH), 67.2 (CH_2), 127.2 (2 × CH), 127.3 (2 × CH), 127.5 (4 × CH), 127.6 (2 × CH), 128.3 (CH), 128.4 (CH), 128.7 (2 × CH), 129.0 (2 × CH), 129.9 (2 × CH), 135.0 (C), 136.4 (C), 139.6 (C), 139.7 (C), 140.3 (C), 140.8 (C), 155.8 (C), 172.1 (C); *m/z* (ESI) 488.1840 (MNa^+. $C_{30}H_{27}NNaO_4$ requires 488.1832).

Methyl (2*S*)-2-(benzyloxycarbonylamino)-3-[(2''-naphthyl)phen-4'-yl] propanoate (159h)

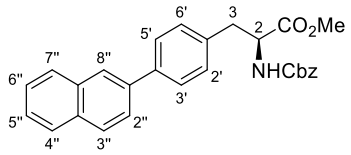

Methyl (2*S*)-2-(benzyloxycarbonylamino)-3-[(2''-naphthyl)phen-4'-yl]propanoate (**159h**) was synthesised as described in general procedure 1 using methyl (2*S*)-2-(benzyloxycarbonylamino)-3-(4-hydroxyphenyl)propanoate (0.155 g, 0.472 mmol), perfluoro-1-butanesulfonyl fluoride (0.120 mL, 0.687 mmol), 2-naphthaleneboronic acid (0.0825 g, 0.480 mmol), XPhos Pd G2 (0.0120 g, 0.0150 mmol, 3 mol%) and potassium phosphate (0.304 g, 1.43 mmol) in acetonitrile (1.5 mL) and water (1 mL) at 90 °C. Purification by flash column chromatography, eluting with 5–10% ethyl acetate in hexane gave methyl (2*S*)-2-(benzyloxycarbonylamino)-3-[(2''-naphthyl)phen-4'-yl]propanoate (**159j**) (0.170 g, 81%) as a colourless oil. ν_{max}/cm^{-1} (neat) 3346 (NH), 3320, 3059, 2978 (CH), 1776 (C=O), 1651 (C=O), 1538, 1318, 1249, 1050, 1022; $[\alpha]_D^{25}$ +62.8 (*c* 0.1, $CHCl_3$); δ_H (400 MHz, $CDCl_3$) 3.17 (1H, dd, *J* 13.9, 6.1 Hz, 3-*H*H), 3.24 (1H, dd, *J* 13.9, 5.7 Hz 3-H*H*), 3.78 (3H, s, OCH_3), 4.72–4.79 (1H, m, 2-H), 5.12 (1H, d, *J* 12.0 Hz, C*H*HPh), 5.17 (1H, d, *J* 12.0 Hz, CH*H*Ph), 5.33 (1H, d, *J* 8.3 Hz, 2-NH), 7.23 (2H, d, *J* 7.8 Hz, 2'-H and 6'-H), 7.29–7.38 (5H, m, Ph), 7.47–7.55 (2H, m, 3'-H and 5'-H), 7.64–7.67 (2H, m, 6''-H and 7''-H), 7.73 (1H, dd, *J* 8.5, 1.8 Hz, 3''-H), 7.87–7.94 (3H, m, 4''-H, 5''-H and 8'-H), 8.03 (1H, d, *J* 1.8 Hz, 1''-H); δ_C (101 MHz, $CDCl_3$) 38.0 (CH_2), 52.5 (CH_3), 54.9 (CH), 67.1 (CH_2), 125.5 (CH), 125.8 (CH), 126.1 (CH), 126.4 (CH), 127.7 (2 × CH), 127.8 (CH), 128.2 (2 × CH), 128.29 (CH), 128.32 (CH), 128.55 (CH), 128.65 (2 × CH), 129.9 (2 × CH), 132.7 (C), 133.8 (C), 135.0 (C), 136.4 (C), 138.1 (C), 140.0 (C), 155.8 (C), 172.1 (C); *m/z* (ESI) 462.1688 (MNa^+. $C_{28}H_{25}NNaO_4$ requires 462.1676).

Methyl (2*S*)-2-(benzyloxycarbonylamino)-3-(4''-fluorobiphen-4'-yl)propanoate (159k)

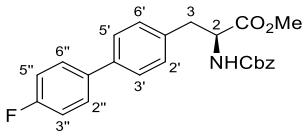

Methyl (*2S*)-2-(benzyloxycarbonylamino)-3-(4''-fluorobiphen-4'-yl)propanoate (**159k**) was synthesised as described in general procedure 1 using methyl (2*S*)-2-(benzyloxycarbonylamino)-3-(4-hydroxyphenyl)propanoate (0.155 g, 0.471 mmol), perfluoro-1-butanesulfonyl fluoride (0.120 mL, 0.680 mmol), 4-fluorophenylboronic acid (0.110 g, 0.729 mmol), XPhos Pd G2 (0.0120 g, 0.0150 mmol, 3 mol%) and potassium phosphate (0.307 g, 1.45 mmol) in acetonitrile (1.5 mL) and water (1 mL) at 60 °C. Purification by flash column chromatography, eluting with 20% ethyl acetate in hexane gave methyl (2*S*)-2-(benzyloxycarbonylamino)-3-(4''-fluorobiphen-4'-yl)propanoate (**159k**) (0.127 g, 69%) as a pale yellow solid. Mp 108–109 °C; ν_{max}/cm^{-1} (neat); 3343 (NH), 1741 (C=O), 1705 (C=O), 1519, 1491, 1214; $[\alpha]_D^{25}$ +54.1 (*c* 0.1, $CHCl_3$); δ_H (400 MHz, $CDCl_3$) 3.12 (1H, dd, *J* 13.8, 6.0 Hz, 3-*H*H), 3.19 (1H, dd, *J* 13.8, 5.6 Hz, 3-H*H*), 3.75 (3H, s, OCH_3), 4.66–4.75 (1H, m, 2-H), 5.09 (1H, d, *J* 12.4 Hz, C*H*HPh), 5.13 (1H, d, *J* 12.4 Hz, CH*H*Ph), 5.26 (1H, d, *J* 8.3 Hz, 2-NH), 7.01–7.18 (4H, m, 2'-H, 6'-H, 3''-H and 5''-H), 7.29–7.39 (5H, m, 7.45, Ph), 7.44 (2H, d, *J* 8.0 Hz, 3'-H and 5'-H), 7.48–7.56 (2H, m, 2''-H and 6''-H); δ_C (101 MHz, $CDCl_3$) 37.9 (CH_2), 52.6 (CH_3), 54.9 (CH), 67.2 (CH_2), 115.8 (2 × CH, d, $^2J_{CF}$ 21.4 Hz), 127.3 (2 × CH), 128.3 (2 × CH), 128.4 (CH), 128.7 (2 × CH, d, $^3J_{CF}$ 8.0 Hz), 128.7 (2 × CH) 129.9 (2 × CH), 134.9 (C), 136.3 (C), 136.9 (C), 139.2 (C), 155.8 (C), 162.6 (C, d, $^1J_{CF}$ 246.3 Hz), 172.1 (C); *m/z* (ESI) 430.1432 (MNa^+. $C_{24}H_{22}FNNaO_4$ requires 430.1425).

Methyl (2*S*)-2-(benzyloxycarbonylamino)-3-[4''-(chlorobiphen-4'-yl] propanoate (159c)

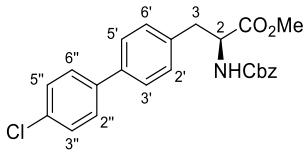

Methyl (2*S*)-2-(benzyloxycarbonylamino)-3-(4-hydroxyphenyl)propanoate (**159c**) (0.155 g, 0.475 mmol) and potassium phosphate (0.300, 1.41 mmol) in dry acetonitrile (1.5 mL) was degassed under argon for 0.2 h. To this was added was added perfluoro-1-butanesulfonyl fluoride (0.120 mL, 0.680 mmol). The reaction tube was sealed, heated to 60 °C, and stirred for 2 h. To this was added 4-chlorophenylboronic acid (0.106 g, 0.678 mmol), XPhos Pd G2 (4.00 mg, 0.00508 mmol) and water (1.0 mL). The reaction mixture was degassed for 0.2 h and stirred at 50 °C for 2 h. Additional XPhos Pd G2 (4.00 mg, 0.00508 mmol) was added and the reaction mixture stirred at 50 °C for 2 h. Another portion of XPhos Pd G2 (4.00 mg, 0.00508 mmol) was added and the reaction mixture stirred at 50 °C for 16 h. A further three batches of XPhos Pd G2 (4.00 mg, 0.00508 mmol) were added every 2 h. After the final portion of catalyst the reaction mixture was stirred at 50 °C for 16 h. After cooling to room temperature, the reaction mixture was diluted in ethyl acetate (30 mL) and washed with water (3 × 30 mL). The organic layer was dried ($MgSO_4$), filtered and concentrated *in vacuo*. Purification by flash column chromatography, eluting with 5% ethyl acetate in toluene gave methyl (2*S*)-2-(benzyloxycarbonylamino)-3-[4''-(chlorobiphen-4'-yl]propanoate (**159c**) (0.0624 g, 31%) as a white solid. Mp 90–92 °C; ν_{max}/cm^{-1} (neat) 3341 (NH), 3031, 2955 (CH), 1717 (C=O), 1515, 1487, 1347, 1258, 1212; $[\alpha]_D^{21}$ +53.0 (*c* 0.1, $CHCl_3$); δ_H (400 MHz, $CDCl_3$) 3.13 (1H, dd, *J* 13.9, 5.7 Hz, 3-*H*H), 3.21 (1H, dd, *J* 13.9, 6.1 Hz 3-H*H*), 3.75 (3H, s, OCH_3), 4.68–4.75 (1H, m, 2-H), 5.10 (1H, d, *J* 12.0 Hz, C*H*HPh), 5.14 (1H, d, *J* 12.0 Hz, CH*H*Ph), 5.30 (1H, d, *J* 8.3 Hz, 2-NH), 7.16–7.20 (2H, m, 2'-H and 6'-H), 7.30–7.52 (11H, m, Ph, 3'-H, 5'-H, 2''-H, 3''-H, 5''-H and 6''-H); δ_C (101 MHz, $CDCl_3$) 37.9 (CH_2), 52.5 (CH_3), 54.9 (CH), 67.1 (CH_2), 127.2 (2 × CH), 128.2 (2 × CH), 128.3 (3 × CH), 128.6 (2 × CH), 129.0 (2 × CH), 129.9 (2 × CH), 133.5 (C), 135.3 (C), 136.3 (C), 138.9 (C), 139.2 (C), 155.7 (C), 172.0 (C); *m/z* (ESI) 446.1131 (MNa^+. $C_{24}H_{22}{}^{35}ClNNaO_4$ requires 446.1130)

Methyl (2*S*)-2-(benzyloxycarbonylamino)-3-(4''-cyanobiphen-4'-yl)propanoate (159l)

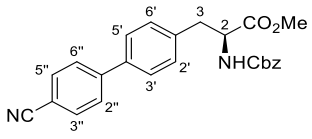

Methyl (2*S*)-2-(benzyloxycarbonylamino)-3-(4''-cyanobiphen-4'-yl)propanoate (**159l**) was synthesised as described in general procedure 1 using methyl (2*S*)-2-(benzyloxycarbonylamino)-3-(4-hydroxyphenyl)propanoate (0.156 g, 0.473 mmol), perfluoro-1-butanesulfonyl fluoride (0.120 mL, 0.680 mmol), 4-cyanophenylboronic acid (0.155 g, 0.939 mmol), XPhos Pd G2 (0.0120 g, 0.0150 mmol, 3 mol%) and potassium phosphate (0.303 g, 1.42 mmol) in acetonitrile (1.5 mL) and water (1 mL) at 80 °C. Purification by flash column chromatography, eluting with 20% ethyl acetate in hexane gave methyl (2*S*)-2-(benzyloxycarbonylamino)-3-(4''-cyanobiphen-4'-yl)propanoate (**159l**) (0.153 g, 79%) as a white solid. Mp 107–109 °C; ν_{max}/cm^{-1} (neat) 3339 (NH), 2955 (CH), 2226 (CN), 1716 (C=O), 1609 (C=C), 1497; $[\alpha]_D^{25}$ +65.2 (*c* 0.1, $CHCl_3$); δ_H (400 MHz, $CDCl_3$) 3.13 (1H, dd, *J* 13.9, 6.5 Hz, 3-*H*H), 3.22 (1H, dd, *J* 13.9, 5.7 Hz, 3-H*H*), 3.75 (3H, s, OCH_3), 4.66–4.76 (1H, m, 2-H), 5.00–5.17 (2H, m, CH_2Ph), 5.27 (1H, d, *J* 8.3 Hz, NH), 7.21 (2H, d, *J* 7.9 Hz, 2'-H and 6'-H), 7.27–7.38 (5H, m, Ph), 7.49 (2H, d, *J* 7.9 Hz, 3'-H and 5'-H), 7.65 (2H, d, *J* 8.2 Hz, 2''-H and 6''-H), 7.72 (2H, d, *J* 8.2 Hz, 3''-H and 5''-H); δ_C (101 MHz, $CDCl_3$) 38.0 (CH_2), 52.6 (CH_3), 54.9 (CH), 67.2 (CH_2), 111.1 (C), 119.0 (C), 127.5 (2 × CH), 127.7 (2 × CH), 128.3 (2 × CH), 128.4 (CH), 128.7 (2 × CH), 130.2 (2 × CH), 132.7 (2 × CH), 136.3 (C), 136.6 (C), 138.1 (C), 145.7 (C), 155.7 (C), 171.9 (C); *m/z* (ESI) 415.1651 (MH^+. $C_{25}H_{22}N_2O_4$ requires 415.1652).

Methyl (2*S*)-2-(benzyloxycarbonylamino)-3-(4''-acetylbiphen-4'-yl)propanoate (159e)

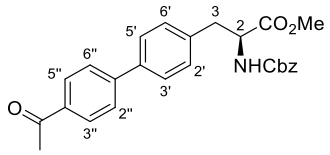

Methyl (2*S*)-2-(benzyloxycarbonylamino)-3-(4''-acetylbiphen-4'-yl)propanoate (**159e**) was synthesised as described in general procedure 1 using methyl (2*S*)-2-(benzyloxycarbonylamino)-3-(4-hydroxyphenyl)propanoate (0.15 g, 0.46 mmol), perfluoro-1-butanesulfonyl fluoride (0.12 mL, 0.68 mmol), 4-acetylphenylboronic acid (0.10 g, 0.68 mmol), XPhos Pd G2 (0.012 g, 0.015 mmol, 3 mol%) and potassium phosphate (0.29 g, 1.4 mmol) in acetonitrile (1.5 mL) and water (1 mL) at 60 °C. Purification by flash column chromatography, eluting with 20% ethyl acetate in hexane gave methyl (2*S*)-2-(benzyloxycarbonylamino)-3-(4''-acetylbiphen-4'-yl)propanoate (**159e**) (0.16 g, 81%) as a white solid. Mp 125–128 °C; ν_{max}/cm^{-1} (neat) 3332 (NH), 2952 (CH), 1716 (C=O), 1676 (C=O), 1522, 1354, 1264, 1207, 733; $[\alpha]_D^{25}$ +55.5 (*c* 0.1, $CHCl_3$); δ_H (400 MHz, $CDCl_3$) 2.64 (3H, s, 4''-$COCH_3$), 3.13 (1H, dd, *J* 13.9, 6.2 Hz, 3-*H*H), 3.22 (1H, dd, *J* 13.9, 5.7 Hz, 3-H*H*), 3.76 (3H, s, OCH_3), 4.68–4.75 (1H, m, 2-H), 5.09 (1H, d, *J* 12.0 Hz, C*H*HPh), 5.13 (1H, d, *J* 12.0 Hz, CH*H*Ph), 5.27 (1H, d, *J* 8.2 Hz, 2-NH), 7.20 (2H, d, *J* 8.4 Hz, 2'-H and 6'-H), 7.27–7.38 (5H, m, Ph), 7.54 (2H, d, *J* 8.4 Hz, 3'-H and 5'-H), 7.66 (2H, d, *J* 8.4 Hz, 2''-H and 6''-H), 8.03 (2H, d, *J* 8.4 Hz, 3''-H and 5''-H); δ_C (101 MHz, $CDCl_3$) 26.8 (CH_3), 38.0 (CH_2), 52.6 (CH_3), 54.9 (CH), 67.2 (CH_2), 127.2 (2 × CH), 127.6 (2 × CH), 128.2 (CH), 128.4 (2 × CH), 128.7 (2 × CH), 129.1 (2 × CH), 130.0 (2 × CH), 136.0 (C), 136.1 (C), 136.3 (C), 138.8 (C), 145.4 (C), 155.7 (C), 172.0 (C), 197.9 (C); *m/z* (ESI) 454.1631 (MNa^+. $C_{26}H_{25}NNaO_5$ requires 454.1625).

Methyl (2*S*)-2-(benzyloxycarbonylamino)-3-(2''-methoxybiphen-4'-yl)propanoate (159m)

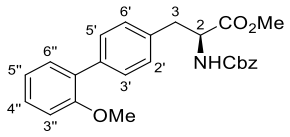

Methyl (2*S*)-2-(benzyloxycarbonylamino)-3-(2''-methoxybiphen-4'-yl)propanoate (**159m**) was synthesised as described in general procedure 1 using methyl (2*S*)-2-(benzyloxycarbonylamino)-3-(4-hydroxyphenyl)propanoate (0.155 g, 0.471 mmol), perfluoro-1-butanesulfonyl fluoride (0.120 mL, 0.680 mmol), 2-methoxyphenylboronic acid (0.139 g, 0.915 mmol), XPhos Pd G2 (0.012 g, 0.015 mmol, 3 mol%) and potassium phosphate (0.307 g, 1.45 mmol) in acetonitrile (1.5 mL) and water (1 mL) at 60 °C. Purification by flash column chromatography, eluting with 30% ethyl acetate in hexane gave methyl (2*S*)-2-(benzyloxycarbonylamino)-3-(2''-methoxybiphen-4'-yl)propanoate (**159m**) (0.163 g, 81%) as a clear oil. ν_{max}/cm^{-1} (neat) 3331 (NH), 2951 (CH), 2365, 1715 (C=O), 1510, 1487, 1240, 1214, 1058, 1023, 757; $[\alpha]_D^{25}$ +50.8 (*c* 0.1, $CHCl_3$); δ_H (400 MHz, $CDCl_3$) 3.13 (1H, dd, *J* 14.0, 6.4 Hz, 3-*H*H), 3.18 (1H, dd, *J* 14.0, 5.6 Hz, 3-H*H*), 3.75 (3H, s, OCH_3), 3.80 (4''-OCH_3), 4.65–4.73 (1H, m, 2-H), 5.06–5.16 (2H, m, CH_2Ph), 5.26 (1H, d, *J* 8.3 Hz, 2-NH), 6.98 (1H, br d, *J* 8.4 Hz, 3''-H), 7.02 (1H, td, *J* 7.5, 1.1 Hz, 5''-H), 7.11–7.16 (2H, m, 3'-H and 5'-H), 7.28–7.37 (7H, m, 2'-H, 6'-H and Ph), 7.43–7.48 (4''-H and 6''-H); δ_C (101 MHz, $CDCl_3$) 38.0 (CH_2), 52.5 (CH_3), 54.9 (CH), 55.6 (CH_3), 67.2 (CH_2), 111.4 (CH), 121.0 (CH), 128.2 (CH), 128.3 (CH), 128.7 (2 × CH), 128.8 (CH) 129.1 (2 × CH), 129.9 (2 × CH), 130.3 (C), 130.9 (2 × CH), 134.3 (C), 136.4 (C), 137.5 (C), 155.8 (C), 156.6 (C), 172.2 (C); *m/z* (ESI) 442.1629 (MNa^+. $C_{25}H_{25}NNaO_5$ requires 442.1625).

Methyl (2*S*)-2-(benzyloxycarbonylamino)-3-(4”-methoxybiphen-4’-yl)propanoate (159b)

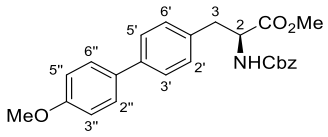

Methyl (2*S*)-2-(benzyloxycarbonylamino)-3-(4”-methoxybiphen-4’-yl)propanoate (**159b**) was synthesised as described in general procedure 1 using methyl (2*S*)-2-(benzyloxycarbonylamino)-3-(4-hydroxyphenyl)propanoate (0.155 g, 0.471 mmol), perfluoro-1-butanesulfonyl fluoride (0.120 mL, 0.680 mmol), 4-methoxyphenylboronic acid (0.110 g, 0.729 mmol), XPhos Pd G2 (0.0120 g, 0.0150 mmol, 3 mol%) and potassium phosphate (0.307 g, 1.45 mmol) in acetonitrile (1.5 mL) and water (1 mL) at 60 °C. Purification by flash column chromatography, eluting with 20% ethyl acetate in hexane gave methyl (2*S*)-2-(benzyloxycarbonylamino)-3-(4”-methoxybiphen-4’-yl)propanoate (**159b**) (0.135 g, 68%) as a white solid. Mp 102–104 °C; ν_{max}/cm^{-1} (neat) 2924 (CH), 2855, 1717 (C=O), 1501, 1246, 907; $[\alpha]_D^{17}$ +27.3 (*c* 0.1, $CHCl_3$); δ_H (400 MHz, $CDCl_3$) 3.12 (1H, dd, *J* 13.9, 6.0 Hz, 3-*H*H), 3.18 (1H, dd, *J* 13.9, 5.6 Hz, 3-H*H*), 3.75 (3H, s, OCH_3), 3.85 (4”-OCH_3), 4.65–4.73 (1H, m, 2-H), 5.09 (1H, d, *J* 12.0 Hz, C*H*HPh), 5.13 (1H, d, *J* 12.0 Hz, CH*H*Ph), 5.24 (1H, d, *J* 8.3 Hz, 2-NH), 6.94–7.00 (2H, m, 3”-H and 5”-H), 7.11–7.16 (2H, m, 3’-H and 5’-H), 7.28–7.37 (5H, m, Ph), 7.43–7.53 (4H, m, 2’-H, 6’-H, 2”-H and 6”-H); δ_C (101 MHz, $CDCl_3$) 38.0 (CH_2), 52.5 (CH_3), 54.9 (CH), 55.5 (CH_3), 67.1 (CH_2), 114.4 (2 × CH), 127.0 (2 × CH), 128.2 (2 × CH), 128.25 (CH), 128.34 (2 × CH), 128.7 (2 × CH), 129.8 (2 × CH), 133.4 (C), 134.2 (C), 136.4 (C), 139.8 (C), 155.8 (C), 159.3 (C), 172.1 (C); *m/z* (ESI) 420.1805 (MH^+. $C_{25}H_{26}NO_5$ requires 420.1805).

Methyl (2*S*)-2-(benzyloxycarbonylamino)-3-(4”-dimethylaminobiphen-4’-yl)propanoate (159o)

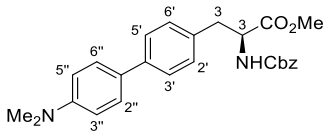

Methyl (2*S*)-2-(benzyloxycarbonylamino)-3-(4”-dimethylaminobiphen-4’-yl)propanoate (**159o**) was synthesised as described in general procedure 1 using methyl (2*S*)-2-(benzyloxycarbonylamino)-3-(4-hydroxyphenyl)propanoate (0.452 g, 1.37 mmol), perfluoro-1-butanesulfonyl fluoride (0.370 mL, 2.05 mmol), 4-dimethylaminophenylboronic acid (0.451 g, 2.73 mmol), XPhos Pd G2 (0.0140 g, 0.0180 mmol, 3 mol%) and potassium phosphate (0.875 g, 4.12 mmol) in acetonitrile (4.5 mL) and water (3 mL) at 80 °C. Purification by flash column chromatography, eluting with 20% ethyl acetate in hexane followed by recrystallisation in chloroform/hexane gave methyl (2*S*)-2-(benzyloxycarbonylamino)-3-(4’’-dimethylaminobiphen-4’-yl)propanoate (**159o**) (0.398 g, 67%) as a pale yellow solid. Mp 144–146 °C; ν_{max}/cm^{-1} (neat) 3343 (NH), 2952 (CH), 1713 (C=O), 1609 (C=C), 1505, 1347, 1207, 1060; $[\alpha]_D^{25}$ +60.4 (*c* 0.1, $CHCl_3$); δ_H (400 MHz, $CDCl_3$) 3.00 (6H, s, N(CH_3)$_2$), 3.11 (1H, dd, *J* 14.0, 6.0 Hz, 3-*H*H), 3.16 (1H, dd, *J* 14.0, 5.6 Hz, 3-H*H*), 3.74 (3H, s, OCH_3), 4.62–4.73 (1H, m, 2-H), 5.09 (1H, d, *J* 12.4 Hz, C*H*HPh), 5.13 (1H, d, *J* 12.4 Hz, CH*H*Ph), 5.24 (1H, d, *J* 8.3 Hz, NH), 6.80 (2H, d, *J* 8.8 Hz, 3”-H and 5”-H), 7.10 (2H, d, *J* 8.2 Hz, 3’-H and 5’-H), 7.26–7.40 (5H, m, Ph), 7.46 (2H, d, *J* 8.2 Hz, 2’-H and 6’-H), 7.48 (2H, d, *J* 8.8 Hz, 2”-H and 6”-H); δ_C (101 MHz, $CDCl_3$) 37.9 (CH_2), 40.7 (2 × CH_3), 52.5 (CH_3), 54.9 (CH), 67.1 (CH_2), 112.9 (2 × CH), 126.6 (2 × CH), 127.7 (2 × CH), 128.2 (2 × CH), 128.3 (CH), 128.7 (2 × CH), 128.8 (C), 129.7 (2 × CH), 133.3 (C), 136.4 (C), 140.2 (C), 150.1 (C), 155.8 (C), 172.2 (C); *m/z* (ESI) 433.2133 (MH^+. $C_{26}H_{29}N_2O_4$ requires 433.2122).

Methyl (2*S*)-2-(benzyloxycarbonylamino)-3-[4'-phenyl(thiophen-3''-yl)]propanoate (159p)

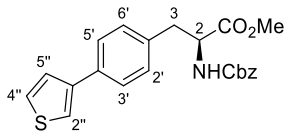

Methyl (2*S*)-2-(benzyloxycarbonylamino)-3-[4'-phenyl(thiophen-3''-yl)]propanoate (**159p**) was synthesised as described in general procedure 1 using methyl (2*S*)-2-(benzyloxycarbonylamino)-3-(4-hydroxyphenyl)propanoate (0.156 g, 0.474 mmol), perfluoro-1-butanesulfonyl fluoride (0.120 mL, 0.680 mmol), 3-thienylboronic acid (0.0909 g, 0.710 mmol), XPhos Pd G2 (0.0120 g, 0.0150 mmol, 3 mol%) and potassium phosphate (0.300 g, 1.41 mmol) in acetonitrile (1.5 mL) and water (1 mL) at 80 °C. Purification by flash column chromatography, eluting with 20% ethyl acetate in hexane gave methyl (2*S*)-2-(benzyloxycarbonylamino)-3-[4'-phenyl(thiophen-3''-yl)]propanoate (**159p**) (0.127 g, 68%) as a white solid. Mp 126–128 °C; ν_{max}/cm^{-1} (neat) 3408 (NH), 2962 (CH), 1745 (C=O), 1713 (C=O), 1505, 1441, 1207; $[\alpha]_D^{25}$ +15.4 (*c* 0.1, $CHCl_3$); δ_H (400 MHz, $CDCl_3$) 3.11 (1H, dd, *J* 14.0, 6.0 Hz, 3-*H*H), 3.18 (1H, dd, *J* 14.0, 5.6 Hz, 3-H*H*), 3.74 (3H, s, OCH_3), 4.65–4.74 (1H, m, 2-H), 5.09 (1H, d, *J* 12.4 Hz, C*H*HPh), 5.14 (1H, d, *J* 12.4 Hz, CH*H*Ph), 5.31 (1H, d, *J* 8.4 Hz, NH), 7.14 (2H, d, *J* 8.0 Hz, 3'-H and 5'-H), 7.29–7.44 (8H, m, 2''-H, 4''-H, 5''-H and Ph), 7.51 (2H, d *J* 8.0 Hz, 2'-H and 6'-H); δ_C (101 MHz, $CDCl_3$) 38.0 (CH_2), 52.4 (CH_3), 54.9 (CH), 67.1 (CH_2), 120.3 (CH), 126.29 (CH), 126.35 (CH), 126.7 (2 × CH), 128.2 (2 × CH), 128.3 (CH), 128.6 (2 × CH), 129.8 (2 × CH), 134.7 (C), 134.8 (C), 136.3 (C), 142.0 (C), 155.7 (C), 172.0 (C); *m/z* (ESI) 418.1087 (MNa^+. $C_{22}H_{21}NNaO_4S$ requires 418.1083).

(2*S*)-2-Amino-3-(4”-phenylbiphen-4’-yl)propanoic acid hydrochloride (160i)

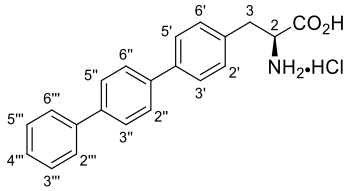

(2*S*)-2-Amino-3-(4”-phenylbiphen-4’-yl)propanoic acid hydrochloride (**160i**) was synthesised according to general procedure 2 using methyl (2*S*)-2-(benzyloxycarbonylamino)-3-(4”-phenylbiphen-4’-yl)propanoate (**159j**) (0.150 g, 0.322 mmol) and caesium carbonate (0.136 g, 0.385 mmol). Recrystallisation from methanol and diethyl ether gave (2*S*)-2-amino-3-(4”-phenylbiphen-4’-yl)propanoic acid hydrochloride (**160i**) (0.0650 g, 53%) as a white solid. Mp 275–280 °C (decomposed); ν_{max}/cm^{-1} (neat) 3418 (OH), 3027 (NH), 2930 (CH), 2356, 2337, 1680 (C=O), 1594 (C=C), 1483; $[\alpha]_D^{15}$ +12.0 (*c* 0.1, MeOH); δ_H (400 MHz, CD_3OD) 3.22 (1H, dd, *J* 14.4, 8.0 Hz, 3-*H*H), 3.38 (1H, dd, *J* 14.4, 5.6 Hz, 3-H*H*), 4.28–4.33 (1H, m, 2-H), 7.32–7.50 (5H, m, ArH), 7.61–7.73 (8H, m, ArH); δ_C (101 MHz, CD_3OD) 37.0 (CH_2), 55.1 (CH), 127.9 (2 × CH), 128.3 (3 × CH), 128.5 (2 × CH), 128.6 (2 × CH), 129.9 (2 × CH), 131.1 (2 × CH), 134.7 (C), 140.6 (C), 141.5 (C), 141.6 (C), 141.8 (C), 171.2 (C); *m/z* (ESI) 318.1491 (MH^+. $C_{21}H_{20}NO_2$ requires 318.1489).

(2*S*)-2-Amino-3-[(2’’-naphthyl)phen-4’-yl]propanoic acid hydrochloride (160g)

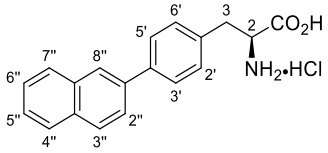

(2*S*)-2-Amino-3-[(2’’-naphthyl)phen-4’-yl]propanoic acid hydrochloride (**160g**) was synthesised according to general procedure 2 using methyl (2*S*)-2-(benzyloxycarbonylamino)-3-[(2’’-naphthyl)phen-4’-yl]propanoate (**159h**) (0.17 g, 0.38 mmol) and caesium carbonate (0.16 g, 0.49 mmol). Recrystallisation from methanol and diethyl ether gave (2*S*)-2-amino-3-[(2’’-naphthyl)phen-4’-yl]propanoic acid hydrochloride (**160g**) (0.027 g, 27%) as a white solid. Mp 236–

240 °C; ν_{max}/cm^{-1} (neat) 3331 (NH), 2856 (CH), 1768 (C=O), 1692 (C=O), 1598, 1491, 1392, 1324, 1183, 1119; $[\alpha]_D^{23}$ –11.0 (*c* 0.1, MeOH); δ_H (400 MHz, CD_3OD) 3.24 (1H, dd, *J* 14.1, 7.6 Hz, 3-*H*H), 3.39 (1H, dd, *J* 14.1, 5.6 Hz, 3-H*H*), 4.32 (1H, dd, *J* 7.6, 5.6 Hz, 2-H), 7.41–7.54 (4H, m, 2'-H, 3'-H, 6''-H and 7''-H), 7.75–7.81 (3H, m, 5'-H, 6'-H and 3''-H), 7.83–7.96 (3H, m, 4''-H, 5''-H and 8''-H), 8.09 (1H, br s, 1''-H); δ_C (101 MHz, CD_3OD) 37.0 (CH_2), 55.1 (CH), 126.2 (CH), 126.5 (CH), 127.1 (CH), 127.4 (CH), 128.6 (CH), 128.9 (2 × CH), 129.2 (CH), 129.6 (CH), 131.1 (2 × CH), 134.2 (C), 134.7 (C), 135.2 (C), 139.1 (C), 141.9 (C), 171. 2 (C); *m/z* (ESI) 292.1335 (MH^+. $C_{19}H_{18}NO_2$ requires 292.1332).

(2*S*)-2-Amino-3-(4''-fluorobiphen-4'-yl)propanoic acid hydrochloride (160j)

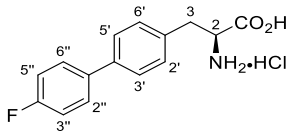

(2*S*)-2-Amino-3-(4''-fluorobiphen-4'-yl)propanoic acid hydrochloride (**160j**) was synthesised according to general procedure 2 using methyl (2*S*)-2-(benzyloxycarbonylamino)-3-(4''-fluorobiphen-4'-yl)propanoate (**159k**) (0.107 g, 0.263 mmol) and caesium carbonate (0.114 g, 0.350 mmol). Recrystallisation from methanol and diethyl ether gave (2*S*)-2-amino-3-(4''-fluorobiphen-4'-yl)propanoic acid hydrochloride (**160j**) (0.041 g, 53%) as an off-white solid. Mp 288–292 °C (decomposed); ν_{max}/cm^{-1} (neat) 2895 (CH), 2162 (CH), 1720 (C=O), 1601 (C=C), 1494, 1232 1156, 812; $[\alpha]_D^{25}$ −5.4 (*c* 0.1, MeOH); δ_H (400 MHz, CD_3OD) 3.22 (1H, dd, *J* 14.6, 7.5 Hz, 3-*H*H), 3.36 (1H, dd, *J* 14.6, 5.4 Hz, 3-H*H*), 4.29 (1H, dd, *J* 7.5, 5.4 Hz, 2-H), 7.17 (2H, t, *J* 8.5 Hz, 3''-H and 5''-H), 7.39 (2H, d, *J* 7.9 Hz, 3'-H and 5'-H), 7.57–7.66 (4H, m, 2'-H, 6'-H, 2''-H and 6''-H); δ_C (101 MHz, CD_3OD) 36.9 (CH_2), 55.1 (CH), 116.6 (2 × CH, d, $^2J_{CF}$ 21.7 Hz), 128.6 (2 × CH), 129.7 (2 × CH, d, $^3J_{CF}$ 8.1 Hz), 131.1 (2 × CH), 134.7 (C), 138.2 (C), 141.0 (C), 164.0 (C, d, $^1J_{CF}$ 245.2 Hz), 171.2 (C); *m/z* (ESI) 260.1089 (MH^+. $C_{15}H_{15}FNO_2$ requires 260.1081).

(2*S*)-2-Amino-3-(4''-acetylbiphen-4'-yl)propanoic acid hydrochloride (160e)

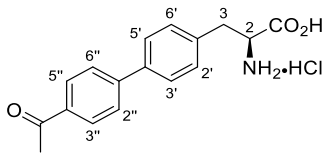

(2*S*)-2-Amino-3-(4''-acetylbiphen-4'-yl)propanoic acid hydrochloride (**160e**) was synthesised according to general procedure 2 using methyl (2*S*)-2-(benzyloxycarbonylamino)-3-(biphen-4'-yl)propanoate (**159e**) (0.052 g, 0.12 mmol) and caesium carbonate (0.051 g, 0.16 mmol). Recrystallisation from methanol and diethyl ether gave (2*S*)-2-amino-3-(4''-acetylbiphen-4'-yl)propanoic acid (**160e**) (0.030 g, 77%) as a white solid. Mp 230–234 °C; ν_{max}/cm^{-1} (neat) 3480 (NH), 2888 (CH), 1762 (C=O), 1645, 1551, 1479, 1294, $[\alpha]_D^{23}$ –18.0 (*c* 0.1, MeOH); δ_H (400 MHz, CD_3OD) 2.64 (3H, s, 4''-$COCH_3$), 3.22 (1H, dd, *J* 14.5, 7.6 Hz, 3-*H*H), 3.38 (1H, dd, *J* 14.5, 5.4 Hz, 3-H*H*), 4.31 (1H, dd, *J* 7.6, 5.4 Hz, 2-H), 7.44 (2H, d, *J* 8.0 Hz, 2'-H and 6'-H), 7.72 (2H, d, *J* 8.0 Hz, 3'-H and 5'-H), 7.78 (2H, d, *J* 8.4 Hz, 2''-H and 6''-H), 8.08 (2H, d, *J* 8.4 Hz, 3''-H and 5''-H); δ_C (101 MHz, CD_3OD) 26.7 (CH_3), 37.0 (CH_2), 55.0 (CH), 128.1 (2 × CH), 128.9 (2 × CH), 130.2 (2 × CH), 131.2 (2 × CH), 135.8 (C), 137.3 (C), 140.6 (C), 146.5 (C), 171.2 (C), 200.1 (C); *m/z* (ESI) 284.1287 (MH^+. $C_{17}H_{18}NO_3$ requires 284.1281).

(2*S*)-2-Amino-3-(2''-methoxybiphen-4'-yl)propanoic acid hydrochloride (160k)

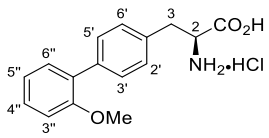

(2*S*)-2-Amino-3-(2''-methoxybiphen-4'-yl)propanoic acid hydrochloride (**160k**) was synthesised according to general procedure 2 using methyl (2*S*)-2-(benzyloxycarbonylamino)-3-(2''-methoxybiphen-4'-yl)propanoate (**159m**) (0.118 g, 0.291 mmol) and caesium carbonate (0.119 g, 0.365 mmol). Recrystallisation from methanol and diethyl ether gave (2*S*)-2-amino-3-(2''-methoxybiphen-4'-yl)propanoic acid hydrochloride (**160k**) (0.046 g, 52%) as a white

solid. Mp 215–218 °C; ν_{max}/cm^{-1} (neat) 2912 (CH), 1724 (C=O), 1594 (C=C), 1483, 1232, 751; $[\alpha]_D^{24}$ +7.8 (*c* 0.1, MeOH); δ_H (400 MHz, CD_3OD) 3.20 (1H, dd, *J* 14.5, 7.9 Hz, 3-*H*H), 3.38 (1H, dd, *J* 14.5, 5.0 Hz, 3-H*H*), 3.78 (3H, s, OCH_3), 4.28 (1H, dd, *J* 7.9, 5.0 Hz, 2-H), 7.00 (1H, t, *J* 7.9 Hz, 5''-H), 7.06 (1H, d, *J* 8.3 Hz, 3''-H), 7.22–7.37 (4H, m, 2'-H, 6'-H, 4''-H and 6''-H), 7.49 (2H, d, *J* 7.8 Hz, 3'-H and 5'-H); δ_C (101 MHz, CD_3OD) 37.0 (CH_2), 55.3 (CH), 56.0 (CH_3), 112.6 (CH), 121.9 (CH), 130.0 (CH), 130.1 (2 × CH), 131.26 (2 × CH), 131.32 (CH), 131.5 (C), 134.0 (C), 139.7 (C), 157.9 (C), 171.4 (C); *m/z* (ESI) 272.1291 (MH^+. $C_{16}H_{18}NO_3$ requires 272.1281).

(2*S*)-2-Amino-3-(4''-methoxybiphen-4'-yl)propanoic acid hydrochloride (160b)

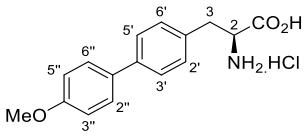

(2*S*)-2-Amino-3-(4''-methoxybiphen-4'-yl)propanoic acid (**160b**) was synthesised according to general procedure 2 using methyl (2*S*)-2-(benzyloxycarbonylamino)-3-(4''-methoxybiphen-4'-yl)propanoate (**159b**) (0.122 g, 0.290 mmol) and caesium carbonate (0.123 g, 0.378 mmol). Recrystallisation from methanol and diethyl ether gave (2*S*)-2-amino-3-(4''-methoxybiphen-4'-yl)propanoic acid (**160b**) (0.0636 g, 71%) as a white solid. Mp 249–254 °C; ν_{max}/cm^{-1} (neat) 3255 (NH), 2928 (CH), 1731 (C=O), 1605, 1495, 1248, 811; $[\alpha]_D^{18}$ +56.5 (*c* 0.1, MeOH); δ_H (400 MHz, CD_3OD) 3.19 (1H, dd, *J* 14.6, 7.9 Hz, 3-*H*H), 3.36 (1H, dd, *J* 14.6, 5.4 Hz, 3-H*H*), 3.84 (3H, s, 4''-OCH_3), 4.28 (1H, dd, *J* 7.9, 5.4 Hz, 2-H), 6.97–7.04 (2H, m, 3''-H and 5''-H), 7.33–7.39 (2H, m, 3'-H and 5'-H), 7.52–7.64 (4H, m, 2'-H, 6'-H, 2''-H and 6''-H); δ_C (101 MHz, CD_3OD) 36.9 (CH_2), 55.1 (CH), 55.8 (CH_3), 115.3 (2 × CH), 128.2 (2 × CH), 128.9 (2 × CH), 130.9 (2 × CH), 133.8 (C), 134.2 (C), 141.7 (C), 160.9 (C), 171.2 (C); *m/z* (ESI) 272.1281 (MH^+. $C_{16}H_{18}NO_3$ requires 272.1281).

(2*S*)-2-Amino-3-(4''-dimethylaminobiphen-4'-yl)propanoic acid hydrochloride (160l)

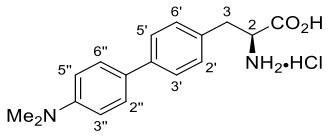

(2*S*)-2-Amino-3-(4''-dimethylaminobiphen-4'-yl)propanoic acid hydrochloride (**160l**) was synthesised according to general procedure 2 using methyl (2*S*)-2-(benzyloxycarbonylamino)-3-(4''-dimethylaminobiphen-4'-yl)propanoate (**159o**) (0.070 g, 0.16 mmol) and caesium carbonate (0.069 g, 0.21 mmol). Recrystallisation from methanol and diethyl ether gave (2*S*)-2-amino-3-(4''-dimethylaminobiphen-4'-yl)propanoic acid hydrochloride (**160l**) (0.044 g, 95%) as a colourless solid. Mp 234–238 °C (decomposed); ν_{max}/cm^{-1} (neat) 2906 (CH), 2704 (OH), 1719 (C=O), 1498, 1400, 1231, 1139, 808; $[\alpha]_D^{15}$ +16.1 (*c* 0.1, MeOH); δ_H (400 MHz, CD_3OD) 3.23 (1H, dd, *J* 14.5, 7.4 Hz, 3-*H*H), 3.32 (6H, s, $N(CH_3)_2$), 3.36 (1H, dd, *J* 14.5, 5.7 Hz, 3-H*H*), 4.28–4.32 (1H, m, 2-H), 7.43 (2H, d, *J* 8.2 Hz, 3''-H and 5''-H), 7.67 (2H, d, *J* 8.2 Hz, 2''-H and 6''-H), 7.77 (2H, d, *J* 8.4 Hz, 3'-H and 5'-H), 7.85 (2H, d, *J* 8.4 Hz, 2'-H and 6'-H); δ_C (101 MHz, CD_3OD) 36.9 (CH_2), 47.2 (2 × CH_3), 55.0 (CH), 122.2 (2 × CH), 128.8 (2 × CH), 130.0 (2 × CH), 131.3 (2 × CH), 135.9 (C), 139.8 (C), 143.3 (C), 143.9 (C), 171.1 (C); *m/z* (APCI) 283.1455 ($[M–H]^-$. $C_{17}H_{19}N_2O_2$ requires 283.1452)

(2*S*)-2-Amino-3-[4'-phenyl(thiophen-3''-yl)]propanoic acid hydrochloride (160m)

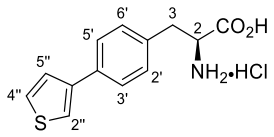

(2*S*)-2-Amino-3-[4'-phenyl(thiophen-3''-yl)]propanoic acid hydrochloride (**160m**) was synthesised as according to general procedure 2 using methyl (2*S*)-2-(benzyloxycarbonylamino)-3-[3''-phenyl-(thiophen-3''-yl)]propanoate (**159p**)

(0.063 g, 0.16 mmol) and caesium carbonate (0.068 g, 0.21 mmol). Recrystallisation from methanol and diethyl ether gave (2*S*)-2-amino-3-[4'-phenyl(thiophen-3''-yl)]propanoic acid hydrochloride (**160m**) (0.016 g, 36%) as an off-white solid. Mp 238–240 °C (decomposed); ν_{max}/cm^{-1} (neat) 2908 (CH), 1731 (C=O), 1494, 1254, 772; $[\alpha]_D^{18}$ +35.2 (*c* 0.1, MeOH); δ_H (400 MHz, CD_3OD) 3.18 (1H, dd, *J* 14.6, 7.6 Hz, 3-*H*H), 3.35 (1H, dd, *J* 14.6, 4.8 Hz, 3-H*H*), 4.26 (1H, dd, *J* 7.6, 4.8 Hz, 2-H), 7.34 (2H, d, *J* 7.8 Hz, 3'-H and 5'-H), 7.43–7.52 (2H, m, ArH), 7.63–7.65 (1H, m, ArH), 7.68 (2H, d, *J* 7.8 Hz, 2'-H and 6'-H); δ_C (101 MHz, CD_3OD) 37.1 (CH_2), 55.2 (CH), 121.6 (CH), 127.0 (CH), 127.5 (CH), 128.0 (2 × CH), 131.0 (2 × CH), 134.3 (C), 136.9 (C), 142.9 (C), 171.3 (C); *m/z* (ESI) 248.0741 (MH^+. $C_{13}H_{14}NO_2S$ requires 248.0740).

2-Oxo-2*H*-chromen-6-ylboronic acid (161)[173]

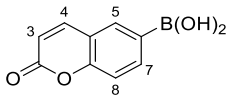

A solution of 6-aminochromen-2-one (0.300 g, 1.86 mmol) in water (1.5 mL) and hydrochloric acid (37% in water, 388 μL) was cooled to 0 °C. A solution of sodium nitrite (0.154 g, 2.23 mmol) in water (0.75 mL) was added dropwise. The syringe was subsequently rinsed with water (0.3 mL) and the rinsings added to the reaction mixture. The reaction mixture was for stirred 0.25 h after which a solution of tetrahydroxydiboron (0.334 g, 3.72 mmol) and sodium acetate (0.305 g, 3.72 mmol) in water (9 mL) was added. The reaction mixture was warmed to room temperature and stirred for 0.3 h. The reaction mixture was acidified to pH 1 (6 M hydrochloric acid) and extracted with ethyl acetate (2 × 30 mL) followed by a 4:1 mixture of chloroform:2-propanol (2 × 30 mL). Purification was achieved using a reverse phase Biotage Isolera One purification system eluting in 5–95% acetonitrile in water. The product fractions were lyophilised to give 2-oxo-2*H*-chromen-6-ylboronic acid (**161**) (0.0874 g, 25%) as a white solid. Mp 300–310 °C (decomposed); NMR data were consistent with the literature.[173] δ_H (400 MHz, CD_3OD) 6.41 (1H, d, *J* 8.6 Hz, 3-H), 7.30 (1H, d, *J* 8.6 Hz, 4-H), 7.90–7.98 (3H, m, 3 × ArH); δ_C (101 MHz, CD_3OD) 113.7, 116.8. 119.7, 135.5, 138.6, 146.0, 156.7, 162.8; *m/z* (ESI) 188 ($[M-H]^-$.100%).

Methyl (2*S*)-2-(benzyloxycarbonylamino)-3-[4'-(2''-oxo-2''*H*'-chromen-6''-yl)phenyl]propanoate (159t)

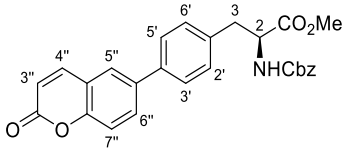

Methyl (2*S*)-2-(benzyloxycarbonylamino)-3-[4'-(2''-oxo-2''*H*'chromen-6''-yl)phenyl]propanoate (**159t**) was synthesised as described in general procedure 1 using methyl (2*S*)-2-(benzyloxycarbonylamino)-3-(4-hydroxyphenyl)propanoate (0.0668 g, 0.200 mmol), perfluoro-1-butanesulfonyl fluoride (0.120 mL, 0.680 mmol), 2-oxo-2*H*-chromen-6-ylboronic acid (**161**) (0.0589 g, 0.310 mmol), and potassium phosphate (0.133 g, 0.626 mmol) in acetonitrile (1.0 mL) and water (0.4 mL) at 80 °C. XPhos Pd G2 (0.00480 g, 0.00610 mmol) was dissolved in tetrahydrofuran (0.3 mL) and added in batches (3 × 0.1 mL). Purification by flash column chromatography eluting with 80% diethyl ether in hexane followed by a second purification by flash column chromatography eluting with 1% methanol in dichloromethane gave methyl (2*S*)-2-(benzyloxycarbonylamino)-3-[4'-(2''-oxo-2''*H*'-chromen-6''-yl)phenyl]propanoate (**159t**) (0.0230 g, 25%) as a white solid. Mp 58–60 °C; ν_{max}/cm^{-1} (neat) 3321 (NH), 1710 (C=O), 1622, 1572, 1435, 1256, 1210, 1131, 1102, 1054, 1017, 931, 896; $[\alpha]_D^{18}$ +50.3 (*c* 0.1, $CHCl_3$); δ_H (400 MHz, $CDCl_3$) 3.13 (1H, dd, *J* 13.6, 6.0 Hz, 3-*H*H). 3.21 (1H, dd, *J* 13.6, 5.6 Hz, 3-H*H*), 3.76 (3H, s, OCH_3), 4.66–4.75 (1H, m, 2-H), 5.09 (1H, d, *J* 12.4 Hz, C*H*HPh), 5.13 (1H, d, *J* 12.4 Hz, CH*H*Ph), 5.27 (1H, d, *J* 8.4 Hz, 2-NH), 6.47 (1H, d, *J* 9.4 Hz, 3''-H), 7.20 (2H, d, *J* 8.0 Hz, 2'-H and 6'-H), 7.30–7.41 (5H, m, CH_2Ph), 7.40 (1H, d, *J* 8.6 Hz, 7''-H), 7.48 (2H, d, *J* 8.0 Hz, 3'-H and 5'-H), 7.64 (1H, d, *J* 2.4 Hz, 5''-H) 7.72 (1H, dd, *J* 8.6, 2.4 Hz, 6''-H), 7.76 (1H, d, *J* 9.4 Hz, 4''-H); δ_C (101 MHz, $CDCl_3$) 38.0 (CH_2), 52.6 (CH_3), 54.9 (CH), 67.2 (CH_2), 117.2 (CH). 117.4 (CH), 119.2 (C), 126.1 (CH), 127.4 (2 × CH), 128.3 (2 × CH), 128.4 (CH), 128.7 (2 × CH), 130.1 (2 × CH), 130.8 (CH), 135.6 (C), 136.3 (C), 137.5 (C), 138.4 (C), 143.6 (CH), 153.6 (C), 155.8 (C), 160.8 (C), 172.0 (C); *m/z* (ESI) 461.1695 (MH^+. $C_{27}H_{24}NO_6$ requires 461.1686).

(2*R*)-2-(benzyloxycarbonylamino)-3-(4'-hydroxyphenyl)propanoate (162)[292]

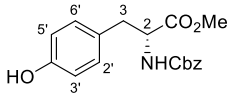

Sodium hydrogencarbonate (0.273 g, 3.25 mmol) in water (3 mL) was added to a solution of D-tyrosine methyl ester hydrochloride (0.301 g, 1.30 mmol) in ethyl acetate (3 mL). The reaction mixture was cooled to 0 °C. Benzyl chloroformate (0.280 mL, 1.94 mmol) was added dropwise. The reaction mixture was warmed to room temperature and stirred for 18 h. The reaction mixture was cooled to 0 °C and a further quantity of benzyl chloroformate (0.180 mL, 1.25 mmol) was added. The reaction mixture was warmed to room temperature and stirred for a further 4 h. The reaction mixture was diluted in ethyl acetate (50 mL) and washed with water (3 × 50 mL). The organic layer was dried ($MgSO_4$) and concentrated *in vacuo*. Purification by flash column chromatography, eluting with 20–40% ethyl acetate in hexane gave (2*R*)-2-(benzyloxycarbonylamino)-3-(4'-hydroxyphenyl)propanoate (**162**) (0.353 g, 83%) as a clear oil. NMR data were consistent with the literature.[9] δ_H (400 MHz, CD_3OD) 3.02 (2H dd, *J* 13.9, 6.5 Hz, 3-*H*H), 3.71 (3H, s, OCH_3), 4.57–4.66 (1H, m , 2-H), 5.02–5.17 (2H, m, C*H*$_2$Ph), 5.31 (1H, d, *J* 8.4 Hz, NH), 6.69 (2H, d, *J* 8.2 Hz, 3'-H and 5-'H) 6.92 (2H, d, *J* 8.2 Hz, 2'-H and 6'-H), 7.27–7.38 (5H, m, Ph); δ_C (101 MHz, CD_3OD) 37.5 (CH_2), 52.5 (CH_3), 55.1 (CH), 67.2 (CH_2), 115.7 (2 × CH), 127.2 (CH), 128.2 (2 × CH), 128.3 (CH), 128.6 (2 × CH), 130.4 (2 × CH), 136.2 (C), 155.3 (C), 156.0 (C), 172.4 (C); *m/z* (ESI) 330 (MH^+. 100%).

Methyl (2*R*)-2-(benzyloxycarbonylamino)-3-(4"-dimethylaminobiphen-4'-yl)propanoate (163)

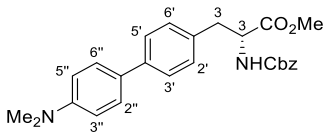

Methyl (2*R*)-2-(benzyloxycarbonylamino)-3-(4"-dimethylaminobiphen-4'-yl)propanoate was synthesised as described in general procedure 1 using methyl (2*R*)-2-(benzyloxycarbonylamino)-3-(4-hydroxyphenyl)propanoate (0.153 g, 0.464

mmol), perfluoro-1-butanesulfonyl fluoride (0.120 mL, 0.680 mmol), 4-dimethylaminophenylboronic acid (0.116g, 0.703 mmol), XPhos Pd G2 (0.0120 g, 0.0150 mmol, 3 mol%) and potassium phosphate (0.116 g, 0.703 mmol) in acetonitrile (1.5 mL) and water (1 mL) at 80 °C. Purification by flash column chromatography, eluting with 20% ethyl acetate in hexane gave methyl (2*R*)-2-(benzyloxycarbonylamino)-3-(4''-dimethylaminobiphen-4'-yl)propanoate (**163**) (0.043 g, 22%) as a pale yellow solid. $[\alpha]_D^{20}$ −37.6 (*c* 0.1, $CHCl_3$); Spectroscopic data was in accordance with methyl (2*S*)-2-(benzyloxycarbonylamino)-3-(4''-dimethylaminobiphen-4'-yl)propanoate.

(2*R*)-2-Amino-3-(4''-dimethylaminobiphen-4'-yl)propanoic acid hydrochloride (164)

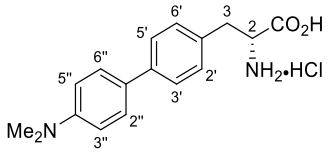

(2*R*)-2-Amino-3-(4''-dimethylaminobiphen-4'-yl)propanoic acid hydrochloride (**164**) was synthesised as described in general procedure 2 using methyl (2*R*)-2-(benzyloxycarbonylamino)-3-(4''-dimethylaminobiphen-4'-yl)propanoate (**163)** (0.038 g, 0.089 mmol) and caesium carbonate (0.038 g, 0.18 mmol). Recrystallisation in a few drops of methanol in diethyl ether gave (2*R*)-2-amino-3-(4''-dimethylaminobiphen-4'-yl)propanoic acid hydrochloride (0.018 g, 66%) as a colourless solid. Spectroscopic data was in accordance with (2*S*)-2-amino-3-(4''-dimethylaminobiphen-4'-yl)propanoic acid hydrochloride (**160l**).

(2*S*)-2-[(9*H*-Fluoren-9-ylmethoxycarbonyl)amino]-3-(4''-dimethylaminobiphen-4'-yl)propanoic acid (168)

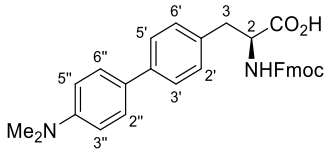

(2*S*)-2-Amino-3-(4''-dimethylaminobiphen-4'-yl)propanoic acid hydrochloride (**160l**) (0.150 g, 0.470 mmol) was dissolved in 1,4-dioxane (1.5 mL) and water (1.5 mL). Sodium hydrogen carbonate (0.160 g, 0.474 mmol) and *N*-(9-fluorenylmethoxycarbonyloxy)succinimide (0.159 g, 1.88 mmol) were added and the reaction mixture was stirred at 25 °C for 24 h. The reaction mixture was concentrated *in vacuo*. The reaction mixture was diluted in water (20 mL) and acidified to pH 2 using 1 M hydrochloric acid and extracted with ethyl acetate (3 × 20 mL). The combined organic layers were dried ($MgSO_4$), filtered and concentrated *in vacuo*. Purification by flash column chromatography, eluting with 10% methanol in acetone afforded (2*S*)-2-[(9*H*-fluoren-9-ylmethoxycarbonyl)amino]-3-(4''-dimethylaminobiphen-4'-yl)propanoic acid (**168**) (0.115 g, 49%) as a white solid. Mp 212–215 °C; ν_{max}/cm^{-1} (neat) 3322 (NH), 2921 (CH), 1686 (C=O), 1609 (C=C), 1502, 1033, 809; $[\alpha]_D^{15}$ +46.6 (*c* 0.1, DMSO); δ_H (400 MHz, DMSO-d_6) 2.90 (6H, s, $N(CH_3)_2$), 2.91–3.00 (1H, m, 3-*H*H), 3.11–3.17 (1H, m, 3-H*H*), 3.96–4.21 (3H, m, 2-H, OC*H*HCH and OCH_2CH), 4.26–4.36 (1H, m, OCH*H*CH), 6.74 (2H, d, *J* 8.8 Hz, ArH), 7.19 (2H, d, *J* 8.0 Hz, ArH), 7.24–7.42 (8H, m, ArH), 7.58–7.66 (2H, m, ArH), 7.87 (2H, d, *J* 6.4 Hz, ArH); ^{13}C data unavailable due to compound decomposition in DMSO; *m/z* (ESI) 507.2296 (MH^+. $C_{32}H_{31}N_2O_4$ requires 507.2278).

3.3.2 Computational Data

Quantum mechanical calculations were performed in Gaussian 5. The structure of amino acid **160l** was fully optimised (no imaginary frequencies) using density functional theory (DFT) at the B3LYP/6-31G(d,p) level.[179] HOMO and LUMO visualisation were achieved following full population analysis.

Optimised structure and total energy of **160l**:

E = −919.79494259

C −0.4171000000 0.2537000000 0.0156000000

C 0.4347000000 −0.7981000000 0.3830000000

C 1.8133000000 −0.6024000000 0.4325000000

C 2.3573000000 0.6417000000 0.1139000000

C 1.5167000000 1.6921000000 −0.2537000000

C 0.1372000000 1.5021000000 −0.3020000000

C −1.8640000000 0.0512000000 −0.0359000000

C −2.3969000000 −1.1372000000 −0.5558000000

C −3.7763000000 −1.3273000000 −0.6051000000

C −4.6383000000 −0.3371000000 −0.1345000000

C −4.1158000000 0.8470000000 0.3852000000

C −2.7372000000 1.0429000000 0.4340000000

H 0.0091000000 −1.7796000000 0.6404000000

H 2.4731000000 −1.4324000000 0.7249000000

H 1.9424000000 2.6740000000 −0.5078000000

H −0.5221000000 2.3319000000 −0.5978000000

H −1.7203000000 −1.9186000000 −0.9334000000

H −4.1850000000 −2.2614000000 −1.0178000000

H −4.7927000000 1.6292000000 0.7591000000

H −2.3288000000 1.9762000000 0.8499000000

C 3.8815000000 0.8548000000 0.1679000000

H 4.1638000000 1.5951000000 −0.5513000000

H 4.1612000000 1.1837000000 1.1469000000

C 4.5969000000 −0.4708000000 −0.1522000000

H 4.1714000000 −0.9018000000 −1.0343000000

N 4.4337000000 −1.4002000000 0.9749000000

H 4.6331000000 −2.3317000000 0.6705000000

H 5.0637000000 −1.1475000000 1.7093000000

C 6.0956000000 −0.2026000000 −0.3835000000

O 6.7375000000 0.8828000000 0.2908000000

H 6.2861000000 1.0569000000 1.1199000000

O 6.7572000000 −0.9352000000 −1.1639000000

N −6.0932000000 −0.5407000000 −0.1863000000

C −6.6517000000 −0.4321000000 1.1691000000

H −6.6741000000 0.5961000000 1.4644000000

H −7.6460000000 −0.8274000000 1.1779000000

H −6.0416000000 −0.9860000000 1.8517000000

C −6.7007000000 0.4820000000 −1.0500000000

H −6.1752000000 0.5204000000 −1.9812000000

H −7.7262000000 0.2343000000 −1.2290000000

H −6.6430000000 1.4357000000 −0.5683000000

3.3.3 Peptide Synthesis

Analysis: High resolution mass spectrometry (HRMS) was performed on an Agilent 6200 series TOF/65000 series Q-TOF High Resolution Mass Spectrometer using ESI^- mode.

Synthesis: Peptides were synthesised on a CEM Liberty Blue peptide synthesis instrument using the Fmoc/^{t}Bu protecting group strategy and standard DIC/OxymaPure activation, using Rink amide resin. Cleavage from the resin was performed using 95% TFA, 2.5% H_2O and 2.5% TIPS. Purification was performed on a Dionex P680 semi-preparative HPLC system using a Phenomenex Luna C18, 5 µm, 150 × 10 mm column at a flow rate of 3 mL/min. A gradient of 10 to 60% solution B was run using a binary solvent system consisting of solution A (H_2O + 0.1% TFA) and B (MeCN + 0.1% TFA). Reverse-phase HPLC analysis was performed on a Shimadzu system with a UV-Vis detector monitoring at 214 nm and 280 nm. The column used was a Phenomenex, Aeris, 5 µm, peptide XB-C18, 150 × 4.6 mm at a flow rate of 1 mL/min. A gradient of 10 to 60% solution B was run using a binary solvent system consisting of solution A (H_2O + 0.1% TFA) and B (MeCN + 0.1% TFA). Peptide content was analysed on a Thermo Scientific NanoDrop One UV-Vis spectrophotometer.

H-160I-Gly-Gly-Leu-Ser-Lys-Ile-Val-Lys(dnp)-Gly-NH_2 (169)

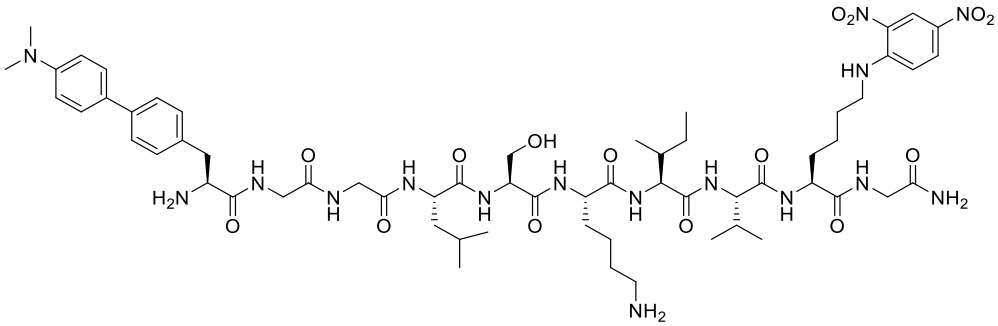

H-Gly-Gly-Leu-Ser(O^{t}Bu)-Lys(N_e-Boc)-Ile-Val-Lys(dnp)-Gly-resin was synthesised through standard microwave-assisted SPPS, using Rink Amide MBHA resin (0.33 mmol/g) on a 0.1 mmol scale. After the synthesis was complete, the resin was washed with DMF (3 × 3 mL). (2*S*)-2-[(9*H*-Fluoren-9-ylmethoxycarbonyl)amino]-3-(4''-dimethylaminobiphen-4'-yl)propanoic acid (**168**)

was subsequently incorporated *via* manual coupling to give peptide **169**. H-Gly-Gly-Leu-Ser(O^{t}Bu)-Lys(N_e-Boc)-Ile-Val-Lys(dnp)-Gly-resin (0.05 mmol) was coupled to (2*S*)-2-[(9*H*-fluoren-9-ylmethoxycarbonyl)amino]-3-(4''-dimethylaminobiphen-4'-yl)propanoic acid (**168**) (38 mg, 0.075 mmol, 1.5 eq), DIPEA (26 mL, 0.15 mmol, 3 eq), PyBOP® (52 mg, 0.1 mmol, 2 eq) in DMF (1.5 mL) for 3 h at room temperature. Fmoc-deprotection was achieved by suspending the resin in 20% morpholine in DMF (1 mL), which was gently mixed for 1 h. Full deprotection and cleavage was subsequently achieved with 95% TFA, 2.5% water and 2.5% triisopropylsilane (5 mL total volume) which was added to the resin and mixed for 2 h. The reaction mixture was evaporated under a flow of nitrogen gas followed by precipitation of the peptide in cold diethyl ether (50 mL). The precipitate was dissolved in 1:1 H_2O/MeCN and lyophilised to give a yellow solid. The crude material was purified using a gradient of 10 to 60% solution B.

MS (ESI) *m/z*: $[M - H]^-$ Calcd for $C_{61}H_{91}N_{16}O_{15}$ 1287.9; Found 1287.9.

HPLC trace for peptide **169**, indicating retention time and purity:

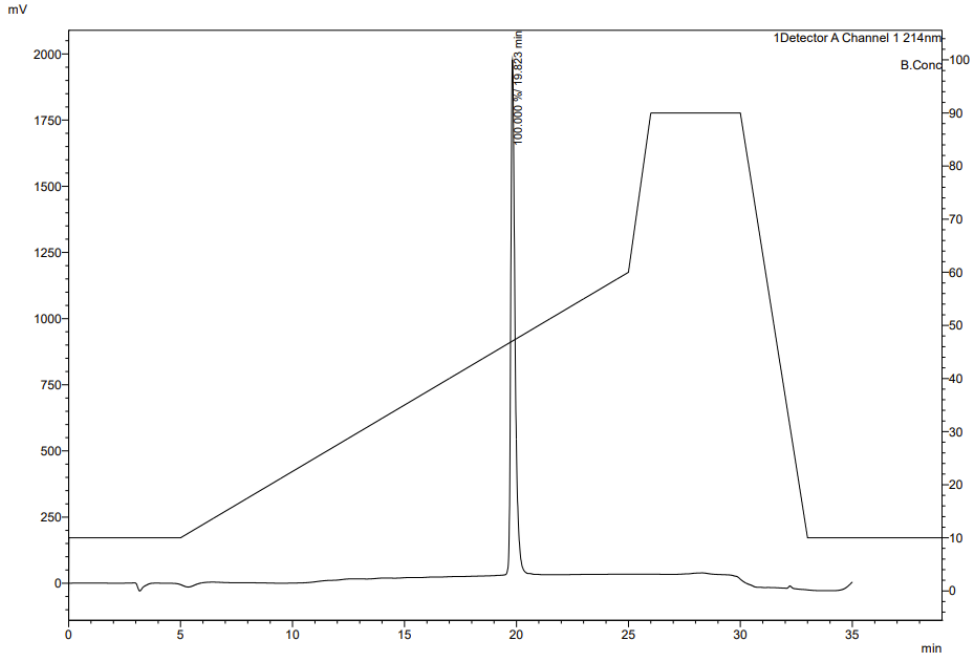

Retention time 19.8 min, purity >99% (20-minute gradient).

3.3.4 Determination of Förster Distance for Peptide 169 and Kinetic Parameters for Trypsin Digestion

Determination of Förster distance (R_0) for amino acid 160l /lysine(dnp) pair

Förster distance, R_0, was determined using the equation given in section **3.2.2.**

Emission and absorption spectra of amino acid **160l** and Lys(dnp) were recorded in methanol at a concentration of 5 mM. Förster distance calculation was performed in excel using template provided by Hink and Visser.[291] This gave a Forster distance between the FRET pair of 36.45 Å.

Determination of kinetic parameters for trypsin digestion of peptide 169

Kinetic measurements were performed using a Horiba Duetta Fluorescence and Absorbance spectrometer at 25 °C. A trypsin stock solution (8.11 mM) was prepared in 1 mM HCl and stored on ice. Solutions were prepared containing 3-morpholinopropanesulfonic acid (MOPS) buffer (20 mM, pH 7.0), trypsin (0.01 mM), various concentrations of peptide (0.50–2.50 mM) and water to give a total volume of 2 mL. Emission spectra were recorded at an excitation wavelength of 300 nm every 10 s over a 400 s time period. Emission data was repeated in triplicate for each concentration of peptide. To calculate the catalytic parameters K_M and k_{cat}, average emission intensity at 405 nm over time was plotted for each concentration. Initial velocity was calculated over the first 50 s using linear fitting in Origin.[182] K_M and k_{cat} were subsequently calculated from Lineweaver-Burk plot of the reciprocal initial velocity versus peptide concentration. This gave a K_M values of 0.33 ± 0.073 mM and a k_{cat} value of 0.73 ± 0.057 s^{-1} (n = 3).

3.3.5 Liposome preparation and analysis

Liposome preparation

Liposomes were prepared as described in literature.[293] L-α-Phosphatidylcholine (egg yolk) (75 mg) and cholesterol (11 mg) (7:1 PC:cholesterol) were dissolved in chloroform (15 mL). The solution was concentrated *in vacuo* to give a thin film on the flask wall. 10 mM sodium phosphate buffer (PBS pH 7.4) (10 mL) was added. The flask was swirled in a water bath at 37 °C for 10 minutes to form a suspension. The suspension was kept at 25 °C for 2 h, sonicated for 3 minutes, then kept at 25 °C for a further 2 hours. The suspension was centrifuged at 4000 rcf for 0.5 h. The pellet was resuspended in 10 mM PBS (10 mL) to give a 7.5 mg/mL PC liposome concentration. Liposomes were stored in the fridge and allowed to come to room temperature prior to use.

Liposome sample preparation

The liposome solution was diluted to the desired concentration in potassium phosphate buffer (pH 7.4). A stock solution of compound of interest was prepared in methanol at 0.2 mg/mL. Liposome sample solutions of 5 μM were prepared by addition of the stock solution into the liposome solution. The sample solutions were inverted several times, then the absorption and emission analysed.

3.4 Arylalkynyl Analogues of Phenylalanine Experimental

3.4.1 One-pot synthesis of arylalkynyl amino acids

Methyl (2*S*)-2-(benzyloxycarbonylamino)-3-[4'-(phenylethynyl)phenyl]propanoate (170a)

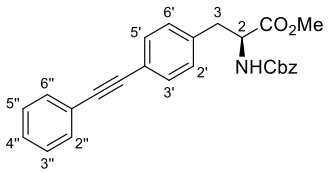

In an oven-dried microwave vial, a solution of methyl (2*S*)-2-(benzyloxycarbonylamino)-3-(4-hydroxyphenyl)propanoate (0.156 g, 0.474 mmol), caesium carbonate (0.460 g, 1.41 mmol) and perfluoro-1-butanesulfonyl fluoride (0.120 mL, 0.710 mmol) in dry acetonitrile (2.5 mL) was degassed under argon for 0.2 h. The reaction vessel was sealed and the reaction mixture heated to 60 °C and stirred for 2 h. To this was added phenylacetylene (0.160 g, 1.41 mmol) and XPhos Pd G2 (0.0180 g, 0.0229 mmol). The reaction mixture was degassed for a further 0.2 h and stirred at 70 °C for 3.5 h. After cooling to room temperature, the reaction mixture was diluted in ethyl acetate (50 mL) and washed with water (3 × 50 mL). The organic layer was dried ($MgSO_4$), filtered and concentrated *in vacuo*. Purification by flash column chromatography eluting with 20% ethyl acetate in hexane followed by trituration in hexane gave methyl (2*S*)-2-(benzyloxycarbonylamino)-3-[4'-(phenylethynyl)phenyl]propanoate (0.157 g, 80%) (**170a**) as a brown solid. Mp 73–76 °C; ν_{max}/cm^{-1} (neat) 3338 (NH), 3034, 2955 (CH), 2358 (C≡C), 1721 (C=O), 1510, 1438, 1255, 1203, 1052, 1019, 755; $[\alpha]_D^{18}$ +60.1 (*c* 0.1, $CHCl_3$); δ_H (400 MHz, $CDCl_3$) 3.08 (1H, dd, *J* 14.0, 6.0 Hz, 3-*H*H), 3.16 (1H, dd, *J* 14.0, 5.6 Hz, 3-H*H*), 3.72 (3H, s, OCH_3), 4.62–4.72 (1H, m, 2-H), 5.08 (1H, d, *J* 12.2 Hz, C*H*HPh), 5.13 (1H, d, *J* 12.2 Hz, CH*H*Ph), 5.24 (1H, d, *J* 8.4 Hz, 2-NH), 7.08 (2H, d, *J* 8.0 Hz, 2'-H and 6'-H), 7.30–7.41 (8H, m, 8 × ArH), 7.44 (2H, d, *J* 8.0 Hz, 3'-H and 5'-H), 7.50–7.55 (2H, m, 2 × ArH); δ_C (101 MHz, $CDCl_3$) 38.2 (CH_2), 52.4 (CH_3), 54.7 (CH), 67.0 (CH_2), 89.0 (C), 89.6 (C), 122.1 (C), 123.2 (C), 128.1 (2 × CH), 128.2 (CH), 128.3 (CH), 128.4 (2 × CH), 128.6 (2 × CH), 129.3 (2

× CH), 131.6 (2 × CH), 131.8 (2 × CH), 136.0 (C), 136.2 (C), 155.6 (C), 171.8 (C); *m/z* (ESI) 414.1703 (MH^+. $C_{26}H_{24}NO_4$ requires 414.1700).

Methyl (2*S*)-2-(benzyloxycarbonylamino)-3-[4'-(4''-methoxyphenylethynyl)phenyl]propanoate (170b)

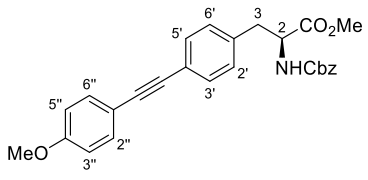

Methyl (2*S*)-2-(benzyloxycarbonylamino)-3-[4'-(4''-methoxyphenylethynyl)phenyl]propanoate was synthesised as described for methyl (2*S*)-2-(benzyloxycarbonylamino)-3-[4'-(phenylethynyl)phenyl]propanoate (**170a**) using methyl (2*S*)-2-(benzyloxycarbonylamino)-3-(4-hydroxyphenyl)propanoate (0.155 g, 0.470 mmol), caesium carbonate (0.460 g, 1.41 mmol), perfluoro-1-butanesulfonyl fluoride (0.120 mL, 0.710 mmol), 4-methoxyphenylacetylene (0.180 mL, 1.41 mmol), and XPhos Pd G2 (0.0180 g, 0.0229 mmol) in dry acetonitrile (2.5 mL). Purification by flash column chromatography eluting with 20% ethyl acetate in hexane gave methyl (2*S*)-2-(benzyloxycarbonylamino)-3-[4'-(4''-methoxyphenylethynyl)phenyl]propanoate (**170b**) (0.137 g, 65%) as a pale brown solid. Mp 89–93 °C; ν_{max}/cm^{-1} (neat) 3328 (NH), 2943 (CH), 1742, 1696 (C=O), 1602, 1518, 1442, 1240, 1019, 821; $[\alpha]_D^{16}$ +82.0 (*c* 0.1, $CHCl_3$); δ_H (400 MHz, $CDCl_3$) 3.08 (1H, dd, *J* 14.0, 6.0 Hz, 3-*H*H), 3.16 (1H, dd, *J* 14.0, 5.6 Hz, 3-H*H*), 3.72 (3H, s, OCH_3), 3.83 (3H, s, OCH_3), 4.62–4.70 (1H, m, 2-H), 5.08 (1H, d, *J* 12.4 Hz, C*H*HPh), 5.13 (1H, d, *J* 12.4 Hz, CH*H*Ph), 5.24 (1H, d, *J* 8.4 Hz, 2-NH), 6.88 (2H, d, *J* 8.4 Hz, 3''-H and 5''-H), 7.07 (2H, d, *J* 8.0 Hz, 2'-H and 6'-H), 7.32–7.40 (5H, m, 5 × ArH), 7.42 (2H, d, *J* 8.0 Hz, 3'-H and 5'-H), 7.46 (2H, d, *J* 8.4 Hz, 2''-H and 6''-H); δ_C (101 MHz, $CDCl_3$) 38.2 (CH_2), 52.4 (CH_3), 54.7 (CH), 55.3 (CH_3), 67.0 (CH_2), 87.7 (C), 89.6 (C), 114.0 (2 × CH), 115.3 (C), 122.5 (C), 128.1 (2 × CH), 128.2 (CH), 128.5 (2 × CH), 129.3 (2 × CH), 131.6 (2 × CH), 133.0 (2 × CH), 135.7 (C), 136.2 (C), 155.6 (C), 159.6 (C), 171.8 (C); *m/z* (ESI) 444.1813 (MH^+. $C_{27}H_{26}NO_5$ requires 444.1805).

General Procedure 3: One-pot Nonaflate Formation and Sonogashira Cross-Coupling Reaction

In an oven-dried microwave vial, a solution of methyl (2*S*)-2-(*tert*-butoxycarbonylamino)-3-(4-hydroxyphenyl)propanoate (1 equiv.) and caesium carbonate (3 equiv.) in dry acetonitrile (0.33 M) was degassed under argon for 0.2 h. To this was added perfluoro-1-butanesulfonyl fluoride (1.5 equiv.). The reaction mixture was heated to 60 °C and stirred for 2 h. To this was added acetylene (1.5 equiv.), XPhos Pd G2 (5 mol%). The reaction mixture was stirred at 70 °C for 3.5 h. After cooling to room temperature, the reaction mixture was diluted in ethyl acetate (30 mL) and washed with water (3 × 30 mL). The combined organic layer was dried ($MgSO_4$), filtered and concentrated *in vacuo*. Purification by flash column chromatography gave the diphenylacetylene amino acids.

Methyl (2*S*)-2-(*tert*-butoxycarbonylamino)-3-[4'-(phenylethynyl)phenyl]propanoate (172a)

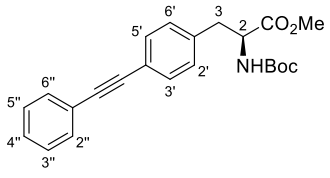

Methyl (2*S*)-2-(*tert*-butoxycarbonylamino)-3-[4'-(phenylethynyl)phenyl]propanoate (**172a**) was synthesised as described in the general procedure 3 using methyl (2*S*)-2-(*tert*-butoxycarbonylamino)-3-(4-hydroxyphenyl)propanoate (0.140 g, 0.474 mmol), caesium carbonate (0.460 g, 1.41 mmol), perfluoro-1-butanesulfonyl fluoride (0.130 mL, 0.710 mmol), phenylacetylene (0.160 mL, 1.41 mmol) and XPhos Pd G2 (0.0180 mg, 0.0230 mmol) in acetonitrile (1.5 mL). Purification by flash column chromatography, eluting with 20% ethyl acetate in hexane gave methyl (2*S*)-2-(*tert*-butoxycarbonylamino)-3-[4'-(phenylethynyl)phenyl]propanoate (**172a**) (0.156 g, 88%) as a brown solid. Mp 37–39 °C; ν_{max}/cm^{-1} (neat) 3354 (NH), 2977 (CH), 2363, 1749 (C=O), 1713 (C=O), 1509, 1365, 1164; $[\alpha]_D^{18}$ +80.7 (*c* 0.1, $CHCl_3$); δ_H (400 MHz, $CDCl_3$) 1.43 (9H, s, 3.09), 3.06 (1H, dd, *J* 14.0, 6.4 Hz, 3-*H*H), 3.14 (1H, dd, *J* 14.0, 6.0 Hz, 3-H*H*), 3.72 (3H, s, OCH_3), 4.56–4.63 (1H, m, 2-H), 4.99 (1H, d, *J*

8.2 Hz, 2-NH), 7.12 (2H, d, *J* 7.8 Hz, 2'-H and 6'-H), 7.29–7.40 (3H, m, 3''-H, 4''-H and 5''-H), 7.46 (2H, d, *J* 7.8 Hz, 3'-H and 5'-H), 7.49–7.54 (2H, m, 2''-H and 6''-H); δ_C (101 MHz, $CDCl_3$) 28.4 (3 × CH_3), 38.5 (CH_2), 52.4 (CH_3), 54.5 (CH), 80.2 (C), 89.2 (C), 89.7 (C), 122.1 (C), 123.4 (C), 128.4 (CH), 128.5 (2 × CH), 129.5 (2 × CH), 131.7 (2 × CH), 131.9 (2 × CH), 136.5 (C), 155.2 (C), 172.3 (C); *m/z* (APCI) 280.1339 [(MH–$CO_2{}^t$Bu)+H]$^+$. $C_{18}H_{17}NO_2H$ requires 280.1332].

Methyl (2*S*)-2-(*tert*-butoxycarbonylamino)-3-[4'-(1''-ethynylnaphthalene)phenyl]propanoate (172b)

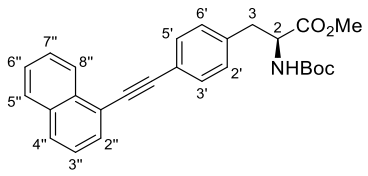

Methyl (2*S*)-2-(*tert*-butoxycarbonylamino)-3-[4'-(1''-ethynylnaphthalene)phenyl]propanoate (**172b**) was synthesized as described in the general procedure 3 using methyl (2*S*)-2-(*tert*-butoxycarbonylamino)-3-(4-hydroxyphenyl)propanoate (0.200 g, 0.679 mmol), caesium carbonate (0.655 g, 2.01 mmol), perfluoro-1-butanesulfonyl fluoride (0.180 mL, 1.02 mmol), 1-ethynylnaphthalene (0.290 mL, 2.01 mmol) and XPhos Pd G2 (0.0260 mg, 0.0330 mmol) in acetonitrile (3.0 mL). Purification by flash column chromatography, eluting in 20% diethyl ether in hexane followed by a second purification by flash column chromatography eluting in 5% ethyl acetate in toluene gave methyl (2*S*)-2-(*tert*-butoxycarbonylamino)-3-[4'-(1''-ethynylnaphthalene)phenyl]propanoate (**172b**) (0.198 g, 67%) as a yellow oil. ν_{max}/cm^{-1} (neat) 3360 (NH), 2977 (CH), 1743 (C=O), 1710 (C=O) 1504, 1364, 1162, 800, 774; $[\alpha]_D^{25}$ +62.3 (*c* 0.1, $CHCl_3$); δ_H (400 MHz, $CDCl_3$) 1.45 (9H, s, 3 × CH_3), 3.09 (1H, dd, *J* 13.6, 6.0 Hz, 3-*H*H), 3.18 (1H, dd, *J* 13.6, 5.8 Hz, 3-H*H*), 3.74 (3H, s, OCH_3), 4.55–4.70 (1H, m, 2-H), 5.03 (1H, d, *J* 8.4 Hz, 2-NH), 7.17 (2H, d, *J* 8.0 Hz, 2'-H and 6'-H), 7.46 (1H, dd, *J* 8.0, 7.2 Hz, 3''-H), 7.50–7.63 (4H, m, 3'-H, 5'-H, 5''-H and 7''-H), 7.76 (1H, dd, *J* 7.2, 1.2 Hz, Ar–H), 7.82–7.89 (2H, m, 6''-H and Ar–H), 8.44 (1H, d, *J* 8.0 Hz, 8''-H); δ_C (101 MHz, $CDCl_3$) 28.4 (3 × CH_3), 38.5 (CH_2), 52.4 (CH_3), 54.5 (CH), 80.2 (C), 87.8 (C), 94.2 (C), 121.0 (C), 122.3 (C),

125.4 (CH), 126.3 (CH), 126.6 (CH), 126.9 (CH), 128.5 (CH), 128.9 (CH), 129.6 (2 × CH), 130.5 (CH), 131.9 (2 × CH), 133.3 (C), 133.4 (C), 136.7 (C), 155.2 (C), 172.3 (C); *m/z* (ESI) 330.1489 [(MH–$CO_2{}^t$Bu)+H]$^+$. $C_{22}H_{19}NO_2H$ requires 330.1489].

Methyl (2*S*)-2-(*tert*-butoxycarbonylamino)-3-[4'-(2''-ethynylnaphthalene)phenyl]propanoate (172c)

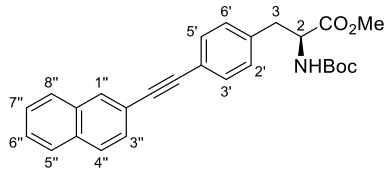

Methyl (2*S*)-2-(*tert*-butoxycarbonylamino)-3-[4'-(2''-ethynylnaphthalene)phenyl]propanoate (**172c**) was synthesised as described in the general procedure 3 using methyl (2*S*)-2-(*tert*-butoxycarbonylamino)-3-(4-hydroxyphenyl)propanoate (0.149 g, 0.505 mmol), caesium carbonate (0.495 g, 1.52 mmol), perfluoro-1-butanesulfonyl fluoride (0.140 mL, 0.762 mmol), 2-ethynylnaphthalene (0.229 g, 1.50 mmol) and XPhos Pd G2 (0.0200 mg, 0.0254 mmol) in acetonitrile (2.5 mL). Purification by flash column chromatography, eluting with 20% ethyl acetate in hexane followed by flash column chromatography eluting in 50–100% dichloromethane in hexane gave methyl (2*S*)-2-(*tert*-butoxycarbonylamino)-3-[4'-(2''-ethynylnaphthalene)phenyl]propanoate (**172c**) (0.137 g, 63%) as a brown solid. Mp 104–107 °C; ν_{max}/cm^{-1} (neat) 3361 (NH), 2980 (CH), 2359, 1736 (C=O), 1686 (C=O), 1509, 1247, 1163, 1012, 818; $[\alpha]_D^{18}$ +60.0 (*c* 0.1, $CHCl_3$); δ_H (400 MHz, $CDCl_3$) 1.44 (9H, s, 3 × CH_3), 3.07 (1H, dd, *J* 13.8, 6.2 Hz, 3-*H*H), 3.15 (1H, dd, *J* 13.8, 5.6 Hz, 3-H*H*), 3.73 (3H, s, OCH_3), 4.56–4.66 (1H, m, 2-H), 5.00 (1H, d, *J* 8.4 Hz, NH), 7.14 (2H, d, *J* 8.0 Hz, 2'-H and 6'-H), 7.46–7.53 (4H, m, 3'-H, 5'-H, 3''-H and 4''-H), 7.57 (1H, dd, *J* 8.6, 1.6 Hz, 8''-H), 7.77–7.87 (3H, m, 5''-H, 6''-H and 7''-H), 8.05 (1H, br s, 1''-H); δ_C (101 MHz, $CDCl_3$) 28.4 (3 × CH_3), 38.5 (CH_2), 52.4 (CH_3), 54.5 (CH), 80.2 (C), 89.6 (C), 90.1 (C), 120.7 (C), 122.2 (C), 126.7 (CH), 126.8 (CH), 127.9 (2 × CH), 128.2 (CH), 128.5 (CH), 129.5 (2 × CH), 131.6 (CH), 131.9 (2 × CH), 132.9 (C), 133.2 (C), 136.6 (C), 155.2 (C), 172.3 (C); *m/z* (ESI) 330.1488 [(MH–$CO_2{}^t$Bu)+H]$^+$. $C_{22}H_{19}NO_2H$ requires 330.1489].

Methyl (2*S*)-2-(*tert*-butoxycarbonylamino)-3-[4'-(4''-methoxyphenylethynyl)phenyl]propanoate (172d)

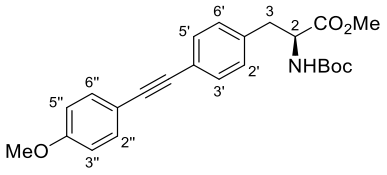

Methyl (2*S*)-2-(*tert*-butoxycarbonylamino)-3-[4'-(4''-methoxyphenylethynyl)phenyl]propanoate (**172d**) was synthesised as described in the general procedure 3 using methyl (2*S*)-2-(*tert*-butoxycarbonylamino)-3-(4-hydroxyphenyl)propanoate (0.202 g, 0.684 mmol), caesium carbonate (0.653 g, 2.00 mmol), perfluoro-1-butanesulfonyl fluoride (0.180 mL, 1.02 mmol), 4'-methoxyphenylacetylene (0.260 mL, 2.01 mmol) and XPhos Pd G2 (0.0260 mg, 0.0330 mmol) in acetonitrile (3.0 mL). Purification by flash column chromatography, eluting with 20% ethyl acetate in hexane gave methyl (2*S*)-2-(*tert*-butoxycarbonylamino)-3-[4'-(4''-methoxyphenylethynyl)phenyl]propanoate (**172d**) (0.248 g, 89%) as a brown solid. Mp 86–88 °C; ν_{max}/cm^{-1} (neat) 3369 (NH), 2954 (CH), 1739 (C=O), 1692 (C=C), 1518, 1240, 1164, 825; $[\alpha]_D^{16}$ +60.6 (*c* 0.1, $CHCl_3$); δ_H (400 MHz, $CDCl_3$) 1.42 (9H, s, 3 × CH_3) 3.05 (1H, dd, *J* 14.0, 6.4 Hz, 3-*H*H), 3.13 (1H, dd, *J* 14.0, 5.6 Hz, 3-H*H*), 3.71 (3H, s, OCH_3), 3.83 (3H, s, OCH_3), 4.51–4.64 (1H, m, 2-H), 4.98 (1H, d, *J* 8.3 Hz, 2-NH), 6.87 (2H, d, *J* 7.9 Hz, 3''-H and 5''-H), 7.10 (2H, d, *J* 7.8 Hz, 2'-H and 6'-H), 7.40–7.49 (4H, m, 3'-H, 5'-H, 2''-H and 6''-H); δ_C (101 MHz, $CDCl_3$) 28.4 (3 × CH_3), 38.4 (CH_2), 52.4 (CH_3), 54.4 (CH), 55.4 (CH_3), 80.1 (C), 87.9 (C), 89.7 (C), 114.1 (2 × CH), 115.5 (C), 122.5 (C), 129.4 (2 × CH), 131.7 (2 × CH), 133.1 (2 × CH), 136.1 (C), 155.2 (C), 159.7 (C), 172.3 (C); *m/z* (ESI) 432.1791 (MNa^+. $C_{24}H_{27}NO_5Na$ requires 432.1781).

Methyl (2*S*)-2-(*tert*-butoxycarbonylamino)-3-[4'-(4''-dimethylaminophenylethynyl)phenyl]propanoate (172e)

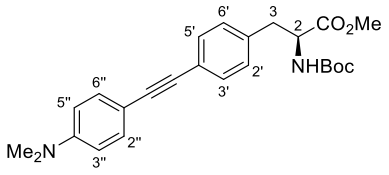

Methyl (2*S*)-2-(*tert*-butoxycarbonylamino)-3-[4'-(4''-dimethylaminophenylethynyl)phenyl]propanoate (**172e**) was synthesised as described in the general procedure 3 using methyl (2*S*)-2-(*tert*-butoxycarbonylamino)-3-(4-hydroxyphenyl)propanoate (0.281 g, 0.951 mmol), caesium carbonate (0.917 g, 2.81 mmol), perfluoro-1-butanesulfonyl fluoride (0.240 mL, 1.42 mmol), 4'-dimethylaminophenylacetylene (0.410 g, 2.82 mmol) and XPhos Pd G2 (0.0360 mg, 0.0460 mmol) in acetonitrile (4 mL). Purification by flash column chromatography, eluting with 20% ethyl acetate in hexane gave methyl (2*S*)-2-(*tert*-butoxycarbonylamino)-3-[4'-(4''-dimethylaminophenylethynyl)phenyl]propanoate (**172e**) (0.368 g, 91%) as a green solid. Mp 126–128 °C; ν_{max}/cm^{-1} (neat) 3346 (NH), 2928 (CH), 1731 (C=O), 1688 (C=C), 1609 (C=C), 1522, 1168, 815; $[\alpha]_D^{16}$ +72.4 (*c* 0.1, $CHCl_3$); δ_H (400 MHz, $CDCl_3$) 1.43 (9H, s, 3 × CH_3), 2.99 (6H, s, $N(CH_3)_2$), 3.02–3.15 (2H, m, 3-H_2), 3.71 (3H, s, OCH_3), 4.53–4.62 (1H, m, 2-H), 4.97 (1H, d, *J* 8.2 Hz, NH), 6.66 (2H, d, *J* 7.6 Hz, 3''-H and 5''-H), 7.08 (2H, d, *J* 8.1 Hz, 2'-H and 6'-H), 7.36–7.44 (4H, m, 3'-H, 5'-H, 2''-H and 6''-H); δ_C (101 MHz, $CDCl_3$) 28.4 (3 × CH_3), 38.4 (CH_2), 40.4 (2 × CH_3), 52.4 (CH_3), 54.5 (CH), 80.1 (C), 87.2 (C), 90.9 (C), 110.2 (C), 112.0 (2 × CH), 123.0 (C), 129.4 (2 × CH), 131.6 (2 × CH), 132.8 (2 × CH), 135.6 (C), 150.3 (C), 155.2 (C), 172.4 (C); *m/z* (APCI) 423.2289 (MH^+. $C_{25}H_{30}N_2O_4H$ requires 423.2278).

Methyl (2*S*)-2-(*tert*-butoxycarbonylamino)-3-[4'-(4''-cyanophenylethynyl)phenyl]propanoate (172f)

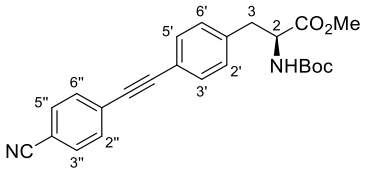

Methyl (2*S*)-2-(*tert*-butoxycarbonylamino)-3-[4'-(4''-cyanophenylethynyl)phenyl]propanoate (**172f**) was synthesised as described in the general procedure 3 using methyl (2*S*)-2-(*tert*-butoxycarbonylamino)-3-(4-hydroxyphenyl)propanoate (0.150 g, 0.508 mmol), caesium carbonate (0.495 g, 1.52 mmol), perfluoro-1-butanesulfonyl fluoride (0.140 mL, 0.762 mmol), 4'-cyanophenylacetylene (0.194 g, 1.53 mmol) and XPhos Pd G2 (0.0200 mg, 0.0254 mmol) in acetonitrile (2.5 mL). Purification by flash column chromatography, eluting with 20–30% ethyl acetate in hexane gave methyl (2*S*)-2-(*tert*-butoxycarbonylamino)-3-[4'-(4''-cyanophenylethynyl)phenyl]propanoate (**172f**) (0.111 g, 51%) as a yellow solid. Mp 128–130 °C; ν_{max}/cm^{-1} (neat) 3358 (NH), 2955 (CH), 2205 (CN), 1726 (C=O), 1674 (C=C), 1293, 1053, 832; $[\alpha]_D^{15}$ +27.1 (*c* 0.1, MeOH); δ_H (400 MHz, $CDCl_3$) 1.42 (9H, s, 3 × CH_3), 3.06 (1H, dd, *J* 14.0, 6.4 Hz, 3-*H*H), 3.16 (1H, dd, *J* 14.0, 5.8 Hz, 3-H*H*), 3.72 (3H, s, OCH_3), 4.55–4.64 (1H, m, 2-H), 4.99 (1H, d, *J* 8.3 Hz, 2-NH), 7.15 (2H, d, *J* 8.2 Hz, 2'-H and 6'-H), 7.47 (2H, d, *J* 8.2 Hz, 3'-H and 5'-H), 7.59 (2H, d, *J* 8.4 Hz, 2''-H and 6''-H), 7.63 (2H, d, *J* 8.4 Hz, 3''-H and 5''-H); δ_C (101 MHz, $CDCl_3$) 28.3 (3 × CH_3), 38.4 (CH_2), 52.3 (CH_3), 54.3 (CH), 80.1 (C), 87.9 (C), 93.6 (C), 111.5 (C), 118.5 (C), 120.9 (C), 128.2 (C), 129.5 (2 × CH), 131.9 (2 × CH), 132.1 (4 × CH), 137.5 (C), 155.0 (C), 172.1 (C); *m/z* (ESI) 305.1297 [(MH–$CO_2{}^t$Bu)+H]$^+$. $C_{19}H_{16}N_2O_2H$ requires 305.1285].

Methyl (2*S*)-2-(*tert*-butoxycarbonylamino)-3-[4'-(4''-fluorophenylethynyl)phenyl]propanoate (172g)

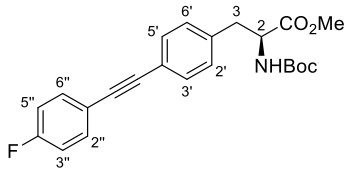

Methyl (2*S*)-2-(*tert*-butoxycarbonylamino)-3-[4'-(4''-fluorophenylethynyl)phenyl]propanoate (**172g**) was synthesised as described in the general procedure 3 using methyl (2*S*)-2-(*tert*-butoxycarbonylamino)-3-(4-hydroxyphenyl)propanoate (0.201 g, 0.681 mmol), caesium carbonate (0.653 g, 2.00 mmol), perfluoro-1-butanesulfonyl fluoride (0.180 mL, 1.02 mmol), 4'-fluorophenylacetylene (0.241 g, 2.01 mmol) and XPhos Pd G2 (0.0260 mg, 0.0330 mmol) in acetonitrile (2.5 mL). Purification by flash column chromatography, eluting with 20% ethyl acetate in hexane gave methyl (2*S*)-2-(*tert*-butoxycarbonylamino)-3-[4'-(4''-fluorophenylethynyl)phenyl]propanoate (**172g**) (0.256 g, 95%) as a brown solid. Mp 153–156 °C; ν_{max}/cm^{-1} (neat) 3368 (NH), 2977 (CH), 2359, 1743 (C=O), 1710 (C=O), 1515, 1501, 1366, 1219, 1156, 835; $[\alpha]_D^{16}$ +75.1 (*c* 0.1, $CHCl_3$); δ_H (400 MHz, $CDCl_3$) 1.42 (9H, s, 3 × CH_3), 3.05 (1H, dd, *J* 14.0, 6.0 Hz, 3-*H*H), 3.14 (1H, dd, *J* 14.0, 6.0 Hz, 3-H*H*), 3.71 (3H, s, OCH_3), 4.55–4.64 (1H, m, 2-H), 4.99 (1H, d, *J* 7.5 Hz, NH), 7.00–7.07 (2H, m, 3''-H and 5''-H), 7.12 (2H, d, *J* 8.2 Hz, 2'-H and 6'-H), 7.44 (2H, d, *J* 8.2 Hz, 3'-H and 5'-H), 7.46–7.52 (2H, m, 2''-H and 6''-H); δ_C (101 MHz, $CDCl_3$) 28.4 (3 × CH_3), 38.5 (CH_2), 52.4 (CH_3), 54.4 (CH), 80.2 (C), 88.6 (C), 88.9 (C), 115.8 (2 × CH, d, $^2J_{CF}$ 22.0 Hz), 119.5 (C, d, $^4J_{CF}$ 3.6 Hz), 121.9 (C), 129.5 (2 × CH), 131.8 (2 × CH), 133.6 (2 × CH, d, $^3J_{CF}$ 8.4 Hz), 136.6 (C), 155.2 (C), 162.6 (C, $^1J_{CF}$ 249.6 Hz), 172.3 (C); *m/z* (APCI) 298.1247 [(MH–$CO_2{}^t$Bu)+H]$^+$. $C_{18}H_{16}FNO_2$ requires 298.1238].

Methyl (2*S*)-2-(*tert*-butoxycarbonylamino)-3-[4'-(2''-ethynylpyridine)phenyl]propanoate (172h)

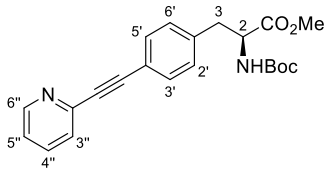

Methyl (2*S*)-2-(*tert*-butoxycarbonylamino)-3-[4'-(2''-ethynylpyridine)phenyl]propanoate (**172h**) was synthesised as described in general procedure 3 using methyl (2*S*)-2-(*tert*-butoxycarbonylamino)-3-(4-hydroxyphenyl)propanoate (0.152 g, 0.515 mmol), caesium carbonate (0.496 g, 1.52 mmol), perfluoro-1-butanesulfonyl fluoride (0.140 mL, 0.762 mmol), 2-ethynylpyridine (0.150 g, 1.52 mmol) and XPhos Pd G2 (0.0200 mg, 0.0254 mmol) in acetonitrile (2.5 mL) at 85 °C. Purification by flash column chromatography, eluting with 5% diethyl ether in dichloromethane gave methyl (2*S*)-2-(*tert*-butoxycarbonylamino)-3-[4'-(2''-ethynylpyridine)phenyl]propanoate (**172h**) (0.0570 g, 30%) as a green solid. Mp 148–150 °C; ν_{max}/cm^{-1} (neat) 3347 (NH), 2977 (CH), 2366, 2223, 1745 (C=O), 1702 (C=O), 1583 (C=C), 1508, 1466, 1362, 1160, 783; $[\alpha]_D^{20}$ +19.2 (*c* 0.1, $CHCl_3$); δ_H (400 MHz, $CDCl_3$) 1.41 (9H, s, 3 × CH_3), 3.05 (1H, dd, *J* 14.0, 6.0 Hz, 3-*H*H), 3.14 (1H, dd, *J* 14.0, 5.6 Hz, 3-H*H*), 3.71 (3H, s, OCH_3), 4.57–4.64 (1H, m, 2-H), 5.00 (1H, d, *J* 8.0 Hz, NH), 7.13 (2H, d, *J* 8.0 Hz, 2'-H and 6'-H), 7.23 (1H, ddd, *J* 7.6, 4.8, 1.2 Hz, 3''-H), 7.48–7.54 (3H, m, 3'-H, 5'-H and 5''-H), 7.67 (1H, td, *J* 7.6, 2.0 Hz, 4''-H), 8.61 (1H, br d, *J* 4.0 Hz, 6''-H); δ_C (101 MHz, $CDCl_3$) 28.4 (3 × CH_3), 38.5 (CH_2), 52.4 (CH_3), 54.4 (CH), 80.2 (C), 88.9 (C), 89.1 (C), 121.1 (C), 122.9 (CH), 127.3 (CH), 129.5 (2 × CH), 132.3 (2 × CH), 136.3 (CH), 137.4 (C), 143.6 (C), 150.2 (CH), 155.1 (C), 172.2 (C); *m/z* (APCI) 381.1810 (MH^+. $C_{22}H_{24}N_2O_4H$ requires 381.1809).

(2*S*)-2-Amino-3-[4'-(phenylethynyl)phenyl]propanoic acid hydrochloride (147a)

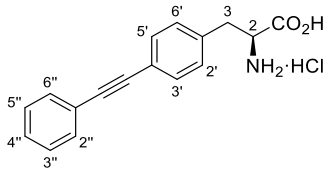

To a stirred solution of methyl (2*S*)-2-(*tert*-butoxycarbonylamino)-3-[4'-(phenylethynyl)phenyl]propanoate (**172a**) (0.112 g, 0.294 mmol) in 1,4-dioxane (2 mL), methanol (3 mL) and water (1.75 mL) was added caesium carbonate (0.125 g, 0.382 mmol). The reaction mixture was stirred at 55 °C for 17 h. 1,4-Dioxane (1 mL) was added and the reaction stirred for a further 5 h at 55 °C. The reaction mixture was concentrated *in vacuo*, diluted in water (20 mL), acidified to pH 1 using 2 M hydrochloric acid and extracted with ethyl acetate (3 × 30 mL). The combined organic layers were dried ($MgSO_4$), filtered and concentrated *in vacuo*. Without further purification, (2*S*)-2-(*tert*-butoxycarbonylamino)-3-[4'-(phenylethynyl)phenyl]propanoic acid (0.102 mg, 0.279 mmol) was dissolved in 4 M hydrochloric acid in 1,4-dioxane (2 mL). The reaction mixture was stirred at room temperature for 1 h. The reaction mixture was concentrated *in vacuo* and azeotroped with chloroform then methanol to give (2*S*)-2-amino-3-[4'-(phenylethynyl)phenyl]propanoic acid hydrochloride (**147a**) (0.0370 g, 42%) as a white solid. Mp 258–260 °C (decomposed); ν_{max}/cm^{-1} (neat) 2921 (CH), 2349 (C≡C), 1725 (C=O), 1596, 1510, 1441, 1389, 1226, 1208, 1155, 1111, 1055, 2020, 849; $[\alpha]_D^{17}$ −7.1 (*c* 0.1, MeOH); δ_H (400 MHz, CD_3OD) 3.17 (1H, dd, *J* 14.4, 7.8 Hz, 3-*H*H), 3.35 (1H, dd, *J* 14.4, 5.6 Hz, 3-H*H*), 4.25 (1H, dd, *J* 7.8, 5.6 Hz, 2-H), 7.33 (2H, d, *J* 8.0 Hz, 2'-H and 6'-H), 7.34–7.39 (3H, m, 3 × ArH), 7.47–7.57 (4H, m, 4 × ArH); δ_C (101 MHz, CD_3OD) 37.2 (CH_2), 55.1 (CH), 89.6 (C), 90.7 (C), 124.2 (C), 124.4 (C), 129.6 (3 × CH), 130.7 (2 × CH), 132.5 (2 × CH), 133.2 (2 × CH), 136.2 (C), 171.2 (C); *m/z* (ESI) 266.1176 (MH^+. $C_{17}H_{16}NO_2$ requires 266.1176).

(2*S*)-2-(*tert*-Butoxycarbonylamino)-3-[4'-(1'' ethynylnaphthalene)phenyl]propanoic acid (177)

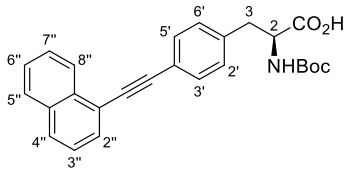

To a stirred solution of methyl (2*S*)-2-(*tert*-butoxycarbonylamino)-3-[4'-(1''-ethynylnaphthalene)phenyl]propanoate (**172b**) (172 mg, 0.401 mmol) in methanol (6 mL) and 1,4-dioxane (3 mL) at 60 °C was added caesium carbonate (170 mg, 0.522 mmol) followed by water (3 mL). The reaction mixture was stirred at 60 °C overnight then cooled to room temperature and concentrated *in vacuo*. The reaction mixture diluted in water (20 mL), acidified to pH 1 using 1 M aqueous hydrochloric acid and extracted with ethyl acetate (3 × 20 mL). The organic layers were combined, dried ($MgSO_4$), filtered and concentrated *in vacuo* to give (2*S*)-2-(*tert*-butoxycarbonylamino)-3-[4'-(1''-ethynylnaphthalene)phenyl]propanoic acid (**177**) in a quantitative yield as a pale yellow solid (166 mg). Mp 71–74 °C; ν_{max}/cm^{-1} (neat) 3320 (NH), 2977 (CH), 2928, 2362, 1715 (C=O), 1505, 1394, 1162, 767; $[\alpha]_D^{17}$ +31.1 (*c* 0.1, $CHCl_3$); NMR spectra showed a 2:1 mixture of rotamers. Only signals for the major rotamer are recorded. δ_H (400 MHz, $CDCl_3$) 1.45 (9H, s, 3 × CH_3), 3.14 (1H, dd, *J* 14.0, 6.8 Hz, 3-*H*H), 3.27 (1H, dd, *J* 14.0, 6.4 Hz, 3-H*H*), 4.59–4.69 (1H, m, 2-H), 5.02 (1H, d, *J* 8.4 Hz, NH), 7.19–7.25 (2H, m, 2'-H and 6'-H), 7.43 (1H, dd, *J* 8.4, 7.2 Hz, 3''-H), 7.48–7.64 (4H, m, 3'-H, 5'-H, 5''-H and 7''-H), 7.74 (1H, d, *J* 7.2 Hz, Ar–H), 7.84 (2H, m, 6''-H and Ar–H), 8.43 (1H, d, *J* 8.4 Hz, 8''-H), 10.73 (1H, br s, OH); δ_C (101 MHz, $CDCl_3$) 28.4 (3 × CH_3), 37.9 (CH_2), 54.3 (CH), 80.6 (C), 87.9 (C), 94.2 (C), 121.0 (C), 122.3 (C), 125.4 (CH), 126.3 (CH), 126.6 (CH), 126.9 (2 × CH), 128.4 (CH), 128.8 (CH), 129.7 (CH), 130.5 (CH), 131.9 (2 × CH), 133.30 (C), 133.35 (C), 136.5 (C), 155.5 (C), 176.5 (C); *m/z* (ESI) 414.1704 ($[M-H]^-$. $C_{26}H_{24}NO_4$ requires 414.1711).

(2*S*)-2-Amino-3-[4'-(1''-ethynylnaphthalene)phenyl]propanoic acid hydrochloride (176)

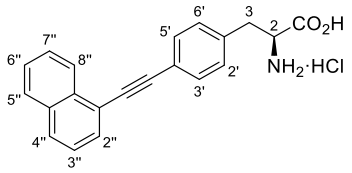

To a stirred solution of (2*S*)-2-(*tert*-butoxycarbonylamino)-3-[4'-(1''-ethynylnaphthalene)phenyl]propanoic acid (**177**) (101 mg, 0.243 mmol) in 1,4-dioxane (1 mL) was added 4 M hydrochloric acid in 1,4-dioxane (1 mL) dropwise. The reaction mixture was stirred at room temperature for 23 h. The reaction mixture was cooled to 0 °C for 0.5 h and filtered. The precipitate was washed with diethyl ether and dried to give (2*S*)-2-amino-3-[4'-(1''-ethynylnaphthalene)phenyl]propanoic acid hydrochloride (**176**) as an off-white solid (48.9 mg, 64%). Spectroscopic data was consistent with the literature.[294] δ_H (400 MHz, CD_3OD) 3.17 (1H, dd, *J* 14.4, 8.0 Hz, 3-*H*H), 3.38 (1H, dd, *J* 14.4, 5.2 Hz, 3-H*H*), 4.15 (1H, dd, *J* 8.0, 5.2 Hz, 2-H), 7.39 (2H, d, *J* 8.2 Hz, 2'-H and 6'-H), 7.46–7.64 (3H, m, 3 × ArH), 7.67 (2H, d, *J* 8.2 Hz, 3'-H and 5'-H), 7.75 (1H, dd, *J* 7.2, 1.2 Hz), 7.88–7.95 (2H, m, ArH), 8.38 (1H, d, *J* 8.0 Hz, ArH); δ_C (101 MHz, CD_3OD) 37.1, 54.9, 88.7, 94.8, 121.7, 124.1. 126.4, 126.8, 127.6, 128.0, 129.5, 130.0, 130.9, 131.4, 133.1, 134.4, 134.7, 136.2, 171.0; *m/z* (ESI) 316.1334 (M^+. $C_{21}H_{18}NO_2$ requires 316.1332).

(2*S*)-2-(*tert*-Butoxycarbonylamino)-3-[4'-(1''-ethynylnaphthalene)phenyl]-1-propanamide-L-phenylalanine methyl ester (178)

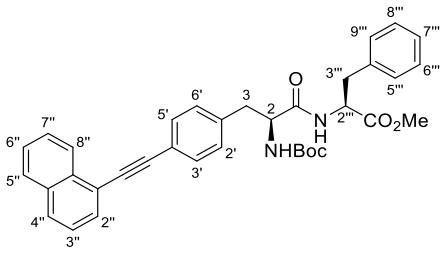

To a stirred solution of (2*S*)-2-(*tert*-butoxycarbonylamino)-3-[4'-(1''-ethynylnaphthalene)phenyl]propanoic acid (**177**) (39.0 mg, 0.0940 mmol) in acetonitrile (3 mL) at 0 °C was added L-phenylalanine methyl ester hydrochloride

(22.0 mg, 0.102 mmol) and 1-hydroxybenzotriazole hydrate (6.00 mg, 0.0470 mmol). The reaction mixture was stirred at 0 °C for 5 minutes prior to the addition of *N,N*-diisopropylethylamine (0.0490 mL, 0.282 mmol) and PyBOP® (75.0 mg, 0.141 mmol) and stirred for a further 0.5 h. The reaction mixture was warmed to room temperature overnight then concentrated *in vacuo*. The reaction mixture was subsequently diluted in ethyl acetate (30 mL), washed with 1 M hydrochloric acid (30 mL) and then brine (30 mL). The organic layer was dried ($MgSO_4$), filtered and concentrated *in vacuo*. Purification by flash column chromatography eluting in 30% ethyl acetate in hexane (2*S*)-2-(*tert*-Butoxycarbonylamino)-3-[4'-(1''-ethynylnaphthalene)phenyl]-1-propanamide-L-phenylalanine methyl ester (**178**) as a white solid (42.7 mg, 79%). Mp 122–125 °C; ν_{max}/cm^{-1} (neat) 3309 (NH), 3290 (NH), 2965 (CH), 1741 (C=O), 1654 (C=O), 1511, 1366, 1216, 755; $[\alpha]_D^{17}$ +60.0 (*c* 0.1, $CHCl_3$); δ_H (400 MHz, $CDCl_3$) 1.43 (9H, s, 3 × CH_3), 3.00–3.14 (4H, m, 3-H_2 and 3'''-H_2), 3.70 (3H, s, OCH_3), 4.37 (1H, d, *J* 6.0 Hz, 2'''-H), 4.74–4.86 (1H, m, 2-H), 5.00 (1H, br s, NH), 6.29 (1H, d, *J* 7.2 Hz, NH), 7.00–7.06 (2H, m, 5'''-H and 9'''-H), 7.19–7.30 (5H, m, 2'-H, 6'-H, 6'''-H, 7'''-H and 8'''-H), 7.46 (1H, dd, *J* 8.0, 7.2 Hz, 3''-H), 7.51–7.62 (4H, m, 3'-H, 5'-H, 5''-H and 7''-H), 7.75 (1H, dd, *J* 7.2, 1.4 Hz, 4''-H), 7.82–7.89 (2H, m, 2''-H and 6''-H), 8.42 (1H, dd, *J* 8.0, 0.8 Hz, 8''-H); δ_C (101 MHz, $CDCl_3$) 28.4 (3 × CH_3), 38.1 (CH_2), 38.4 (CH_2), 52.5 (CH_3), 53.4 (CH), 55.7 (CH), 80.5 (C), 87.8 (C), 94.2 (C), 121.0 (C), 122.2 (C), 125.4 (CH), 126.3 (CH), 126.6 (CH), 126.9 (CH), 127.3 (CH), 128.5 (CH), 128.7 (2 × CH), 128.9 (CH), 129.3 (2 × CH), 129.6 (2 × CH), 130.5 (CH), 132.0 (2 × CH), 133.3 (C), 133.4 (C), 135.7 (C), 137.1 (C), 155.4 (C), 170.7 (C), 171.5 (C); *m/z* (ESI) 599.2513 (MNa^+. $C_{36}H_{36}N_2O_5Na$ requires 599.2516).

(2*S*)-2-(*tert*-Butoxycarbonylamino)-3-[4'-(1''-ethynylnaphthalene)phenyl]-1-propanamide-L-tryptophan methyl ester (179)

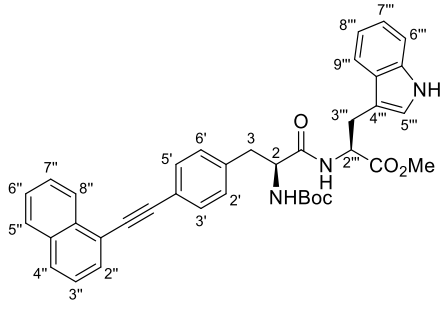

To a stirred solution of (2*S*)-2-(*tert*-butoxycarbonylamino)-3-[4'-(1''-ethynylnaphthalene)phenyl]propanoic acid (**177**) (56.0 mg, 0.135 mmol) in acetonitrile (2.5 mL) at 0 °C was added L-tryptophan methyl ester hydrochloride (38.0 mg, 0.148 mmol) and 1-hydroxybenzotriazole hydrate (9.00 mg, 0.0675 mmol). The reaction mixture was stirred at 0 °C for 5 minutes prior to the addition of *N,N*-diisopropylethylamine (0.0700 mL, 0.405 mmol) and PyBOP® (105 mg, 0.203 mmol) and stirred for a further 0.5 h. The reaction mixture was warmed to room temperature overnight then concentrated *in vacuo*. The reaction mixture was subsequently diluted in ethyl acetate (30 mL), washed in 1 M hydrochloric acid (30 mL) and then brine (30 mL). The organic layer was dried ($MgSO_4$), filtered and concentrated *in vacuo*. Purification by flash column chromatography eluting in 40% ethyl acetate in hexane gave (2*S*)-2-(*tert*-Butoxycarbonylamino)-3-[4'-(1''-ethynylnaphthalene)phenyl]-1-propanamide-L-tryptophan methyl ester (**179**) as a white solid (63.0 mg, 76%). Mp 88–91 °C; ν_{max}/cm^{-1} (neat) 3314 (NH), 2979 (CH), 2921 (CH), 1656 (C=O), 1506, 1438, 1336, 1250, 1213, 1161, 742; $[\alpha]_D^{17}$ +55.6 (*c* 0.1, $CHCl_3$); δ_H (400 MHz, $CDCl_3$) 1.41 (9H, s, 3 × CH_3), 3.04 (2H, d, *J* 6.8 Hz, 3'''-H_2), 3.25 (1H, dd, *J* 14.6, 5.6 Hz, 3-*H*H), 3.30 (1H, dd, *J* 14.6, 5.6 Hz, 3-H*H*), 3.66 (3H, s, OCH_3), 4.17–4.45 (1H, m, 2'''-H), 4.82–4.93 (1H, m, 2-H), 5.07 (1H, d, *J* 5.6 Hz, NH), 6.38 (1H, d, *J* 7.2 Hz, NH), 6.87 (1H, d, *J* 2.8 Hz, 5'''-H), 7.11 (1H, t, *J* 7.4 Hz, 8'''-H), 7.15–7.22 (3H, m, 3 × ArH), 7.33 (1H, d, *J* 8.0 Hz, 6'''-H), 7.41–7.62 (6H, m, 6 × ArH), 7.76 (1H, dd, *J* 7.2, 1.2 Hz, 2''-H), 7.82–7.90 (2H, m, 4''-H and 6''-H), 8.25 (1H, br s, NH), 8.43 (1H, dd, *J* 8.0, 0.8 Hz, 8''-H); δ_C (101 MHz, $CDCl_3$) 27.7 (CH_2), 28.4 (3 × CH_3), 38.6 (CH_2), 52.5 (CH_3), 53.1 (CH), 55.7 (CH), 80.3 (C), 87.8 (C), 94.3 (C), 109.7 (C), 111.5 (CH), 118.5 (CH), 119.8 (CH), 120.9 (C), 122.0 (C), 122.4 (CH), 123.0 (CH), 125.4 (CH), 126.3 (CH), 126.6 (CH), 126.9 (CH), 127.6 (C), 128.5 (CH), 128.9 (CH), 129.6 (2 ×

CH), 130.5 (CH), 131.9 (2 × CH), 133.3 (C), 136.2 (C), 137.2 (C), 155.4 (C), 170.8 (2 × C), 171.9 (C); *m/z* (ESI) 638.2622 (MNa^+. $C_{38}H_{37}N_3O_5Na$ requires 638.2625).

3.4.2 Synthesis of expanded of arylalkynyl amino acid library

Methyl (2*S*)-2-(*tert*-butoxycarbonylamino)-3-[4'-(trimethylsilylethynyl)phenyl]propanoate (180)[227]

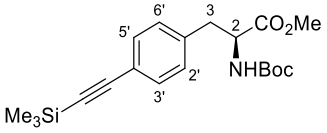

In an oven-dried flask under argon, methyl (2*S*)-2-(*tert*-butoxycarbonylamino)-3-(4-hydroxyphenyl)propanoate (0.150 g, 0.508 mmol) was dissolved in dry acetonitrile (2.5 mL) and degassed for 0.2 h. Triethylamine (0.210 mL, 1.52 mmol) and perfluoro-1-butanesulfonyl fluoride (0.140 mL, 0.762 mmol) were added. The reaction mixture was heated to 60 °C and stirred for 2 h. Trimethylsilyl acetylene (0.220 mL, 1.52 mmol) and XPhos Pd G2 (0.0120, 0.0150 mmol) were added. The reaction mixture was degassed for 0.2 h, heated to 70 °C and stirred for 5 h. A further portion of trimethylsilyl acetylene (0.040 mL, 0.276 mmol) and XPhos Pd G2 (0.0120, 0.0150 mmol) were added. The reaction mixture was degassed for 0.2 h, heated to 70 °C and stirred for 18 h. The reaction mixture was cooled to room temperature, diluted in ethyl acetate (30 mL) and washed with water (3 × 30 mL). The organic layer was dried ($MgSO_4$), filtered and concentrated *in vacuo*. Purification by flash column chromatography, eluting in 20% diethyl ether in hexane gave methyl (2*S*)-2-(*tert*-butoxycarbonylamino)-3-[4'-(trimethylsilylethynyl)phenyl]propanoate (**180**) (0.180 g, 96%) as an orange oil. $[\alpha]_D^{22}$ +72.1 (*c* 0.1, $CHCl_3$); NMR data was in accordance with previously reported.[227] δ_H (400 MHz, $CDCl_3$) 0.24 (9H, s, $Si(CH_3)_3$), 1.42 (9H, s, 3 × CH_3), 3.03 (1H, dd, *J* 14.0, 6.0 Hz, 3-*H*H), 3.10 (1H, dd, *J* 14.0, 5.6 Hz, 3-H*H*), 3.69 (3H, s, OCH_3), 4.52–4.60 (1H, m, 2-H), 4.94 (1H, d, *J* 8.4 Hz, 2-NH), 7.06 (2H, d, *J* 8.2 Hz, 2'-H and 6'-H), 7.39 (2H, d, *J* 8.2 Hz, 3'-H and 5'-H); δ_C (101 MHz, $CDCl_3$) 0.10 (3 × CH_3), 28.4 (3 × CH_3), 38.4 (CH_2), 52.4 (CH_3), 54.4 (CH), 80.2 (C), 94.5 (C), 104.9

(C), 122.0 (C), 139.3 (2 × CH) 132.2 (2 × CH), 136.8 (C), 155.1 (C), 172.2 (C); *m/z* (ESI) 276 [(M–$CO_2{}^tBu$)+H^+. 100%].

Methyl (±)-2-(*tert*-butoxycarbonylamino)-3-(4'-ethynylphenyl)propanoate (181)[201]

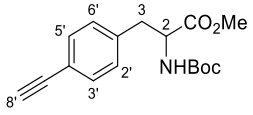

In an oven-dried flask under argon, methyl (2*S*)-2-(*tert*-butoxycarbonylamino)-3-[4'-(trimethylsilylethynyl)phenyl]propanoate (0.0700 g, 0.187 mmol) (**180**) was dissolved in dry tetrahydrofuran (2 mL) and cooled to 0 °C under argon. Anhydrous 1 M tetrabutylammonium fluoride in tetrahydrofuran (0.560 mL, 0.560 mmol) was added dropwise over 5 minutes. The reaction mixture was stirred for 0.25 h at 0 °C then concentrated *in vacuo*. Purification by flash column chromatography, eluting with 20% ethyl acetate in hexane gave methyl (±)-2-(*tert*-butoxycarbonylamino)-3-(4'-ethynylphenyl)propanoate (**181**) (0.0430 g, 75%) as a pale orange oil. NMR data were consistent with the literature.[201] δ_H (400 MHz, $CDCl_3$) 1.42 (9H, s, 3 × CH_3), 2.95–3.16 (3H, m, 3-H_2 and 8'-H), 4.53–4.63 (1H, m, 2-H), 4.97 (1H, d, *J* 8.0 Hz, 2-NH), 7.09 (2H, d, *J* 8.0 Hz, 2'-H and 6'-H), 7.42 (2H, d, *J* 8.0 Hz, 3'-H and 5'-H); δ_C (101 MHz, $CDCl_3$) 28.4 (3 × CH_3), 38.4 (CH_2), 52.4 (CH_3), 54.4 (CH), 77.4 (CH), 80.2 (C), 80.4 (C), 121.0 (C), 129.4 (2 × CH), 132.4 (2 × CH), 137.1 (C), 155.1 (C), 172.2 (C); *m/z* (ESI) 204 (MH^+. 100%).

Methyl (±)-2-(*tert*-butoxycarbonylamino)-3-[4'-(4''-cyanophenylethynyl)phenyl]propanoate ((±) 172f)

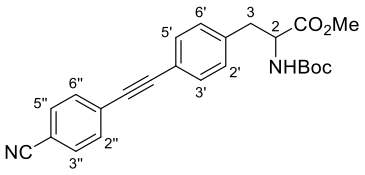

In an oven-dried flask under argon, 4-iodobenzonitrile (0.0980 g, 0.424 mmol), bis(triphenylphosphine)palladium(II) dichloride (0.0120 g, 0.0171 mmol), copper iodide (0.00650 g, 0.0341 mmol) and methyl (±)-2-(*tert*-butoxycarbonylamino)-3-

(4'-ethynylphenyl)propanoate (**181**) (0.100 g, 0.330 mmol) were dissolved in dry *N*,*N*'-dimethylformamide (6 mL) and anhydrous triethylamine (14 mL) and degassed under argon for 0.3 h. The reaction mixture was heated to 90 °C for 0.67 h then allowed to gradually return to room temperature over 3 h. Additional bis(triphenylphosphine)palladium(II) dichloride (0.0120 g, 0.0171 mmol) and copper iodide (0.00650 g, 0.0341 mmol) were added. The reaction was heated to 90 °C for 0.67 h then allowed to gradually return to room temperature over 4 h. The reaction mixture was concentrated *in vacuo*, diluted in ethyl acetate (50 mL) and washed with water (2 × 50 mL) and brine (2 × 50 mL). The organic layer was dried ($MgSO_4$), filtered and concentrated *in vacuo*. Purification by flash column chromatography eluting with 0–2% ethyl acetate in dichloromethane gave methyl (±)-2-(*tert*-butoxycarbonylamino)-3-[4'-(4''-cyanophenylethynyl)phenyl]propanoate (**(±) 172f**) (0.124 g, 93%) as a yellow solid. Spectroscopic data were consistent with previously synthesised as described above.

Methyl (±)-2-(*tert*-butoxycarbonylamino)-3-[4'-(3''-cyanophenylethynyl)phenyl]propanoate (172j)

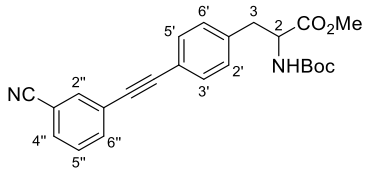

In an oven-dried flask under argon, methyl (±)-2-(*tert*-Butoxycarbonylamino)-3-(4'-ethynylphenyl)propanoate (**181**) (0.102 g, 0.336 mmol) and 3-bromobenzonitrile (0.0783 g, 0.430 mmol) were dissolved in *N*,*N*'- dimethylformamide (4 mL) and anhydrous triethylamine (10 mL) and degassed for 0.3 h. To this was added bis(triphenylphosphine)palladium(II) dichloride (0.0120 g, 0.0171 mmol) and copper iodide (0.00650 g, 0.0341 mmol) in dry, degassed *N*,*N*'-dimethylformamide (1 mL) and anhydrous triethylamine (2 mL). The reaction mixture was heated to 90 °C for 0.5 h then allowed to gradually return to room temperature for 4 h. Additional bis(triphenylphosphine)palladium(II) dichloride (0.0120 g, 0.0171 mmol) and copper iodide (0.00650 g, 0.0341 mmol) in dry, degassed *N*,*N*'-dimethylformamide (1 mL) and anhydrous triethylamine (2 mL) was added. The reaction mixture was degassed under argon for 0.3 h, heated to 90 °C for 0.5 h then allowed to gradually return to room temperature over 16 h. The reaction mixture was

concentrated *in vacuo*, diluted in ethyl acetate (50 mL) and washed with water (2 × 50 mL) and brine (2 × 50 mL). The organic layer was dried ($MgSO_4$), filtered and concentrated *in vacuo*. Purification by flash column chromatography eluting with 50–60% diethyl ether in hexane gave methyl (±)-2-(*tert*-butoxycarbonylamino)-3-[4'-(3''-cyanophenylethynyl)phenyl]propanoate (**172j**) (0.0690, 52%) as an off-white solid. Mp 112–114 °C; ν_{max}/cm^{-1} (neat) 3372 (NH), 2976 (CH), 2231 (C≡C), 1712 (C=O), 1508, 1438, 1365, 1249, 1164, 1057, 1020, 797; δ_H (400 MHz, $CDCl_3$) 1.42 (9H, s, 3 × CH_3), 3.05 (1H, dd, *J* 14.0, 6.4 Hz, 3-*H*H), 3.15 (1H, dd, *J* 14.0, 6.0 Hz, 3-H*H*), 3.72 (3H, s, OCH_3), 4.59 (1H, m, 2-H), 5.01 (1H, d, *J* 8.4 Hz, 2-NH), 7.14 (2H, d, *J* 8.0 Hz, 2'-H and 6'-H), 7.42–7.48 (3H, m, 3'-H, 5'-H and 5''-H), 7.59 (1H, dt, *J* 7.6, 1.6 Hz, 6''-H), 7.71 (1H, dt, *J* 8.0, 1.6 Hz, 4''-H), 7.78 (1H, s, 2''-H); δ_C (101 MHz, $CDCl_3$) 28.4 (3 × CH_3), 38.5 (CH_2), 52.4 (CH_3), 54.4 (CH), 80.2 (C), 87.2 (C), 91.7 (C), 113.0 (C), 118.2 (C), 121.1 (C), 125.0 (C), 129.4 (CH), 129.6 (2 × CH), 131.5 (CH), 132.0 (2 × CH), 135.0 (CH), 135.7 (CH), 137.4 (C), 155.1 (C), 172.2 (C); *m/z* (ESI) 305.1283 (MH^+. $C_{24}H_{25}N_2O_4$ requires 305.1285).

Methyl (±)-2-(*tert*-butoxycarbonylamino)-3-[4'-(4''-methylsulfonylphenylethynyl)phenyl]propanoate (172k)

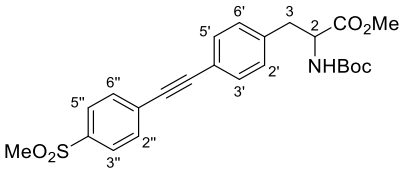

Methyl (±)-2-(*tert*-butoxycarbonylamino)-3-[4'-(4''-methylsulfonylphenylethynyl)phenyl]propanoate (**172k**) was synthesised as described for methyl (±)-2-(*tert*-butoxycarbonylamino)-3-[4'-(3''-cyanophenylethynyl)phenyl]propanoate (**172j**) using methyl (±)-2-(*tert*-butoxycarbonylamino)-3-(4'-ethynylphenyl)propanoate (**181**) (0.100 g, 0.330 mmol), 4-bromophenyl methylsulfone (0.101 g, 0.424 mmol), bis(triphenylphosphine)palladium(II) dichloride (0.0240 g, 0.0342 mmol) and copper iodide (0.0130 g, 0.0683 mmol) in dry *N*,*N*'-dimethylformamide (6 mL) and anhydrous triethylamine (14 mL). Purification by flash column chromatography eluting with 30–40% ethyl acetate in hexane gave methyl (±)-2-(*tert*-butoxycarbonylamino)-3-[4'-(4''-methylsulfonylphenylethynyl)phenyl]propanoate (**172k**) (0.127 g, 84%) as an off-white solid. Mp 138–140 °C; ν_{max}/cm^{-1} (neat) 3363

(NH), 2980 (CH), 2223 (C≡C), 1733 (C=O), 1686 (C=O), 1591, 1520, 1438, 1367, 1294, 1245, 1148, 1133, 1086, 1053, 1014, 968, 833; δ_H (400 MHz, $CDCl_3$) 1.42 (9H, s, 3 × CH_3), 3.00–3.10 (4H, m, 3-*H*H and SO_2CH_3), 3.16 (1H, dd, *J* 13.6, 6.0 Hz, 3-H*H*), 3.72 (3H, s, OCH_3), 4.56–4.64 (1H, m, 2-H), 5.00 (1H, d, *J* 8.0 Hz, 2-NH), 7.15 (2H, d, *J* 8.4 Hz, 2'-H and 6'-H), 7.48 (2H, d, *J* 8.4 Hz, 3'-H and 5'-H), 7.68 (2H, d, *J* 8.4 Hz, 2''-H and 6''-H), 7.92 (2H, d, *J* 8.4 Hz, 3''-H and 5''-H); δ_C (101 MHz, $CDCl_3$) 28.4 (3 × CH_3), 38.6 (CH_2), 44.6 (CH_3), 52.5 (CH_3), 54.4 (CH), 80.2 (C), 87.9 (C), 93.4 (C), 121.1 (C), 127.6 (2 × CH), 129.3 (C), 129.7 (2 × CH), 132.1 (2 × CH), 132.4 (2 × CH), 137.6 (C), 139.7 (C), 155.1 (C), 172.2 (C); *m/z* (ESI) 358.1110 [(MH–CO_2*t*Bu)+H]$^+$. $C_{19}H_{20}NO_4S$ requires 358.1108).

Methyl (±)-2-(*tert*-butoxycarbonylamino)-3-[4'-(4''-acetylphenylethynyl)phenyl]propanoate (172l)

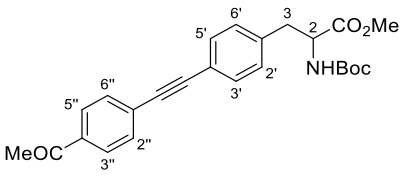

Methyl (±)-2-(*tert*-butoxycarbonylamino)-3-[4'-(4''-acetylphenylethynyl)phenyl]propanoate (**172l**) was synthesised as described for methyl (±)-2-(*tert*-butoxycarbonylamino)-3-[4'-(3''-cyanophenylethynyl)phenyl]propanoate (**172j**) using methyl (±)-2-(*tert*-butoxycarbonylamino)-3-(4'-ethynylphenyl)propanoate (**181**) (0.101 g, 0.333 mmol), 4-bromoacetophenone (0.0882 g, 0.443 mmol), bis(triphenylphosphine)palladium(II) dichloride (0.0240 g, 0.0342 mmol) and copper iodide (0.0130 g, 0.0683 mmol) in dry *N*,*N*'-dimethylformamide (6 mL) and anhydrous triethylamine (14 mL). Purification by flash column chromatography eluting with 2–4% diethyl ether in dichloromethane gave methyl (±)-2-(*tert*-butoxycarbonylamino)-3-[4'-(4''-acetylphenylethynyl)phenyl]propanoate (**172l**) (0.0850 g, 61%) as a white solid. Mp 127–129 °C; ν_{max}/cm^{-1} (neat) 3364 (NH), 2973 (CH), 1735 (C=O), 1677 (C=O), 1599, 1519, 1436, 1362, 1248, 1165, 1052, 1013, 962, 832; δ_H (400 MHz, $CDCl_3$) 1.42 (9H, s, 3 × CH_3), 2.61 (3H, s, 4''-$COCH_3$), 3.06 (1H, dd, *J* 14.0, 6.0 Hz, 3-*H*H), 3.15 (1H, dd, *J* 14.0, 5.6 Hz, 3-H*H*), 3.72 (3H, s, OCH_3), 4.55–4.64 (1H, m, 2-H), 5.00 (1H, d, *J* 8.4 Hz, 2-NH), 7.14 (2H, d, *J* 8.4 Hz, 2'-H and 6'-H), 7.48 (2H, d, *J* 8.4 Hz, 3'-H and 5'-H), 7.59 (2H, d, *J* 8.4 Hz, 2''-

H and 6''-H), 7.93 (2H, d, *J* 8.4 Hz, 3''-H and 5''-H); δ_C (101 MHz, $CDCl_3$) 26.8 (CH_3), 28.4 (3 × CH_3), 38.5 (CH_2), 52.4 (CH_3), 54.4 (CH), 80.2 (C), 88.9 (C), 92.6 (C), 121.5 (C), 128.3 (C), 128.4 (2 × CH), 129.6 (2 × CH), 131.8 (2 × CH), 132.0 (2 × CH), 136.3 (C), 137.2 (C), 155.2 (C), 172.2 (C), 197.4 (C); *m/z* (ESI) 321.1367 ([(MH–$CO_2{}^t$Bu)+H]$^+$. $C_{20}H_{20}NO_3$ requires 321.1365).

Methyl (±)-2-(*tert*-butoxycarbonylamino)-3-[4'-(1''-ethynylnaphthalene)phenyl]propanoate ((±) 172b)

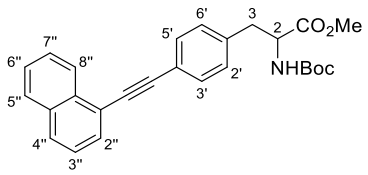

Methyl (±)-2-(*tert*-butoxycarbonylamino)-3-[4'-(1''-ethynylnaphthalene)phenyl]propanoate (**(±) 172b**) was synthesised as described for methyl (±)-2-(*tert*-butoxycarbonylamino)-3-[4'-(3''-cyanophenylethynyl)phenyl]propanoate (**172j**) using methyl (±)-2-(*tert*-butoxycarbonylamino)-3-(4'-ethynylphenyl)propanoate (**181**) (0.101 g, 0.333 mmol), 1-bromonaphthalene (0.600 mL, 0.424 mmol), bis(triphenylphosphine)palladium(II) dichloride (0.0240 g, 0.0342 mmol) and copper iodide (0.0130 g, 0.0683 mmol) in dry *N*,*N*'-dimethylformamide (6 mL) and anhydrous triethylamine (14 mL). Purification by flash column chromatography eluting with 0–2% ethyl acetate in dichloromethane gave methyl (±)-2-(*tert*-butoxycarbonylamino)-3-[4'-(1''-ethynylnaphthalene)phenyl]propanoate (**(±) 172b**) (0.0511 g, 36%) as a yellow oil. Spectroscopic data was consistent with previously synthesised (**172b**) as described above.

Methyl (±)-2-(*tert*-butoxycarbonylamino)-3-[4'-(1''-ethynyl-6''-napthoate)phenyl]propanoate (172m)

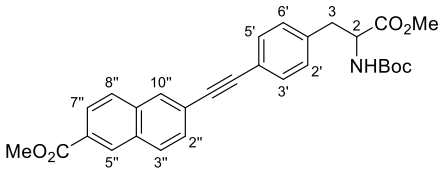

Methyl (±)-2-(*tert*-butoxycarbonylamino)-3-[4'-(1''-ethynyl-6''-napthoate)phenyl]propanoate was synthesised as described for methyl (±)-2-(*tert*-butoxycarbonylamino)-3-[4'-(3''-cyanophenylethynyl)phenyl]propanoate (**172j**) using methyl (±)-2-(*tert*-butoxycarbonylamino)-3-(4'-ethynylphenyl)propanoate (**181**) (0.101 g, 0.333 mmol), methyl 6-bromo-2-naphthoate (0.113 g, 0.426 mmol), bis(triphenylphosphine)palladium(II) dichloride (0.0240 g, 0.0342 mmol) and copper iodide (0.0130 g, 0.0683 mmol) in dry *N*,*N*'-dimethylformamide (6 mL) and anhydrous triethylamine (14 mL). Purification by flash column chromatography eluting with 0–2% ethyl acetate in dichloromethane gave methyl (±)-2-(*tert*-butoxycarbonylamino)-3-[4'-(1''-ethynyl-6''-napthoate)phenyl]propanoate (**172m**) (0.104 g, 65%) as an off-white solid. Mp 151–154 °C; ν_{max}/cm^{-1} (neat) 3373 (NH), 2952 (CH), 1742 (C=O), 1705 (C=O), 1626, 1508, 1434, 1367, 1265, 1218, 1175, 1095, 1059, 1020, 973, 891; δ_H (400 MHz, $CDCl_3$) 1.43 (9H, s, 3 × CH_3), 3.07 (1H, dd, *J* 14.0, 6.4 Hz, 3-*H*H), 3.16 (1H, dd, *J* 14.0, 6.0 HZ, 3-H*H*), 3.73 (3H, s, OCH_3), 3.99 (3H, s, 6''-CO_2CH_3), 4.56–4.65 (1H, m, 2-H), 5.01 (1H, d, *J* 8.4 Hz, 2-NH), 7.14 (2H, d, *J* 8.4 Hz, 2'-H and 6'-H), 7.51 (2H, d, *J* 8.4 Hz, 3'-H and 5'-H), 7.62 (1H, dd, *J* 8.4, 1.2 Hz, 2''-H), 7.85 (1H, d, *J* 8.4 Hz, 8''-H), 7.47 (1H, d, *J* 8.4 Hz, 3''-H), 8.03–8.10 (2H, m, 7''-H and 10''-H), 8.58 (1H, s, 5''-H); δ_C (101 MHz, $CDCl_3$) 28.4 (3 × CH_3), 38.5 (CH_2), 52.5 (2 × CH_3), 54.4 (CH), 80.2 (C), 89.7 (C), 91.0 (C), 121.8 (C), 123.3 (C), 126.1 (CH), 128.11 (CH), 128.14 (C), 129.3 (CH), 129.5 (CH), 129.6 (2 × CH), 130.9 (CH), 131.2 (CH), 131.95 (C), 132.01 (2 × CH), 135.2 (C), 137.0 (C), 155.2 (C), 167.2 (C), 172.3 (C); *m/z* (ESI) 387.1485 ([(MH–$CO_2{}^tBu$)+H]$^+$. $C_{24}H_{21}NO_4$ requires 287.1471).

Methyl (±)-2-(*tert*-butoxycarbonylamino)-3-[4'-(1''-ethynyl-4''-naphthonitrile)phenyl]propanoate (172n)

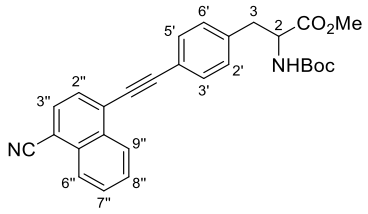

In an oven-dried flask under argon, a solution of methyl (±)-2-(*tert*-butoxycarbonylamino)-3-(4'-ethynylphenyl)propanoate (**181**) (0.100 g, 0.330 mmol), 4-bromo-1-naphthonitrile (0.0980 g, 0.424 mmol), copper iodide (0.00650 g, 0.0341 mmol) and XPhos Pd G2 (0.00650 g, 0.00826 mmol) in anhydrous triethylamine (14 mL) and dry *N*,*N*'-dimethylformamide (6 mL) was degassed under argon for 0.33 h. The reaction mixture was heated to 70 °C for 3 h. After cooling to room temperature, a further portion of copper iodide (0.00650 g, 0.0341 mmol) and XPhos Pd G2 (0.00650 g, 0.00826 mmol) was added. The reaction mixture was degassed for 0.33 h and heated to 70 °C for 17 h. The reaction mixture was concentrated *in vacuo*, diluted in ethyl acetate (50 mL) and washed with water (2 × 50 mL) and brine (2 × 50 mL). The organic layer was dried ($MgSO_4$), filtered and concentrated *in vacuo*. Purification by flash column chromatography eluting with 20% ethyl acetate in hexane gave methyl (±)-2-(*tert*-butoxycarbonylamino)-3-[4'-(1''-ethynyl-4''-naphthonitrile)phenyl]propanoate (**172n**) (0.0860, 61%) as a yellow solid. Mp 148–150 °C; ν_{max}/cm^{-1} (neat) 3361 (NH), 2969 (CH), 2211 (C≡C), 1737 (C=O), 1709 (C=O), 1510, 1365, 1221, 1154, 1056, 1018, 829; δ_H (400 MHz, $CDCl_3$) 1.42 (9H, s, 3 × CH_3), 3.09 (1H, dd, *J* 13.6, 6.4 Hz, 3-*H*H), 3.19 (1H, dd, *J* 13.6, 6.0 Hz, 3-*H*H), 3.74 (3H, s, OCH_3), 4.59–4.68 (1H, m, 2-H), 5.04 (1H, d, *J* 8.0 Hz, 2-NH), 7.20 (2H, d, *J* 8.0 Hz, 2'-H and 6'-H), 7.59 (2H, d, *J* 8.0 Hz, 3'-H and 5'-H), 7.68–7.78 (3H, m, 2''-H, 6''-H and 8''-H), 7.87 (1H, d, *J* 7.6 Hz, 3''-H), 8.23–8.28 (1H, m, 9''-H), 8.46–8.51 (1H, m, 7''-H); δ_C (101 MHz, $CDCl_3$) 28.4 (3 × CH_3), 38.6 (CH_2), 52.5 (CH_3), 54.4 (CH), 80.2 (C), 86.6 (C), 98.3 (C), 110.1 (C), 117.8 (C), 121.2 (C), 125.7 (CH), 126.7 (C), 127.1 (CH), 128.4 (CH), 129.05 (CH), 129.14 (CH), 129.7 (2 × CH), 131.9 (CH), 132.1 (2 × CH), 132.3 (C), 132.9 (C), 137.8 (C), 155.1 (C), 172.2 (C); *m/z* (QTOF) 355.1441 ($[(MH–CO_2{}^tBu)+H]^+$. $C_{23}H_{19}N_2O_2$ requires 355.1441).

Methyl (±)-2-(*tert*-butoxycarbonylamino)-3-[4'-(4''-ethynylquinoline)phenyl]propanoate (172o)

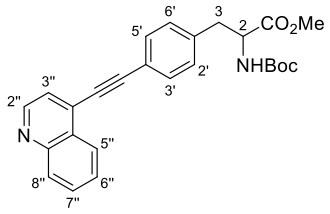

Methyl (±)-2-(*tert*-butoxycarbonylamino)-3-[4'-(4''-ethynylquinoline)phenyl]propanoate (**172o**) was synthesised as described for methyl (±)-2-(*tert*-butoxycarbonylamino)-3-[4'-(3''-cyanophenylethynyl)phenyl]propanoate (**172j**) using methyl (±)-2-(*tert*-butoxycarbonylamino)-3-(4'-ethynylphenyl)propanoate (**181**) (0.100 g, 0.330 mmol), 4-bromoquinoline (0.0880 g, 0.424 mmol), bis(triphenylphosphine)palladium(II) dichloride (0.0240 g, 0.0342 mmol) and copper iodide (0.0130 g, 0.0683 mmol) in dry *N*,*N*'-dimethylformamide (6 mL) and anhydrous triethylamine (14 mL). Purification by flash column chromatography eluting with 10% ethyl acetate in dichloromethane gave methyl (±)-2-(*tert*-butoxycarbonylamino)-3-[4'-(4''-ethynylquinoline)phenyl]propanoate (**172o**) (0.107 g, 75%) as a yellow oil. ν_{max}/cm^{-1} (neat) 3364 (NH), 2976 (CH), 2215 (C≡C), 1743 (C=O), 1704 (C=O), 1577, 1500, 1436, 1391, 1364, 1249, 1216, 1161, 1054, 1018, 909, 844; δ_H (400 MHz, $CDCl_3$) 1.42 (9H, s, 3 × CH_3), 3.08 (1H, dd, *J* 13.8, 6.4 Hz, 3-*H*H), 3.17 (1H, dd, *J* 13.8, 5.6 Hz, 3-H*H*), 3.72 (3H, s, OCH_3), 4.54–4.67 (1H, m, 2-H), 5.13 (1H, d, *J* 8.0 Hz, 2-NH), 7.18 (2H, d, *J* 8.2 Hz, 2'-H and 6'-H), 7.53 (1H, d, *J* 4.4 Hz, 3''-H), 7.57 (2H, d, *J* 8.2 Hz, 3'-H and 5'-H), 7.57–7.64 (1H, m, 7''-H), 7.74 (1H, ddd, *J* 8.2, 6.8, 1.4 Hz, 6''-H) 8.12 (1H, d, *J* 8.2 Hz, 5''-H), 8.33 (1H, dd, *J* 8.4, 1.4 Hz, 8''-H), 8.88 (1H, d, *J* 4.4 Hz, 2''-H); δ_C (101 MHz, $CDCl_3$) 28.4 (3 × CH_3), 38.5 (CH_2), 52.4 (CH_3), 54.4 (CH), 80.1 (C), 85.3 (C), 98.5 (C), 121.0 (C), 123.6 (CH), 126.1 (CH), 127.3 (CH), 127.8 (C), 129.7 (2 × CH), 129.8 (C), 130.0 (2 × CH), 132.2 (2 × CH), 137.9 (C), 148.2 (C), 149.9 (CH), 155.1 (C), 172.2 (C); *m/z* (ESI) 456.2026 (MNa^+. $C_{26}H_{26}N_2O_4Na$ requires 456.2020).

Methyl (±)-2-(*tert*-butoxycarbonylamino)-3-[4'-(7''-ethynylquinoline)phenyl]propanoate (172p)

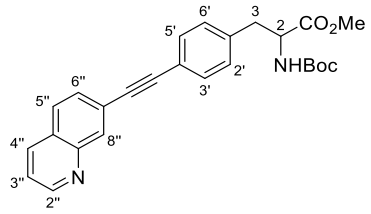

Methyl (±)-2-(*tert*-butoxycarbonylamino)-3-[4'-(7''-ethynylquinoline)phenyl]propanoate (**172p**) was synthesised as described for methyl (±)-2-(*tert*-butoxycarbonylamino)-3-[4'-(3''-cyanophenylethynyl)phenyl]propanoate (**172j**) using methyl (±)-2-(*tert*-butoxycarbonylamino)-3-(4'-ethynylphenyl)propanoate (**181**) (0.998 g, 0.329 mmol), 7-bromoquinoline (0.893 g, 0.429 mmol), bis(triphenylphosphine)palladium(II) dichloride (0.0240 g, 0.0342 mmol) and copper iodide (0.0130 g, 0.0683 mmol) in dry *N*,*N*'-dimethylformamide (6 mL) and anhydrous triethylamine (14 mL). Purification by flash column chromatography eluting with 0–10% ethyl acetate in dichloromethane gave methyl (±)-2-(*tert*-butoxycarbonylamino)-3-[4'-(7''-ethynylquinoline)phenyl]propanoate (**172p**) (0.709, 50%) as a pale brown solid. Mp 145–148 °C; ν_{max}/cm^{-1} (neat) 3357 (NH), 2977 (CH), 1743 (C=O), 1708 (C=O), 1617, 1511, 1436, 1365, 1251, 1256, 1165, 1055, 1020, 837; δ_H (400 MHz, $CDCl_3$) 1.42 (9H, s, 3 × CH_3), 3.06 (1H, dd, *J* 14.0, 6.4 Hz, 3-*H*H), 3.15 (1H, dd, *J* 14.0, 6.0 Hz, 3-H*H*), 3.71 (3H, s, OCH_3), 4.55–4.65 (1H, m, 2-H), 5.09 (1H, d, *J* 8.0 Hz, 2-NH) 7.14 (2H, d, *J* 8.2 Hz, 2'-H and 6'-H), 7.30–7.46 (1H, m, 3''-H), 7.51 (2H, d, *J* 8.2 Hz, 3'-H and 5'-H), 7.62 (1H, d, *J* 8.4 Hz, 6''-H), 7.71–7.88 (1H, m, 5''-H), 8.13 (1H, d, *J* 8.0 Hz, 4''-H), 8.28 (1H, s, 8''-H), 8.99 (1H, br s, 2''-H); δ_C (101 MHz, $CDCl_3$) 28.4 (3 × CH_3), 38.4 (CH_2), 52.4 (CH_3), 54.4 (CH), 80.1 (C), 89.3 (C), 91.2 (C), 121.7 (C), 124.5 (C), 128.1 (CH), 129.3 (2 × CH), 129.5 (3 × CH), 132.0 (2 × CH), 132.8 (CH), 135.8 (CH), 137.0 (2 × C), 148.2 (C), 151.1 (CH), 155.2 (C), 172.2 (C); *m/z* (ESI) 431.1978 (MH^+. $C_{26}H_{27}N_2O_4$ requires 431.1965).

Methyl (±)-2-(*tert*-butoxycarbonylamino)-3-[4'-(5''-ethynylquinoline)phenyl]propanoate (172q)

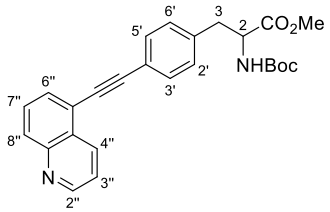

Methyl (±)-2-(*tert*-butoxycarbonylamino)-3-[4'-(5''-ethynylquinoline)phenyl]propanoate (**172q**) was synthesised as described for methyl (±)-2-(*tert*-butoxycarbonylamino)-3-[4'-(3''-cyanophenylethynyl)phenyl]propanoate (**172j**) using methyl (±)-2-(*tert*-butoxycarbonylamino)-3-(4'-ethynylphenyl)propanoate (**181**) (0.101 g, 0.333 mmol), 5-bromoquinoline (0.0897 g, 0.431 mmol), bis(triphenylphosphine)palladium(II) dichloride (0.0240 g, 0.0342 mmol) and copper iodide (0.0130 g, 0.0683 mmol) in dry *N*,*N*'-dimethylformamide (6 mL) and anhydrous triethylamine (14 mL). Purification by flash column chromatography eluting with 10% ethyl acetate in dichloromethane gave methyl (±)-2-(*tert*-butoxycarbonylamino)-3-[4'-(5''-ethynylquinoline)phenyl]propanoate (**172q**) (0.0953 g, 68%) as a pale brown solid. Mp 110–113 °C; ν_{max}/cm^{-1} (neat) 2977 (CH), 1744 (C=O), 1710 (C=O), 1497, 1391, 1365, 1166, 1050, 1020, 804; δ_H (400 MHz, $CDCl_3$) 1.43 (9H, s, 3 × CH_3), 3.08 (1H, dd, *J* 13.6, 6.0 Hz, 3-*H*H), 3.17 (1H, dd, *J* 13.6, 5.6 Hz, 3-H*H*), 3.73 (3H, s, OCH_3), 4.53–4.66 (1H, m, 2-H), 5.06 (1H, d, *J* 8.4 Hz, 2-NH), 7.17 (2H, d, *J* 8.0 Hz, 2'-H and 6'-H), 7.50 (1H, dd, *J* 8.4, 4.0 Hz, 3''-H), 7.56 (2H, d, *J* 8.0 Hz, 3'-H and 5'-H), 7.68 (1H, dd, *J* 8.2, 7.2 Hz, 7''-H), 7.79 (1H, d, *J* 7.2 Hz, 6''-H), 8.10 (1H, d, *J* 8.2 Hz, 8''-H), 8.71 (1H, d, *J* 8.4 Hz, 4''-H), 8.96 (1H, br s, 2''-H); δ_C (101 MHz, $CDCl_3$) 28.4 (3 × CH_3), 38.5 (CH_2), 52.4 (CH_3), 54.4 (CH), 80.2 (C), 86.5 (C), 94.8 (C), 121.4 (C), 121.7 (C), 121.8 (CH), 128.7 (C), 129.1 (CH), 129.6 (2 × CH), 130.4 (CH), 130.7 (CH), 131.9 (2 × CH), 134.7 (CH), 137.1 (C), 148.2 (C), 151.0 (CH), 155.2 (C), 172.2 (C); *m/z* (ESI) 431.1960 (MH^+. $C_{26}H_{27}N_2O_4$ requires 431.1965).

Methyl (±)-2-(*tert*-butoxycarbonylamino)-3-[4'-(4''-ethynyl-6''-cyanoquinoline)phenyl]propanoate (172r)

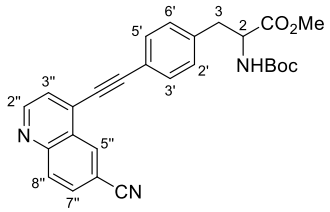

Methyl (±)-2-(*tert*-butoxycarbonylamino)-3-[4'-(4''-ethynyl-6''-cyanoquinoline)phenyl]propanoate (**172r**) was synthesised as described for methyl (±)-2-(*tert*-butoxycarbonylamino)-3-[4'-(3''-cyanophenylethynyl)phenyl]propanoate (**172j**) using methyl (±)-2-(*tert*-butoxycarbonylamino)-3-(4'-ethynylphenyl)propanoate (**181**) (0.100 g, 0.330 mmol), 4-bromoquinoline-6-carbonitrile (0.0997 g, 0.428 mmol), bis(triphenylphosphine)palladium(II) dichloride (0.0240 g, 0.0342 mmol) and copper iodide (0.0130 g, 0.0683 mmol) in dry *N*,*N*'-dimethylformamide (6 mL) and anhydrous triethylamine (14 mL). Purification by flash column chromatography eluting with 10% ethyl acetate in dichloromethane gave methyl (±)-2-(*tert*-butoxycarbonylamino)-3-[4'-(4''-ethynyl-6''-cyanoquinoline)phenyl]propanoate (**172r**) (0.131 g, 87%) as a yellow solid. Mp 69–71 °C; ν_{max}/cm^{-1} (neat) 2976 (CH), 2209 (C≡C), 1707 (C=O), 1574, 1496, 1438, 1364, 1159, 1054, 1018, 855; δ_H (400 MHz, $CDCl_3$) 1.44 (9H, s, 3 × CH_3), 3.11 (1H, dd, *J* 13.6, 6.4 Hz, 3-*H*H), 3.21 (1H, dd, *J* 13.6, 6.0 Hz, 3-H*H*), 3.75 (3H, s, OCH_3), 4.58–4.65 (1H, m, 2-H), 5.06 (1H, d, *J* 8.4 Hz, 2-NH), 7.23 (2H, d, *J* 8.4 Hz, 2'-H and 6'-H), 7.62 (2H, d, *J* 8.4 Hz, 3'-H and 5'-H), 7.65 (1H, d, *J* 4.4 Hz, 3''-H), 7.89 (1H, dd, *J* 8.6, 1.6 Hz, 7''-H), 8.20 (1H, dd, *J* 8.6, 0.4 Hz, 8''-H), 8.72 (1H, dd, *J* 1.6, 0.4 Hz, 5''-H), 9.01 (1H, d, *J* 4.4 Hz, 2''-H); δ_C (101 MHz, $CDCl_3$) 28.4 (3 × CH_3), 38.6 (CH_2), 52.5 (CH_3), 54.5 (CH), 80.3 (C), 84.0 (C), 100.7 (C), 111.0 (C), 118.8 (C), 120.3 (C), 125.0 (CH), 127.3 (C), 129.9 (2 × CH), 130.67 (C), 130.71 (CH), 131.6 (CH), 132.4 (2 × CH), 132.6 (CH), 138.7 (C), 149.2 (C), 152.8 (CH), 155.1 (C), 172.2 (C); *m/z* (ESI) 456.1917 (MH^+. $C_{27}H_{26}N_3O_4$ requires 456.1917).

Methyl (±)-2-(*tert*-butoxycarbonylamino)-3-[4'-(4''-ethynyl-7''-nitrobenzofuran)phenyl]propanoate (172s)

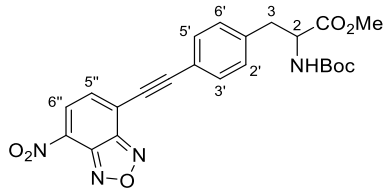

In an oven-dried flask under argon, a solution of methyl (±)-2-(*tert*-butoxycarbonylamino)-3-(4'-ethynylphenyl)propanoate (**181**) (0.100 g, 0.330 mmol), 4-chloro-7-nitrobenzo-2-oxa-1,3-diazole (0.0855 g, 0.418 mmol), bis(triphenylphosphine)palladium(II) dichloride (0.0240 g, 0.0342 mmol) and copper iodide (0.0130 g, 0.0683 mmol) in dry tetrahydrofuran (4 mL) and anhydrous triethylamine (14 mL) was degassed under argon for 0.5 h. The reaction mixture was shielded from light and stirred at room temperature for 1.5 h. The reaction mixture was concentrated *in vacuo* and purified by flash column chromatography eluting with 10–30% ethyl acetate in hexane followed by a second purification by flash column chromatography eluting with 2% ethyl acetate in dichloromethane to give methyl (±)-2-(*tert*-butoxycarbonylamino)-3-[4'-(4''-ethynyl-7''-nitrobenzofuran)phenyl]propanoate (**172s**) (0.0465 g, 30%) as a yellow solid. Mp 60–64 °C; ν_{max}/cm^{-1} (neat) 3368 (NH), 2977 (CH), 2203 (C≡C), 1739 (C=O), 1704 (C=O), 1541, 1523, 1438, 1366, 1332, 1160, 1063, 1018, 994, 862; δ_H (400 MHz, $CDCl_3$) 1.42 (9H, s, 3 × CH_3), 3.08 (1H, dd, *J* 13.6, 6.4 Hz, 3-*H*H), 3.20 (1H, dd, *J* 13.6, 6.0 Hz, 3-H*H*), 3.73 (3H, s, OCH_3), 4.56–4.66 (1H, m, 2-H), 5.03 (1H, d, *J* 8.4 Hz, 2-NH), 7.22 (2H, d, *J* 8.0 Hz, 2'-H and 6'-H), 7.61 (2H, d, *J* 8.0 Hz, 3'-H and 5'-H), 7.69 (1H, d, *J* 7.6 Hz, 5''-H), 8.50 (1H, d, *J* 7.6 Hz, 6''-H); δ_C (101 MHz, $CDCl_3$) 28.4 (3 × CH_3), 38.7 (CH_2), 52.5 (CH_3), 54.4 (CH), 80.3 (C), 83.7 (C), 104.5 (C), 119.8 (C), 121.6 (C), 129.9 (2 × CH), 130.5 (CH), 131.6 (CH), 132.7 (2 × CH), 135.6 (C), 139.5 (C), 142.7 (C), 150.9 (C), 155.1 (C), 172.1 (C); *m/z* (ESI) 367.1037 ($[(MH–CO_2{}^tBu)+H]^+$. $C_{18}H_{14}N_4O_5$ requires 367.1037).

Methyl (±)-2-(*tert*-butoxycarbonylamino)-3-[4'-(6''-ethynylcoumarin)phenyl]propanoate (172t)

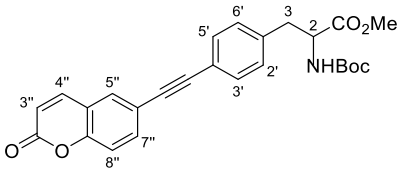

In an oven-dried flask under argon, a solution of methyl (±)-2-(*tert*-butoxycarbonylamino)-3-(4'-ethynylphenyl)propanoate (**181**) (0.100 g, 0.330 mmol), 6-bromochromen-2-one (0.0970 g, 0.429 mmol), bis(triphenylphosphine)palladium(II) dichloride (0.0120 g, 0.0171 mmol) and copper iodide (0.0650 g, 0.0341 mmol) in dry *N*,*N*'-dimethylformamide (6 mL) and anhydrous triethylamine (14 mL) was degassed under argon for 0.5 h. The reaction mixture was heated to 70 °C and stirred for 2.5 h. A second portion of bis(triphenylphosphine)palladium(II) dichloride (0.0120 g, 0.0171 mmol) and copper iodide (0.0650 g, 0.0341 mmol) was added and the reaction mixture was further degassed under argon for 0.5 h. The reaction mixture was stirred at 70 °C for 4 h, concentrated *in vacuo*, diluted in ethyl acetate (50 mL) and washed with water (2 × 50 mL) and brine (2 × 50 mL). The organic layer was dried ($MgSO_4$), filtered and concentrated *in vacuo*. Purification by flash column chromatography eluting with 2–5% ethyl acetate in dichloromethane gave methyl (±)-2-(*tert*-butoxycarbonylamino)-3-[4'-(6''-ethynylcoumarin)phenyl]propanoate (**172t**) (0.0490 g, 33%) as an off white solid. Mp 133–136 °C; ν_{max}/cm^{-1} (neat) 3347 (NH), 2973 (CH), 1712 (C=O), 1623, 1568, 1508, 1433, 1364, 1221, 1161, 1122, 1093, 1019, 906, 821; δ_H (400 MHz, $CDCl_3$) 1.42 (9H, s, 3 × CH_3), 3.06 (1H, dd, *J* 14.0, 6.0 Hz, 3-*H*H), 3.15 (1H, dd, *J* 14.0, 5.6 Hz, 3-H*H*), 4.55–4.66 (1H, m, 2-H), 5.00 (1H, d, *J* 8.0 Hz, 2-NH), 6.46 (1H, d, *J* 9.6 Hz, 3''-H), 7.14 (2H, d, *J* 8.0 Hz, 2'-H and 6'-H), 7.28–7.32 (1H, m, 8''-H) 7.46 (2H, d, *J* 8.0 Hz, 3'-H and 5'-H), 7.63–7.77 (3H, m, 3 × ArH); δ_C (101 MHz, $CDCl_3$) 28.4 (3 × CH_3), 38.5 (CH_2), 52.4 (CH_3), 54.4 (CH), 80.2 (C), 87.8 (C), 90.0 (C), 117.3 (CH), 117.6 (CH), 119.0 (C), 120.0 (C), 121.5 (C), 129.6 (2 × CH), 130.9 (CH), 131.9 (2 × CH), 135.0 (CH), 137.1 (C), 142.9 (CH), 153.7 (C), 155.1 (C), 160.3 (C), 172.2 (C); *m/z* (ESI) 348.1234 ([MH–$CO_2{}^tBu$]$^+$. $C_{21}H_{17}NO_6$ requires 348.1230).

Methyl (±)-2-(*tert*-butoxycarbonylamino)-3-[4'-(2''-ethynyl-9''*H*-xanthen-9''-one)phenyl]propanoate (172u)

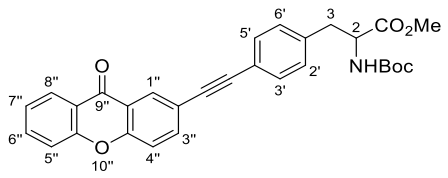

Methyl (**±**)-2-(*tert*-butoxycarbonylamino)-3-[4'-(2''-ethynyl-9''*H*-xanthen-9''-one)phenyl]propanoate (**172u**) was synthesised as described for methyl (±)-2-(*tert*-butoxycarbonylamino)-3-[4'-(3''-cyanophenylethynyl)phenyl]propanoate (**172j**) using methyl (±)-2-(*tert*-butoxycarbonylamino)-3-(4'-ethynylphenyl)propanoate (**181**) (0.0964 g, 0.0.318 mmol), 2-bromo-9*H*-xanthen-9-one (0.119 g, 0.433 mmol), bis(triphenylphosphine)palladium(II) dichloride (0.0240 g, 0.0342 mmol) and copper iodide (0.0130 g, 0.0683 mmol) in *N*,*N*'-dimethylformamide (6 mL) and anhydrous triethylamine (14 mL). Purification by flash column chromatography eluting first with 3% diethyl ether in dichloromethane followed by 5% ethyl acetate in dichloromethane gave methyl (±)-2-(*tert*-butoxycarbonylamino)-3-[4'-(2''-ethynyl-9''*H*-xanthen-9''-one)phenyl]propanoate (**172u**) (0.0763 g, 48%) as a white solid. Mp 165–167 °C; ν_{max}/cm^{-1} (neat) 3344 (NH), 2977 (CH), 1711 (C=O), 1660, 1614, 1511, 1488, 1465, 1365, 1312, 1217, 1165, 1109, 1057, 1020, 871; δ_H (400 MHz, $CDCl_3$) 1.43 (9H, s, 3 × CH_3), 3.07 (1H, dd, *J* 14.0, 6.4 Hz, 3-*H*H), 3.15 (1H, dd, *J* 14.0, 6.0 Hz, 3-H*H*), 3.73 (3H, s, OCH_3), 4.54–4.64 (1H, m, 2-H), 5.01 (1H, d, *J* 8.0 Hz, 2-NH), 7.14 (2H, d, *J* 8.0 Hz, 2'-H and 6'-H), 7.40 (1H, ddd, *J* 8.0, 7.0, 1.2 Hz, 7''-H), 7.45–7.52 (4H, m, 3'-H, 5'-H, 4''-H and 5''-H), 7.74 (1H, ddd, *J* 8.0, 7.0, 1.8 Hz, 6''-H), 7.83 (1H, dd, *J* 8.8, 2.0 Hz, 3''-H), 8.35 (1H, dd, *J* 8.0, 1.8 Hz, 8''-H), 8.49 (1H, d, *J* 2.0 Hz, 1''-H); δ_C (101 MHz, $CDCl_3$) 28.4 (3 × CH_3), 38.5 (CH_2), 52.5 (CH_3), 54.4 (CH), 80.2 (C), 88.2 (C), 90.0 (C), 118.2 (CH), 118.5 (CH), 119.5 (C), 121.7 (C), 121.91 (C), 121.94 (C), 124.4 (CH), 127.0 (CH), 129.6 (2 × CH), 130.2 (CH), 132.0 (2 × CH), 135.2 (CH), 136.9 (C), 137.6 (CH), 155.2 (C), 155.8 (C), 156.2 (C), 172.3 (C), 176.6 (C); *m/z* (ESI) 520.1741 (MNa^+. $C_{30}H_{27}NO_6Na$ requires 520.1731).

Methyl (±)-2-(*tert*-butoxycarbonylamino)-3-[4'-(3''-ethynyl-9''*H*-xanthen-9''-one)phenyl]propanoate (172v)

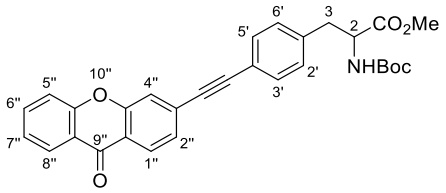

Methyl (±)-2-(*tert*-butoxycarbonylamino)-3-[4'-(3''-ethynyl-9''*H*-xanthen-9''-one)phenyl]propanoate (**172v**) was synthesised as described for methyl (±)-2-(*tert*-butoxycarbonylamino)-3-[4'-(3''-cyanophenylethynyl)phenyl]propanoate (**172j**) using methyl (±)-2-(*tert*-butoxycarbonylamino)-3-(4'-ethynylphenyl)propanoate (**181**) (0.101 g, 0.333 mmol), 3-bromo-9*H*-xanthen-9-one (0.119 g, 0.433 mmol), bis(triphenylphosphine)palladium(II) dichloride (0.0240 g, 0.0342 mmol) and copper iodide (0.0130 g, 0.0683 mmol) in dry *N*,*N*'-dimethylformamide (6 mL) and anhydrous triethylamine (14 mL). Purification by flash column chromatography eluting first with 1:5:50 and then 1:2:20 ethyl acetate:toluene:dichloromethane gave methyl (±)-2-(*tert*-butoxycarbonylamino)-3-[4'-(3''-ethynyl-9''*H*-xanthen-9''-one)phenyl]propanoate (**172v**) as a white solid. Mp 158–161 °C; ν_{max}/cm^{-1} (neat) 3338 (NH), 2977 (CH), 2214 (C≡C), 1744 (C=O), 1712 (C=O), 1657, 1619, 1605, 1551, 1464, 1419, 1365, 1323, 1213, 1165, 1107, 1056, 1020, 968, 839; δ_H (400 MHz, $CDCl_3$) 1.43 (9H, s, 3 × CH_3), 3.07 (1H, dd, *J* 13.6, 6.4 Hz, 3-*H*H), 3.17 (1H, dd, *J* 13.6, 6.0 Hz, 3-H*H*), 3.73 (3H, s, OCH_3), 4.57–4.64 (1H, m, 2-H), 5.02 (1H, d, *J* 8.0 Hz, 2-NH), 7.16 (2H, d, *J* 8.4 Hz, 2'-H and 6'-H), 7.39 (1H, ddd, *J* 8.0, 7.2, 1.2 Hz, 7''-H), 7.46–7.52 (4H, m, 3'-H, 5'-H, 2''-H and 5''-H), 7.63 (1H, d, *J* 1.6 Hz, 4''-H), 7.73 (1H, ddd, 8.8, 7.2, 1.8 Hz, 6''-H), 8.30 (1H, d, *J* 8.0 Hz, 1''-H), 8.33 (1H, dd, *J* 8.0, 1.8 Hz, 8''-H); δ_C (101 MHz, $CDCl_3$) 28.4 (3 × CH_3), 38.6 (CH_2), 52.5 (CH_3), 54.4 (CH), 80.2 (C), 88.4 (C), 93.5 (C), 118.2 (CH), 120.8 (CH), 121.2 (C), 121.4 (C), 122.1 (C), 124.3 (CH), 126.88 (CH), 126.91 (CH), 127.2 (CH), 129.7 (2 × CH), 130.1 (C), 132.1 (2 × CH), 135.1 (CH), 137.6 (C), 155.2 (C), 156.0 (C), 156.3 (C), 172.2 (C), 176.8 (C); *m/z* (ESI) 498.1917 (MH^+. $C_{30}H_{28}NO_6$ requires 498.1911).

Methyl (±)-2-(*tert*-butoxycarbonylamino)-3-[4'-(7''-ethynylquinolin-4-one) phenyl]propanoate (172w)

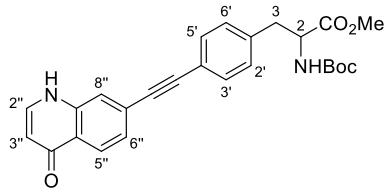

In an oven-dried flask under argon, a solution of methyl (±)-2-(*tert*-butoxycarbonylamino)-3-(4'-ethynylphenyl)propanoate (**181**) (0.100 g, 0.330 mmol), 7-bromoquinolin-4-ol (0.0968 g, 0.432 mmol), bis(bis(triphenylphosphine)palladium(II) dichloride (0.0120 g, 0.0171 mmol) and copper iodide (0.0650 g, 0.0341 mmol) in dry *N*,*N*'-dimethylformamide (6 mL) and anhydrous triethylamine (14 mL) was degassed under argon for 30 minutes. The reaction mixture was heated to 60 °C and stirred for 4 h. A second portion of bis(triphenylphosphine)palladium(II) dichloride (0.0120 g, 0.0171 mmol) and copper iodide (0.0650 g, 0.0341 mmol) was added and the reaction mixture was further degassed for 0.5 h. The reaction mixture was stirred at 60 °C for 16 h, concentrated *in vacuo,* diluted in ethyl acetate (50 mL) and washed with water (2 × 50 mL) and brine (2 × 50 mL). The organic layer was dried ($MgSO_4$), filtered and concentrated *in vacuo*. Purification by flash column chromatography eluting with 1–10% methanol in dichloromethane gave methyl (±)-2-(*tert*-butoxycarbonylamino)-3-[4'-(7''-ethynylquinolin-4-one)phenyl]propanoate (**172w**) (0.0443 g, 30%) as a pale yellow solid. Mp 208–210 °C; ν_{max}/cm^{-1} (neat) 3230 (NH), 2920 (CH), 1703 (C=O), 1633, 1606, 1556, 1502, 1462, 1365, 1159, 1055, 815; δ_H (400 MHz, $CDCl_3$) 1.42 (9H, s, 3 × CH_3), 3.03 (1H, dd, *J* 13.6, 6.4 Hz, 3-*H*H), 3.12 (1H, dd, *J* 13.6, 6.0 Hz, 3-H*H*), 3.71 (3H, s, OCH_3), 4.48–4.62 (1H, m, 2-H), 5.07 (1H, d, *J* 8.4 Hz, 2-NH), 6.35 (1H, d, *J* 7.2 Hz, 3''-H), 7.13 (2H, d, *J* 8.2 Hz, 2'-H and 6'-H), 7.45 (2H, d, *J* 8.2 Hz, 3'-H and 5'-H), 7.48 (1H, dd, *J* 8.4, 1.6 Hz, 6''-H), 7.67–7.78 (2H, m, 2''-H and 8''-H), 8.38 (1H, d, *J* 8.4 Hz, 5''-H), 11.69 (1H, br s, 1'-NH); δ_C (101 MHz, $CDCl_3$) 28.4 (3 × CH_3), 38.6 (CH_2), 53.5 (CH_3), 54.5 (CH), 80.4 (C), 88.7 (C), 92.1 (C), 110.0 (CH), 121.4 (CH), 125.6 (C), 126.0 (CH), 127.1 (C, CH), 127.3 (C), 129.6 (2 × CH), 132.1 (2 × CH), 137.3 (C), 139.7 (CH), 140.2 (C), 155.3 (C), 172.3 (C), 178.9 (C); *m/z* (QTOF) 447.1940 (MH^+. $C_{26}H_{27}N_2O_5$ requires 447.1914).

(2*S*)-2-(*tert*-Butoxycarbonylamino)-3-(4'-ethynylphenyl)propanoic acid (182)[227]

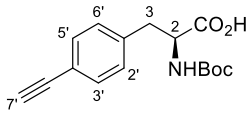

Methyl (2*S*)-2-(*tert*-butoxycarbonylamino)-3-[4'-(trimethylsilylethynyl)phenyl]propanoate (**180**) (2.32 g, 6.17 mmol) was dissolved in a 1:1 mixture of diethyl ether:methanol (142 mL). Aqueous 1 M sodium hydroxide (40 mL) was added dropwise over 0.17 h after which the reaction mixture was stirred for a further 1 h. The reaction mixture was adjusted to pH 7 using 6 M hydrochloric acid and concentrated *in vacuo*. The reaction mixture was diluted in water (100 mL), acidified to pH 2 and extracted with ethyl acetate (3 × 100 mL). Purification by flash column chromatography eluting with 2:2:96 acetic acid:diethyl ether:dichloromethane gave (2*S*)-2-(*tert*-butoxycarbonylamino)-3-(4'-ethynylphenyl)propanoic acid (**182**) as a pale orange solid (1.62 g, 91%). Mp 126–129 °C (lit.[227] 125.5–126.2 °C); NMR data were consistent with the literature.[227] NMR spectra showed a 2:1 mixture of rotamers. Only data for the major rotamer were recorded. δ_H (400 MHz, $CDCl_3$) 1.42 (9H, s, 3 × CH_3), 3.02–3.25 (3H, m, 3-H_2 and 7'-H), 4.55–4.66 (1H, m, 2-H), 4.99 (1H, d, *J* 8.0 Hz, 2-NH), 7.14 (2H, d, *J* 8.2 Hz, 2'-H and 6'-H), 7.43 (2H, d, *J* 8.2 Hz, 3'-H and 5'-H), 11.07 (1H, br s, OH); δ_C (101 MHz, $CDCl_3$) 28.4 (3 × CH_3), 37.9 (CH_2), 54.3 (CH), 80.6 (C), 82.0 (C), 83.5 (CH), 121.1 (C), 129.5 (2 × CH), 132.4 (2 × CH), 137.0 (C), 155.4 (C), 175.7 (C); *m/z* (QTOF) 288 ($[M-H]^-$. 100%).

(2*S*)-2-(*tert*-Butoxycarbonylamino)-3-[4'-(4"-cyanophenylethynyl)phenyl]propanoic acid (184a)

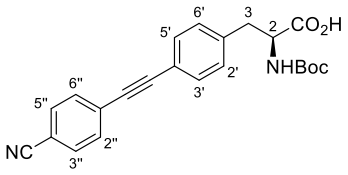

In an oven-dried flask under argon, a solution of (2*S*)-2-(*tert*-butoxycarbonylamino)-3-(4'-ethynylphenyl)propanoic acid (**182**) (0.0422 g, 0.146 mmol) and 4-

iodobenzonitrile (0.0509 g, 0.222 mmol) in dry *N,N'*-dimethylformamide (3 mL) and triethylamine (7 mL) was degassed under argon for 0.2 h. To this was added copper iodide (0.00330 g, 0.0173 mmol) and bis(triphenylphosphine)palladium(II) dichloride (0.00600 g, 0.00855 mmol). The solution was degassed for a further 0.1 h then stirred at 90 °C for 0.67 h. The reaction mixture was allowed to gradually come to room temperature and stirred for a further 2.5 h. Additional copper iodide (0.00330 g, 0.0173 mmol) and bis(triphenylphosphine)palladium(II) dichloride (0.00600 g, 0.00855 mmol) were added and the reaction mixture was degassed under argon for 0.1 h. The reaction mixture was stirred at 90 °C for 0.67 h and then room temperature for a further 3 h. The reaction mixture was concentrated *in vacuo*, diluted in ethyl acetate (50 mL), acidified to pH 1 using 1 M aqueous hydrochloric acid and washed with water (2 × 50 mL) and brine (2 × 50 mL). The organic layer was dried ($MgSO_4$), filtered and concentrated *in vacuo*. The crude material was purified by flash column chromatography eluting first with dichloromethane followed by 2:1:97 acetic acid:methanol:dichloromethane. Trituration from a mixture of chloroform and hexane gave (2*S*)-2-(*tert*-butoxycarbonylamino)-3-[4'-(4''-cyanophenylethynyl)phenyl]propanoic acid (**184a**) as a white solid (0.0467 g, 82%). Mp 154–156 °C; ν_{max}/cm^{-1} (neat) 3343 (NH), 2973 (CH), 2930, 2216 (CN), 1684 (C=O), 1602 (C=C) 1509, 1250, 1160, 834; $[\alpha]_D^{17}$ +18.9 (*c* 0.1, $CHCl_3$); NMR spectra showed a 2:1 mixture of rotamers. Only data for the major rotamer were recorded: δ_H (400 MHz, $CDCl_3$) 1.42 (9H, s, 3 × CH_3), 3.09 (1H, dd, *J* 14.4, 6.4 Hz, 3-*H*H), 3.15–3.28 (1H, m, 3-H*H*), 4.57–4.68 (1H, m, 2-H), 5.01 (1H, d, *J* 8.0 Hz, 2-NH), 7.21 (2H, d, *J* 7.8 Hz, 2'-H and 6'-H), 7.48 (2H, d, *J* 7.8 Hz, 3'-H and 5'-H), 7.57 (2H, d, *J* 8.8 Hz, 2''-H and 6''-H), 7.61 (2H, d, *J* 8.8 Hz, 3''-H and 5''-H), 9.65 (1H, br s, OH); δ_C (101 MHz, $CDCl_3$) 28.4 (3 × CH_3), 38.0 (CH_2), 54.3 (CH), 80.6 (C), 88.1 (C), 93.7 (C), 111.6 (C), 118.6 (C), 121.1 (C), 128.3 (C), 129.7 (2 × CH), 132.2 (6 × CH), 137.4 (C), 155.4 (C), 176.1 (C); *m/z* (ESI) 389.1506 ($[M-H]^-$. $C_{23}H_{21}N_2O_4$ requires 389.1507).

Methyl (2*S*)-2-(*tert*-butoxycarbonylamino)-3-[4'-(1''-ethynyl-6''-naphthoate)phenyl]propanoic acid (184b)

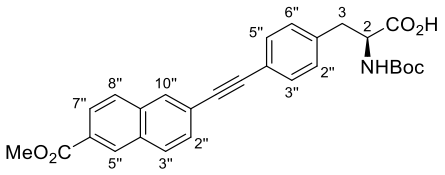

In an oven-dried flask under argon, a solution of (2*S*)-2-(*tert*-butoxycarbonylamino)-3-(4'-ethynylphenyl)propanoic acid (**182**) (0.102 g, 0.353 mmol), methyl 6-bromo-2-naphthoate (0.124 g, 0.468 mmol) copper iodide (0.00640 g, 0.0336 mmol) and bis(triphenylphosphine)palladium(II) dichloride (0.0126 g, 0.0180 mmol) in dry *N,N'*-dimethylformamide (6 mL) and triethylamine (14 mL) was degassed for 0.4 h. The reaction mixture was stirred at 90 °C for 0.6 h. The reaction mixture was warmed to room temperature and stirred for a further 3.5 h. Additional copper iodide (0.00630 g, 0.0330 mmol) and bis(triphenylphosphine)palladium(II) dichloride (0.0126 g, 0.0180 mmol) was added and the reaction mixture was degassed for 0.2 h. The reaction mixture was stirred at 90 °C for 0.6 h and then room temperature for a further 15 h. The reaction mixture was concentrated *in vacuo*, diluted in ethyl acetate (50 mL), acidified to pH 1 using 6 M aqueous hydrochloric acid and washed with water (2 × 50 mL) and brine (2 × 50 mL). The organic layer was dried ($MgSO_4$), filtered and concentrated *in vacuo*. Purification by flash column chromatography eluting with dichloromethane followed by 2:1:97 acetic acid:methanol:dichloromethane gave methyl (2*S*)-2-(*tert*-butoxycarbonylamino)-3-[4'-(1''-ethylnyl-6''-naphthoate)phenyl]propanoic acid (**184b**) as an off-white solid (0.129 g, 76%). Mp 173–175 °C; ν_{max}/cm^{-1} (neat) 3354 (NH), 2982 (CH), 2943 (CH), 1716 (C=O), 1686 (C=O), 1627 (C=C), 1513, 1435, 1367, 1287, 1267, 1251, 1222, 1163, 1140, 1097, 915, 821, 770; $[\alpha]_D^{17}$ +42.0 (*c* 0.1, $CHCl_3$); NMR spectra showed a 2:1 mixture of rotamers. Only data for the major rotamer were recorded: δ_H (400 MHz, $CDCl_3$) 1.44 (3H, s, 3 × CH_3), 3.13 (1H, dd, *J* 14.0, 6.4 Hz, 3-*H*H), 3.18–3.28 (1H, m, 3-H*H*), 4.58–4.70 (1H, m, 2-H), 5.08 (1H, d, *J* 8.0 Hz, 2-NH), 7.21 (2H, d, *J* 8.0 Hz, 2'-H and 6'-H), 7.52 (2H, d, *J* 8.0 Hz, 3'-H and 5'-H), 7.57 (1H, dd, *J* 8.4, 1.6 Hz, 2''-H), 7.78 (1H, d, *J* 8.6 Hz, 8''-H), 7.84 (1H, d, *J* 8.4 Hz, 3''-H), 7.99 (1H, s, 10''-H), 8.02 (1H, dd, *J* 8.6, 1.6 Hz, 7''-H), 8.51 (1H, s, 5''-H); δ_C (101 MHz, $CDCl_3$) 28.4 (3 × CH_3), 38.0 (CH_2), 52.4 (CH_3), 54.4 (CH), 80.5 (C), 89.7 (C), 91.0

(C), 121.8 (C), 123.2 (C), 126.0 (CH), 127.9 (C), 128.0 (CH), 129.3 (CH), 129.4 (CH), 129.7 (2 × CH), 130.8 (CH), 131.1 (CH), 131.8 (C), 132.0 (2 × CH), 135.1 (C), 136.9 (C), 155.5 (C), 167.2 (C), 176.1 (C); *m/z* (ESI) 472.1765 ($[M-H]^-$. $C_{28}H_{26}NO_6$ requires 472.1766).

(2*S*)-2-(*tert*-Butoxycarbonylamino)-3-[4'-(4"-ethynyl-1"-naphthonitrile)phenyl]propanoic acid (184c)

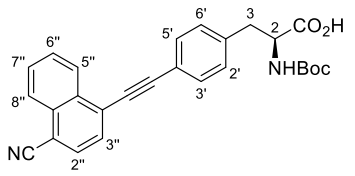

In an oven-dried flask under argon, a solution of (2*S*)-2-(*tert*-butoxycarbonylamino)-3-(4'-ethynylphenyl)propanoic acid (**182**) (0.0964 g, 0.333 mmol) in dry *N,N'*-dimethylformamide (6 mL) and triethylamine (14 mL) was degassed under argon for 0.4 h. To this was added 4-bromo-1-naphthonitrile (0.101 g, 0.433 mmol), copper iodide (0.00650 g, 0.0341 mmol) and XPhos Pd G2 (0.00680 g, 0.00864 mmol). The reaction mixture was degassed under argon for a further 0.2 h then stirred at 70 °C for 4.3 h. The reaction mixture was degassed and an additional portion of copper iodide (0.00660 g, 0.0347 mmol) and XPhos Pd G2 (0.00690 g, 0.00877 mmol) was added and the reaction stirred at 70 °C for 16 h. The reaction mixture was concentrated *in vacuo*, diluted in water (50 mL), acidified to pH 1 using 6 M hydrochloric acid and extracted with ethyl acetate (3 × 50 mL). The combined organic layers were washed with brine (50 mL), dried ($MgSO_4$) and concentrated *in vacuo*. Purification by flash column chromatography eluting with 2:1:96 acetic acid:methanol:dichloromethane gave (2*S*)-2-(*tert*-butoxycarbonylamino)-3-[4'-(4''-ethynyl-1''-naphthonitrile)phenyl]propanoic acid (**184c**) as a pale yellow solid (0.108 g, 73%). Mp 145–148 °C; ν_{max}/cm^{-1} (neat) 2970 (NH), 2934, 2208 (CN), 1712 (C=O), 1512, 1390, 1367, 1159, 1052, 1020, 836, 759; $[\alpha]_D^{17}$ +22.8 (*c* 0.1, $CHCl_3$); NMR spectra showed a 2:1 mixture of rotamers. Only data for the major rotamer were recorded: δ_H (400 MHz, $CDCl_3$) 1.44 (9H, s, 3 × CH_3), 3.14 (1H, d, *J* 13.6, 6.0 Hz, 3-*H*H), 3.20–3.32 (1H, m, 3-H*H*), 4.57–4.74 (1H, m, 2-H), 5.07 (1H, d, *J* 7.6 Hz, 2-NH), 7.27 (2H, d, *J* 7.6 Hz, 2'-H and 6'-H), 7.59 (2H, d, *J* 7.6 Hz, 3'-H and 5'-H), 7.63–7.73 (3H, m, 3''-H, 6''-H and 8''-H), 7.81 (1H, d, *J* 7.6 Hz, 5''-H), 8.18–8.25

(1H, m, 7''-H), 8.43 (1H, d, *J* 8.0 Hz, 2''-H), 10.73 (1H, br s, OH); δ_C (101 MHz, $CDCl_3$) 28.4 (3 × CH_3), 38.0 (CH_2), 54.5 (CH), 80.6 (C), 82.0 (C), 86.6 (C), 98.2 (C), 110.0 (C), 117.7 (C), 121.3 (C), 125.7 (CH), 126.6 (C), 127.0 (CH), 128.4 (CH), 129.0 (CH), 129.1 (CH), 129.8 (2 × CH), 131.8 (CH), 132.1 (2 × CH), 132.8 (C), 137.6 (C), 155.5 (C), 175.4 (C); *m/z* (ESI) 439.1662 ($[M-H]^-$. $C_{27}H_{23}N_2O_4$ requires 439.1663).

(2*S*)-2-(*tert*-Butoxycarbonylamino)-3-[4'-(6''-ethynylchromen-2''-one)phenyl]propanoic acid (184d)

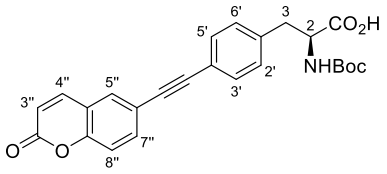

(2*S*)-2-(*tert*-Butoxycarbonylamino)-3-[4'-(6''-ethynylchromen-2''-one)phenyl]propanoic acid (**184d**) was synthesised as described for methyl (2*S*)-2-(*tert*-butoxycarbonylamino)-3-[4'-(4''-ethynyl-1''-naphthonitrile)phenyl]propanoic acid **(184c)** using (2*S*)-2-(*tert*-butoxycarbonylamino)-3-(4'-ethynylphenyl)propanoic acid (**182**) (0.0900 g, 0.311 mmol), 6-bromo-2*H*-chromen-2-one (0.0910 g, 0.404 mmol), copper iodide (0.0118 g, 0.0622 mmol) and XPhos Pd G2 (0.0122 g, 0.0155 mmol) in dry *N,N'*-dimethylformamide (6 mL) and triethylamine (14 mL). Purification by flash column chromatography eluting first with 2–7% methanol in 5% toluene in chloroform followed by 7–10% methanol in chloroform gave (2*S*)-2-(*tert*-butoxycarbonylamino)-3-[4'-(6''-ethynylchromen-2''-one)phenyl]propanoic acid (**184d**) as a brown solid (0.0998 g, 73%). Mp 133–136 °C; ν_{max}/cm^{-1} (neat) 2973 (NH), 2926, 2359, 1710 (C=O), 1568, 1508, 1367, 1161, 1127, 1094, 907, 821, 753; $[\alpha]_D^{17}$ +27.8 (*c* 0.1, $CHCl_3$); NMR spectra showed a 2:1 mixture of rotamers. Only data for the major rotamer were recorded: δ_H (400 MHz, $CDCl_3$) 1.42 (9H, s, 3 × CH_3), 3.01–3.29 (2H, m, 3-H_2), 4.52–4.71 (1H, m, 2-H), 4.98–5.14 (1H, m, 2-NH), 6.45 (1H, d, *J* 9.6 Hz, 3''-H), 7.20 (2H, d, *J* 7.6 Hz, 2'-H and 6'-H), 7.29 (1H, d, *J* 8.4 Hz, 8''-H), 7.46 (2H, d, *J* 7.6 Hz, 3'-H and 5'-H), 7.57–7.64 (2H, m, 5''-H and 7''-H), 7.66 (1H, d, *J* 9.6 Hz, 4''-H), 9.96 (1H, br s, OH); δ_C (101 MHz, $CDCl_3$) 28.4 (3 × CH_3), 38.0 (CH_2), 54.3 (CH), 80.6 (C), 87.9 (C), 90.0 (C), 117.3 (CH), 117.5 (CH), 119.0 (C), 119.9 (C), 121.5 (C), 129.7 (2 × CH), 130.9

(CH), 131.9 (2 × CH), 135.0 (CH), 137.0 (C), 142.9 (CH), 153.7 (C), 155.5 (C), 160.4 (C), 175.8 (C); *m/z* (ESI) 432.1461 ([M−H]$^-$. $C_{25}H_{22}NO_6$ 432.1453).

(2*S*)-2-(*tert*-Butoxycarbonylamino)-3-[4'-(5''-ethynylquinoline)phenyl]propanoic acid (184e)

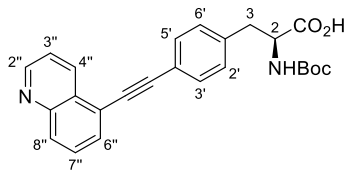

(2*S*)-2-(*tert*-Butoxycarbonylamino)-3-[4'-(5''-ethynylquinoline)phenyl]propanoic acid was synthesised as described for methyl (2*S*)-2-(*tert*-butoxycarbonylamino)-3-[4'-(methyl 6''-ethylnyl-2''-naphthoate)phenyl]propanoic acid **(184b)** using (2*S*)-2-(*tert*-butoxycarbonylamino)-3-(4'-ethynylphenyl)propanoic acid (**182**) (0.0970 g, 0.354 mmol), 5-bromoquinoline (0.0910 g, 0.437 mmol), copper iodide (0.0129 g, 0.0677 mmol), bis(triphenylphosphine)palladium(II) dichloride (0.0229 g, 0.0326 mmol) in dry *N,N'*-dimethylformamide (6 mL) and triethylamine (14 mL). The reaction mixture was concentrated *in vacuo*, diluted in ethyl acetate (50 mL), acidified to pH 4 using 1 M aqueous hydrochloric acid and washed with water (2 × 50 mL) and brine (2 × 50 mL). The organic layer was dried ($MgSO_4$), filtered and concentrated *in vacuo*. Purification by flash column chromatography eluting with 0–7% methanol in dichloromethane gave (2*S*)-2-(*tert*-butoxycarbonylamino)-3-[4'-(5''-ethynylquinoline)phenyl]propanoic acid (**184e**) as a pale brown solid (0.0676 g, 49%). Mp 180–185 °C (decomposed); ν_{max}/cm^{-1} (neat) 3357 (NH), 2971 (CH), 2925, 1686 (C=O), 1526, 1339, 1265, 1216, 1165, 1051, 802; $[\alpha]_D^{18}$ +20.6 (*c* 0.1, MeOH); δ_H (400 MHz, CD_3OD) 1.39 (9H, s, 3 × CH_3), 2.81–3.00 (1H, m, 3-*H*H), 3.18–3.25 (1H, m, 3-H*H*), 4.27–4.43 (1H, m, 2-H), 7.32 (2H, d, *J* 7.8 Hz, 2'-H and 6'-H), 7.58 (2H, d, *J* 7.8 Hz, 3'-H and 5'-H), 7.66 (1H, dd, *J* 8.4, 4.0 Hz, 3''-H), 7.74–7.81 (1H, m, 7''-H), 7.83 (1H, d, *J* 7.2 Hz, 6''-H), 8.04 (1H, d, *J* 8.4 Hz, 8''-H), 8.81 (1H, d, *J* 8.4 Hz, 4''-H), 8.87–8.94 (1H, m, 2''-H); δ_C (101 MHz, CD_3OD) 28.7 (3 × CH_3), 38.8 (CH_2), 49.3 (CH), 80.5 (C), 86.4 (C), 96.4 (C), 122.3 (C), 122.9 (C), 123.4 (CH), 129.9 (CH), 130.0 (C), 130.7 (CH), 130.8 (2 × CH), 132.0 (CH), 132.7 (2 × CH), 132.8 (C), 136.5 (CH), 140.2 (C), 148.6 (C), 151.8 (CH), 157.8 (C); *m/z* (ESI) 417.1824 (MH^+. $C_{25}H_{25}N_2O_4$ requires 417.1809).

(2*S*)-2-(*tert*-Butoxycarbonylamino)-3-[4'-(7''-ethynylquinoline)phenyl]propanoic acid (184f)

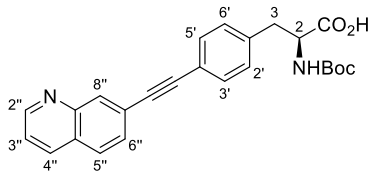

(2*S*)-2-(*tert*-Butoxycarbonylamino)-3-[4'-(7''-ethynylquinoline)phenyl]propanoic acid (**184f**) was synthesised as described for methyl (2*S*)-2-(*tert*-butoxycarbonylamino)-3-[4'-(1''-ethylnyl-6''-naphthoate)phenyl]propanoic acid (**184b**) using (2*S*)-2-(*tert*-butoxycarbonylamino)-3-(4'-ethynylphenyl)propanoic acid (**182**) (0.102 g, 0.353 mmol), 7-bromoquinoline (0.0958 g, 0.460 mmol), copper iodide (0.0145 g, 0.0761 mmol), bis(triphenylphosphine)palladium(II) dichloride (0.0249 g, 0.0355 mmol) in dry *N,N'*-dimethylformamide (6 mL) and triethylamine (14 mL). Purification by flash column chromatography eluting in 2:2:96 acetic acid:methanol:dichloromethane followed by a second purification by flash column chromatography eluting with 5–10% methanol in dichloromethane gave (2*S*)-2-(*tert*-butoxycarbonylamino)-3-[4'-(7''-ethynylquinoline)phenyl]propanoic acid as a pale brown solid (**184f**) (0.0921 g, 63%). Mp 128–131 °C; ν_{max}/cm^{-1} (neat) 2969 (CH), 2363, 1735 (C=O), 1713 (C=O), 1515, 1368, 1221, 1207, 1164; $[\alpha]_D^{18}$ +7.6 (*c* 0.1, $CHCl_3$); NMR spectra showed a 14:1 mixture of rotamers. Only data for the major rotamer were recorded: δ_H (400 MHz, $CDCl_3$) 1.48 (9H, s, 3 × CH_3), 3.09–3.36 (2H, m, 3-H_2), 4.54–4.74 (1H, m, 2-H), 5.34 (1H, d, *J* 5.6 Hz, 2-NH), 7.33 (2H, d, *J* 7.8 Hz, 2'-H and 6'-H), 7.42–7.51 (1H, m, 3''-H), 7.60 (1H, d, *J* 7.8 Hz, 3'-H and 5'-H), 7.65 (1H, d, *J* 8.4 Hz, 6''-H), 7.80 (1H, d, *J* 8.4 Hz, 5''-H), 8.16 (1H, s, 8''-H), 8.23 (1H, d, *J* 8.0 Hz, 4''-H), 8.83–8.99 (1H, m, 2''-H); δ_C (101 MHz, $CDCl_3$) 28.5 (3 × CH_3), 38.5 (CH_2), 54.7 (CH), 79.9 (C), 88.8 (C), 92.6 (C), 121.2 (C), 121.7 (CH), 125.9 (C), 128.1 (CH), 130.1 (3 × CH), 130.3 (CH), 132.0 (2 × CH), 132.2 (C), 137.8 (CH), 138.2 (C), 146.0 (C), 149.6 (CH), 155.4 (C), 174.4 (C); *m/z* (ESI) 417.1812 (MH^+. $C_{25}H_{25}N_2O_4$ requires 417.1809).

3.4.3 Synthesis of arylalkynyl BODIPY analogue

4,4-Difluoro-8-phenyl-1,3,5,7-tetramethyl-4-bora-*3a*,*4a*-diaza-*s*-indacene (190)[235]

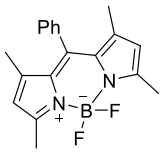

In an oven-dried flask under argon, to a solution of benzaldehyde (0.360 mL, 3.56 mmol) in dry dichloromethane (14 mL) under argon was added 2,4-dimethylpyrrole (0.920 mL, 8.90 mmol) followed by one drop of trifluoroacetic acid. The reaction mixture was stirred at room temperature for 15 h under argon. *p*-Chloranil (0.875 g, 3.56 mmol) was added and the reaction mixture was stirred for a further 1.25 h. Anhydrous triethylamine (3.40 mL, 24.9 mmol) was added followed by boron trifluoride diethyl etherate (3.10 mL, 24.9 mmol). The reaction mixture was stirred at room temperature for 1.25 h then concentrated *in vacuo*. Purification by flash column chromatography eluting with 2% ethyl acetate in petroleum ether gave 4,4-difluoro-8-phenyl-1,3,5,7-tetramethyl-4-bora-*3a*,*4a*-diaza-*s*-indacene (**190**) (0.240 g, 20%) as a red solid. NMR data were consistent with the literature.[235] Mp 170–173 °C (lit.[236] 172–174 °C); δ_H (400 MHz, $CDCl_3$) 1.37 (6H, s, 2 × CH_3), 2.56 (6H, s, 2 × CH_3), 5.98 (2H, s, 2-H and 6-H), 7.26–7.29 (2H, m, 2'-H and 6'-H) 7.45–7.51 (3H, m, 3'-H, 4'-H and 5'-H); δ_C (101 MHz, $CDCl_3$) 14.5 (2 × CH_3), 14.7 (2 × CH_3), 121.4 (CH), 128.1 (2 × CH), 129.1 (2 × CH), 129.3 (2 × CH), 131.6 (C), 135.2 (C), 141.9 (C), 143.3 (C), 155.6 (C); *m/z* (QTOF) 325 (MH^+. 100%).

4,4-Difluoro-6-iodo-8-phenyl-1,3,5,7-tetramethyl-4-bora-*3a*,*4a*-diaza-*s*-indacene (191)[295]

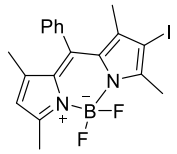

In an oven-dried flask under argon, to a solution of 4,4-difluoro-8-phenyl-1,3,5,7-tetramethyl-4-bora-*3a*,*4a*-diaza-*s*-indacene (**190**) (0.185 g, 0.571 mmol) in dry dichloromethane (47 mL) at 0 °C was added *N*-iodosuccinimide (0.122 g, 0.542 mmol) in dry dichloromethane (16 mL) dropwise over 0.5 h. The reaction was stirred for a further 1 h and then concentrated *in vacuo*. Purification by flash column chromatography eluting with 30% dichloromethane in hexane gave 4,4-difluoro-6-iodo-8-phenyl-1,3,5,7-tetramethyl-4-bora-*3a*,*4a*-diaza-*s*-indacene (**191**) as red solid (0.162 g, 66%). Mp 171–173 °C; ^{1}H NMR data were consistent with the literature.[295] δ_H (400 MHz, $CDCl_3$) 1.38 (6H, s, 2 × CH_3), 2.57 (3H, s, CH_3), 2.63 (3H, s, CH_3), 6.04 (1H, s, 2-H), 7.23–7.29 (2H, m, 2'-H and 6'-H), 7.47–7.42 (3H, m, 3'-H, 4'-H and 5'-H); δ_C (101 MHz, $CDCl_3$) 14.7 (CH_3), 14.9 (CH_3), 15.9 (CH_3), 16.8 (CH_3), 84.4 (C), 122.4 (CH), 128.0 (2 × CH), 129.4 (CH), 129.4 (2 × CH), 131.1 (C), 132.0 (C), 135.0 (C), 141.7 (C), 143.4 (C), 145.3 (C), 154.7 (C), 157.9 (C); *m/z* (ESI) 451 (MH^+. 100%).

(2*S*)-2-(*tert*-Butoxycarbonylamino)-3-[4'-(4'',4''-difluoro-6''-ethynyl-8''-phenyl-1'',3'',5'',7''-tetramethyl-4''-bora-*3''a*,*4''a*-diaza-*s*-indacene)pheny]propanoic acid (192)

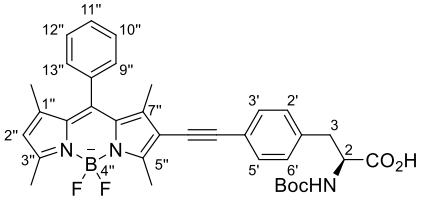

(2*S*)-2-(*tert*-Butoxycarbonylamino)-3-[4'-(4'',4''-difluoro-6''-ethynyl-8''-phenyl-1'',3'',5'',7''-tetramethyl-4''-bora-*3''a*,*4''a*-diaza-*s*-indacene)pheny]propanoic acid (**192**) was synthesised as described for methyl (2*S*)-2-(*tert*-butoxycarbonylamino)-3-

[4'-(methyl 6''-ethylnyl-2''-naphthoate)phenyl]propanoic acid **(184b)** using (2*S*)-2-(*tert*-butoxycarbonylamino)-3-(4'-ethynylphenyl)propanoic acid (**182**) (0.0895 g, 0.309 mmol), 4,4-difluoro-6-iodo-8-phenyl-1,3,5,7-tetramethyl-4-bora-*3a*,*4a*-diaza-*s*-indacene **(191)** (0.181 g, 0.402 mmol), copper iodide (0.0115 g, 0.0604 mmol), bis(triphenylphosphine)palladium(II) dichloride (0.0215 g, 0.0306 mmol) in dry *N,N'*-dimethylformamide (6 mL) and triethylamine (14 mL). The reaction mixture was concentrated *in vacuo*, diluted in water (50 mL) and extracted with ethyl acetate (3 × 50 mL). The combined organic layers were washed with brine (20 mL), dried ($MgSO_4$), filtered and concentrated *in vacuo*. Purification by flash column chromatography eluting with 2–10% methanol in dichloromethane gave (2*S*)-2-(*tert*-butoxycarbonylamino)-3-[4'-(4'',4''-difluoro-6''-ethynyl-8''-phenyl-1'',3'',5'',7''-tetramethyl-4''-bora-*3''a*,*4''a*-diaza-*s*-indacene)pheny]propanoic acid (**192**) (0.148 g, 77%) as a deep purple solid. Mp 171–173 °C; ν_{max}/cm^{-1} (neat) 2940 (NH), 2926, 2363 (CH), 2338, 1717 (C=O), 1538, 1511, 1399, 1364, 1314, 1182, 1160, 1056, 977, 933; $[\alpha]_D^{18}$ +1.6 (*c* 0.03, $CHCl_3$); δ_H (400 MHz, DMSO-d_6) 1.32 (9H, s, 3 × CH_3), 1.37 (3H, s, CH_3), 1.44 (3H, s, CH_3), 2.51 (3H, s, CH_3), 2.58 (3H, s, CH_3), 2.77–2.91 (1H, m, 3-*H*H), 2.96–3.09 (1H, m, 3-H*H*), 3.92–4.11 (1H, m, 2-H), 6.30 (1H, s, 2''-H), 6.89–6.97 (1H, m, 2-NH), 7.25 (2H, d, *J* 8.0 Hz, 2'-H and 6'-H), 7.33–7.43 (4H, m, 3'-H, 5'-H, 9''-H, and 13''-H), 7.54–7.64 (3H, m, 10''-H, 11''-H and 12''-H); δ_C (101 MHz, DMSO-d_6) 12.8 (CH_3), 13.2 (CH_3), 14.2 (CH_3), 14.5 (CH_3), 28.2 (3 × CH_3), 36.5 (CH_2), 55.1 (CH), 78.2 (C), 79.2 (C), 81.4 (C), 95.9 (C), 114.2 (C), 120.6 (C), 122.9 (CH), 127.8 (2 × CH), 129.4 (CH), 129.5 (2 × CH), 129.6 (2 × CH), 130.9 (2 × CH), 132.2 (C), 133.7 (C), 138.9 (C), 141.4 (C), 142.5 (C), 145.2 (C), 154.6 (C), 155.5 (C), 158.4 (C), 173.6 (C); *m/z* (ESI) 610.2696 ($[M-H]^-$. $C_{35}H_{35}BF_2N_3O_4$ requires 610.2700).

Methyl (2*S*)-2-amino-3-[4'-(trimethylsilylethynyl)phenyl]propanoate (195)

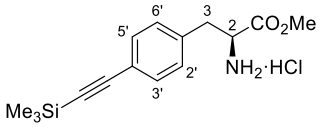

4 M Hydrochloric acid in 1,4-dioxane (4.4 mL) was added dropwise to a stirring solution of methyl (2*S*)-2-(*tert*-butoxycarbonylamino)-3-[4'-(trimethylsilylethynyl)phenyl]propanoate (**180**) (0.535 g, 1.42 mmol) in 1,4-dioxane

(4.4 mL) at room temperature. The reaction mixture was stirred for a further 6.5 h then concentrated *in vacuo*. Purification by flash column chromatography eluting with 1:49:50, triethylamine:hexane:ethyl acetate gave methyl (2*S*)-2-amino-3-[4'-(trimethylsilylethynyl)phenyl]propanoate (**195**) (0.350 g, 90%) as an off white solid. Mp 56–58 °C; ν_{max}/cm^{-1} (neat) 3400 (NH), 2957 (CH), 2155 (C≡C), 1732 (C=O), 1506, 1253, 1168, 995, 833; $[\alpha]_D^{16}$ + 4.9 (*c* 0.1, $CHCl_3$); δ_H (400 MHz, $CDCl_3$) 0.23 (9H, s, $Si(CH_3)_3$), 1.52 (2H, br s, 2-NH_2), 2.86 (1H, dd, *J* 13.4, 7.2 Hz, 3-*H*H), 3.05 (1H, dd, *J* 13.4, 4.4 Hz, 3-H*H*), 3.69 (4H, m, 2-H and OCH_3), 7.12 (2H, d, *J* 8.0 Hz, 2'-H and 6'-H), 7.39 (2H, d, *J* 8.0 Hz, 3'-H and 5'-H); δ_C (101 MHz, $CDCl_3$) 0.1 (3 × CH_3), 41.2 (CH_2), 52.1 (CH_3), 55.7 (CH), 94.3 (C), 105.0 (C), 121.8 (C), 129.3 (2 × CH), 132.2 (2 × CH), 137.9 (C), 175.4 (C); *m/z* (ESI) 276.1417 (MH^+. $C_{15}H_{22}NO_2Si$ requires 276.1414).

Methyl (2*S*)-2-(*N*-palmitoylamino)-3-[4'-(trimethylsilylethynyl)phenyl]propanoate (196)

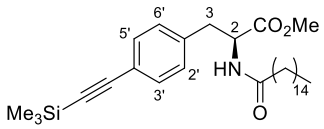

In an oven-dried flask, palmitic acid (0.188 g, 0.733 mmol) and *O*-(benzotriazol-1-yl)-*N*,*N*,*N*',*N*'-tetramethyluronium (HBTU) (0.306 g, 0.806 mmol) were suspended in dry acetonitrile (9 mL) under argon. To this was added *N*,*N*'-diisopropylethylamine (0.420 mL, 2.42 mmol) and the reaction was stirred at room temperature for 0.17 h. Methyl (2*S*)-2-amino-3-[4'-(trimethylsilylethynyl)phenyl]propanoate (**195**) (0.202 g, 0.733 mmol) was added slowly in dry acetonitrile (9 mL). The reaction mixture was stirred at room temperature for 17 h then concentrated *in vacuo*. The reaction mixture was dissolved in dichloromethane (50 mL) and washed with water (50 mL) followed by 1 M aqueous hydrochloric acid (50 mL), saturated aqueous sodium bicarbonate (50 mL) and brine (50 mL). The organic layer was dried ($MgSO_4$) and concentrated *in vacuo*. Purification by flash column chromatography eluting with 20% ethyl acetate in hexane afforded methyl (2*S*)-2-(*N*-palmitoylamino)-3-[4'-(trimethylsilylethynyl)phenyl]propanoate (**196**) as a white solid (0.329 g, 87%). Mp 57–79 °C; ν_{max}/cm^{-1} (neat) 3325 (NH), 2915 (CH), 2849 (CH), 2159 (C≡C), 1741

(C=O), 1647 (C=O), 1527, 1248, 1204, 865, 837; $[\alpha]_D^{17}$ +29.4 (*c* 0.1, $CHCl_3$); δ_H (400 MHz, $CDCl_3$) 0.23 (9H, s, $Si(CH_3)_3$), 0.87 (3H, t, *J* 6.6 Hz, CH_3), 1.19–1.32 (24H, m, 12 × CH_2), 1.52–1.62 (2H, m, CH_2), 2.11–2.17 (2H, m, CH_2), 3.06 (1H, dd, *J* 14.0, 6.0 Hz, 3-*H*H), 3.13 (1H, dd, *J* 14.0, 6.0 Hz, 3-H*H*), 3.70 (3H, s, OCH_3), 4.87 (1H, dt, *J* 7.6, 6.0 Hz, 2-H), 5.89 (1H, d, *J* 7.6 Hz, 2-NH), 7.12 (2H, d, *J* 8.2 Hz, 2'-H and 6'-H), 7.38 (2H, d, *J* 8.2 Hz, 3'-H and 5'-H); δ_C (101 MHz, $CDCl_3$) 0.1 (3 × CH_3), 14.2 (CH_3), 22.8 (CH_2), 25.7 (CH_2), 29.3 (CH_2), 29.4 (CH_2), 29.5 (CH_2), 29.6 (CH_2), 29.7 (CH_2), 29.77 (2 × CH_2), 29.80 (3 × CH_2), 32.0 (CH_2), 36.7 (CH_2), 38.0 (CH_2), 52.4 (CH_3), 52.9 (CH), 94.5 (C), 104.9 (C), 122.1 (C), 129.3 (2 × CH), 132.2 (2 × CH), 136.7 (C), 172.1 (C), 172.8 (C); *m/z* (ESI) 514.3712 (MH^+. $C_{31}H_{52}NO_3Si$ requires 514.3711).

(2*S*)-2-(*N*-Palmitoylamino)-3-(4'-ethynylphenyl)propanoic acid (197)

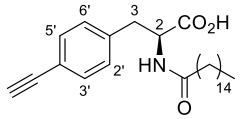

Methyl (2*S*)-2-(*N*-palmitoylamino)-3-[4'-(trimethylsilylethynyl)phenyl]propanoate (**196**) (0.262 g, 0.510 mmol) was dissolved in 50:50 methanol:diethyl ether (2.8 mL). Aqueous 1 M sodium hydroxide (1.02 mL, 1.02 mmol) was added slowly and the reaction mixture was stirred at room temperature for 2 h. The reaction mixture was concentrated *in vacuo*, suspended in water (50 mL), acidified to pH 2 (6 M aqueous hydrochloric acid) and extracted with 4:1 chloroform:isopropyl alcohol (3 × 50 mL). The organic layers were combined, dried ($MgSO_4$) and concentrated *in vacuo* to give (2*S*)-2-(*N*-palmitoylamino)-3-(4'-ethynylphenyl)propanoic acid (**197**) as a white solid (0.209 g, 96%). Mp 97–100 °C; ν_{max}/cm^{-1} (neat) 3327 (NH), 3276, 2917 (CH), 2849 (CH), 1717 (C=O), 1650 (C=O), 1518, 1508, 1203, 847; $[\alpha]_D^{16}$ +42.4 (*c* 0.1, $CHCl_3$); δ_H (400 MHz, $CDCl_3$) 0.88 (3H, t, *J* 6.4 Hz, CH_3), 1.17–1.33 (24H, m, 12 × CH_2), 1.51–1.61 (2H, m, CH_2), 2.09–2.25 (2H, m, CH_2), 3.07 (1H, s, 8'-H), 3.12 (1H, dd, *J* 14.4, 6.4 Hz, 3-*H*H), 3.25 (1H, dd, *J* 14.0, 5.6 Hz, 3-H*H*), 4.83–4.91 (1H, m, 2-H), 5.93 (1H, d, *J* 7.2 Hz, 2-NH), 7.12 (2H, d, *J* 8.2 Hz, 2'-H and 6'-H), 7.43 (2H, d, *J* 8.2 Hz, 3'-H and 5'-H); δ_C (101 MHz, $CDCl_3$) 14.3 (CH_3), 22.9 (CH_2), 25.7 (CH_2), 29.3 (CH_2), 29.47 (CH_2), 29.52 (CH_2), 29.6 (CH_2), 29.79 (CH_2), 29.82 (CH_2), 29.9 (4 × CH_2), 32.1 (CH_2), 36.6 (CH_2), 37.3 (CH_2), 53.1 (CH), 77.7 (CH), 83.4 (C), 121.3

(C), 129.5 (2 × CH), 132.5 (2 × CH), 136.7 (C), 174.1 (2 × C); *m/z* (ESI) 426.3016 ([M−H]$^-$. $C_{27}H_{40}NO_3$ requires 426.3014).

(2*S*)-2-(*N*-Palmitoylamino)-3-[4'-(4'',4''-difluoro-6''-ethynyl-8''-phenyl-1'',3'',5'',7''-tetramethyl-4''-bora-*3''a*,*4''a*-diaza-*s*-indacene))pheny]propanoic acid (194)

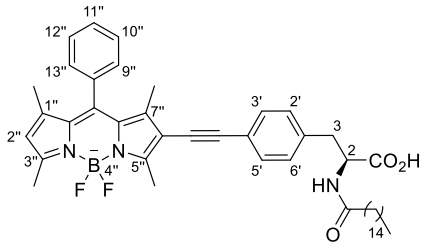

(2*S*)-2-(*N*-Palmitoylamino)-3-[4'-(4'',4''-difluoro-6''-ethynyl-8''-phenyl-1'',3'',5'',7''-tetramethyl-4''-bora-*3''a*,*4''a*-diaza-*s*-indacene))pheny]propanoic acid 194**X**) was synthesised as described for methyl (2*S*)-2-(*tert*-butoxycarbonylamino)-3-[4'-(methyl 6''-ethylnyl-2''-naphthoate)phenyl]propanoic acid **(184b)** using (2*S*)-2-(*N*-palmitoylamino)-3-(4'-ethynylphenyl)propanoic acid (**196**) (0.110 g, 0.258 mmol), 4,4-difluoro-8-phenyl-1,3,5,7-tetramethyl-4-bora-*3a*,*4a*-diaza-*s*-indacene **(191)** (0.151 g, 0.335 mmol), copper iodide (0.00980 g, 0.0515 mmol), bis(triphenylphosphine)palladium(II) dichloride (0.0180 g, 0.0256 mmol) in dry *N,N'*-dimethylformamide (4.7 mL) and triethylamine (11 mL). The reaction mixture was concentrated *in vacuo*, diluted in water (50 mL) and extracted with ethyl acetate (3 × 50 mL). The combined organic layers were washed with brine (20 mL), dried ($MgSO_4$), filtered and concentrated *in vacuo*. Purification by flash column chromatography eluting with 0–10% methanol in dichloromethane gave (2*S*)-2-(*N*-palmitoylamino)-3-[4'-(4'',4''-difluoro-6''-ethynyl-8''-phenyl-1'',3'',5'',7''-tetramethyl-4''-bora-*3''a*,*4''a*-diaza-*s*-indacene))pheny]propanoic acid (**194**) as a deep purple solid (0.121 g, 63%). Mp 133–135 °C; ν_{max}/cm^{-1} (neat) 3230 (NH), 2921 (CH), 2851 (CH), 1739 (C=O), 1537, 1513, 1402, 1316, 1275, 1191, 1163, 1061, 982, 721; $[\alpha]_D^{19}$ +34.9 (*c* 0.05, MeOH); δ_H (400 MHz, DMSO-d_6) 0.82 (3H, t, *J* 6.8 Hz, CH_3), 0.92–1.05 (2H, m, CH_2), 1.08–1.31 (24H, m, 12 × CH_2), 1.37 (3H, s, CH_3), 1.43 (3H, s, CH_3), 1.88–2.06 (2H, m, CH_2), 2.50 (3H, s, CH_3), 2.56 (3H, s, CH_3), 2.83 (1H, dd, *J* 13.8, 9.2 Hz, 3-*H*H), 3.10 (1H, dd, *J* 13.8, 4.4 Hz, 3-H*H*), 4.34 (1H, br s, 2-H), 6.30 (1H, s, 2''-H), 7.20 (2H, d, *J* 7.8 Hz, 2'-H and 6'-H), 7.32 (2H, d, *J*

7.8 Hz, 3'-H and 5'-H), 7.36–7.42 (2H, m, 9''-H and 13''-H), 7.55–7.63 (3H, m, 10''-H, 11''-H and 12''-H), 7.75 (1H, br s, 2-NH); δ_C (101 MHz, DMSO-d_6) 12.7 (CH_3), 13.2 (CH_3), 14.0 (CH_3), 14.2 (CH_3), 14.5 (CH_3), 22.1 (CH_2), 25.4 (CH_2), 28.5 (CH_2), 28.8 (CH_2), 29.0 (CH_2), 29.06 (CH_2), 29.08 (CH_2), 29.13 (CH_2), 29.16 (CH_2), 29.19 (2 × CH_2), 29.22 (CH_2), 31.3 (CH_2), 35.4 (CH_2), 37.1 (CH_2), 53.8 (CH), 81.1 (C), 96.0 (C), 114.3 (C), 120.3 (C), 122.7 (CH), 127.7 (2 × CH), 129.4 (2 × CH and C), 129.5 (C), 129.6 (3 × CH), 130.6 (2 × CH), 132.1 (C), 133.7 (C), 139.2 (C), 141.2 (C), 142.3 (C), 145.0 (C), 154.6 (C), 158.2 (C), 171.7 (C); *m/z* (QTOF) 748.4463 ($[M-H]^-$. $C_{46}H_{57}BF_2N_3O_3$ requires 748.4474).

3.4.4 Dipeptide synthesis, late-stage Sonogashira cross-coupling and click chemistry reactions.

(2*S*)-2-(*tert*-Butoxycarbonylamino)-3-(4'-ethynylphenyl)-1-propanamide-L-alanine *tert*-butyl ester (183)

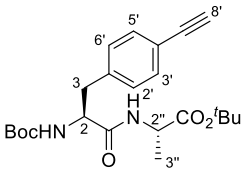

To a stirred solution of (2*S*)-2-(*tert*-butoxycarbonylamino)-3-(4'-ethynylphenyl)propanoic acid (**182**) (0.200 g, 0.691 mmol) in acetonitrile (16 mL) was added L-alanine *tert*-butyl ester hydrochloride (0.138 g, 0.760 mmol) and 1-hydroxybenzotriazole hydrate (0.0470 g, 0.346 mmol). The reaction mixture was stirred at 0 °C for 5 minutes prior to the addition of *N,N*-diisopropylethylamine (0.360 mL, 2.07 mmol) and PyBOP® (0.539 g, 1.04 mmol). After 0.5 h, the reaction mixture was warmed to room temperature and allowed to stir overnight. Following concentration *in vacuo*, the reaction mixture was diluted in ethyl acetate (50 mL), washed with 1 M hydrochloric acid (50 mL) and brine (50 mL). The organic layer was dried ($MgSO_4$), filtered and concentrated *in vacuo*. Purification by flash column chromatography eluting with 1% methanol in chloroform gave (2*S*)-2-(*tert*-butoxycarbonylamino)-3-(4'-ethynylphenyl)-1-propanamide-L-alanine *tert*-butyl ester (**183**) as a white solid (0.225 g, 78%). Mp 102–104 °C; ν_{max}/cm^{-1} (neat) 3346

(NH), 3261 (NH), 2977 (CH), 1736 (C=O), 1672, 1649, 1554, 1509, 1452, 1365, 1321, 1284, 1248, 1153, 1105, 1045, 854; $[\alpha]_D^{21}$ +21.0 (*c* 0.1, $CHCl_3$); δ_H (400 MHz, $CDCl_3$) 1.31 (3H, d, *J* 7.2 Hz, 3''-H_3), 1.38 (9H, s, 3 × CH_3), 1.43 (9H, s, 3 × CH_3), 2.95–3.10 (3H, m, 3-H_2 and 8'-H), 4.27–4.43 (2H, m, 2-H and 2''-H), 5.07 (1H, d, *J* 8.4 Hz, 2-NH), 6.54 (1H, d, *J* 7.2 Hz, 2''-NH), 7.15 (2H, d, *J* 8.2 Hz, 2'-H and 6'-H), 7.39 (2H, d, *J* 8.2 Hz, 3'-H and 5'-H); δ_C (101 MHz, $CDCl_3$) 18.7 (CH_3), 28.0 (3 × CH_3), 28.3 (3 × CH_3), 38.5 (CH_2), 48.8 (CH), 55.5 (CH), 77.3 (CH), 80.3 (C), 82.2 (C), 83.5 (C), 120.8 (C), 129.5 (2 × CH), 132.4 (2 × CH), 137.7 (C), 155.4 (C), 170.4 (C), 171.7 (C); *m/z* (ESI) 439.2200 (MNa^+. $C_{23}H_{32}N_2O_5Na$ requires 439.2203).

(2*S*)-2-(*tert*-Butoxycarbonylamino)-3-(4'-(methyl 1''*H*-1'',2'',3''-triazol-1''-ylacetate)phenyl)-1-propanamide-L-alanine *tert*-butyl ester (201)

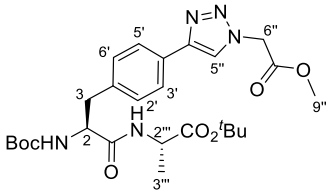

To a stirred solution of (2*S*)-2-(*tert*-butoxycarbonylamino)-3-(4'-ethynylphenyl)-1-propanamide-L-alanine *tert*-butyl ester (**183**) (50.0 mg, 0.120 mmol) and methyl azidoacetate (11.7 μL, 0.120 mmol) in dichloromethane (2.2 mL) and water (2.2 mL) was added copper(II) sulfate pentahydrate (6.00 mg, 0.0240 mmol) followed by sodium ascorbate (9.50 mg, 0.0480 mmol). The reaction mixture was stirred at room temperature for 15 h then diluted in water (20 mL) and extracted with dichloromethane (3 × 20 mL). The organic layer was subsequently washed with brine (20 mL), dried ($MgSO_4$), filtered and concentrated *in vacuo*. Purification by flash column chromatography eluting with 50% ethyl acetate in hexane gave (2*S*)-2-(*tert*-butoxycarbonylamino)-3-(4'-(methyl 1''*H*-1'',2'',3''-triazol-1''-ylacetate)phenyl)-1-propanamide-L-alanine *tert*-butyl ester (**201**) (52.6 mg, 83%) as a white solid. Mp 72–74 °C; ν_{max}/cm^{-1} (neat) 3288 (NH), 2980, 2916 (CH), 2849, 1738 (C=O), 1654, 1533, 1456, 1366, 1217, 1149, 1047, 1021, 845; $[\alpha]_D^{18}$ +47.9 (*c* 0.1, $CHCl_3$); δ_H (400 MHz, $CDCl_3$) 1.32 (3H, d, *J* 6.8 Hz, 3'''-H_3), 1.41 (9H, s, 3 × CH_3), 1.42 (9H, s, 3 × CH_3), 3.10 (2H, d, *J* 6.4 Hz, 3-H_2), 3.82 (3H, s, 9''-H_3), 4.30–4.45 (2H, m, 2-H and 2'''-H), 4.91–5.08 (1H, m, 2-NH), 5.22 (2H, s, 6''-H_2), 6.50 (1H, d, *J* 7.2 Hz, 2'''-

NH), 7.27 (2H, d, *J* 8.4 Hz, 2'-H and 6'-H), 7.77 (2H, d, *J* 8.4 Hz, 3'-H and 5'-H), 7.88 (1H, s, 5''-H); δ_C (101 MHz, $CDCl_3$) 18.7 (CH_3), 28.0 (3 × CH_3), 28.4 (3 × CH_3), 38.3 (CH_2), 48.9 (CH), 50.9 (CH_2), 53.2 (CH_3), 55.6 (CH), 80.4 (C), 82.2 (C), 120.9 (CH), 126.2 (2 × CH), 129.2 (C), 130.1 (2 × CH), 136.9 (C), 148.2 (C), 155.5 (C), 166.8 (C), 170.5 (C), 171.8 (C); *m/z* (ESI) 554.2600 (MNa^+. $C_{26}H_{37}N_5O_7Na$ requires 554.2585).

(2*S*)-2-(*tert*-Butoxycarbonylamino)-3-(4'-(1''-benzyl-1''*H*-1'',2'',3''-triazole)phenyl)-1-propanamide-L-alanine *tert*-butyl ester (202)

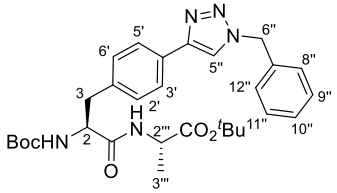

To a stirred solution of (2*S*)-2-(*tert*-butoxycarbonylamino)-3-(4'-ethynylphenyl)-1-propanamide-L-alanine *tert*-butyl ester (**183**) (27.0 mg, 0.0648 mmol) and benzyl azide (8.1 μL) in dichloromethane (125 μL) and water (125 μL) was added copper sulfate pentahydrate (3.20 mg, 0.0130 mol) followed by sodium ascorbate (5.10 mg, 0.0259 mmol). The reaction mixture was stirred at room temperature for 15 h then diluted in water (20 mL) and extracted with dichloromethane (3 × 20 mL). The organic layer was subsequently washed with brine (20 mL), dried ($MgSO_4$), filtered and concentrated *in vacuo* to give (2*S*)-2-(*tert*-butoxycarbonylamino)-3-(4'-(1''-benzyl-1''*H*-1'',2'',3''-triazole)phenyl)-1-propanamide-L-alanine *tert*-butyl ester (**202**) (37.0 mg, 100%) as a white solid. Mp 93–95 °C; ν_{max}/cm^{-1} (neat) 3358 (NH), 2981 (CH), 2362, 1735 (C=O), 1685, 1658 (C=O), 1508, 1456, 1366, 1226, 1149, 1049, 1024, 720; $[\alpha]_D^{19}$ +50.2 (*c* 0.1, $CHCl_3$); δ_H (400 MHz, $CDCl_3$) 1.31 (3H, d, *J* 7.2 Hz, 3'''-H_3), 1.39 (9H, s, 3 × CH_3), 3.00–3.14 (2H, m, 3-H_2), 4.28–4.44 (2H, m, 2-H and 2'''-H), 4.94–5.10 (1H, m, 2-NH), 5.56 (2H, s, 6''-H_2), 6.51 (1H, d, *J* 7.2 Hz, 2'''-NH), 7.23 (2H, d, *J* 7.8 Hz, 2'-H and 6'-H), 7.26–7.43 (5H, m, 5 × ArH), 7.64 (1H, s, 5''-H), 7.71 (2H, d, *J* 7.8 Hz, 3'-H and 5'-H); δ_C (101 MHz, $CDCl_3$) 18.7 (CH_3), 28.0 (3 × CH_3), 28.4 (3 × CH_3), 38.3 (CH_2), 48.9 (CH), 54.3 (CH_2), 55.6 (CH), 80.3 (C), 82.1 (C), 119.5 (CH), 126.0 (2 × CH), 128.2 (2 × CH), 128.9 (CH), 129.3

(2 × CH), 129.4 (C), 130.0 (2 × CH), 134.8 (C), 136.7 (C), 148.1 (C), 155.4 (C), 170.6 (C), 171.7 (C); *m/z* (ESI) 572.2856 (MNa^+. $C_{30}H_{39}N_5O_5Na$ requires 572.2843).

Fluorescein 5-(*N*-3-azidopropyl)thiourea (204)

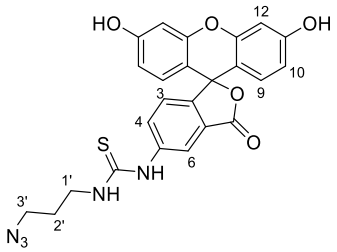

In an oven-dried flask, fluorescein 5-isothiocyanate (0.100 g, 0.257 mmol) was dissolved in dry *N,N'*-dimethylformamide (8 mL) under argon. To this was added *N,N*-diisopropylethylamine (0.100 mL, 0.574 mmol) and 3-azidopropylamine (39.0 μL, 0.286 mmol). The reaction was shielded from light and stirred at room temperature for 40 h. The reaction mixture was concentrated *in vacuo*, diluted in ethyl acetate (30 mL) and washed with water (10 mL) and brine (10 mL). The organic layer was dried ($MgSO_4$), filtered and concentrated *in vacuo*. Purification by flash column chromatography eluting with dichloromethane followed by 10% methanol in dichloromethane gave fluorescein 5-(*N*-3-azidopropyl)thiourea (**204**) (68.0 mg, 52%) as an orange solid. Mp 104–107 °C; ν_{max}/cm^{-1} (neat) 2926 (CH), 2095, 1736 (C=O), 1580, 1534, 1455, 1294, 1264, 1210, 1171, 1156, 850; δ_H (400 MHz, CD_3OD) 1.92 (2H, quin, *J* 6.8 Hz, 2'-H_2), 3.42 (2H, t, *J* 6.8 Hz, 1'-H_2), 3.70 (2H, t, *J* 6.8 Hz, 3'-H_2), 6.54 (2H, dd, *J* 8.8, 2.4 Hz, 10-H), 6.67 (2H, d, *J* 2.4 Hz, 12-H), 6.69 (2H, d, *J* 8.6 Hz, 9-H), 7.15 (1H, d, *J* 8.4 Hz, 3-H), 7.74 (1H, dd, *J* 8.4, 2.0 Hz, 4-H), 8.12 (1H, d, *J* 2.0 Hz 6-H); δ_C (101 MHz, CD_3OD) 29.3 (CH_2), 43.1 (CH_2), 50.3 (CH_2), 103.5 (2 × CH), 111.6 (C), 113.8 (2 × CH), 120.3 (CH), 125.8 (CH), 129.3 (C), 130.4 (2 × CH), 131.9 (CH), 142.3 (C), 149.3 (C), 154.3 (2 × C), 161.8 (C), 171.2 (C), 183.0 (C); *m/z* (QTOF) 490.1181 (MH^+. $C_{24}H_{20}N_5O_5S$ requires 489.1107).

_N_-(3'-Azidopropyl)-5-(dimethylamino)naphthalene-1-sulfonamide (206)[296]

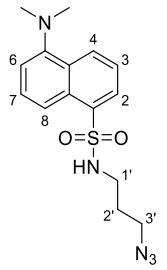

To a stirred solution of 3-azidopropylamine (145 μL, 1.48 mmol) and triethylamine (62.0 μL, 0.444 mmol) in dichloromethane (0.35 mL) was added a solution of dansyl chloride (0.102 g, 0.378 mmol) in dichloromethane (2.8 mL). The reaction mixture was stirred at room temperature for 17 h then concentrated *in vacuo*. Purification by flash column chromatography eluting with dichloromethane followed by 5% methanol in dichloromethane gave *N*-(3'-azidopropyl)-5-(dimethylamino)naphthalene-1-sulfonamide (**206**) (0.132 mg, 98%) as a yellow oil. NMR data were consistent with the literature.[296] δ_H (400 MHz, $CDCl_3$) 1.64 (2H, quint, *J* 6.4 Hz, 2'-H_2), 2.89 (6H, s, 2 × CH_3), 2.98 (2H, q, *J* 6.4 Hz, 1'-H_2), 3.24 (2H, t, *J* 6.4 Hz, 3'-H_2), 5.10 (1H, t, *J* 6.4 Hz, NH), 7.19 (1H, d, *J* 7.4 Hz, 6-H), 7.53 (1H, dd, *J* 8.6, 7.4 Hz, 7-H), 7.56 (1H, dd, *J* 8.8, 7.6 Hz, 3-H), 8.25 (1H, dd, *J* 7.6, 1.6 Hz, 4-H), 8.29 (1H, d, *J* 8.8 Hz, 8.6 Hz, 8-H), 8.55 (1H, d, *J* 8.8 Hz, 2-H); δ_C (101 MHz, $CDCl_3$) 28.9 (CH_2), 40.9 (CH_2), 45.5 (2 × CH_3), 48.8 (CH_2), 115.4 (CH), 118.6 (CH), 123.3 (CH), 128.6 (CH), 129.6 (C), 129.9 (CH), 130.0 (C), 130.8 (CH), 134.5 (C), 152.2 (C); *m/z* (QTOF) 334 (MH^+. 100%).

(2*S*)-2-(*tert*-Butoxycarbonylamino)-3-[4'-(1"*H*-1",2",3"-triazol-1"-{*N*-propyl-16"-(dimethylamino)naphthalene-11"-sulfonamide]pheny}-1-propanamide-L-alanine *tert*-butyl ester (207)

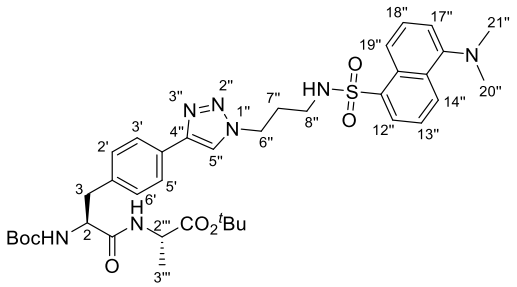

To a stirred solution of (2*S*)-2-(*tert*-butoxycarbonylamino)-3-(4'-ethynylphenyl)-1-propanamide-L-alanine *tert*-butyl ester (**183**) (45.5 mg, 0.109 mmol) and *N*-(3'-azidopropyl)-5-(dimethylamino)naphthalene-1-sulfonamide (**206**) (36.4 mg, 0.109 mmol) in dichloromethane (250 μL) and water (250 μL) was added copper sulfate pentahydrate (5.40 mg, 0.0218 mmol) followed by sodium ascorbate (8.6 mg, 0.0436 mmol). The reaction mixture was stirred at room temperature for 15 h then diluted in water (20 mL) and extracted with dichloromethane (3 × 20 mL). The organic layer was subsequently washed with brine (20 mL), dried ($MgSO_4$), filtered and concentrated *in vacuo*. Purification by flash column chromatography eluting with 60–70% ethyl acetate in hexane afforded 2*S*)-2-(*tert*-butoxycarbonylamino)-3-[4'-(1"*H*-1",2",3"-triazol-1"-{*N*-propyl-16"-(dimethylamino)naphthalene-11"-sulfonamide}phenyl]-1-propanamide-L-alanine *tert*-butyl ester (**207**) (70.0 mg, 85%) as a green solid. Mp 105–107 °C; ν_{max}/cm^{-1} (neat) 3278 (NH), 2979 (CH), 2935 (CH), 1655 (C=O), 1452, 1392, 1365, 1311, 1228, 1142, 789; $[\alpha]_D^{19}$ +10.0 (*c* 0.1, $CHCl_3$); δ_H (400 MHz, CD_3OD) 1.26–1.39 (12H, m, 3 × CH_3, and 3"'-H_3),1.44 (9H, s, 3 × CH_3), 1.97 (2H, quin, *J* 6.8 Hz, 7"-H_2), 2.76–2.89 (9H, m, 3-*H*H, 8"-H_2, 20"-H_3 and 21"-H_3), 3.18 (1H, dd, *J* 14.0, 4.8 Hz, 3-H*H*), 4.23–4.43 (4H, m, 2-H, 6"-H_2 and 2"'-H), 7.23 (1H, d, *J* 7.6 Hz, 17"-H), 7.34 (2H, d, *J* 8.0 Hz, 2'-H and 6'-H), 7.48 (1H, dd, *J* 8.4, 7.2 Hz, 13"-H), 7.57 (1H, dd, *J* 8.6, 7.6 Hz, 18"-H), 7.66 (2H, d, *J* 8.0 Hz, 3'-H and 5'-H), 7.91 (1H, s, 5"-H), 8.14 (1H, dd, *J* 7.2, 1.2 Hz, 14"-H), 8.35 (1H, d, *J* 8.6 Hz, 19"-H), 8.50 (1H, d, *J* 8.4 Hz, 12"-H); δ_C (101 MHz, CD_3OD) 17.7 (CH_3), 28.2 (3 × CH_3), 28.7 (3 × CH_3), 31.2 (CH_2), 39.1 (CH_2), 40.7 (CH_2), 45.8 (2 × CH_3), 48.4 (CH_2), 50.2 (CH), 56.9 (CH), 80.6 (C), 82.7 (C), 116.4

(CH), 120.3 (CH), 122.2 (CH), 124.3 (CH), 126.7 (2 × CH), 129.3 (CH), 130.0 (C), 130.4 (CH), 130.8 (C), 131.0 (2 × CH), 131.1 (C), 131.3 (CH), 136.6 (C), 139.0 (C), 148.5 (C), 153.3 (C), 157.6 (C), 173.2 (C), 173.9 (C); *m/z* (QTOF) 772.3454 (MNa^+. $C_{38}H_{51}N_7O_7SNa$ requires 772.3463).

N-(3'-Azidopropyl)-5-((*3aS*,*4S*,*6aR*)-2-oxohexahydro-1*H*-thieno[3,4-*d*]imidazol-4-yl)pentanamide (209)[297]

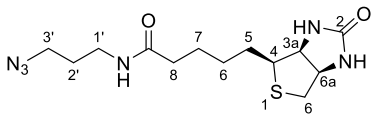

In an oven-dried flask under argon, D-biotin (0.200 g, 0.819 mmol) was suspended in dry *N,N'*-dimethylformamide (5 mL) in a sealed tube and heated to 55 °C. After cooling to room temperature, a solution of carbonyldiimidazole (0.207 g, 1.64 mmol) in *N,N'*-dimethylformamide (3 mL) was added dropwise and the reaction mixture stirred for 3 h. 1-Azido-3-aminopropylamine (161 μL, 1.64 mmol) was added and the reaction mixture stirred at room temperature for 15 h. The reaction mixture was concentrated *in vacuo* and purified by recrystallisation in a mixture of 1-butanol/acetic acid/ water (70:7:10) to give *N*-(3'-azidopropyl)-5-((*3aS*,*4S*,*6aR*)-2-oxohexahydro-1*H*-thieno[3,4-*d*]imidazol-4-yl)pentanamide (**209**) (0.055 g, 21%). The remaining crude material was re-purified by recrystallisation followed by flash column chromatography eluting with 10% methanol in dichloromethane to give *N*-(3-azidopropyl)-5-((*3aS*,*4S*,*6aR*)-2-oxohexahydro-1*H*-thieno[3,4-d]imidazol-4-yl)pentanamide (**209**) (0.064 g, 24%) as a white solid. Mp 148–150 °C; NMR data were consistent with the literature.[296] δ_H (400 MHz, CD_3OD) 1.39–1.49 (2H, m, CH_2), 1.76 (2H, t, *J* 6.8 Hz, 2'-H_2), 1.54–1.80 (4H, m, 2 × CH_2), 2.21 (2H, t, *J* 6.8 Hz, 8-H_2), 2.71 (1H, d, *J* 12.6 Hz, 6-*H*H), 2.93 (1H, dd, *J* 12.6, 4.6 Hz, 6-H*H*), 3.17–3.22 (1H, m, 4-H), 3.25 (2H, t, *J* 6.8 Hz, 1'-H_2), 3.36 (2H, t, *J* 6.8 Hz, 3'-H_2), 4.30 (1H, dd, *J* 7.6, 4.4 Hz, 3a-H), 4.49 (1H, dd, *J* 7.6, 4.6 Hz, 6a-H); δ_C (101 MHz, CD_3OD) 26.8 (CH_2), 29.5 (CH_2), 29.7 (CH_2), 29.8 (CH_2), 36.8 (CH_2), 37.7 (CH_2), 41.0 (CH_2), 50.1 (CH_2), 57.0 (CH), 61.6 (CH), 63.4 (CH), 166.1 (C), 176.2 (C); *m/z* (QTOF) 325 ($[M-H]^-$. 100%).

(2*S*)-2-(*tert*-Butoxycarbonylamino)-3-[4'-(1"*H*-[1''2"3'']triazol-1"-{*N*-propyl-14"-((*16"aS*,*15"S*,*20"aR*)-18"-oxohexahydro-1*H*-thieno[15",16''-d]imidazol-15"-yl)pentanamide})phenyl]-1-propanamide-L-alanine *tert*-butyl ester (210)

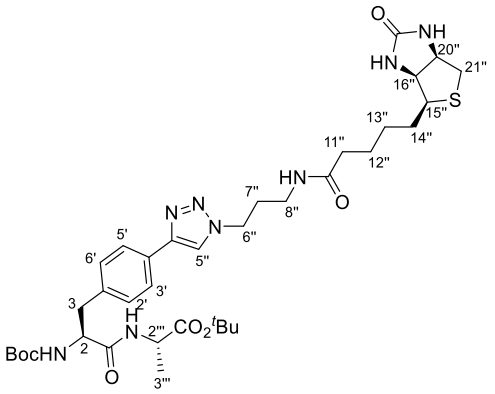

To a stirred solution of (2*S*)-2-(*tert*-butoxycarbonylamino)-3-(4'-ethynylphenyl)-1-propanamide-L-alanine *tert*-butyl ester (**183**) (70.0 mg, 0.168 mmol) and *N*-(3'-azidopropyl)-5-((*3aS*,*4S*,*6aR*)-2-oxohexahydro-1*H*-thieno[3,4-d]imidazol-4-yl)pentanamide (**209**) (55.0 mg, 0.168) in *tert*-butanol (1 mL), dichloromethane (1.5 mL) and water (1.5 mL) was added copper sulfate pentahydrate (8.30 mg, 0.0336 mmol) followed by sodium ascorbate (13.3 mg, 0.0672 mmol). The reaction mixture was stirred at room temperature for 19 h, diluted in water (50 mL) and extracted with dichloromethane (2 × 50 mL). The combined organic layers were washed with brine (30 mL), dried ($MgSO_4$), filtered and concentrated *in vacuo*. Purification by flash column chromatography eluting with 5–10% methanol in dichloromethane gave (2*S*)-2-(*tert*-butoxycarbonylamino)-3-[4'-(1''*H*-[1"2"3"]triazol-1"-{*N*-propyl-14"-((*16"aS*,*15"S*,*20"aR*)-18"-oxohexahydro-1*H*-thieno[15",16"-d]imidazol-15''-yl)pentanamide})phenyl]-1-propanamide-L-alanine *tert*-butyl ester (**210**) (107 mg, 86%) as a white solid. Mp 130–134 °C; ν_{max}/cm^{-1} (neat) 3342 (NH), 2931 (CH), 1691 (C=O), 1645 (C=O), 1450, 1367, 1244, 1147, 1047, 846; $[\alpha]_D^{18}$ +15.0 (*c* 0.1, MeOH); δ_H (400 MHz, CD_3OD) 1.24–1.48 (23H, m, 3'''-H_3, 13"-H_2, 18 × CH_3), 1.51–1.77 (4H, m, 12"-H_2 and 14"-H_2), 2.10–2.23 (4H, m, 7"-H_2 and 11"-H_2), 2.69 (1H, d, *J* 12.8 Hz, 21"-*H*H), 2.85 (1H, dd, *J* 14.0, 9.6 Hz, 3-*H*H), 2.90 (1H, dd, *J* 12.8, 4.8 Hz, 21"-H*H*), 3.12–3.22 (2H, m, 3-H*H* and 15"-H), 3.26 (2H, t, *J* 6.4 Hz, 8"-H_2), 4.25–4.32 (2H, m, 2-H and 16"-H), 4.38 (1H, dd, *J* 9.6, 4.8 Hz, 2'''-H), 4.44–4.51 (3H, m, 6"-H_2 and 20"-H), 7.35 (2H, d, *J* 7.8 Hz, 2'-H and 6'-H), 7.74 (2H, d, *J* 7.8 Hz, 3'-H and 5'-H), 8.32 (1H, s, 5"-

H); δ_C (101 MHz, CD_3OD) 17.7 (CH_3), 26.8 (CH_2), 28.2 (3 × CH_3), 28.7 (3 × CH_3), 29.5 (CH_2), 29.8 (CH_2), 31.1 (CH_2), 36.8 (CH_2), 37.5 (CH_2), 39.1 (CH_2), 41.0 (CH_2), 50.2 (CH), 56.9 (CH), 57.0 (CH), 61.6 (CH), 63.3 (CH), 80.6 (C), 82.7 (C), 122.3 (CH), 126.6 (2 × CH), 130.1 (C), 131.1 (2 × CH), 139.0 (C), 148.7 (C), 157.6 (C), 166.1 (C), 173.2 (C), 174.0 (C), 176.2 (C); *m/z* (QTOF) 765.3723 (MNa^+. $C_{36}H_{54}N_8O_7SNa$ requires 765.3728).

(2*S*)-2-(*tert*-Butoxycarbonylamino)-3-(4'-ethynylphenyl)-1-propanamide-L-phenylalanine methyl ester (211)

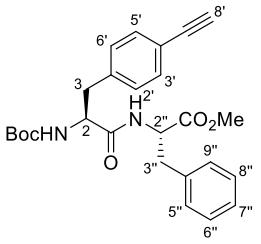

(2*S*)-2-(*tert*-Butoxycarbonylamino)-3-(4'-ethynylphenyl)-1-propanamide-L-phenylalanine methyl ester (**211**) was synthesised as described for (2*S*)-2-(*tert*-butoxycarbonylamino)-3-(4'-ethynylphenyl)-1-propanamide-L-alanine *tert*-butyl ester (**183**) using (2*S*)-2-(*tert*-butoxycarbonylamino)-3-(4'-ethynylphenyl)propanoic acid (**182**) (0.200 g, 0.691 mmol), L-phenylalanine methyl ester hydrochloride (0.164 g, 0.760 mmol), 1-hydroxybenzotriazole hydrate (0.0470 g, 0.346 mmol), *N,N*-diisopropylethylamine (0.360 mL, 2.07 mmol) and PyBOP® (0.539 g, 1.04 mmol) in acetonitrile (16 mL). Purification by flash column chromatography eluting with 30% ethyl acetate in hexane gave (2*S*)-2-(*tert*-butoxycarbonylamino)-3-(4'-ethynylphenyl)-1-propanamide-L-phenylalanine methyl ester (**211**) as a white solid (0.267 g, 86%). Mp 139–142 °C; ν_{max}/cm^{-1} (neat) 3332 (NH), 3303 (NH), 2974 (CH), 1736 (C=O), 1662 (C=O), 1541, 1516, 1367, 1296, 1247, 1163, 1041, 1009; $[\alpha]_D^{21}$ +45.8 (*c* 0.1, $CHCl_3$); δ_H (400 MHz, $CDCl_3$) 1.40 (9H, s, 3 × CH_3), 2.93–3.11 (5H, m, 3-H_2, 8'-H and 3''-H_2), 3.67 (3H, s, OCH_3), 4.24–4.38 (1H, m, 2-H), 4.70–4.82 (1H, m, 2''-H), 4.98 (1H, d, *J* 8.0 Hz, 2-NH), 6.29 (1H, d, *J* 7.6 Hz, 2''-NH), 6.96–7.02 (2H, m, 5''-H and 9''-H), 7.13 (2H, d, *J* 8.0 Hz, 2'-H and 6'-H), 7.20–7.25 (3H, m, 6''-H, 7''-H and 8''-H), 7.39 (2H, d, *J* 8.0 Hz, 3'-H and 5'-H); δ_C (101 MHz, $CDCl_3$) 28.3 (3 × CH_3), 38.0 (CH_2), 38.3 (CH_2), 52.5 (CH_3), 53.4 (CH), 55.6 (CH), 77.4 (CH), 80.4 (C), 83.5 (C), 120.9 (C), 127.3 (CH), 128.7 (2 × CH), 129.3 (2 ×

CH), 129.5 (2 × CH), 132.5 (2 × CH), 135.6 (C), 137.6 (C), 155.3 (C), 170.6 (C), 171.4 (C); *m/z* (ESI) 473.2040 (MNa^+. $C_{26}H_{30}N_2O_5Na$ requires 473.2047).

(2*S*)-2-(*tert*-Butoxycarbonylamino)-3-(4'-ethynylphenyl)-1-propanamide dibenzyl-L-aspartate (212)

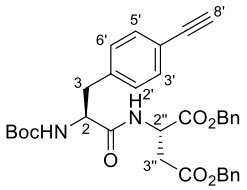

(2*S*)-2-(*tert*-butoxycarbonylamino)-3-(4'-ethynylphenyl)-1-propanamide dibenzyl-L-aspartate (**212**) was synthesised as described for (2*S*)-2-(*tert*-butoxycarbonylamino)-3-(4'-ethynylphenyl)-1-propanamide-L-alanine *tert*-butyl ester (**183**) using (2*S*)-2-(*tert*-butoxycarbonylamino)-3-(4'-ethynylphenyl)propanoic acid (**182**) (0.200 g, 0.691 mmol), L-aspartic acid dibenzyl ester *p*-toluenesulfonate (0.369 g, 0.760 mmol), 1-hydroxybenzotriazole hydrate (0.0470 g, 0.346 mmol), *N,N*-diisopropylethylamine (0.360 mL, 2.07 mmol) and PyBOP® (0.539 g, 1.04 mmol) in acetonitrile (16 mL). Purification by flash column chromatography eluting with 30% ethyl acetate in hexane gave (2*S*)-2-(*tert*-butoxycarbonylamino)-3-(4'-ethynylphenyl)-1-propanamide dibenzyl-L-aspartate (**212**) as a white solid (0.314 g, 78%). Mp 100–102 °C; ν_{max}/cm (neat) 3319 (NH), 2972 (CH), 1730 (C=O), 1685, 1655, 1545, 1520, 1389, 1333, 1303, 1163, 1109, 1047, 984; $[\alpha]_D^{21}$ +13.6 (*c* 0.1, $CHCl_3$); δ_H (400 MHz, $CDCl_3$) 1.39 (3 × CH_3), 2.88 (1H, dd, *J* 17.2, 4.4 Hz, 3''-*H*H), 2.96 (1H, dd, *J* 14.4, 7.2 Hz, 3-*H*H), 3.01–3.10 (3H, m, 3-H*H*, 8'-H and 3''-H*H*), 4.31–4.41 (1H, m, 2-H), 4.83 (1H, dt, *J* 8.0, 4.4 Hz, 2''-H), 4.86–4.95 (1H, m, 2-NH), 5.01 (1H, d, *J* 12.4 Hz, C*H*HPh), 5.06 (1H, d, *J* 12.0 Hz, CH*H*Ph), 5.12 (2H, s, CH_2Ph), 6.90 (1H, d, *J* 8.0 Hz, 2''-NH), 7.11 (2H, d, *J* 8.4 Hz, 2'-H and 6'-H), 7.24–7.40 (12H, m, 12 × Ar-H); δ_C (101 MHz, $CDCl_3$) 28.3 (3 × CH_3), 36.3 (CH_2), 38.2 (CH_2), 48.9 (CH), 55.3 (CH), 67.0 (CH_2), 67.8 (CH_2), 77.4 (CH), 80.4 (C), 83.6 (C), 120.8 (C), 128.50 (2 × CH), 128.54 (2 × CH), 128.6 (CH), 128.65 (CH), 128.73 (2 × CH), 128.75 (2 × CH), 129.5 (2 × CH), 132.4 (2 × CH), 135.1 (C), 135.4 (C), 137.4 (C), 155.3 (C), 170.1 (C), 170.6 (C), 170.9 (C); *m/z* (ESI) 623.2149 (MK^+. $C_{34}H_{36}N_2O_7K$ requires 623.2154).

(2*S*)-2-(*tert*-Butoxycarbonylamino)-3-(4'-(4"-cyanophenylethynyl)phenyl)-1-propanamide-L-alanine *tert*-butyl ester (213)

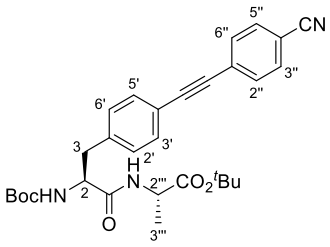

In an oven-dried flask under argon, a solution of (2*S*)-2-(*tert*-butoxycarbonylamino)-3-(4'-ethynylphenyl)-1-propanamide-L-alanine *tert*-butyl ester (**183**) (0.0829 g, 0.216 mmol), 4-iodobenzonitrile (0.0646 g, 0.281 mmol), bis(triphenylphosphine)palladium(II) dichloride (0.00760 g, 0.0108 mmol), copper iodide (0.00410 g, 0.0215 mmol) in dry *N,N'*-dimethylformamide (5 mL) and anhydrous triethylamine (12 mL) was degassed for 0.33 h. The reaction mixture was heated to 90 °C for 0.5 h then allowed to slowly cool to room temperature and stirred for a further 3 h. Additional bis(triphenylphosphine)palladium(II) dichloride (0.00760 g, 0.0108 mmol) and copper iodide (0.00410 g, 0.0215 mmol) were added and the reaction mixture further degassed for 0.33 h prior to stirring at 90 °C for 0.5 h. The reaction mixture was slowly cooled to room temperature, stirred for 3.5 h then concentrated *in vacuo*. The reaction mixture was dissolved in ethyl acetate (50 mL) and washed in water (2 × 50 mL) and brine (2 × 50 mL). Purification by flash column chromatography eluting with 20% ethyl acetate in hexane gave (2*S*)-2-(*tert*-butoxycarbonylamino)-3-(4'-(4"-cyanophenylethynyl)phenyl)-1-propanamide-L-alanine *tert*-butyl ester (**213**) (0.0769 g, 88%) as a white solid. Mp 141–144 °C; ν_{max}/cm^{-1} (neat) 3340 (NH), 2983 (CH), 2212 (C≡C), 1726 (C=O), 1687 (C=O), 1655, 1516, 1367, 1304, 1252, 1157, 1049, 985, 839; $[\alpha]_D^{18}$ +45.0 (*c* 0.1, $CHCl_3$); δ_H (400 MHz, $CDCl_3$) 1.33 (3H, d, *J* 7.2 Hz, 3'''-H_3), 1.41 (9H, s, 3 × CH_3), 1.44 (9H, s, 3 × CH_3), 3.09 (2H, d, *J* 6.4 Hz, 3-H_2), 4.24–4.48 (2H, m, 2-H and 2'''-H), 5.04 (1H, d, *J* 8.4 Hz, 2-NH), 6.43 (1H, d, *J* 7.2 Hz, 2'''-NH), 7.22 (2H, d, *J* 8.2 Hz, 2'-H and 6'-H), 7.46 (2H, d, *J* 8.2 Hz, 3'-H and 5'-H), 7.57 (2H, d, *J* 8.8 Hz, 2"-H and 6"-H), 7.63 (2H, d, *J* 8.8 Hz, 3"-H and 5"-H); δ_C (101 MHz, $CDCl_3$) 18.8 (CH_3), 28.0 (3 × CH_3), 28.4 (3 × CH_3), 38.6 (CH_2), 48.9 (CH), 55.6 (CH), 80.4 (C), 82.3 (C), 87.9 (C), 93.8 (C), 111.5 (C), 118.7 (C), 121.0 (C), 128.4 (C), 129.7 (2 ×

CH), 132.12 (2 × CH), 132.14 (2 × CH), 132.2 (2 × CH), 138.1 (C), 155.4 (C), 170.3 (C), 171.7 (C); *m/z* (ESI) 540.2466 (MNa^+. $C_{30}H_{35}N_3O_5$ requires 540.2469).

(2*S*)-2-(*tert*-Butoxycarbonylamino)-3-(4'-(4''-cyanophenylethynyl)phenyl)-1-propanamide-L-phenylalanine methyl ester (214)

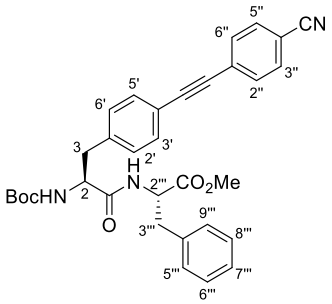

(2*S*)-2-(*tert*-Butoxycarbonylamino)-3-(4'-(4''-cyanophenylethynyl)phenyl)-1-propanamide-L-phenylalanine methyl ester (**214**) was synthesised as described for (2*S*)-2-(*tert*-butoxycarbonylamino)-3-(4'(4''-cyanophenylethynyl)phenyl)-1-propanamide-L-alanine *tert*-butyl ester (**213**) using (2*S*)-2-(*tert*-butoxycarbonylamino)-3-(4'-ethynylphenyl)-1-propanamide-L-phenylalanine methyl ester (**211**) (0.100 g, 0.222 mmol), 4-iodobenzonitrile (0.0659 g, 0.289 mmol), bis(triphenylphosphine)palladium(II) dichloride (0.0156 g, 0.0222 mmol) and copper iodide (0.00840 g, 0.0441 mmol) in dry *N,N'*-dimethylformamide (6 mL) and anhydrous triethylamine (14 mL). Purification by flash column chromatography eluting with 30% ethyl acetate in hexane afforded (2*S*)-2-(*tert*-butoxycarbonylamino)-3-(4'-(4''-cyanophenylethynyl)phenyl)-1-propanamide-L-phenylalanine methyl ester (**214**) (0.0832 g, 68%) as a white solid. Mp 167–169 °C; ν_{max}/cm^{-1} (neat) 3323 (NH), 2929 (CH), 2214 (C≡C), 1739 (C=O), 1687 (C=O), 1657, 1514, 1441, 1248, 1163, 1026, 839; $[\alpha]_D^{18}$ +32.0 (*c* 0.1, $CHCl_3$); δ_H (400 MHz, $CDCl_3$) 1.41 (9H, s, 3 × CH_3), 2.95–3.15 (4H, m, 3-H_2 and 3'''-H_2), 3.69 (3H, s, OCH_3), 4.28–4.41 (1H, m, 2-H) 4.71–4.83 (1H, m, 2'''-H), 4.90–5.02 (1H, m, 2-NH), 6.28 (1H, d, *J* 7.6 Hz, 2'''-NH), 6.98–7.04 (2H, m, 5'''-H and 9'''-H), 7.20 (2H, d, *J* 8.4 Hz, 2'-H and 6'-H), 7.22–7.29 (3H, m, 6'''-H, 7'''-H and 8'''-H), 7.45 (2H, d, *J* 8.4 Hz, 3'-H and 5'-H), 7.58 (2H, d, *J* 8.6 Hz, 2''-H and 6''-H), 7.63 (2H, d, *J* 8.6 Hz, 3''-H and 5''-H); δ_C (101 MHz, $CDCl_3$) 28.4 (3 × CH_3), 38.1 (CH_2), 38.4 (CH_2), 52.5 (CH_3), 53.4 (CH), 55.6 (CH), 80.5 (C), 88.0 (C), 93.7 (C), 111.6 (C), 118.6 (C), 121.0 (C), 127.3 (2 × CH), 128.3 (C), 128.7 (2 × CH), 129.3 (2

× CH), 129.7 (2 × CH), 132.1 (CH), 132.16 (2 × CH), 132.19 (2 × CH), 135.7 (C), 138.1 (C), 155.3 (C), 170.6 (C), 171.5 (C); *m/z* (ESI) 574.2318 (MNa^+. $C_{33}H_{33}N_3O_5Na$ requires 574.2312).

(2*S*)-2-(*tert*-Butoxycarbonylamino)-3-(4'-(4''-cyanophenylethynyl)phenyl)-1-propanamide dibenzyl-L-aspartate (215)

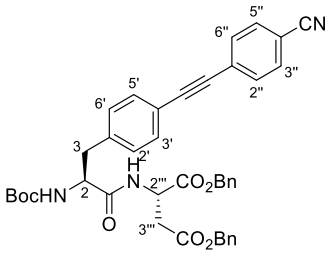

(2*S*)-2-(*tert*-Butoxycarbonylamino)-3-(4'-(4''-cyanophenylethynyl)phenyl)-1-propanamide dibenzyl-L-aspartate (**215**) was synthesised as described for (2*S*)-2-(*tert*-butoxycarbonylamino)-3-(4'-(4''-cyanophenylethynyl)phenyl)-1-propanamide-L-alanine *tert*-butyl ester (**213**) using (2*S*)-2-(*tert*-butoxycarbonylamino)-3-(4'-ethynylphenyl)-1-propanamide dibenzyl-L-aspartate (**212**) (0.0997 g, 0.171 mmol), 4-iodobenzonitrile (0.0523 g, 0.228 mmol), bis(triphenylphosphine)palladium(II) dichloride (0.0122 g, 0.174 mmol) and copper iodide (0.0660 g, 0.0347 mmol) in dry *N,N'*-dimethylformamide (6 mL) and anhydrous triethylamine (14 mL). Purification by flash column chromatography eluting with 30% ethyl acetate in hexane afforded (2*S*)-2-(*tert*-butoxycarbonylamino)-3-(4'-(4''-cyanophenylethynyl)phenyl)-1-propanamide dibenzyl-L-aspartate (**215**) (0.0992 g, 85%) as a white solid. Mp 144–146 °C; ν_{max}/cm^{-1} (neat) 3317 (NH), 2970 (CH), 2212 (C≡C), 1730 (C=O), 1687 (C=O), 1655 (C=O), 1520, 1387, 1365, 1333, 1294, 1165, 1047, 984, 837; $[\alpha]_D^{18}$ +9.0 (*c* 0.1, $CHCl_3$); δ_H (400 MHz, $CDCl_3$) 1.40 (9H, s, 3 × CH_3), 2.89 (1H, dd, *J* 17.2, 4.4 Hz, 3'''-*H*H), 2.99 (1H, dd, *J* 14.0, 6.8 Hz, 3-*H*H), 3.06 (1H, dd, *J* 17.2, 4.4 Hz, 3'''-H*H*), 3.11 (1H, dd, *J* 14.0, 6.0 Hz, 3-H*H*), 4.31–4.44 (1H, m, 2-H), 4.84 (1H, dt, *J* 8.0, 4.4 Hz, 2'''-H), 4.91–4.97 (1H, m, 2-NH), 5.01 (1H, d, *J* 12.2 Hz, C*H*HPh), 5.06 (1H, d, *J* 12.2 Hz, CH*H*Ph), 5.13 (2H, s, CH_2Ph), 6.90 (1H, d, *J* 8.0 Hz, 2'''-NH), 7.18 (2H, d, *J* 8.4 Hz, 2'-H and 6'-H), 7.24–7.38 (10H, m, 10 × ArH), 7.44 (2H, d, *J* 8.4 Hz, 3'-H and 5'-H), 7.56 (2H, d, *J* 8.8 Hz, 2''-H and 6''-H), 7.62 (2H, d *J* 8.8 Hz, 3''-H

and 6''-H); δ_C (101 MHz, $CDCl_3$) 28.4 (3 × CH_3), 36.3 (CH_2), 38.4 (CH_2), 48.9 (CH), 55.3 (CH), 67.0 (CH_2), 67.8 (CH_2), 80.4 (C), 88.0 (C), 93.8 (C), 111.5 (C), 118.7 (C), 120.9 (C), 128.3 (C), 128.47 (2 × CH), 128.49 (2 × CH), 128.6 (CH), 128.66 (CH), 128.73 (2 × CH), 128.8 (2 × CH), 129.7 (2 × CH), 132.10 (2 × CH), 132.13 (2 × CH), 132.2 (2 × CH), 135.1 (C), 135.4 (C), 137.9 (C), 155.3 (C), 170.1 (C), 170.6 (C), 170.9 (C); *m/z* (ESI) 724.2412 (MK^+. $C_{41}H_{39}N_3O_7K$ requires 724.2420).

3.5 Arylalkynyl Analogues of Tyrosine Experimental

3.5.1 Synthesis of arylalkynyl analogues of tyrosine

Methyl (2*S*)-2-[(*tert*-butoxycarbonyl)amino]-3-(3'-bromo-4'-hydroxyphenyl)propanoate (142)[298]

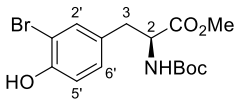

To a stirred solution of methyl (2*S*)-2-[(*tert*-butoxycarbonyl)amino]-3-(4'-hydroxyphenyl)propanoate (**25**) (0.501 g, 1.70 mmol) and *p*-toluenesulfonic acid (0.0325 g, 0.171 mmol) in methanol (3 mL) in a foiled round bottom flask was added a solution of *N*-bromosuccinimide (0.331 g, 1.86 mmol) in methanol (22 mL) from a foiled dropping funnel over 0.58 h. The reaction mixture was stirred at room temperature for 2 h then concentrated *in vacuo*. Purification by flash column chromatography eluting with 5% ethyl acetate in dichloromethane gave methyl (2*S*)-2-[(*tert*-butoxycarbonyl)amino]-3-(3'-bromo-4'-hydroxyphenyl)propanoate (**142**) (0.500 g, 79%) as a white solid. Mp 111–115 °C (lit.[298] 117–119 °C); $[\alpha]_D^{21}$ +45.7 (*c* 0.1, $CHCl_3$); δ_H (400 MHz, $CDCl_3$) 1.43 (9H, s, 3 × CH_3), 2.95 (1H, dd, *J* 14.0, 5.9 Hz, 3-*H*H), 3.05 (1H, dd, *J* 14.0, 5.2 Hz, 3-H*H*), 3.72 (3H, s, OCH_3), 4.47–4.57 (1H, m, 2-H), 4.98 (1H, d, *J* 8.2 Hz, NH), 5.43 (1H, s, OH), 6.90–7.03 (2H, m, 5'-H and 6'-H), 7.23 (1H, d, *J* 1.5 Hz, 2'-H); δ_C (101 MHz, $CDCl_3$) 28.4 (3 × CH_3), 37.4 (CH_2), 52.5 (CH_3), 54.6 (CH), 80.3 (C), 110.3 (C), 116.2 (CH), 129.9 (C), 130.2 (CH), 132.8 (CH), 151.5 (C), 155.2 (C), 172.3 (C); *m/z* (ESI) 396 (MNa^+. 100%).

Methyl (2*S*)-3-[3'-bromo-4'-(methoxymethoxy)phenyl]-2-[(*tert*-butoxycarbonyl)amino]propanoate (143)

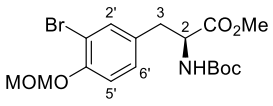

To a stirred solution of methyl (2*S*)-2-[(*tert*-butoxycarbonyl)amino]-3-(3'-bromo-4'-hydroxyphenyl)propanoate (**142**) (0.403 g, 1.08 mmol) and *N,N*-diisopropylethylamine (0.800 mL, 4.32 mmol) in dichloromethane (12 mL) at 0 °C was slowly added bromomethyl methyl ether (0.310 mL, 3.77 mmol). The reaction mixture was stirred at 0 ° for 0.5 h, then warmed to room temperature and stirred for 3 h. The reaction mixture was diluted in dichloromethane (50 mL) and washed with 0.5 M aqueous citric acid solution (2 × 50 mL), saturated sodium bicarbonate (2 × 50 mL) and brine (50 mL). The organic layer was dried ($MgSO_4$), filtered and concentrated *in vacuo*. Purification by flash column chromatography eluting with 30% ethyl acetate in hexane, followed by a second purification by flash column chromatography eluting with 20% ethyl acetate in hexane gave methyl (2*S*)-3-[3'-bromo-4'-(methoxymethoxy)phenyl]-2-[(*tert*-butoxycarbonyl)amino]propanoate (**143**) (0.381 g, 84%) as a colourless oil. $[\alpha]_D^{22}$ +36.8 (*c* 0.1, $CHCl_3$); ν_{max}/cm^{-1} (neat) 3364 (NH), 2978 (CH), 1746 (C=O), 1713 (C=O), 1495, 1366, 1246, 1161, 1045; δ_H (400 MHz, $CDCl_3$) 1.43 (9H, s, 3 × CH_3), 2.96 (1H, dd, *J* 14.0, 6.0 Hz, 3-*H*H), 3.06 (1H, dd, *J* 14.0, 5.6 Hz, 3-H*H*), 3.51 (3H, s, OCH_2OCH_3), 3.73 (3H, s, OCH_3), 4.49–4.57 (1H, m, 2-H), 4.99 (1H, d, *J* 8.2 Hz, NH), 5.22 (2H, s, OCH_2OCH_3), 7.00 (1H, dd, *J* 8.4, 2.0 Hz, 6'-H), 7.07 (2H, d, *J* 8.4 Hz, 5'-H), 7.30 (1H, d, *J* 2.0 Hz, 2'-H); δ_C (101 MHz, $CDCl_3$) 28.4 (3 × CH_3), 37.3 (CH_2), 52.5 (CH_3), 54.5 (CH), 56.5 (CH_3), 80.2 (C), 95.3 (CH_2), 112.9 (C), 116.3 (CH), 129.4 (CH), 131.2 (C), 134.3 (CH), 153.0 (C), 155.2 (C), 172.2 (C); *m/z* (ESI) 440.0677 (MNa^+. $C_{17}H_{24}{}^{79}BrNNaO_6$ requires 440.0679).

Methyl (*2S*)-2-[(*tert*-butoxycarbonyl)amino]-3-(3'-iodo-4'-hydroxyphenyl)propanoate (220)[283]

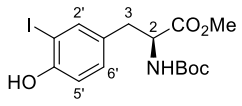

In an oven-dried flask under argon, thionyl chloride (0.100 mL, 1.38 mmol) was added dropwise to a stirred solution of 3-iodo-L-tyrosine (**218**) (0.199 g, 0.648 mmol) in anhydrous methanol (1.3 mL) at 0 °C. The reaction was stirred at 0 °C for 1.5 h. Addition methanol (2 mL) was added and the reaction stirred for a further 2 h. The reaction mixture was concentrated *in vacuo* and the product washed with a cold solution of 20% 2-propanol in chloroform to give 3-iodo-L-tyrosine methyl ester (**219**) (0.152 g, 73%). Without further purification, 3-iodo-L-tyrosine methyl ester (0.050 g, 0.140 mmol) was dissolved in methanol (0.5 mL). To this was added triethylamine (59.0 μL, 0.420 mmol) and the reaction mixture cooled to 0 °C. Di-*tert*-butyl dicarbonate (0.0340 g, 0.154 mmol) in methanol (0.5 mL) was added dropwise over 1 h. The reaction mixture was allowed to gradually warm to room temperature and stirred for 20 h. The reaction mixture was concentrated *in vacuo*, diluted in ethyl acetate (20 mL) and washed with water (20 mL) and brine (20 mL). The organic layer was dried ($MgSO_4$), filtered and concentrated *in vacuo*. Purification by flash column chromatography eluting with 20–30% ethyl acetate in hexane gave methyl (*2S*)-2-[(*tert*-butoxycarbonyl)amino]-3-(3'-iodo-4'-hydroxyphenyl)propanoate (**220**) (0.0326 g, 56%) as a white solid. Mp 100–103 °C; $[\alpha]_D^{20}$ +51.5 (*c* 0.44, $CHCl_3$) [lit.[283] $[\alpha]_D^{23}$ +54.0 (*c* 0.44, $CHCl_3$)]; δ_H (400 MHz, $CDCl_3$) 1.43 (9H, s, 3 × CH_3), 2.93 (1H, dd, *J* 13.6, 6.0 Hz, 3-*H*H), 3.03 (1H, dd, *J* 13.6, 5.6 Hz, 3-H*H*), 3.72 (3H, s, OCH_3), 4.40–4.46 (1H, m, 2-H), 5.02 (1H, d, *J* 8.4 Hz, 2-NH), 5.66 (1H, br s, OH), 6.87 (1H, d, *J* 8.4 Hz, 5'-H), 6.99 (1H, dd, *J* 8.4, 2.0 Hz, 6'-H), 7.42 (1H, s, 2'-H); δ_C (101 MHz, $CDCl_3$) 28.4 (3 × CH_3), 37.1 (CH_2), 52.5 (CH_3), 54.6 (CH), 80.3 (C), 85.6 (C), 115.2 (CH), 130.2 (C), 131.1 (CH), 139.1 (CH), 154.2 (C), 155.2 (C), 172.3 (C); *m/z* (ESI) 420 ([M–H]$^-$. 100%).

Methyl (2*S*)-2-[(*tert*-butoxycarbonyl)amino]-3-(3'-trimethylsilylethynyl-4'-hydroxyphenyl)propanoate (216)[299]

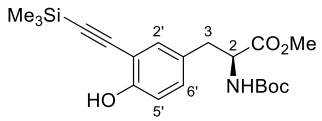

Methyl (2*S*)-2-[(*tert*-butoxycarbonyl)amino]-3-(3'-iodo-4'-hydroxyphenyl)propanoate (**220**) (0.041 g, 0.097 mmol), bis(triphenylphosphine)palladium(II) dichloride (0.0068 g, 0.0097 mmol) and copper iodide (0.0037 g, 0.019 mmol) were put under argon and dissolved in degassed anhydrous tetrahydrofuran (9 mL). To this was added anhydrous triethylamine (40 µL, 0.29 mmol) followed by trimethylsilyl acetylene (40 µL, 0.29 mmol). The reaction mixture was stirred at 30 °C for 5.3 h then concentrated *in vacuo*. The reaction mixture was diluted in ethyl acetate (20 mL), washed with water (20 mL) and brine (20 mL), dried ($MgSO_4$), filtered and concentrated *in vacuo*. Purification by flash column chromatography eluting with 20% ethyl acetate in hexane gave methyl (2*S*)-2-[(*tert*-butoxycarbonyl)amino]-3-(3'-trimethylsilylethynyl-4'-hydroxyphenyl)propanoate (**216**) (0.034 g, 89%) as a brown oil. $[\alpha]_D^{20}$ +39.9 (*c* 1.0, $CHCl_3$) (lit.[299] $[\alpha]_D^{25}$ +39.0 (*c* 1.0, $CHCl_3$)); δ_H (400 MHz, $CDCl_3$) 0.27 (9H, s, $Si(CH_3)_3$), 1.42 (9H, s, 3 × CH_3), 2.92 (1H, dd, *J* 14.0, 6.4 Hz, 3-*H*H), 3.03 (1H, dd, *J* 14.0, 5.6 Hz, 3-H*H*), 3.71 (3H, s, OCH_3), 4.46–4.52 (1H, m, 2-H), 4.96 (1H, d, *J* 7.6 Hz, 2-NH), 5.78 (1H, s, OH), 6.86 (1H, d, *J* 8.4 Hz, 5'-H), 6.99 (1H, dd, *J* 8.4, 1.8 Hz, 6'-H), 7.11 (1H, d, *J* 1.8 Hz, 2'-H); δ_C (101 MHz, $CDCl_3$) 0.1 (3 × CH_3), 28.4 (3 × CH_3), 37.5 (CH_2), 52.4 (CH_3), 54.6 (CH), 80.1 (C), 98.9 (C), 102.6 (C), 109.7 (C), 114.9 (CH), 127.9 (C), 131.7 (CH), 132.4 (CH), 155.2 (C), 156.3 (C), 172.4 (C); *m/z* (ESI) 414 (MNa^+. 100%).

Methyl (2*S*)-2-[(*tert*-butoxycarbonyl)amino]-3-(3'-ethynyl-4'-hydroxyphenyl)propanoate (222)

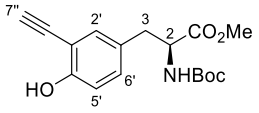

Methyl (2*S*)-2-[(*tert*-butoxycarbonyl)amino]-3-(3'-trimethylsilylethynyl-4'-hydroxyphenyl)propanoate (**216**) (0.034 g, 0.086 mmol) was dissolved in dry tetrahydrofuran (1 mL) and ethanol (24 μL) and cooled to 0 °C under argon. To this was added anhydrous 1 M tetrabutylammonium fluoride in tetrahydrofuran (0.040 mL, 0.043 mmol). The reaction mixture was stirred at 0 °C for 1.5 h and then concentrated *in vacuo*, diluted in ethyl acetate (20 mL) and washed with water (20 mL) then brine (20 mL). The organic layer was dried ($MgSO_4$), filtered and concentrated *in vacuo*. Purification by flash column chromatography eluting with 20% ethyl acetate in hexane gave methyl (2*S*)-2-[(*tert*-butoxycarbonyl)amino]-3-(3'-ethynyl-4'-hydroxyphenyl)propanoate (**222**) (0.019 g, 70%) as a brown oil. $[\alpha]_D^{19}$ +53.6 (*c* 0.1, $CHCl_3$; ν_{max}/cm^{-1} (neat) 3365, 3288 (NH), 2978 (CH), 1738 (C=O), 1693, 1500, 1441, 1365, 1252, 1165, 1059, 1020; δ_H (400 MHz, $CDCl_3$) 1.42 (9H, s, 3 × CH_3), 2.94 (1H, dd, *J* 14.0, 6.0 Hz, 3-*H*H), 3.03 (1H, dd, *J* 14.0, 6.0 Hz, 3-H*H*), 3.45 (1H, s, 7'-H), 3.72 (3H, s, OCH_3), 4.46–4.53 (1H, m, 2-H), 4.98 (1H, d, *J* 8.4 Hz, 2-NH), 6.87 (1H, d, *J* 8.4 Hz, 5'-H), 7.03 (1H, dd, *J* 8.4, 2.2 Hz, 6'-H), 7.13 (1H, d, *J* 2.2 Hz, 2'-H); δ_C (101 MHz, $CDCl_3$) 28.4 (3 × CH_3), 37.5 (CH_2), 52.4 (CH_3), 54.6 (CH), 78.3 (C), 80.2 (C), 84.5 (CH), 108.5 (C), 115.2 (CH), 128.1 (C), 132.0 (CH), 132.8 (CH), 155.2 (C), 156.7 (C), 172.3 (C); *m/z* (ESI) 342.1313 (MNa^+. $C_{17}H_{21}NO_5Na$ requires 342.1312).

4.0 References

1. T. Terai and T. Nagano, *Plugers Arch.*, 2013, **465**, 347–359.
2. A. Miyawaki and Y. Niino, *Mol. Cell*, 2015, **58**, 632–643.
3. A. M. Smith, H. Duan, A. M. Mohs and S. Nie, *Adv. Drug Deliv. Rev.*, 2008, **60**, 1226–1240.
4. A. B. Chinen, C. M. Guan, J. R. Ferrer, S. N. Barnaby, T. J. Merkel and C. A. Mirkin, *Chem. Rev.*, 2015, **115**, 10530–10574.
5. J. Zhang, R. E. Campbell, A. Y. Ting and R. Y. Tsien, *Nat. Rev. Mol. Cell Biol.*, 2002, **3**, 906–918.
6. T. Terai and T. Nagano, *Curr. Opin. Chem. Biol.*, 2008, **12**, 515–521.
7. J. Ma, R. Sun, K. Xia, Q. Xia, Y. Liu and X. Zhang, *Chem. Rev.*, 2024, **124**, 1738–1861.
8. D. Saimi and Z. Chen, *Smart Mol.*, 2023, **1**, e20230002.
9. C. A. Hoelzel and X. Zhang, *ChemBioChem*, 2020, **21**, 1935–1946.
10. J. Králová, M. Jurášek, L. Mikšátková, A. Marešová, J. Fähnrich, P. Cihlářová, P. Drašar, P. Bartůněk and V. Král, *Sci. Rep.*, 2020, **10**, 22053.
11. A. T. Krueger and B. Imperiali, *ChemBioChem*, 2013, **14**, 788–799.
12. A. H. Harkiss and A. Sutherland, *Org. Biomol. Chem.*, 2016, **14**, 8911–8921.
13. Z. Cheng, E. Kuru, A. Sachdeva and M. Vendrell, *Nat. Rev. Chem.*, 2020, **4**, 275–290.
14. R.-r. Feng, M. Wang, W. Zhang and F. Gai, *Chem. Rev.*, 2024, **124**, 6501–6542.
15. R. W. Sinkeldam, N. J. Greco and Y. Tor, *Chem. Rev.*, 2010, **110**, 2579–2619.
16. P. W. Atkins and J. D. Paula, *Atkins' Physical Chemistry* Oxford University Press, Oxford, 9th ed edn., 2012.
17. J. R. Lakowicz, *Principles of Fluorescence Spectroscopy*, Springer New York, NY, 3 edn., 2006.
18. E. Condon, *Phys. Rev.*, 1926, **28**, 1182–1201.
19. J. Franck and E. G. Dymond, *Trans. Faraday Soc.*, 1926, **21**, 536–542.
20. M. Kasha, *Discuss. Faraday Soc.,* 1950, **9**, 14–19.
21. J. C. del Valle and J. Catalán, *J. Phys. Chem. Chem. Phys.*, 2019, **21**, 10061–10069.
22. C. Reichardt, *Chem. Rev.*, 1994, **94**, 2319–2358.
23. M. M. Martin and L. Lindqvist, *J. Lumin.*, 1975, **10**, 381–390.
24. K.-L. Wong, J.-C. G. Bünzli and P. A. Tanner, *J. Lumin.*, 2020, **224**, 117256.
25. J. V. Jun, D. M. Chenoweth and E. J. Petersson, *Org. Biomol. Chem*, 2020, **18**, 5747–5763.
26. M. S. Michie, R. Götz, C. Franke, M. Bowler, N. Kumari, V. Magidson, M. Levitus, J. Loncarek, M. Sauer and M. J. Schnermann, *J. Am. Chem. Soc.*, 2017, **139**, 12406–12409.
27. M. Nepraš, N. Almonasy, F. Bureš, J. Kulhánek, M. Dvořák and M. Mich, *Dyes and Pigments*, 2011, **91**, 466–473.
28. J. D. Bell, A. H. Harkiss, D. Nobis, E. Malcolm, A. Knuhtsen, C. R. Wellaway, A. G. Jamieson, S. W. Magennis and A. Sutherland, *Chem. Commun.*, 2020, **56**, 1887–1890.
29. R. Huang, Q. Qiao, D. Seah, T. Shen, X. Wu, F. de Moliner, C. Wang, N. Ding, W. Chi, H. Sun, M. Vendrell, Z. Xu, Y. Fang and X. Liu, *J. Am. Chem. Soc.,* 2025, **147**, 5258–5268.
30. P. Luu, S. E. Fraser and F. Schneider, *Commun. Biol.*, 2024, **7**, 364.
31. R. Clarke, L. Zeng, B. C. Atkinson, M. Kadodwala, A. R. Thomson and A. Sutherland, *Chem. Sci.*, 2024, **15**, 5944–5949.
32. S. Chen, N. E. Fahmi, C. Bhattacharya, L. Wang, Y. Jin, S. J. Benkovic and S. M. Hecht, *Biochemistry*, 2013, **52**, 8580–8589.

33. T. Kalstrup and R. Blunck, *Proc. Natl. Acad. Sci. U.S.A.*, 2013, **110**, 8272–8277.
34. F. W. J. Teale and G. Weber, *Biochem. J*, 1957, **65**, 476–482.
35. Y. Xiong, C. Shi, L. Li, Y. Tang, X. Zhang, S. Liao, B. Zhang, C. Sun and C. Ren, *New J. Chem.*, 2021, **45**, 15180–15194.
36. T. Koopmans, M. van Haren, L. Q. van Ufford, J. M. Beekman and N. I. Martin, *Biorg. Med. Chem.*, 2013, **21**, 553–559.
37. P. R. Gleason, B. Kolbaba-Kartchner, J. N. Henderson, E. P. Stahl, C. R. Simmons and J. H. Mills, *Biochemistry*, 2021, **60**, 2577–2585.
38. J. N. Henderson, C. R. Simmons, N. E. Fahmi, J. W. Jeffs, C. R. Borges and J. H. Mills, *Biochemistry*, 2020, **59**, 3401–3410.
39. T. L. Dangerfield and K. A. Johnson, *J. Biol. Chem.*, 2020, **295**, 17265–17280.
40. S. M. Kuhn, M. Rubini, M. A. Müller and A. Skerra, *J. Am. Chem. Soc.,* 2011, **133**, 3708–3711.
41. J. Wang, J. Xie and P. G. Schultz, *J. Am. Chem. Soc.*, 2006, **128**, 8738–8739.
42. S.-M. Paek, M. Jeong, J. Jo, Y. M. Heo, Y. T. Han and H. Yun, *Molecules*, 2016, **21**, 951.
43. M. Noden and S. D. Taylor, *J. Org. Chem.,* 2021, **86**, 11407–11418.
44. P. Kele, G. Sui, Q. Huo and R. M. Leblanc, *Tetrahedron: Asymmetry*, 2000, **11**, 4959–4963.
45. Y. Zou, J. Han, A. S. Saghyan, A. F. Mkrtchyan, H. Konno, H. Moriwaki, K. Izawa and V. A. Soloshonok, *Molecules*, 2020, **25**, 2739.
46. R. M. Williams and M. N. Im, *J. Am. Chem. Soc.,* 1991, **113**, 9276–9286.
47. Williams, R. M. In *Peptidomimetics Protocols*; Kazmierski, W. M., Ed.; Humana Press: Totowa, NJ, 1999; pp. 339–356
48. P. J. Sinclair, D. Zhai, J. Reibenspies and R. M. Williams, *J. Am. Chem. Soc.,* 1986, **108**, 1103–1104.
49. A. E. Sorochinsky, J. L. Aceña, H. Moriwaki, T. Sato and V. A. Soloshonok, *Amino Acids*, 2013, **45**, 691–718.
50. J. L. Aceña, A. E. Sorochinsky and V. Soloshonok, *Amino Acids*, 2014, **46**, 2047–2073.
51. A. S. Saghiyan, L. L. Manasyan, A. V. Geolchanyan, A. M. Hovhannisyan, T. V. Ghochikyan, V. S. Haroutunyan, A. A. Avetisyan, K. S. Mirzoyan, V. I. Maleev and V. N. Khrustalev, *Tetrahedron: Asymmetry*, 2006, **17**, 2743–2753.
52. A. S. Saghiyan, S. A. Dadayan, S. G. Petrosyan, L. L. Manasyan, A. V. Geolchanyan, S. M. Djamgaryan, S. A. Andreasyan, V. I. Maleev and V. N. Khrustalev, *Tetrahedron: Asymmetry*, 2006, **17**, 455–467.
53. Y. N. Belokon, V. I. Maleev, A. A. Petrosyan, T. F. Savel"eva, N. S. Ikonnikov, A. S. Peregudov, V. N. Khrustalev and A. S. Saghiyan, *Russ. Chem. Bull.*, 2002, **51**, 1593–1599.
54. A. Popkov, A. Gee, M. Nádvorník and A. Lyčka, *Transition Met. Chem.*, 2002, **27**, 884–887.
55. A. V. Strizhak, V. Y. Postupalenko, V. V. Shvadchak, N. Morellet, E. Guittet, V. G. Pivovarenko, A. S. Klymchenko and Y. Mély, *Bioconjugate Chem.*, 2012, **23**, 2434–2443.
56. M. Sholokh, O. M. Zamotaiev, R. Das, V. Y. Postupalenko, L. Richert, D. Dujardin, O. A. Zaporozhets, V. G. Pivovarenko, A. S. Klymchenko and Y. Mély, *J. Phys. Chem. B,* 2015, **119**, 2585–2595.
57. V. Y. Postupalenko, O. M. Zamotaiev, V. V. Shvadchak, A. V. Strizhak, V. G. Pivovarenko, A. S. Klymchenko and Y. Mely, *Bioconjugate Chem.*, 2013, **24**, 1998–2007.
58. F. Bureš, *RSC Adv.*, 2014, **4**, 58826–58851.

59. L. C. Speight, A. K. Muthusamy, J. M. Goldberg, J. B. Warner, R. F. Wissner, T. S. Willi, B. F. Woodman, R. A. Mehl and E. J. Petersson, *J. Am. Chem. Soc.,* 2013, **135**, 18806–18814.
60. J. G. Marmorstein, V. V. Pagar, E. Hummingbird, I. G. Saleh, H. A. T. Phan, Y. Chang, K. D. Shaffer, Y. Venkatesh, I. J. Dmochowski, K. J. Stebe and E. J. Petersson, *Bioconjugate Chem.*, 2024, **35**, 1913–1922.
61. P. Eggan, S. E. Gordon and W. N. Zagotta, *eLife*, 2024, **13**, RP99854.
62. W. N. Zagotta, B. S. Sim, A. K. Nhim, M. M. Raza, E. G. B. Evans, Y. Venkatesh, C. M. Jones, R. A. Mehl, E. J. Petersson and S. E. Gordon, *eLife*, 2021, **10**, e70236.
63. M. B. Cory, C. M. Jones, K. D. Shaffer, Y. Venkatesh, S. Giannakoulias, R. M. Perez, M. G. Lougee, E. Hummingbird, V. V. Pagar, C. M. Hurley, A. Li, R. H. Mach, R. M. Kohli and E. J. Petersson, *Protein Sci.*, 2023, **32**, e4633.
64. J. J. Ferrie, N. Ieda, C. M. Haney, C. R. Walters, I. Sungwienwong, J. Yoon and E. J. Petersson, *Chem. Commun.*, 2017, **53**, 11072–11075.
65. J. M. Goldberg, L. C. Speight, M. W. Fegley and E. J. Petersson, *J. Am. Chem. Soc.,* 2012, **134**, 6088–6091.
66. C. M. Jones, D. M. Robkis, R. J. Blizzard, M. Munari, Y. Venkatesh, T. S. Mihaila, A. J. Eddins, R. A. Mehl, W. N. Zagotta, S. E. Gordon and E. J. Petersson, *Chem. Sci.,* 2021, **12**, 11955–11964.
67. Z. M. Hostetler, M. B. Cory, C. M. Jones, E. J. Petersson and R. M. Kohli, *ACS Chem. Biol.*, 2020, **15**, 1127–1133.
68. S. Giannakoulias, S. R. Shringari, J. J. Ferrie and E. J. Petersson, *Sci. Rep.,* 2021, **11**, 18406.
69. C. M. Jones, G. A. Petersson and E. J. Petersson, *Arkivoc*, 2021, **2021**, 97–109.
70. I. Sungwienwong, J. J. Ferrie, J. V. Jun, C. Liu, T. M. Barrett, Z. M. Hostetler, N. Ieda, A. Hendricks, A. K. Muthusamy, R. M. Kohli, D. M. Chenoweth, G. A. Petersson and E. J. Petersson, *J. Phys. Org. Chem.*, 2018, **31**.
71. J. B. Grimm, B. P. English, J. Chen, J. P. Slaughter, Z. Zhang, A. Revyakin, R. Patel, J. J. Macklin, D. Normanno, R. H. Singer, T. Lionnet and L. D. Lavis, *Nat. Methods*, 2015, **12**, 244–250.
72. J. Wang, X. Liu, K. Li, T. Shi, Q. Xu, T. Peng, Q. Huang, Z. Gao, H. Zhou, W. Lu and J. Wang, *J. Am. Chem. Soc.,* 2025, **147**, 15205–15215.
73. Z. Xiang and L. Wang, *J. Org. Chem*, 2011, **76**, 6367–6371.
74. M. Mizuno and M. Yamano, *Org. Lett.*, 2005, 7, 3629–3631.
75. J. A. Dale, D. L. Dull and H. S. Mosher, *J. Org. Chem.*, 1969, **34**, 2543–2549.
76. H. S. Lee, J. Guo, E. A. Lemke, R. D. Dimla and P. G. Schultz, *J. Am. Chem. Soc.*, 2009, **131**, 12921–12923.
77. A. Chatterjee, J. Guo, H. S. Lee and P. G. Schultz, *J. Am. Chem. Soc.,* 2013, **135**, 12540–12543.
78. M. Wen, X. Guo, P. Sun, L. Xiao, J. Li, Y. Xiong, J. Bao, T. Xue, L. Zhang and C. Tian, *Chem. Commun.*, 2015, **51**, 8153–8156.
79. S.-H. Park, W. Ko, S.-H. Park, H. S. Lee and I. Shin, *ChemBioChem*, 2020, **21**, 59–63.
80. G. Loving and B. Imperiali, *J. Am. Chem. Soc.,* 2008, **130**, 13630–13638.
81. J. Kollár, P. Hrdlovič, Š. Chmela, M. Sarakha and G. Guyot, *J. Photochem. Photobiol. A Chem.,* 2005, **170**, 151–159.
82. E. Kuru, S. Tekkam, E. Hall, Y. V. Brun and M. S. Van Nieuwenhze, *Nat. Protoc.* 2015, **10**, 33–52.
83. I. Dufau and H. Mazarguil, *Tetrahedron Lett.*, 2000, **41**, 6063–6066.
84. Y. Zhao, M. C. Pirrung and J. Liao, *Mol. Biosyst.,* 2012, **8**, 879–887.
85. T. Oyama, L. Mendive-Tapia, V. Cowell, A. Kopp, M. Vendrell and L. Ackermann, *Chem. Sci.*, 2023, **14**, 5728–5733.

86. S. Benson, F. de Moliner, A. Fernandez, E. Kuru, N. L. Asiimwe, J.-S. Lee, L. Hamilton, D. Sieger, I. R. Bravo, A. M. Elliot, Y. Feng and M. Vendrell, *Nat. Commun.*, 2021, **12**, 2369.
87. Y.-B. Ruan, Y. Yu, C. Li, N. Bogliotti, J. Tang and J. Xie, *Tetrahedron*, 2013, **69**, 4603–4608.
88. F. Nadal-Bufi, R. V. Nithun, F. de Moliner, X. Lin, S. Habiballah, M. Jbara and M. Vendrell, *ACS Cent. Sci.*, 2025, **11**, 66–75.
89. F. de Moliner, Z. Konieczna, L. Mendive-Tapia, R. S. Saleeb, K. Morris, J. A. Gonzalez-Vera, T. Kaizuka, S. G. N. Grant, M. H. Horrocks and M. Vendrell, *Angew. Chem. Int. Ed.*, 2023, **62**, e202216231.
90. S. Uchiyama, K. Kimura, C. Gota, K. Okabe, K. Kawamoto, N. Inada, T. Yoshihara and S. Tobita, *Chem. Eur. J.,* 2012, **18**, 9552–9563.
91. R. Micikas, A. Acharyya, F. Gai and A. B. Smith, III, *Org. Lett.*, 2021, **23**, 1247–1250.
92. T. Haldar, S. Chatterjee, M. N. Alam, P. Maity and S. Bagchi, *J. Phys. Chem. B*, 2022, **126**, 10732–10740.
93. K. Zhang, I. A. Ahmed, H. T. Kratochvil, W. F. DeGrado, F. Gai and H. Jo, *Chem. Commun.*, 2019, **55**, 5095–5098.
94. I. A. Ahmed, J. M. Rodgers, C. Eng, T. Troxler and F. Gai, *Phys. Chem. Chem. Phys.*, 2019, **21**, 12843–12849.
95. K. P. Fong, I. A. Ahmed, M. Mravic, H. Jo, O. V. Kim, R. I. Litvinov, J. W. Weisel, W. F. DeGrado, F. Gai and J. S. Bennett, *Biochemistry*, 2021, **60**, 1722–1730.
96. M. R. Hilaire, I. A. Ahmed, C.-W. Lin, H. Jo, W. F. DeGrado and F. Gai, *Proc. Natl. Acad. Sci. U.S.A.***,** 2017, **114**, 6005–6009.
97. M. Winn, D. Francis and J. Micklefield, *Angew. Chem.*, 2018, **130**, 6946–6949.
98. C. E. Boville, D. K. Romney, P. J. Almhjell, M. Sieben and F. H. Arnold, *J. Org. Chem.,* 2018, **83**, 7447–7452.
99. T. Narancic, S. A. Almahboub and K. E. O'Connor, *World J. Microbiol. Biotechnol.*, 2019, **35**, 67.
100. G. I. D. Cooper, I. Saha, J. Newman, R. H. Shin and P. G. Harran, *J. Org. Chem.,* 2024, **89**, 14665–14672.
101. K. L. Rich, M. Négrerie, J. Li, S. Elliott, R. W. Thornburg and J. W. Petrich, *Photochem. Photobiol.*, 1993, **58**, 28–30.
102. Y.Chen, R.L.Rich, F.Gai and J.W.Petrich, *J. Phys. Chem.*, 1993, **97**, 1770–1780.
103. S. Lepthien, M. G. Hoesl, L. Merkel and N. Budisa, *Proc. Natl. Acad. Sci. U.S.A.,* 2008, **105**, 16095–16100.
104. W.-C. Chao, J.-Y. Shen, C.-H. Yang, Y.-K. Lan, J.-H. Yuan, L.-J. Lin, H.-C. Yang, J.-F. Lu, J.-S. Wang, K. Wee, Y.-H. Chen and P.-T. Chou, *Biophys. J.*, 2016, **110**, 1732–1743.
105. S. M. Twine, L. Murphy, R. S. Phillips, P. Callis, M. T. Cash and A. G. Szabo, *J. Phys. Chem. B*, 2003, **107**, 637–645.
106. R. L. Rich, F. Gai, J. W. Lane, J. W. Petrich and A. W. Schwabacher, *J. Am. Chem. Soc.,* 1995, **117**, 733–739.
107. W.-W. Park, K. M. Lee, B. S. Lee, Y. J. Kim, S. H. Joo, S. K. Kwak, T. H. Yoo and O.-H. Kwon, *Angew. Chem. Int. Ed.*, 2020, **59**, 7089–7096.
108. L. D. Newton, S. I. Pascu, R. M. Tyrrell and I. M. Eggleston*, Org. Biomol. Chem***.**, 2019, **17**, 467–471.
109. M. G. Hoesl, M. Larregola, H. Cui and N. Budisa, *J. Pept. Sci.*, 2010, **16**, 589–595.
110. Y. Chen, F. Gai and J. W. Petrich, *J. Phys. Chem*, 1994, **98**, 2203–2209.
111. A. B. Pardee, V. G. Shore and L. S. Prestidge, *Biochim. Biophys. Acta*, 1956, **21**, 406–407.

112. R. F. W. Jackson, N. Wishart, A. Wood, K. James and M. J. Wythes, *J. Org. Chem.*, 1992, **57**, 3397–3404.
113. R. F. Jackson, I. Rilatt and L. Caggiano, *Synlett*, 2005, 2701–2719.
114. J. D. Bell, T. E. F. Morgan, N. Buijs, A. H. Harkiss, C. R. Wellaway and A. Sutherland, *J. Org. Chem.*, 2019, **84**, 10436–10448.
115. L. M. Riley, T. N. McLay and A. Sutherland, *J. Org. Chem.*, 2023, **88**, 2453–2463.
116. A. C. Dodds, H. G. Sansom, S. W. Magennis and A. Sutherland, *Org. Lett.*, 2023, **25**, 8942–8946.
117. J. P. Martin, N. R. Fetto and M. J. Tucker, *Phys. Chem. Chem. Phys*, 2016, **18**, 20750–20757.
118. M. J. Tucker, R. Oyola and F. Gai, *Biopolymers*, 2006, **83**, 571–576.
119. M. De Zotti, S. Bobone, A. Bortolotti, E. Longo, B. Biondi, C. Peggion, F. Formaggio, C. Toniolo, A. Dalla Bona, B. Kaptein and L. Stella, *Chem. Biodiversity*, 2015, **12**, 513–527.
120. J. Liu, J. Strzalka, A. Tronin, J. S. Johansson and J. K. Blasie, *Biophys. J.*, 2009, **96**, 4176–4187.
121. D. T. Meier, L.-H. Tu, S. Zraika, M. F. Hogan, A. T. Templin, R. L. Hull, D. P. Raleigh and S. E. Kahn, *J. Biol. Chem.*, 2015, **290**, 30475–30485.
122. P. Marek, R. Gupta and D. P. Raleigh, *ChemBioChem*, 2008, **9**, 1372–1374.
123. K. N. Aprilakis, H. Taskent and D. P. Raleigh, *Biochemistry*, 2007, **46**, 12308–12313.
124. H. Taskent-Sezgin, P. Marek, R. Thomas, D. Goldberg, J. Chung, I. Carrico and D. P. Raleigh, *Biochemistry*, 2010, **49**, 6290–6295.
125. I. M. Pazos, I. A. Ahmed, M. I. L. Berríos and F. Gai, *Anal. Biochem.*, 2015, **483**, 21–26.
126. M. J. Tucker, J. Tang and F. Gai, *J. Phys. Chem. B.* 2006, **110**, 8105–8109.
127. H. Taskent-Sezgin, J. Chung, V. Patsalo, S. J. Miyake-Stoner, A. M. Miller, S. H. Brewer, R. A. Mehl, D. F. Green, D. P. Raleigh and I. Carrico, *Biochemistry*, 2009, **48**, 9040–9046.
128. S. J. Miyake-Stoner, A. M. Miller, J. T. Hammill, J. C. Peeler, K. R. Hess, R. A. Mehl and S. H. Brewer, *Biochemistry*, 2009, **48**, 5953–5962.
129. S. R. Anderson, M. R. Gopal, A. P. Spangler, M. A. Jones, D. J. R. Wyllis and A. M. Kunjapur, *ChemCatChem*, 2025, **17**, e202401979.
130. P. M. T. Ferreira, L. S. Monteiro, G. Pereira, E. M. S. Castanheira and C. G. Frost, *Eur. J. Org. Chem.*, 2013, 550–556.
131. S. Chen, L. Wang, N. E. Fahmi, S. J. Benkovic and S. M. Hecht, *J. Am. Chem. Soc.*, 2012, **134**, 18883–18885.
132. S. Wang, H. Liu, S. Zhao, Q. Wu, Z. Yang, D. Yang, Y. Lv, Q. Su, S.-T. Zhang and B. Yang, *Chem. Sci.,* 2025, **16**, 3275–3284.
133. T. Förster, *Angew. Chem. Int. Ed. Engl.,* 1969, **8**, 333–343.
134. A. R. Mohite and R. G. Bhat, *J. Org. Chem.*, 2012, **77**, 5423–5428.
135. A. S. Abreu, E. M. S. Castanheira, P. M. T. Ferreira, L. S. Monteiro, G. Pereira and M.-J. R. P. Queiroz, *Eur. J. Org. Chem.*, 2008, **2008**, 5697–5703.
136. M. Suhartono, M. Weidlich, T. Stein, M. Karas, G. Dürner and M. W. Göbel, *Eur. J. Org. Chem.*, 2008, **2008**, 1608–1614.
137. J. Maity, D. Honcharenko and R. Strömberg, *Tetrahedron Lett.*, 2015, **56**, 4780–4783.
138. R. McGrory, R. Clarke, O. Marshall and A. Sutherland, *Org Biomol Chem*, 2023, **21**, 6932–6939.
139. A. Gupta, B. P. Garreffi and M. Guo, *Chem. Commun.*, 2020, **56**, 12578–12581.
140. S. Chen, N. E. Fahmi, L. Wang, C. Bhattacharya, S. J. Benkovic and S. M. Hecht, *J. Am. Chem. Soc.*, 2013, **135**, 12924–12927.

141. W. Wang, M. M. Lorion, O. Martinazzoli and L. Ackermann, *Angew. Chem. Int. Ed.*, 2018, **57**, 10554–10558.
142. L. Mendive-Tapia, D. Mendive-Tapia, C. Zhao, D. Gordon, S. Benson, M. J. Bromley, W. Wang, J. Wu, A. Kopp, L. Ackermann and M. Vendrell, *Angew. Chem. Int. Ed.*, 2022, **61**, e202117218.
143. J. F. Riordan, M. Sokolovsky and B. L. Vallee, *Biochemistry*, 1967, **6**, 358–+.
144. S. I. Vdovenko, M. T. Kolycheva, I. I. Gerus and V. P. Kukhar, *Amino Acids*, 1993, **4**, 303–306.
145. V. De Filippis, R. Frasson and A. Fontana, *Protein Sci.*, 2006, **15**, 976–986.
146. A. R. Mezo, R. P. Cheng and B. Imperiali, *J. Am. Chem. Soc.*, 2001, **123**, 3885–3891.
147. H. Singh and S. Verma, *Chem. Commun.*, 2021, **57**, 5290–5293.
148. A. Banerjee, T. D. Panosian, K. Mukherjee, R. Ravindra, S. Gal, D. L. Sackett and S. Bane, *ACS Chem. Biol.*, 2010, **5**, 777–785.
149. P. Cheruku, J.-H. Huang, H.-J. Yen, R. S. Iyer, K. D. Rector, J. S. Martinez and H.-L. Wang, *Chem. Sci.*, 2015, **6**, 1150–1158.
150. G. Pereira, H. Vilaça and P. M. T. Ferreira, *Amino Acids*, 2013, **44**, 335–344.
151. E. Ros, M. Bellido, J. A. Matarin, A. Gallen, M. Martínez, L. Rodríguez, X. Verdaguer, L. Ribas de Pouplana and A. Riera, *RSC Advances*, 2022, **12**, 14321–14327.
152. R. McGrory, PhD Thesis, University of Glasgow, 2023.
153. J. C. Anderson, C.-H. Chang, A. P. Jathoul and A. J. Syed, *Tetrahedron*, 2019, **75**, 347–356.
154. Y. Wei and N. Yoshikai, *Org. Lett.*, 2011, **13**, 5504–5507.
155. A. J. Ross, H. L. Lang and R. F. Jackson, *J. Org. Chem.*, 2010, **75**, 245–248.
156. T. E. Barder, S. D. Walker, J. R. Martinelli and S. L. Buchwald, *J. Am. Chem. Soc.,* 2005, **127**, 4685–4696.
157. T. E. Barder, M. R. Biscoe and S. L. Buchwald, *Organometallics*, 2007, **26**, 2183–2192.
158. I. Rilatt and R. F. W. Jackson, *J. Org. Chem.*, 2008, **73**, 8694–8704.
159. M. Poreba, A. Szalek, W. Rut, P. Kasperkiewicz, I. Rutkowska-Wlodarczyk, S. J. Snipas, Y. Itoh, D. Turk, B. Turk, C. M. Overall, L. Kaczmarek, G. S. Salvesen and M. Drag, *Sci. Rep.* 2017, **7**, 43135.
160. J. C. J. Hintzen, K. D. Beckley, E. L. Goldberg and G. M. Burslem, *Chem. Sci.,* 2026, **17**, 2317–2331.
161. J. V. Olsen, S.-E. Ong and M. Mann, *Mol. Cell. Proteomics,* 2004, **3**.
162. T. K. Mukherjee, *J. Phys. Chem.*, 1970, **74**, 3006–3014.
163. M. W. Kryman, G. A. Schamerhorn, J. E. Hill, B. D. Calitree, K. S. Davies, M. K. Linder, T. Y. Ohulchanskyy and M. R. Detty, *Organometallics*, 2014, **33**, 2628–2640.
164. F. Deng and Z. Xu, *Chin. Chem. Lett.*, 2019, **30**, 1667–1681.
165. P. Wessig, L. John, E. Sperlich and A. Kelling, *Eur. J. Org. Chem.*, 2021, **2021**, 499–511.
166. K. C. C. Aganda, S. Na and A. Lee, *Tetrahedron Lett.*, 2022, **104**.
167. R. McGrory, D. C. Morgan, A. G. Jamieson and A. Sutherland, *Org. Lett.*, 2023, **25**, 5844–5849.
168. S. Akai, T. Ikawa and K. Saito, *Synlett*, 2012, **23**, 2241–2246.
169. C. Amatore, G. Le Duc and A. Jutand, *Chemistry*, 2013, **19**, 10082–10093.
170. R. Martin and S. L. Buchwald, *Acc. Chem. Res.*, 2008, **41**, 1461–1473.
171. X. A. F. Cook, A. de Gombert, J. McKnight, L. R. E. Pantaine and M. C. Willis, *Angew. Chem. Int. Ed. Engl.*, 2021, **60**, 11068–11091.
172. M. Loncaric, D. Gaso-Sokac, S. Jokic and M. Molnar, *Biomolecules*, 2020, **10**.
173. W. Erb, A. Hellal, M. Albini, J. Rouden and J. Blanchet, *Chemistry*, 2014, **20**, 6608–6612.

174. E. A. Braude and F. C. Nachod, *Determination of Organic Structures by Physical Methods*, Academic Press, New York 1955.
175. L. Ma, Q. Ouyang, G. C. Werthmann, H. M. Thompson and E. M. Morrow, *Front. Cell Dev. Biol.* 2017, **5**, 1–12.
176. H. Xiong, P. Kos, Y. Yan, K. Zhou, J. B. Miller, S. Elkassih and D. J. Siegwart, *Bioconjugate Chem.*, 2016, **27**, 1737–1744.
177. J.-T. Hou, W. X. Ren, K. Li, J. Seo, A. Sharma, X.-Q. Yu and J. S. Kim, *Chem. Soc. Rev.*, 2017, **46**, 2076–2090.
178. (a) E. Lippert, *Z. Naturforsch. A*, 1955, **10**, 541–545. (b) N. Mataga, Y. Kaifu and M. Koizumi, *Bull. Chem. Soc. Jpn.*, 1955, **28**, 690–691.
179. W. J. Hehre, R. Ditchfield and J. A. Pople, *J. Phys. Chem.*, 1972, **56**, 2257–2261.
180. J. A. Dean, *Lange's handbook of chemistry*, McGraw-Hill, New York, 1992.
181. R. Bhushan, H. Brückner, *J. Chromatrogr. B,* 2011, **879**, 3148–3161.
182. *Origin*, Version 2023. OriginLab Corporation, Northampton, MA, USA.
183. L. M. Riley, O. Marshall, A. H. Harkiss, H. M. Senn and A. Sutherland, *Org. Lett.*, 2024, **26**, 5391–5395.
184. (a) R. Flamini, I. Tomasi, A. Marrocchi, B. Carlotti and A. Spalletti, *J. Photochem. Photobiol. A Chem.*, 2011, **223**, 140–148. (b) T.-I. Ho, A. Elangovan, H.-Y. Hsu and S.-W. Yang, *J. Phys. Chem. B*, 2005, **109**, 8626–8633.
185. S.-W. Yang, A. Elangovan, K.-C. Hwang and T.-I. Ho, *J. Phys. Chem. B*, 2005, **109**, 16628–16635.
186. M. Kivala and F. Diederich, *Acc. Chem. Res.*, 2009, **42**, 235–248.
187. R. J. Magyar, S. Tretiak, Y. Gao, H. L. Wang and A. P. Shreve, *Chem. Phys. Lett.*, 2005, **401**, 149–156.
188. I. Bylińska, K. Guzow, J. Wójcik and W. Wiczk, *J. Photochem. Photobiol. A Chem.*, 2018, **364**, 679–685.
189. G. Evano, N. Blanchard and M. Toumi, *Chem. Rev.*, 2008, **108**, 3054–3131.
190. C. Palladino, T. Fantoni, L. Ferrazzano, B. Muzzi, A. Ricci, A. Tolomelli and W. Cabri, *ACS Catal.,* 2023, **13**, 12048–12061.
191. M. García-Melchor, M. C. Pacheco, C. Nájera, A. Lledós and G. Ujaque, *ACS Catal.,* 2012, **2**, 135–144.
192. M. Gazvoda, M. Virant, B. Pinter and J. Košmrlj, *Nat. Commun.,* 2018, **9**, 4814.
193. R. S. Giri, S. Roy, G. Dolai, S. R. Manne and B. Mandal, *ChemistrySelect*, 2020, **5**, 2050–2056.
194. N. George, S. Ofori, S. Parkin and S. G. Awuah, *RSC Adv.*, 2020, **10**, 24017–24026.
195. J. W. Chang, A. B. Cognetta, III, M. J. Niphakis and B. F. Cravatt, *ACS Chem. Biol.,* 2013, **8**, 1590–1599.
196. D. Escudero, *Acc. Chem. Res.*, 2016, **49**, 1816–1824.
197. K. Torii, S. Benson, Y. Hori, M. Vendrell and K. Kikuchi, *Chem. Sci.*, 2024, **15**, 1393–1401.
198. R. Subiros-Funosas, V. C. L. Ho, N. D. Barth, L. Mendive-Tapia, M. Pappalardo, X. Barril, R. Ma, C.-B. Zhang, B.-Z. Qian, M. Sintes, O. Ghashghaei, R. Lavilla and M. Vendrell, *Chem. Sci*, 2020, **11**, 1368–1374.
199. M. Bertolini, L. Mendive-Tapia, O. Ghashghaei, A. Reese, C. Lochenie, A. M. Schoepf, M. Sintes, K. Tokarczyk, Z. Nare, A. D. Scott, S. R. Knight, A. R. Aithal, A. Sachdeva, R. Lavilla and M. Vendrell, *ACS Cent. Sci.*, 2024, **10**, 969–977.
200. N. D. Barth, L. Mendive-Tapia, R. Subiros-Funosas, O. Ghashghaei, R. Lavilla, L. Maiorino, X.-Y. He, I. Dransfield, M. Egeblad and M. Vendrell, *Angew. Chem. Int. Ed.*, 2022, **61**, e202113020.
201. S.-L. Xie, J.-Z. Yan, M.-J. Xie, X. Li, F. Zhou, M.-Q. Zheng, X.-L. Wang, J. Feng, Y. Zhang, Y.-N. Duan, Y.-D. Niu, D. Li and H.-D. Xia, *Green Chem.,* 2024, **26**, 323–329.

202. J. V. Jun, E. J. Petersson and D. M. Chenoweth, *J. Am. Chem. Soc.*, 2018, **140**, 9486–9493.
203. A. Kukoyi, H. He and K. Wheeler, *J. Photochem. Photobiol. A Chem.*, 2022, **425**, 113686.
204. M. Aydemir, G. Haykir, S. Demir, E. Aydemir, E. Arslan, H. Selvitopi, M. E. Arslan, A. Kadı, A. P. Monkman and F. Turksoy**, *J. Photochem. Photobiol. A Chem.***, 2026, **470**, 116666.
205. E. Kuru, A. Radkov, X. Meng, A. Egan, L. Alvarez, A. Dowson, G. Booher, E. Breukink, D. I. Roper, F. Cava, W. Vollmer, Y. Brun and M. S. VanNieuwenhze, *ACS Chem. Biol.,* 2019, **14**, 2745–2756.
206. D. Häußler and M. Gütschow, *Heteroat. Chem*, 2015, **26**, 367–373.
207. W. Wang and H. Li, *Tetrahedron Lett.*, 2004, **45**, 8479–8481.
208. A. Katori, E. Azuma, H. Ishimura, K. Kuramochi and K. Tsubaki, *J. Org. Chem.*, 2015, **80**, 4603–4610.
209. B. K. Sharma, A. M. Shaikh and R. M. Kamble, *J. Chem. Sci*, 2015, **127**, 2063–2071.
210. B. Heinz, B. Schmidt, C. Root, H. Satzger, F. Milota, B. Fierz, T. Kiefhaber, W. Zinth and P. Gilch, *Phys. Chem. Chem. Phys.,* 2006, **8**, 3432–3439.
211. A. Grzelakowska, J. Kolińska, M. Zakłos-Szyda and J. Sokołowska, *J. Photochem. Photobiol. A Chem.*, 2020, **387**, 112153.
212. C. Hoppmann, U. Alexiev, E. Irran and K. Rück-Braun, *Tetrahedron Lett.*, 2013, **54**, 4585–4587.
213. Boston University Fluorochromes Brightness Chart, https://www.bu.edu/flow-cytometry/files/2013/06/Fluorochromes-Brightness-Chart.pdf (accessed April 2026).
214. Guilbault, G. G. *Practical Fluorescence*, 2nd ed.; Marcel Dekker: New York, 1990.
215. M.-C. Chen, D.-G. Chen and P.-T. Chou, *ChemPlusChem*, 2021, **86**, 11–27.
216. Q. Zhu, Z. Li, L. Mu, X. Zeng, C. Redshaw and G. Wei, *Spectrochim. Acta A Mol. Biomol. Spectrosc.,* 2018, **188**, 230–236.
217. Z. Liu, G. Li, Y. Wang, J. Li, Y. Mi, D. Zou, T. Li and Y. Wu, *Talanta*, 2019, **192**, 6–13.
218. G. Li, D. Zhu, L. Xue and H. Jiang, *Org. Lett.*, 2013, **15**, 5020–5023.
219. M. Z. Vardaki, V. G. Gregoriou and C. L. Chochos, *RSC Chem. Biol.*, 2024, **5**, 273–292.
220. K. Dodo, K. Fujita and M. Sodeoka, *J. Am. Chem. Soc.*, 2022, **144**, 19651–19667.
221. C. L. Weeks, A. Polishchuk, Z. Getahun, W. F. DeGrado and T. G. Spiro, *J. Raman Spectrosc.*, 2008, **39**, 1606–1613.
222. M. G. Romei, E. V. von Krusenstiern, S. T. Ridings, R. N. King, J. C. Fortier, C. A. McKeon, K. M. Nichols, L. K. Charkoudian and C. H. Londergan, *J. Phys. Chem. B*, 2023, **127**, 85–94.
223. J. D. Flynn, M. Y. Gimmen, D. N. Dean, S. M. Lacy and J. C. Lee, *ChemBioChem*, 2020, **21**, 1582–1586.
224. (a) L. Wei, F. Hu, Y. Shen, Z. Chen, Y. Yu, C.-C. Lin, M. C. Wang and W. Min, *Nat. Methods*, 2014, **11**, 410–412. (b) S. Hong, T. Chen, Y. Zhu, A. Li, Y. Huang and X. Chen, *Angew. Chem. Int. Ed.*, 2014, **53**, 5827–5831.
225. V. Iashin, T. Wirtanen and J. E Perea-Buceta, *Catalysts*, 2022, **12**, 233.
226. J. Santandrea, C. Minozzi, C. Cruché and S. K. Collins, *Angew. Chem. Int. Ed.*, 2017, **56**, 12255–12259.
227. S. Verlinden, S. Ballet and G. Verniest, *Eur. J. Org. Chem.*, 2016, **2016**, 5807–5812.
228. H. Sunahara, Y. Urano, H. Kojima and T. Nagano, *J. Am. Chem. Soc.,* 2007, **129**, 5597–5604.

229. L. Mendive-Tapia, C. Zhao, A. R. Akram, S. Preciado, F. Albericio, M. Lee, A. Serrels, N. Kielland, N. D. Read, R. Lavilla and M. Vendrell, *Nat. Commun.*, 2016, **7**, 10940.
230. R. Subiros-Funosas, L. Mendive-Tapia, J. Sot, J. D. Pound, N. Barth, Y. Varela, F. M. Goñi, M. Paterson, C. D. Gregory, F. Albericio, I. Dransfield, R. Lavilla and M. Vendrell, *Chem. Commun.*, 2017, **53**, 945–948.
231. L. Mendive-Tapia, R. Subiros-Funosas, C. Zhao, F. Albericio, N. D. Read, R. Lavilla and M. Vendrell, *Nat. Protoc*, 2017, **12**, 1588–1619.
232. L. Mendive-Tapia, L. Miret-Casals, N. D. Barth, J. Wang, A. de Bray, M. Beltramo, V. Robert, C. Ampe, D. J. Hodson, A. Madder and M. Vendrell, *Angew. Chem.*, 2023, **135**, e202302688.
233. M. Wang, M. G. H. Vicente, D. Mason and P. Bobadova-Parvanova, *ACS Omega*, 2018, **3**, 5502–5510.
234. N. Kaplaneris, J. Son, L. Mendive-Tapia, A. Kopp, N. D. Barth, I. Maksso, M. Vendrell and L. Ackermann, *Nat. Commun.*, 2021, **12**, 3389.
235. C. Duan, Y. Zhou, G.-G. Shan, Y. Chen, W. Zhao, D. Yuan, L. Zeng, X. Huang and G. Niu, *J. Mater. Chem. C*, 2019, **7**, 3471–3478.
236. Í. A. O. Bozzi, L. A. Machado, E. B. T. Diogo, F. G. Delolo, L. O. F. Barros, G. A. P. Graça, M. H. Araujo, F. T. Martins, L. F. Pedrosa, L. C. d. Luz, E. S. Moraes, F. S. Rodembusch, J. S. F. Guimarães, A. G. Oliveira, S. H. Röttger, D. B. Werz, C. P. Souza, F. Fantuzzi, J. Han, T. B. Marder, H. Braunschweig and E. N. d. S. Júnior, *Chem. Eur. J.,* 2023, **30**, e202303883.
237. J. S. Lindsey, *Acc. Chem. Res.*, 2010, **43**, 300–311.
238. R. L. Gapare and A. Thompson, *Chem. Commun.*, 2022, **58**, 7351–7359.
239. K. Rurack, M. Kollmannsberger and J. Daub, *New J. Chem.*, 2001, **25**, 289–292.
240. C. Liu, X. Gao, J. Yuan and R. Zhang, *TrAC, Trends Anal. Chem.*, 2020, **133**, 116092.
241. R. S. Gamage, J. L. Chasteen and B. D. Smith, *Bioconjug Chem*, 2023, **34**, 961–971.
242. L. J. Morrison, M. P. Barrett, P. C. Steketee, G. Cecchi, O. Kijanga, F. Mramba and H. K. Auty, *Trends Parasitol.*, 2024, **40**, 679–686.
243. L. MacLean, E. Myburgh, J. Rodgers and H. P. Price, *Parasite Immunol.*, 2013, **35**, 283–294.
244. J. Wiedeman and K. Mensa-Wilmot, *Plos One*, 2018, **13**.
245. M. Cayla, F. Rojas, E. Silvester, F. Venter and K. R. Matthews, *Parasite Vector*, 2019, **12**.
246. C.-J. Li, *Acc. Chem. Res.*, 2010, **43**, 581–590.
247. J. P. Brand and J. Waser, *Chem. Soc. Rev.*, 2012, **41**, 4165–4179.
248. C. Hu, J. Mena and I. V. Alabugin, *Nat. Rev. Chem.*, 2023, **7**, 405–423.
249. M.-H. Huang, W.-J. Hao, G. Li, S.-J. Tu and B. Jiang, *Chem. Commun.*, 2018, **54**, 10791–10811.
250. S. J. Hein, D. Lehnherr, H. Arslan, F. J. Uribe-Romo and W. R. Dichtel, *Acc. Chem. Res.*, 2017, **50**, 2776–2788.
251. J. H. Li, D. L. An and J. H. Qin, *Synthesis-Stuttgart*, 2020, **52**, 3818–3836.
252. B. M. Trost and J. T. Masters, *Chem. Soc. Rev.*, 2016, **45**, 2212–2238.
253. H. A. Stefani, A. S. Guarezemini and R. Cella, *Tetrahedron*, 2010, **66**, 7871–7918.
254. J. Lei, L. Su, K. Zeng, T. Chen, R. Qiu, Y. Zhou, C.-T. Au and S.-F. Yin, *Chem. Eng. Sci.*, 2017, **171**, 404–425.
255. H. A. Reichard, M. McLaughlin, M. Z. Chen and G. C. Micalizio, *Eur. J. Org. Chem.*, 2010, **2010**, 391–409.
256. G. Ieronimo, A. Mondelli, F. Tibiletti, A. Maspero, G. Palmisano, S. Galli, S. Tollari, N. Masciocchi, K. M. Nicholas, S. Tagliapietra, G. Cravotto and A. Penoni, *Tetrahedron*, 2013, **69**, 10906–10920.

257. L. Wang, O. Jacobson, D. Avdic, B. H. Rotstein, I. D. Weiss, L. Collier, X. Chen, N. Vasdev and S. H. Liang, *Angew. Chem. Int. Ed.*, 2015, **54**, 12777–12781.
258. H. C. Kolb, M. G. Finn and K. B. Sharpless, *Angew. Chem. Int. Ed.*, 2001, **40**, 2004–2021.
259. M. F. Debets, S. S. van Berkel, S. Schoffelen, F. P. J. T. Rutjes, J. C. M. van Hest and F. L. van Delft, *Chem. Commun.*, 2010, **46**, 97–99.
260. M. F. Debets, S. S. van Berkel, J. Dommerholt, A. J. Dirks, F. P. J. T. Rutjes and F. L. van Delft, *Acc. Chem. Res.*, 2011, **44**, 805–815.
261. N. J. Agard, J. M. Baskin, J. A. Prescher, A. Lo and C. R. Bertozzi, *ACS Chem. Biol.* 2006, **1**, 644–648.
262. J. A. Codelli, J. M. Baskin, N. J. Agard and C. R. Bertozzi, *J. Am. Chem. Soc*, 2008, **130**, 11486–11493.
263. J. C. M. van Hest, K. L. Kiick and D. A. Tirrell, *J. Am. Chem. Soc.*, 2000, **122**, 1282–1288.
264. K. Kirshenbaum, I. S. Carrico and D. A. Tirrell, *ChemBioChem*, 2002, **3**, 235–237.
265. K. E. Beatty, F. Xie, Q. Wang and D. A. Tirrell, *J. Am. Chem. Soc.*, 2005, **127**, 14150–14151.
266. C. Li, E. Henry, N. K. Mani, J. Tang, J.-C. Brochon, E. Deprez and J. Xie, *Eur. J. Org. Chem.*, 2010, **2010**, 2395–2405.
267. E. Benedetti, A. B. E. Veliz, M. Charpenay, L. S. Kocsis and K. M. Brummond, *Org. Lett.*, 2013, **15**, 2578–2581.
268. C. Li, J. Tang and J. Xie, *Tetrahedron*, 2009, **65**, 7935–7941.
269. S. S. Bag, S. Jana and M. K. Pradhan, *Biorg. Med. Chem.*, 2016, **24**, 3579–3595.
270. S. S. Bag and R. Kundu, *J. Org. Chem.*, 2011, **76**, 3348–3356.
271. J. E. Moses and A. D. Moorhouse, *Chem. Soc. Rev.*, 2007, **36**, 1249–1262.
272. Y. L. Angell and K. Burgess, *Chem. Soc. Rev.*, 2007, **36**, 1674–1689.
273. S. Mocanu, G. Ionita and I. Matei, *Spectrochim. Acta A Mol. Biomol. Spectrosc.,* 2020, **237**, 118413.
274. S. Huangfu, X. Yu, Z. Sun, B. Jiang and H. Chen, *Chem. Commun.*, 2024, **60**, 1509–1516.
275. X. Wan, G. Zhang, Z. Ge, R. Narain and S. Liu, *Chem. Asian J.*, 2011, **6**, 2835–2845.
276. J. Li, S. Lin, J. Wang, S. Jia, M. Yang, Z. Hao, X. Zhang and P. R. Chen, *J. Am. Chem. Soc.*, 2013, **135**, 7330–7338.
277. N. Li, R. K. V. Lim, S. Edwardraja and Q. Lin, *J. Am. Chem. Soc.,* 2011, **133**, 15316–15319.
278. S. Hauke, M. Best, T. T. Schmidt, M. Baalmann, A. Krause and R. Wombacher, *Bioconjugate Chem.*, 2014, **25**, 1632–1637.
279. N. Saha, F. N. U. Vidya, R. Xie and V. Agarwal, *J. Am. Chem. Soc.*, 2024, **146**, 30009–30013.
280. U. Hoffmanns and N. Metzler-Nolte, *Bioconjugate Chem.*, 2006, **17**, 204–213.
281. H. Pfeiffer, A. Rojas, J. Niesel and U. Schatzschneider, *Dalton Transactions*, 2009, 4292–4298.
282. D. Nandan, S. K. Behera and R. Ramapanicker, *ChemBioChem*, 2025, **26**, e202500041.
283. N. David, R. Pasceri, R. R. A. Kitson, A. Pradal and C. J. Moody, *Chem. Eur. J.*, 2016, **22**, 10867–10876.
284. X. Zhu, C. C. McAtee and C. S. Schindler, *Org. Lett.*, 2018, **20**, 2862–2866.
285. Walker and S. E. Rokita, *J. Org. Chem.*, 2003, **68**, 1563–1566.
286. Y. Murakami, H. Yanuma and T. Usuki, *Tetrahedron: Asymmetry*, 2012, **23**, 1557–1563.
287. A. T. R. Williams, S. A. Winfield and J. N. Miller, *Analyst*, 1983, **108**, 1067–1071.
288. A. M. Brouwer, *Pure Appl. Chem.*, 2011, **83**.

289. J. F. Popplewell, M. J. Swann, N. J. Freeman, C. McDonnell and R. C. Ford, *Biochim. Biophys. Acta Biomembr.* 2007, **1768**, 13–20.
290. E. Stempel, R. F. X. Kaml, N. Budisa and M. Kalesse, *Biorg. Med. Chem.*, 2018, **26**, 5259–5269.
291. Critical Transfer Distance Determination Between FRET Pairs, http://photobiology.info/Experiments/Biolum-Expt.html (accessed September 2024).
292. S. Lin, Z.-Q. Yang, B. H. B. Kwok, M. Koldobskiy, C. M. Crews and S. J. Danishefsky, *J. Am. Chem. Soc.*, 2004, **126**, 6347–6355.
293. N. v. Rooijen and R. v. Nieuwmegen, *Cell Tissue Res*, 1984, **238**, 355–358.
294. A. S. Saghyan, A. F. Mkrtchyan, Z. Z. Mardiyan, L. A. Hayriyan, A. J. Karapetyan, Y. N. Belokon, P. Ehlers and P. Langer, *ChemistrySelect*, 2019, **4**, 13806–13809.
295. H. Lu, Q. Wang, L. Gai, Z. Li, Y. Deng, X. Xiao, G. Lai and Z. Shen, *Chem. Eur. J.*, 2012, **18**, 7852–7861.
296. X. Cai, W. Lu, C. Ma, Y. Kang, Y. Ren, X. Meng, D. J. Craik, S. Fan, L. Y. Chan and S. Liu, *Chin. J. Chem* . 2025, **43**, 3171–3177.
297. P.-C. Lin, S.-H. Ueng, M.-C. Tseng, J.-L. Ko, K.-T. Huang, S.-C. Yu, A. K. Adak, Y.-J. Chen and C.-C. L. Prof., *Angew. Chem. Int. Ed.*, 2006, **45**, 4286–4290.
298. D. Georgiev, B. W. H. Saes, H. J. Johnston, S. K. Boys, A. Healy and A. N. Hulme, *Molecules*, 2016, **21**, 88.
299. G. Ortar, *Org. Prep. Proced. Int.*, 2002, **34**, 190–193.